



**Molekular und zellbiologischer Ansatz
hin zu neuartigen Medikamenten
gegen *Echinococcus multilocularis***

**Molecular and cell biological approach
towards novel drugs against *Echinococcus multilocularis***

Dissertation zur Erlangung des naturwissenschaftlichen Doktorgrades
der Graduate School of Life Sciences,
Julius-Maximilians-Universität Würzburg,
Klasse Infektion und Immunität
Vorgelegt von

Akito Koike

aus

Ikeda

Würzburg 2022

Eingereicht am:
Bürostempel

Mitglieder des Promotionskomitees:

Vorsitzende/r: Prof. Dr. Christian Janzen

1. Betreuer: Prof. Dr. Klaus Brehm

2. Betreuer: Prof. Dr. Christian Stigloher

3. Betreuer: Prof. Dr. August Stich

(4. Betreuer:)

Tag des Promotionskolloquiums:

Doktorurkunden ausgehändigt am:

1. Table of Contents

| | |
|--|----|
| 1. Table of Contents | 1 |
| 2. Summary / Zusammenfassung | 7 |
| 2.1 Summary | 7 |
| 2.2 Zusammenfassung | 9 |
| 3. Introduction..... | 11 |
| 3.1 Echinococcosis | 11 |
| 3.1.1 Epidemiology..... | 11 |
| 3.1.2 Phylogeny | 12 |
| 3.1.3 Life cycles and body structure of <i>Echinococcus multilocularis</i> | 14 |
| 3.1.4 Symptom and treatment of alveolar echinococcosis | 16 |
| 3.1.5 Stem cells in <i>Echinococcus</i> and other Platyhelminthes | 17 |
| 3.1.6 <i>E. multilocularis</i> in laboratories | 18 |
| 3.2 Protein kinases | 19 |
| 3.2.1 Function and regulation of protein kinases | 19 |
| 3.2.2 Major groups of protein kinases | 20 |
| 3.2.2 Function of PIM kinases and CDC25 phosphatases | 22 |
| 3.3 Benzimidazoles..... | 24 |
| 3.3.1 Structure and utility of benzimidazole | 24 |

Table of Contents

| | | |
|-------|--|----|
| 3.3.2 | Albendazole..... | 25 |
| 3.3.3 | Triclabendazole | 26 |
| 3.4 | Colchicine binding site inhibitors..... | 27 |
| 3.4.1 | Colchicine | 27 |
| 3.4.2 | Combretastatin | 28 |
| 3.4.3 | Derivatives of colchicine binding site inhibitors for flavivirus infection | 29 |
| 3.5 | Tubulins | 30 |
| 3.5.1 | Tubulin families and their function | 30 |
| 3.5.2 | Residues in β -tubulin corelated with benzimidazole resistance..... | 30 |
| 3.5.3 | β -tubulins of <i>Homo sapiens</i> | 32 |
| 3.5.4 | β -tubulins of <i>E. multilocularis</i> | 32 |
| 3.5.5 | β -tubulins of <i>Fasciola hepatica</i> | 34 |
| 3.5.6 | Colchicine binding site..... | 35 |
| 3.6 | Purpose of this research..... | 37 |
| 4 | Materials and methods | 38 |
| 4.1 | Ethical statement..... | 38 |
| 4.2 | Equipment and devices | 38 |
| 4.3 | Chemicals and reagents | 40 |
| 4.3.1 | Commercially available kinase inhibitors..... | 40 |
| 4.3.2 | Commercially available inhibitors of tubulin polymerization | 41 |
| 4.3.3 | Kits..... | 41 |

Table of Contents

| | | |
|-------|--|----|
| 4.3.4 | Reagent/media for <i>Echinococcus</i> /mammalian | 42 |
| 4.3.5 | Reagent/media for yeast | 42 |
| 4.3.6 | Reagent/media for <i>E. coli</i> and plasmid construction..... | 43 |
| 4.3.7 | Reagents /antibodies for imaging analysis..... | 44 |
| 4.4 | Oligonucleotides | 45 |
| 4.4.1 | Primers for both projects | 45 |
| 4.4.2 | Primers for kinase projects | 45 |
| 4.4.3 | Primers for tubulin project..... | 46 |
| 4.5 | Other consumables..... | 47 |
| 4.6 | <i>In vitro</i> cultivation..... | 48 |
| 4.6.1 | <i>In vitro</i> cultivation of <i>E.multilocularis</i> | 48 |
| 4.6.2 | <i>In vitro</i> cultivation of mammalian cells | 49 |
| 4.6.3 | <i>In vitro</i> cultivation of <i>Saccharomyces cerevisiae</i> | 49 |
| 4.7 | <i>In vitro</i> screening | 50 |
| 4.7.1 | Matured vesicle assay | 50 |
| 4.7.2 | Vesicle formation assay | 51 |
| 4.7.3 | Cell viability assay of <i>E.multilocularis</i> | 52 |
| 4.7.4 | Screening with mammalian cell lines | 52 |
| 4.7.5 | Transfection of mammalian cell line and following cell viability assay | 53 |
| 4.8 | Bioinformatic analysis and handling of nucleic acids..... | 57 |
| 4.8.1 | Bioinformatic analysis..... | 57 |

Table of Contents

| | |
|--|----|
| 4.8.2 <i>In silico</i> screening of compounds..... | 59 |
| 4.8.3 <i>In silico</i> analysis of affinity between HsPim1 and inhibitors..... | 60 |
| 4.9 Handling of nucleic acids..... | 61 |
| 4.9.1 PCR with KOD DNA polymerase..... | 61 |
| 4.9.2 Gel electrophoresis..... | 62 |
| 4.9.3 Purification and cloning of PCR products..... | 63 |
| 4.9.4 Transformation of chemically competent <i>E. coli</i> | 63 |
| 4.9.5 Colony PCR..... | 64 |
| 4.9.6 Amplification of plasmid..... | 65 |
| 4.9.7 Sequencing of plasmid..... | 65 |
| 4.9.8 Synthesis of probes for <i>in situ</i> hybridization..... | 66 |
| 4.10 Yeast-two-hybrid..... | 68 |
| 4.11 Imaging analysis..... | 69 |
| 4.11.1 Whole-mount <i>in situ</i> hybridization..... | 69 |
| 4.11.2 Whole-mount immunofluorescence assay..... | 71 |
| 4.11.3 EdU labeling and analysis of EdU positive cells..... | 72 |
| 5. Results..... | 73 |
| 5.1 <i>In vitro</i> screening with kinases inhibitors..... | 73 |
| 5.2 PIM kinases..... | 77 |
| 5.2.1 Characterization of EmpPIM..... | 77 |
| 5.2.2 Expression of <i>empim</i> in stem cells..... | 80 |

Table of Contents

| | |
|--|-----|
| 5.2.3 Interaction between EmPIM and EmCDC25C..... | 83 |
| 5.2.4 Effects of SGI-1776 and CX6258 on <i>E. multilocularis</i> | 90 |
| 5.2.5 <i>In silico</i> screening of EmPIM inhibitors..... | 97 |
| 5.3 Tubulins..... | 102 |
| 5.3.1 Comparison of Echinococcus tubulins and Robinson’s model of <i>H. contortus</i> | 102 |
| 5.3.2 Effect of TCBZ on metacestode vesicles..... | 105 |
| 5.3.3 Effect of TCBZ on the ability of regeneration..... | 117 |
| 5.3.4 Effect of TCBZ on isolated primary cells..... | 120 |
| 5.3.5 Interaction between BZs and each β -tubulin of <i>E. multilocularis</i> | 121 |
| 5.3.6 Trial of colchicine binding site inhibitors on <i>E. multilocularis in vitro</i> | 124 |
| 6 Discussion..... | 126 |
| 6.1 In vitro screening with kinase inhibitors..... | 126 |
| 6.2 PIM kinases..... | 127 |
| 6.2.1 Characterization of EmPIM..... | 127 |
| 6.2.2 Expression of empim in stem cells..... | 128 |
| 6.2.3 Interaction between EmPIM and EmCDC25..... | 130 |
| 6.2.4 Effects of SGI-1776 and CX6258 on <i>E. multilocularis</i> | 132 |
| 6.2.5 <i>In silico</i> screening of EmPim inhibitors..... | 134 |
| 6.2.6 Summary of kinase project and how this research advance the field..... | 135 |
| 6.3 Tubulins..... | 136 |
| 6.3.1 Comparison of Echinococcus tubulin and Robinson’s model of <i>H. contortus</i> | 136 |

Table of Contents

| | |
|--|-----|
| 6.3.2 Effect of TCBZ on metacystode vesicles..... | 137 |
| 6.3.3 Effect of TCBZ on the ability of regeneration..... | 139 |
| 6.3.4 Effect of TCBZ on isolated primary cells..... | 139 |
| 6.3.5 Interaction between BZs and each β -tubulin of <i>E. multilocularis</i> | 140 |
| 6.3.6 Trial of colchicine binding site inhibitors on <i>E. multilocularis in vitro</i> | 144 |
| 6.3.7 Summary of tubulin project and how this research advance the field..... | 146 |
| 7 Bibliography and approval of secondary publication..... | 147 |
| 7.1 Bibliography..... | 147 |
| 7.2 Approval of secondary publication..... | 170 |
| 8 Appendix and curriculum vitae..... | 171 |
| 8.1 List of 400 compounds against EmPim..... | 171 |
| 8.2 List of 20 compounds against EmPim..... | 182 |
| 8.3 List of 31 combretastatin/colchicine-related compounds..... | 189 |
| 8.4 Accession numbers of proteins described in this doctoral dissertation..... | 193 |
| 8.4.1 Kinase project..... | 193 |
| 8.4.2 Tubulin project..... | 195 |
| 8.5 Curriculum vitae..... | 196 |
| 9. Acknowledgement and affidavit..... | 198 |
| 9.1 Acknowledgement..... | 198 |
| 9.2 Affidavit / Eidesstattliche Erklärung..... | 201 |

2. Summary / Zusammenfassung

2.1 Summary

Echinococcosis is one of the most important zoonosis both for human and veterinary medicine. The causative agent of Alveolar Echinococcosis (AE) is *Echinococcus multilocularis*. Metacestode vesicles, the larval stage of this parasitic helminth can infiltrate into the liver and grow asexually like malignant tumors. This can be lethal without appropriate treatments.

The treatment of human AE is limited to surgery and chemotherapy, but surgery is applicable only for smaller percentage of the patients diagnosed in the early stage. Most of patients can only depend on chemotherapy with Albendazole (ABZ). However, ABZ works parasitostatically only, and cannot cure the disease. Therefore, ABZ needs to be taken for longer periods, although it accompanies side effect. Thus, development of new, parasitocidal and selective drug against AE is required. Because the undifferentiated stem cell population of *E. multilocularis* play key role in its longevity and regenerative capacity, stem cell-targeted chemotherapy is important.

In this work, *in vitro* screening of various inhibitors against kinases and tubulins were performed. The screening result demonstrated that inhibitors against human PIM kinases proved to have strong detrimental effects on *E. multilocularis*. Through yeast two hybrid assay, the interaction of parasite PIM kinase (EmPIM) with its cell division cycle 25 (EmCDC25) was indicated and through *in situ* hybridization, the partial localization of EmPIM in the stem cells was observed. Therefore, EmPim is likely to be a positive regulator of cell cycle progression, the same as human Pim1. In addition, 20 compounds against EmPIM were selected through high throughput *in silico* screening and synthesized. One of them has a detrimental effect on *E. multilocularis* comparable to commercially available human pan-PIM inhibitors, but has much weaker toxicity on human cell lines.

Furthermore, triclabendazole (TCBZ), which is approved for another flatworm disease Fascioliasis and target β -tubulins, was tried on *E.multilocularis.*, together with its metabolite triclabendazole-sulfoxide (TCBZSX) With two stem cell markers, EdU labelling and *in situ* hybridization against EmTRIM, damage to stem cells by TCBZSX was shown. In addition, primary cells from treated vesicles could never regenerate new vesicles and the damage to stem cells proved to be irreversible.

Since the early 1980s, ABZ-based chemotherapy has greatly improved the life expectancy of human AE patients. However, it also has the problem of compromising patients' quality of life, due to adverse side effects and lack of parasitocidal effect. The high-throughput *in silico* screening method used in my research of EmPim kinase might identify compounds with selectivity and can overcome the side effect problem in ABZ-based chemotherapy. On the other hand, my research of TCBZ has the potential to develop a practical parasitocidal chemotherapy by combining TCBZ and ABZ.

2.2 Zusammenfassung

Die Echinokokkose ist eine der wichtigsten Zoonosen sowohl für die Human- als auch für die Veterinärmedizin. Der Erreger der alveolären Echinokokkose (AE) ist *Echinococcus multilocularis*. Metazestode Bläschen, das Larvenstadium dieses parasitären Helminthen, können in die Leber eindringen und ungeschlechtlich wie bösartige Tumore wachsen. Dies kann ohne geeignete Behandlung tödlich sein.

Die Behandlung von AE beim Menschen beschränkt sich auf Chirurgie und Chemotherapie, aber die Chirurgie ist nur bei einem kleinen Prozentsatz der Patienten anwendbar, die im Frühstadium diagnostiziert werden. Die meisten Patienten können sich nur auf eine Chemotherapie mit Albendazol (ABZ) verlassen. ABZ wirkt jedoch nur parasitostatisch und kann die Krankheit nicht heilen. Daher muss ABZ über einen längeren Zeitraum eingenommen werden, obwohl es mit Nebenwirkungen einhergeht. Daher ist die Entwicklung eines neuen, parasitentötenden und selektiven Medikaments gegen AE erforderlich. Da die undifferenzierte Stammzellpopulation von *E. multilocularis* eine Schlüsselrolle für seine Langlebigkeit und Regenerationsfähigkeit spielt, ist eine auf Stammzellen abzielende Chemotherapie wichtig.

In dieser Arbeit wurde ein In-vitro-Screening verschiedener Hemmstoffe gegen Kinasen und Tubuline durchgeführt. Das Ergebnis des Screenings zeigte, dass Inhibitoren gegen humane pim-Kinasen starke schädliche Auswirkungen auf *E. multilocularis* haben. Durch ein Hefe-Zwei-Hybrid-System wurde die Interaktion der Parasiten-Pim-Kinase (EmPIM) mit der Zellteilungszyklus 25 (EmCDC25) nachgewiesen, und durch In-situ-Hybridisierung wurde die teilweise Lokalisierung von EmPIM in den Stammzellen beobachtet. Daher ist es wahrscheinlich, dass EmPim ein positiver Regulator der Zellzyklusprogression ist, genau wie menschliches Pim1. Darüber hinaus wurden 20 Verbindungen gegen EmPIM durch Hochdurchsatz-Screening in silico ausgewählt und synthetisiert. Eine von ihnen hat eine schädliche Wirkung auf *E.*

multilocularis, die mit der von handelsüblichen menschlichen pan-PIM-Inhibitoren vergleichbar ist, aber eine viel geringere Toxizität auf menschliche Zelllinien aufweist.

Darüber hinaus wurde Triclabendazol (TCBZ), das für eine andere Plattwurmkrankheit, die Fascioliasis, zugelassen ist und auf β -Tubuline abzielt, zusammen mit seinem Metaboliten Triclabendazol-Sulfoxid (TCBZSX) an *E. multilocularis* getestet. Mit zwei Stammzellmarkern, EdU-Markierung und In-situ-Hybridisierung gegen EmTRIM, wurde eine Schädigung der Stammzellen durch TCBZSX nachgewiesen. Darüber hinaus konnten Primärzellen aus behandelten Vesikeln keine neuen Vesikel regenerieren, und die Schädigung der Stammzellen erwies sich als irreversibel.

Seit Anfang der 1980er Jahre hat die Chemotherapie auf ABZ-Basis die Lebenserwartung von Patienten, die an AE erkrankt sind, erheblich verbessert. Sie bringt jedoch das Problem mit sich, dass sie die Lebensqualität der Patienten aufgrund der unerwünschten Nebenwirkungen und der fehlenden parasitentötenden Wirkung beeinträchtigt. Die Hochdurchsatz-In-silico-Screening-Methode, die in meiner Forschung zur EmPim-Kinase eingesetzt wird, könnte Verbindungen mit Selektivität identifizieren und das Problem der Nebenwirkungen bei der ABZ-basierten Chemotherapie lösen. Andererseits hat meine Forschung zu TCBZ das Potenzial, durch die Kombination von TCBZ und ABZ eine praktische parasitizide Chemotherapie zu entwickeln.

3. Introduction

3.1 Echinococcosis

3.1.1 Epidemiology

Echinococcosis is one of diseases listed in WHO's neglected tropical diseases. This list includes communicable diseases which affect larger population but have not been controlled enough. Echinococcosis is roughly divided into two, alveolar echinococcosis (AE) and cystic echinococcosis (CE). The causative reagent of human AE is the larval stage of tapeworm named *Echinococcus multilocularis* and that of CE is *Echinococcus granulosus*. The diseases are characterized by cystic (CE) or tumor-like, infiltrative (AE) growth of the parasite's metacestode larval stages within the host's inner organs. Both AE and CE can be lethal without appropriate treatment (Brunetti et al., 2010; Kern, 2010).

E. multilocularis is distributed in the Northern hemisphere (Torgerson et al., 2010). On the other hand, CE distributes all over the world except for Antarctica. According to the 2015 WHO Foodborne Diseases Burden Epidemiology Reference Group (FERG), echinococcosis is responsible for 19300 deaths and 871,000 (CE: 184,000 and AE: 688,000) disability-adjusted-life-years (DALYs) each year. The mortality of CE is 1% (non-treatment seeking) and 2% (treatment seeking). The mortality of AE is 2-5% in North America, Central Europe and Northern Europe, but it is 20-30% in Eastern Europe (WHO, 2015). The costs for treatment and loss in the livestock industry also can be enormous. Other than *E. granulosus* and *E. multilocularis*, three other pathogens for echinococcosis, *E. oligarthrus*, *E. Shiquicus* and *E. vogeli* are known but the number of patients is rather small (Spickler, 2020).

3.1.2 Phylogeny

Genus *Echinococcus* belongs to family Taenidae, which also includes the pork tapeworm *Taenia soleum*. The family Taenidae belong to Cestoda (tape worms), the same as *Sparganum proliferum* or *Diphyllobothrium*. Cestoda is one of three groups of neodermata. All members of Neodermata are parasitic. Other two major groups in Neodermata are Trematoda (fluke) and Monogenea. Trematoda includes important parasites such as *Fasciola hepatica* and *Schistosoma mansoni*. Neodermata is part of Neophora. Neophora also includes Tricladida, such as planaria (*Schmidtea mediterranea*) and terrestrial planaria. Different from Neodermata, all members of Tricladida are free living organisms. Neophora is part of Platyhelminth (flatwoms) and other groups in Platyhelminthes are Macrostomida and Polycladida (Collins and Newmark, 2013).

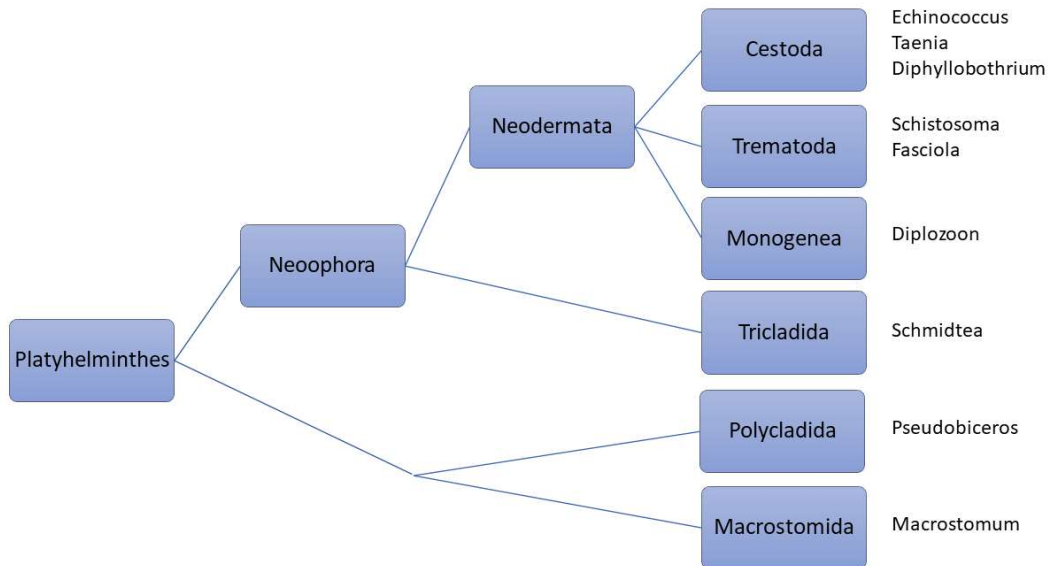


Figure 1: Schematic image of phylogeny in plathyhelminthes
Schematic image of phylogeny based on the figure 2 of Collins and Newmark 2013

Introduction

Platyhelminthes constitutes Lophotrochozoa, together with Annelida (including earthworms) and Mollusca (including octopuses and snails). Lophotrochozoa constitutes Protostomia, together with Ecdysozoa (Olson et al., 2012). Ecdysozoa is the group of nematoda (including *Caenorhabditis*, *Strongyloides* and *Haemonchus*) and Arthropoda (Engelhardt et al., 2022). Protostomia constitutes Bilateria together with Deuterostomia, and Deuterostomia include vertebrata such as *Homo sapience* (Lartillot and Philippe, 2008). Bilateria belongs to Metazoa, and Metazoa belongs to Opisthokonta together with fungi such as *Saccharomyces cerevisiae* and *Aspergillus nidulans*.

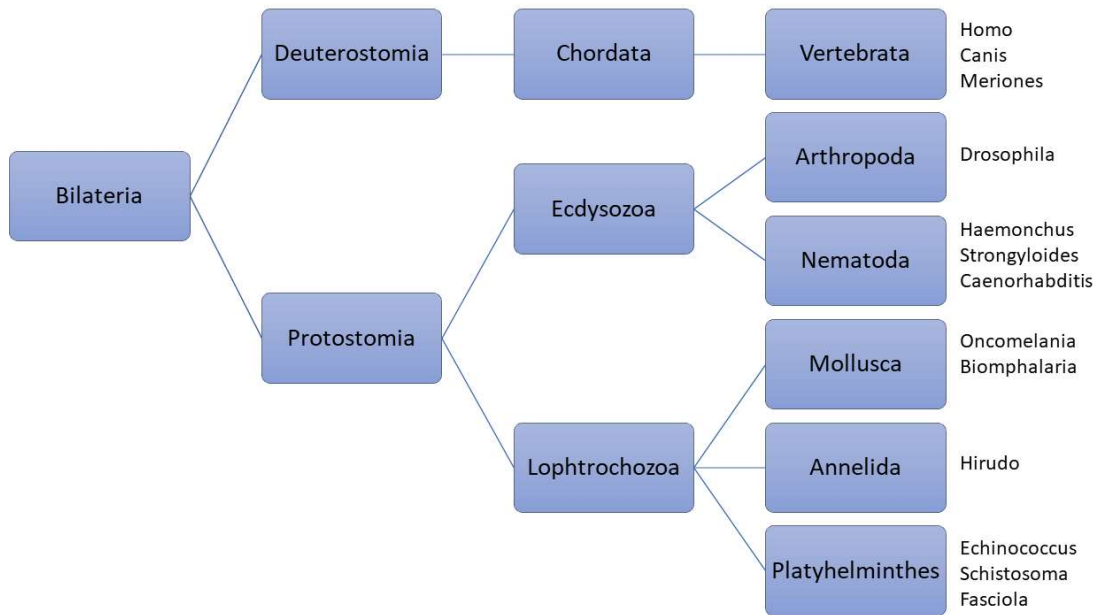


Figure 2: Schematic image of phylogeny in Bilateria
Schematic image of phylogeny , based on the figure 1 in Olson et al. 2012

3.1.3 Life cycles and body structure of *Echinococcus multilocularis*

The definitive hosts of *E. multilocularis* are carnivores of family Canidae such as foxes and dogs. The eggs are spread to the environment with feces of the definitive hosts. The egg shape is round and around 30µm in diameter and a larva of the first stage called oncosphere has already developed in it. The oncosphere have 3 pairs of hooks (Thompson and Eckert, 1982). The oncospheres in the egg are taken by the intermediate hosts orally through contaminated food or water. Various mammals including horses, pigs and primates can be the hosts, but natural and best intermediate hosts are small animals like rodents (Eckert and Deplazes, 2004). In the intermediate hosts, the oncospheres hatches in the intestine and penetrate the epithelium. Through the blood stream, the oncosphere can move to various inner organs, but usually settle in liver. They metamorphose into the stage called metacestodes or metacestode vesicles (Brehm et al., 2006). The body structure of this stage is atypical as larvae of tapeworms. They look like sphere of up to several centimeters in diameter and they do not have dorsal-ventral nor anterior-posterior axis. Two layers, laminated layer and germinal layer, constitute metacestode vesicles. Laminated layer is the outer acellular layer of carbohydrate network, and host proteins are attached on the surface. The inner layer, germinal layer includes alive cells such as muscle cells, nerve cells and stem cells. These stem cells are also called germinative cells. The interior of the cysts is filled with hydatid fluid, a complex mixture of host and parasite factors (Brehm, 2010a). The vesicles grow in number by budding, and infiltrate into the host tissue locally, and sometimes experience metastatic spread like malignant tumors. Once the metacestode vesicles are established, they seem to be immunologically tolerated by the host (Dixon, 1997).

In the optimal hosts like rodents, brood capsules are formed by the invagination of the germinal layers. Inside of the brood capsule, the final larval stage protoscolex is formed (Brehm, 2010b; Koziol et al., 2016). This protoscolexes develop basic structure of the heads of adult worms, and already have hooks and suckers. When the protoscolexes are taken by

Introduction

carnivores through the food chain, the surrounding tissues are digested. The difference in the composition of bile is considered to be important for the host specificity, only carnivores' bile can activate protoscoleces (Smyth, 1968). The protoscoleces attach on the small intestine with their hooks and suckers (Thompson and Eckert, 1983). In the intestine, at the posterior part of the body axis, multiple new segments called proglottids are developed distal to the protoscoleces. *E. multilocularis* develop only 3-5 proglottids and their overall worm length is 4.5 mm. Different from *Fasciola* or *Schmidtea*, cestodes do not have digestive organs and absorb nutrients directly through the surface. The eggs are produced in the matured proglottids and released into the intestine together with the proglottids. When humans take the egg accidentally, the metacestode vesicles can grow slowly but massively. The same as typical intermediate hosts, the oncosphere can settle and grow into metacestode vesicles in the liver. However, even decades after the infection, brood capsules or protoscoleces are rarely formed in human patients, presumably because humans are not optimal intermediate hosts.

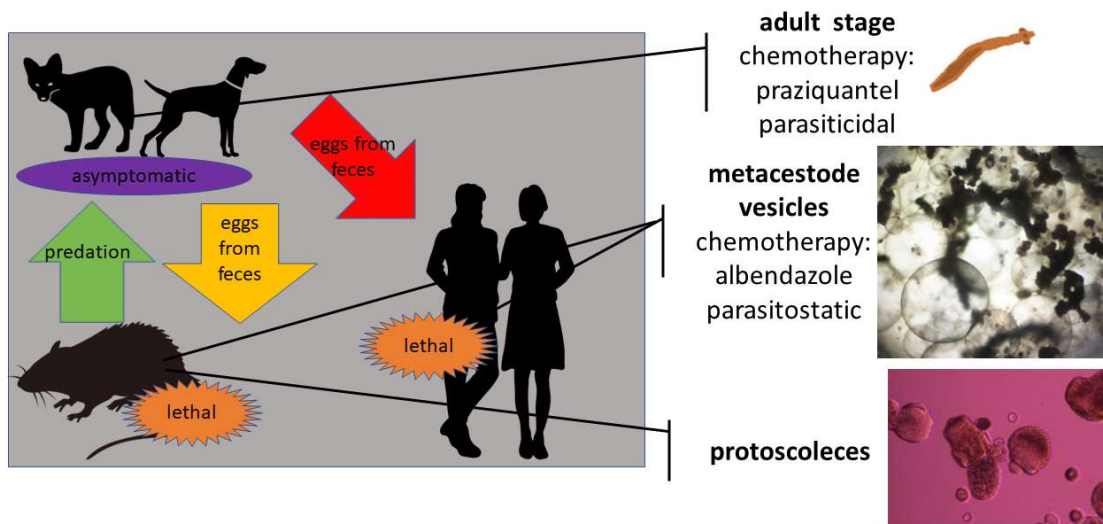


Figure 3: Life cycle of *Echinococcus multilocularis*

Schematic image of *E. multilocularis*'s life cycle. Chemotherapy against each stages are also shown. All photographs are taken/drawn by myself or free materials from silhouette AC.

3.1.4 Symptom and treatment of alveolar echinococcosis

Canine patients with adult worms normally shows weaker or no symptoms. The chemotherapy for adult worms is Praziquantel. In most cases, worms are exterminated after taking just one time medication. (Haller *et al.*, 1998).

Praziquantel paralyzes worms and force them to detach from the tissues and they are removed by the immune systems. It works well when the patients are definitive hosts with adult worms. Because the body structure and gene expression pattern are different from that of adult worms, praziquantel is not effective to metacestode vesicles in human patients.

In the case of human patients, Echinococcosis is usually diagnosed 5-15 years after initial infection, because parasites grow slowly and they only show weak and nonspecific symptoms during this incubation period (Eckert and Deplazes, 2004). Smaller lesions appear typically on the liver first. In later stages of infection, it can spread to other inner organs including lungs and brains (Eckert and Deplazes, 2004). The typical symptoms in later stages include abdominal pain, weight loss and hepatic failure.

Only when the lesions are smaller and limited (approximately 20% of cases), it can be cured by removal of parasite tissue through radical surgery (Brunetti *et al.*, 2010). However, in other cases of advanced stages, only palliative surgery is available. Regardless of the type of surgery, accompanying chemotherapy is usually applied. Medication should be continued at least for 2 years, and 10 years of monitoring is recommended because of frequent relapses. This problem will be described in 3.3.2.

Even though dogs are natural definitive hosts, they can harbor metacestode vesicles, when they take eggs instead of protoscoleces (Eckert and Deplazes, 2004). In such cases, surgical treatment and following chemotherapy (10mg/kg ABZ) for months or years are required (Haller *et al.*, 1998). Eggs are detected also from the feces of domestic cats, and

they have the potential to be definitive hosts (Dyachenko et al., 2008; Eckert and Deplazes, 2004).

3.1.5 Stem cells in *Echinococcus* and other Platyhelminthes

Planarian (e.g. *Schmidtea mediterranea*) are famous for their ability to regenerate. When they are amputated into small pieces, every piece can grow into a new individual. This ability strongly depends on adult somatic stem cells called neoblast (Newmark and Sanchez Alvarado, 2002).

Parasitic flatworms have similar stem cell systems and abilities to regenerate for some extent, although it is not as extreme as in the case of planaria. In fact, *Schistosoma mansoni* is known to regenerate their tissues after the treatment of sublethal dose of praziquantel (Ross et al., 2002). Stem cells in *S. mansoni* are also called neoblasts. They are morphologically similar to planarian neoblasts, express a lot of genes which regulate planarian neoblasts, and have ability to produce differentiated cells (Collins and Newmark, 2013).

Echinococcus multilocularis also has totipotent somatic stem cells called germinative cells. In fact, 25% of cells in the germinal layer are germinative cells. These germinative cells look morphologically homogeneous but can be divided into sub-populations at the molecular level (Koziol et al., 2014). Like in the case of neoblast of *S. mansoni*, germinative cells of *E. multilocularis* express a lot of homologues of planarian neoblast-specific markers but also display some remarkable differences in the gene expression profile. Through the experiment of stem cell depletion with hydroxyurea, their ability of self-renewal has been shown. They are believed to be the only population in metacystode vesicles which can proliferate, and to play important role for their longevity and continuous growth (Koziol et al., 2014)

3.1.6 *E. multilocularis* in laboratories

Previous works from the AG Brehm established *in vitro* cultivation systems for *Echinococcus* larvae and stem cells. In these systems, the growth of the parasite within the host liver can be reconstituted *in vitro*, and major part of the life cycles from early metacestode vesicle to the production of protoscoleces can be mimicked (Brehm, 2010a) Co-cultivation with host feeder cells is especially important to produce large amount of metacestode vesicles. Some factors secreted from continuously proliferating mammalian cell lines seem to be necessary for the growth of metacestode vesicles (Spiliotis et al., 2004) In fact, several researches demonstrated that host-derived factors such as insulin (Hemer et al., 2014), fibroblast growth factor (Förster et al., 2018), or epidermal growth factor (Cheng et al., 2017; Cheng et al., 2020) significantly stimulate parasite development *in vitro*. Metacestode vesicles can grow with cell lines from non-hepatic origins for some extent, but rat liver cell line, Reuber hepatoma (ATCC no. CRL-1600) seems to be the best as feeder cells (Spiliotis et al., 2004).

When the removal of Reuber hepatoma is necessary for the experiment in host-cell-free conditions, axenic condition is used. The feeder cells attached to metacestode vesicles can be removed by cell disruption with osmotic shock but the medium should not be fresh DMEM but the supernatant from the culture of Reuber hepatoma (conditioned medium) (Spiliotis et al., 2004).

This culture in host-cell-free conditions have clear advantage for the isolation of *Echinococcus* genomic DNA without contamination, or preparation of primary cells through trypsinization. These primary cells are rich in stem cells and useful for the stem cell research. These primary cells can be kept for longer period with conditioned medium, and they also can regenerate new vesicles in several weeks (Spiliotis and Brehm, 2009).

Even though it is possible to regenerate new vesicles from, the amount is by far smaller than the original vesicles. To maintain production of large amount of metacestode vesicles,

the passage in laboratory rodents is necessary. With this serial passage, strains can be maintained for decades (Spiliotis and Brehm, 2009). The method of serial passage will be described in 4.6.1. As for the laboratory animals, Mongolian gerbils (*Meriones unguiculatus*) are used in AG Brehm, because they are highly permissible hosts (Spiliotis and Brehm, 2009).

Because the current chemotherapy does not have parasitocidal effect, there is demand for the development of new drugs. After the establishment of stable cultivation method like above, researchers began to consider medium-throughput *in vitro* screening methods to identify lead compounds of new drug efficiently. One of such screening methods is PGI assay established by AG Hemphil in Bern university. This method evaluate structural damage on the vesicles, through the leakage of phosphoglucose isomerase (PGI) into the medium, because hydatid fluid includes plenty of PGI (Stadelmann et al., 2010). This method successfully screened 426 FDA- approved compounds (Stadelmann et al., 2014), but, there is also disadvantage. This method consumes a lot of metacestode vesicles of specific size and age, and preparation for the screening can cost a lot and can be time-consuming. It also cannot identify slow-acting drugs such as ABZ.

3.2 Protein kinases

3.2.1 Function and regulation of protein kinases

Protein kinases are enzymes which catalyzes the transfer of gamma-phosphate groups of high-energy ATP/GTP to free hydroxyl groups on substrate proteins. Most eukaryotic protein kinases phosphorylate hydroxyl groups on serine/threonine, or tyrosine residues (Fabbro et al., 2015). However, there are protein kinases called dual specificity kinases which can target all these three (Dhanasekaran and Premkumar Reddy, 1998). Protein kinases

regulate target proteins through activation and inactivation, together with phosphatases which remove phosphate groups.

These kinds of activation/inactivation play key roles in most of inter and intracellular signal transduction pathway in eukaryotic cells and many other cellular process, such as gene expression, cell cycle progression, or the rearrangement of cytoskeleton (Manning et al., 2002). Mutations in protein kinases can result in abnormal signal transduction and eventually can cause serious diseases including various kind of cancers (Maurer et al., 2011).

Protein kinases of parasitic helminths are considered to be interesting from both biological and clinical points of view (Vicogne et al., 2004) for three reasons. First, a lot of scientific and clinical resources have been invested for the research of kinases because of the importance for the biology of cancers. Plenty of inhibitors against various kinases have been synthesized and are commercially available. Some of them are already used in hospitals or proceeded to clinical trials, and a lot of clinical data have been accumulated. Furthermore, data of 3D structure of human kinases and interacting compounds are also deposited in databases (Brooijmans et al., 2010). Second, these scientific resources also can be used for the research of kinases from non-model organisms, because the functions of protein kinases proved to be conserved among metazoans (Canduri et al., 2007), through the biological research of various organisms. Third, because of their function, all protein kinases have ATP binding pockets, which can be optimal targets of small molecule compounds like ATP competitive inhibitors (Bode and Dong, 2009).

3.2.2 Major groups of protein kinases

Most protein kinases in human genome can be categorized into 7 major groups, based on the similarities in catalytic and accessory domains. The major groups are CKI (casein kinase I), CAMK (calcium/calmodulin-dependent protein kinase), AGC (PKA+PKC+PKG),

TK(Tyrosine kinases), TKL (Tyrosine kinase-like), CMGC (CDKs+MAPKs+GSKs+CDC-like) and STE (Homologous of yeast Sterile 7/11/20 kinases) (Kanev et al., 2019). Each group includes multiple families. Notably, kinases in these 7 categories are also expressed in *E. multilocularis* and some of them already have been intensively studied (Cheng et al., 2017; Cheng et al., 2020; Förster et al., 2018; Gelmedin et al., 2008; Hemer and Brehm, 2012; Hemer et al., 2014; Montagne et al., 2019; Spiliotis et al., 2006; Stoll et al., 2021; Tsai et al., 2013).

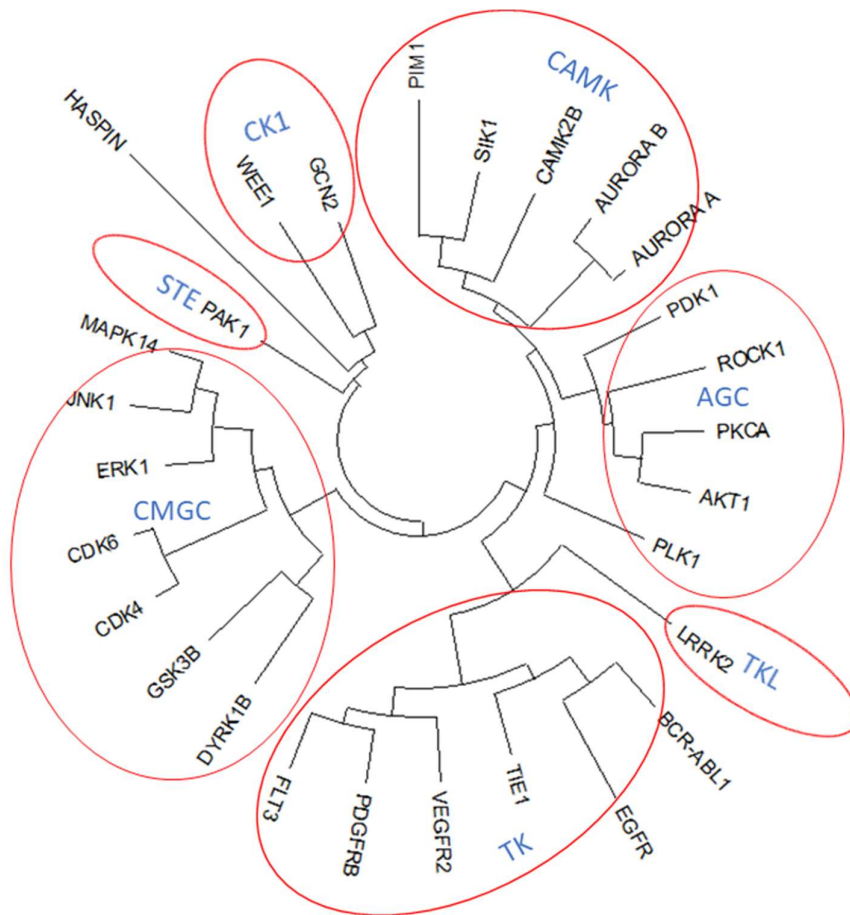


Figure 4: Phylogenetic tree of human kinase

Phylogenetic tree of human kinases was generated based on the alignment of kinase domain. 7 major groups of human kinome are shown. Amino acid sequences were gained from UniProt and kinase domains were detected with SMART. The alignment was made with ClustalW. The statistical method for the tree was maximum likelihood. The alignment and tree were processed and visualized with MEGA11.

3.2.2 Function of PIM kinases and CDC25 phosphatases

The proto-oncogene threonine threonine kinase PIM (proviral integration site for Moloney murine leukemia virus) constitute one family of CaMK (Ca²⁺/Calmodulin-dependent protein kinase-related) group. In the human genome, three PIM kinases homologues are encoded, Pim1, Pim2 and Pim3. PIM kinases are involved in various functions including transcriptional regulation, cell cycle progression and apoptosis. Especially, a lot of substrates of PIM kinases play important roles in cell cycle progression. All three PIM kinases are oncoproteins which are overexpressed in several cancers such as prostate cancer (Chen et al., 2005), myeloma (Cheng et al.; Nair et al., 2017), leukemia (Chen et al., 2009; Lin et al., 2010), non-Hodgkin lymphoma (Cohen et al., 2004) and breast cancer (Brasó-Maristany et al., 2016; Horiuchi et al., 2016).

There is one conspicuous characteristic in the structure of human PIM kinases. Both N terminal and C terminal amino acid sequences outside of the kinase domain are relatively short, and do not have any regulatory domains. Most of the kinases and phosphatases activate and inactivate one another, through phosphorylation and dephosphorylation (Johnson and Noble, 1996), but PIM kinases are believed to be constitutively active (Qian et al., 2005). They are only regulated by transcription, translation and proteasomal degradation (Amaravadi and Thompson, 2005).

In most of the period in the cell cycle, CDK1=CDC2 (cyclin dependent kinase 1=cyclin dependent kinase 2) is inactivated by WEE1 and MYT1 (Membrane-associated tyrosine- and threonine-specific cdc2-inhibitory kinase) through inhibitory phosphorylation at T14 and Y15 (Chow et al., 2011). CDC25C is also kept inactivated by C-TAK1 (Cdc twentyfive associated kinase1). Before G2-M transition, PIM1 activates CDC25C and inactivates C-TAK1 through phosphorylation (Bachmann et al., 2006). Activated CDC25C removes phosphate groups of CDK1 at T14 and Y15. By the activated complex of cyclin B and CDK1, the cell cycle is

Introduction

driven from G2 phase to M phase (Bachmann *et al.*, 2006). Similarly, CDK2 and CDK4 are kept inactivated in most of the cell cycle through phosphorylation. Before G1-S transition, PIM1 activates CDC25A (Mochizuki *et al.*, 1999), and activated CDC25A removes phosphate groups on T14/Y15 of CDK2 and Y17 of CDK4. The cell cycle is driven from G1 to S phase by the activated complex of cyclinE-CDK2 and cyclinD-CDK4 (Donzelli and Draetta, 2003).

Other than cell cycle progression, kinases of PIM family have several functions. For example, PIM1 and PIM3 inactivate BAD and regulate apoptosis negatively. PIM1 and CDC25A also impede apoptosis through the inactivation of ASK1 (Gu *et al.*, 2009; Shen and Huang, 2012). All 3 PIM kinases promote transcriptional activity and nuclear localization of Notch1 through phosphorylation at S2152 (Santio *et al.*).

SGI-1776 is an ATP competitive pan-Pim inhibitor, but it also inhibits FLT-3 and HASPIN (Chen *et al.*, 2009). As an anticancer drug for non-Hodgkin's lymphoma, prostate cancer and leukemia, SGI-1776 proceeded to clinical trial phase I but it had discontinued in 2010, because QTc prolongation was observed as a side effect.

CX-6258 is another ATP competitive pan-Pim kinase inhibitor (Haddach *et al.*, 2012). It also has effect on FLT3 (Bogusz *et al.*, 2017) and HASPIN (Melms *et al.*, 2020).

3.3 Benzimidazoles

3.3.1 Structure and utility of benzimidazole

Derivatives of benzimidazoles (BZ) such as albendazole (ABZ) are widely used anthelmintics, which specifically target β -tubulin component of the cytoskeleton (Gull et al., 1987; Robinson et al., 2004). Benzimidazole is a bicyclic compound which is literally a fusion of benzene and imidazole. The position number on the molecule is shown in Fig.5. Various derivatives of benzimidazoles have been developed, mainly by the modification of position 1,2,and 6.

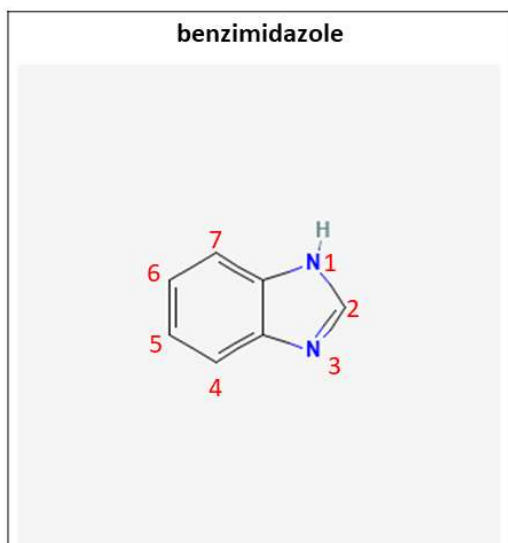


Figure 5: 2D Structure of benzimidazole

The 2D structure was downloaded from PubChem. Red number indicates the position on the molecule.

Their utility as anthelmintics relies on more intense binding to helminth β -tubulins than to those of mammals, although both molecules are up to >75% identical on the amino acid sequence level.

3.3.2 Albendazole

The standard chemotherapy for human echinococcosis is albendazole (ABZ). Since the beginning of 1980s, ABZ has been used for the medication against human Echinococcosis (Morris et al., 1983). ABZ is metabolized into albendazole-sulfoxide (ABZSX), and both ABZ and ABZSX have effect on parasites.

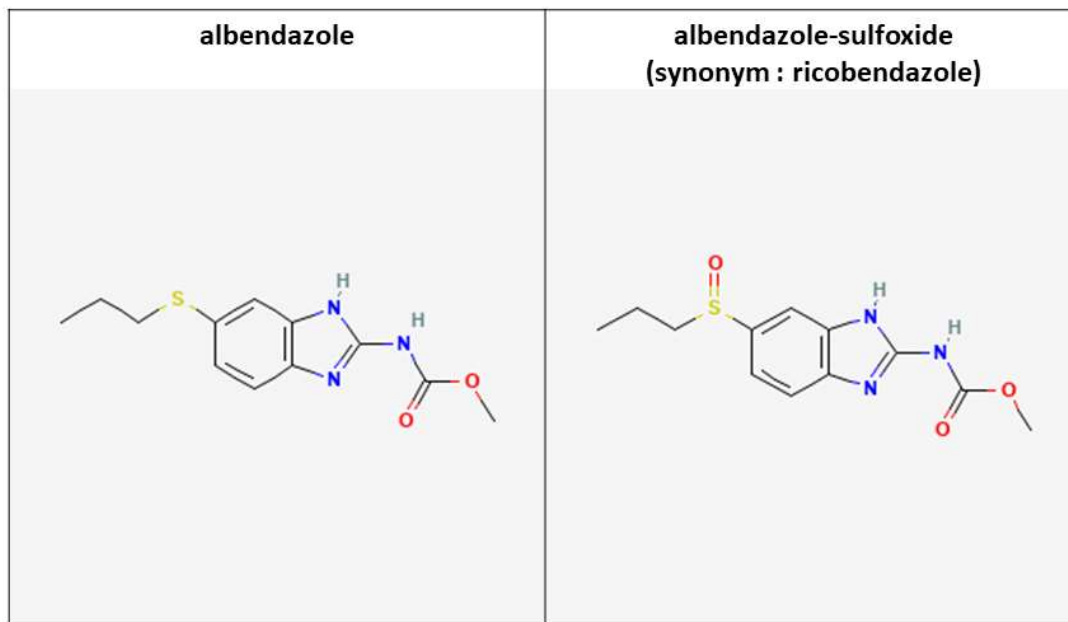


Figure 6: 2D Structure of ABZ and ABZSX sulfoxide

The 2D structure was downloaded from PubChem.

Other than surgery ABZ is currently the only available treatment for AE, but it accompanies side effects. Different from praziquantel for adult worms, ABZ does not have parasitocidal effect. It only has parasitostatic effect (Ingold et al., 1999; Reuter et al., 2010). Therefore, ABZ should be taken continuously for very long period. Because of the adverse side effect above, the burden of continuous medication is not negligible for patients. In some cases, withdrawal of the drug is necessary because of severe side effects, but it can result in relapse. Therefore, new, selective, and parasitocidal drugs are necessary.

3.3.3 Triclabendazole

Triclabendazole (TCBZ) is another derivative of benzimidazole. It is approved for chemotherapy against fascioliasis by liver fluke *Fasciola hepatica* / *Fasciola gigantica* and paragonimiasis by lung fluke *Paragonimus sp* (Boray et al., 1983; Keiser et al., 2005). The same as ABZ, TCBZ is metabolized into triclabendazole-sulfoxide (TCBZSX) and both TCBZ and TCBZSX have activity against parasites. It includes chloride atoms and thiomethyl group, but it does not have a carbamate moiety. These characteristics clearly distinguish TCBZ from classical BZ derivatives.

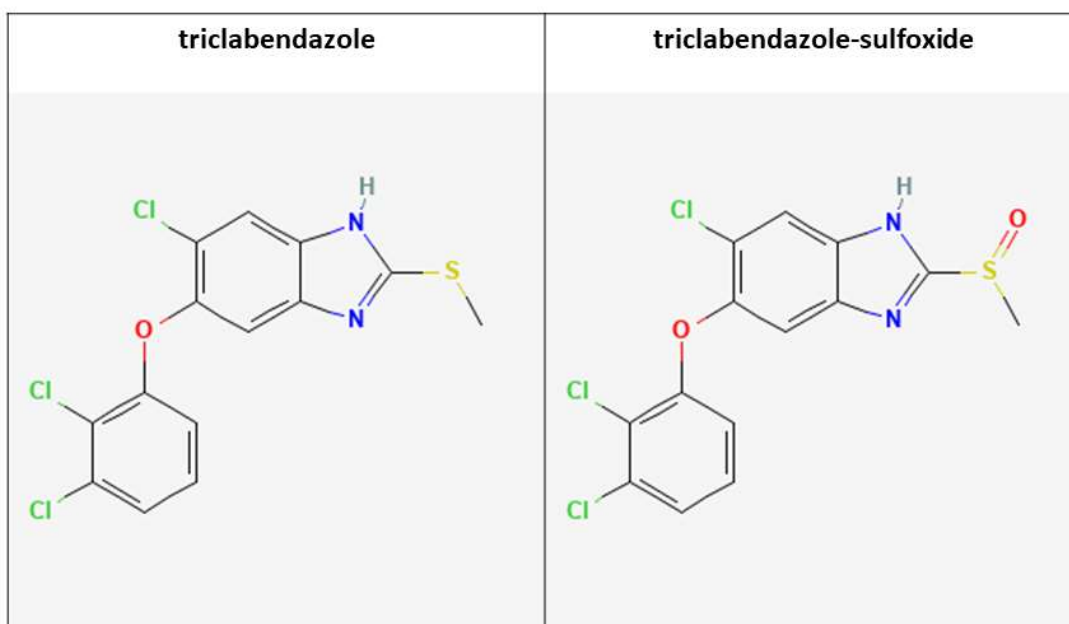


Figure 7: 2D Structure of TCBZ and TCBZSX

The 2D structure was downloaded from PubChem.

Continuous medication is usually not required for human fascioliasis. In most cases, eggs in feces disappeared in 12 hours after taking tablets. TCBZ works on every stage, but ABZ only works on adults (Alvarez et al., 2009; Fairweather and Boray, 1999).

TCBZ is also approved for livestock. In the randomized blinded trial in Cote d'Ivoire, eggs disappeared from 95% of cattle in 28 days after treatment with single dose of TCBZ. In contrast, eggs disappeared from 70% of cattle which were treated with ABZ (Kouadio et al., 2021). This result indicates that juvenile worms survived ABZ treatment, but they could not survive TCBZ treatment. This does not contradict to the cases of human fascioliasis.

3.4 Colchicine binding site inhibitors

3.4.1 Colchicine

Colchicine is originally an alkaloid found in the seeds and bulbs of *Colchicum autumnale*, a plant in order Liliales. The same as BZs, it inhibit polymerization of tubulins. It is highly toxic and known to cause cell cycle arrest (Bischoff and Holtzer, 1968). Because it interferes cell cycle, it is used for the analysis of chromosomal karyotype (Rishi and Rishi, 1979) and development of breed improvement of plants such as polyploid watermelons (Zhang et al., 2019).

As for clinical use, colchicine have anti-inflammatory effect because it can supresses neutrophils (Dalbeth et al., 2014). It was once used as a remedy for gout (Talbot, 1978). However, steroids or NSAIDS are preferred now because of its narrower therapeutic index (van Durme et al., 2021).

Former member of our laboratory once tried colchicine on *E. multilocularis*. In that experiment, the transport of glycoconjugates from tegument cell body to the tegumental distal syncytium, which is also microtubule-dependent, was inhibited by colchicine treatment (Koziol, personal communication).

3.4.2 Combretastatin

Combretastatin A-4 is originally isolated from plants of *Combretum caffrum*, a species of bushwillow in Africa. It also inhibits polymerization of tubulins by binding to colchicine-binding site (Chaudhuri et al., 2000). A lot of derivatives have been developed, mainly as prodrugs against cancers (Sekar et al., 2022). Combretastatin A-4 phosphate affects cytoskeleton of immature endothelial cells in tumor vascular system by binding to microtubules. It also induces cell death through apoptosis and/or mitotic catastrophe pathways (Jaroch et al., 2016). As vascular disrupting agent (VDA), it is expected to be used in combination with other chemotherapy and radiotherapy (Siemann et al., 2009).

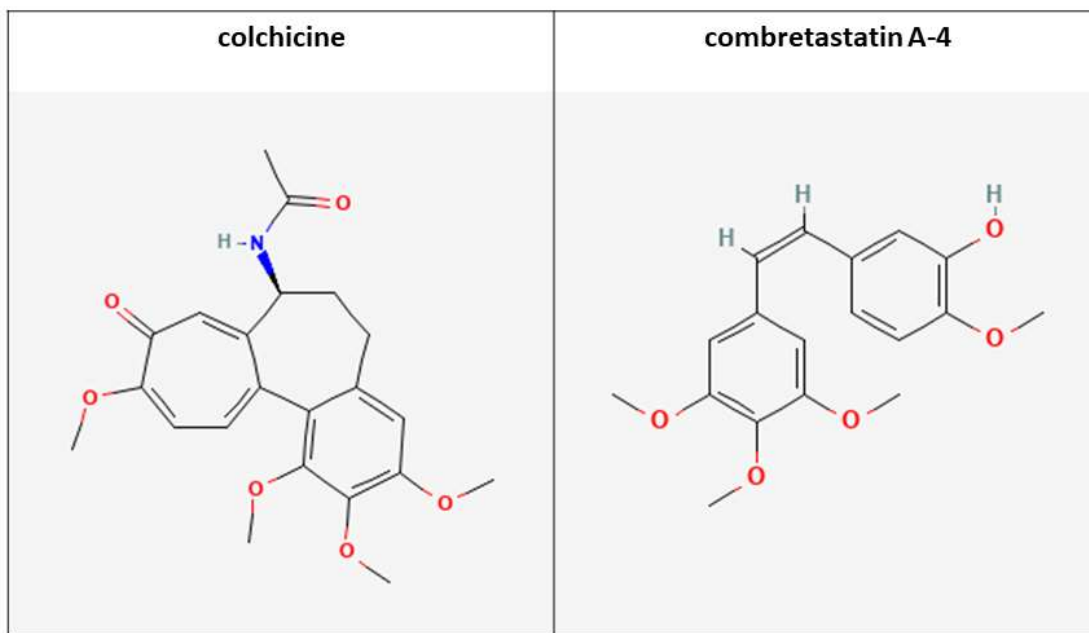


Figure 8: 2D Structure of colchicine and combretastatin A-4

The 2D structures were downloaded from PubChem.

3.4.3 Derivatives of colchicine binding site inhibitors for flavivirus infection

Family Fraviviridae includes pathogens of important vector-borne diseases such as dengue, Zika and West Nile. Recent studies proved that microtubules and cytoskeleton are involved in the mechanism of flavivirus replication cycles (Foo and Chee, 2015). In the case of dengue, microtubules play important role for the intracellular transport of viral particles (Greber, 2002) , and tubulin expression was elevated in the patients of dengue hemorrhagic fever (Thayan et al., 2009). There are plenty of inhibitors of tubulin polymerization including colchicine, combretastatin and BZs, but either of them has some adverse side effect and it is difficult to use them for these viral infections. Therefore, Klein laboratory members in Heidelberg university focused on human carboxylesterase (hCE1). They synthesized derivatives of colchicine and combretastatin, which have moieties of cyclopentyl esters with phenylglycine or leucine (Needham et al., 2011). Cyclopentyl ester moieties is hydrolyzed by hCE1 and form cyclopentanol and the corresponding carboxylate. The toxicity of these prodrugs with additional moieties should have been weakened for most of cell types. However, in the preferential targets of flavivirus, such as lineages of monocyte and hepatocytes (Blackley et al., 2007; Martina et al., 2009), hCE1 is highly expressed (Hosokawa, 2008; Macaev et al., 2013), and the prodrugs are converted into active forms by hydrolysis of moieties. In the experiment of Klein laboratory, analogues with leucin-based moieties were successfully cleaved by hCE1, but those with phenylglycine-based moieties remained to be uncleaved. In the viral replication assay, the parental compounds colchicine and combretastatin showed the strongest activity, but some of analogues such as VB-033 and VB-087 (supplement list 8.3) showed relatively good activity, even though their toxicities against HeLa and Huh-7 were much lower than parental compounds. (Richter et al., 2019).

3.5 Tubulins

3.5.1 Tubulin families and their function

Members of tubulin families provide the backbone of many cellular substructures including mitotic and meiotic spindles, cytoskeletal network and axonemes of cilia and flagella (Findeisen et al., 2014). Especially, α -tubulin and β -tubulin form heterodimer and the heterodimers form microtubuli. When BZs attach to β -tubulins, the conformation of domains are changed and dimerization with α -tubulins will be inhibited (Robinson *et al.*, 2004). On the other hand, colchicine-binding domains spans both α -tubulin and β -tubulin, and colchicine binding site inhibitors inhibits polymerization of the heterodimer (Massarotti et al., 2012).

3.5.2 Residues in β -tubulin corelated with benzimidazole resistance

Because benzimidazoles are widely used for fungi, helminth, or some other pests, a lot of resistant strain appeared. The mutant strains of *Haemonchus contortus*, a nematode which causes displaced abomasum in ruminants, have been studied in detail. Resistant strain with conserved mutation F200Y in HcTubB1 (Kwa et al., 1994), and other resistant strains with F200Y in HcTubB2 were reported independently (Prichard, 2001). Also in fungi, multiple resistant strains of *Aspergillus nidulans* with mutation in benA (β -tubulin) have been found. 2 out of 18 have F200Y mutation, 4 out of 18 strains have another mutation E198A and 12 out of 18 strains have H6Y or H6L mutation (Jung et al., 1992).

In addition, A165V mutation of benA makes *Aspergillus nidulans* supersensitive to carbendazim, nocodazole and benomyl, but resistant to thiabendazole (Jung and Oakley, 1990). The difference between carbendazim and thiabendazole is only position 2 carbon, and this indicated that the 165th residue interact with position 2 carbon of benzimidazole.

Introduction

Saccharomyces cerevisiae with mutation F167Y in tub-2 (β -tubulin) are 3-4 folds resistant to carbendazim and nocodazole, but 8 folds more susceptible to benomyl. The difference between benomyl and carbendazim is position 1 carbon, and this experiment indicated that the 167th residue interact with position 1 carbon of BZs (Li et al., 1996). On the other hand, benomyl-resistant *Neurospora crassa* had F167Y mutation (Orbach et al., 1986). These results look contradicting because the same mutation in two different species had opposite effect on the resistance to benomyl. However, both examples support the importance of 167th residue for the interaction with BZs.

Robinson et. al. positioned ABZSX manually around BZ resistance-correlated positions of *H. contortus*'s β -tubulin model. 6th, 165th, 167th, 198th, 200th residues appeared in the examples above, form a cluster within a small volume of molecular structure in the model (Robinson *et al.*, 2004).

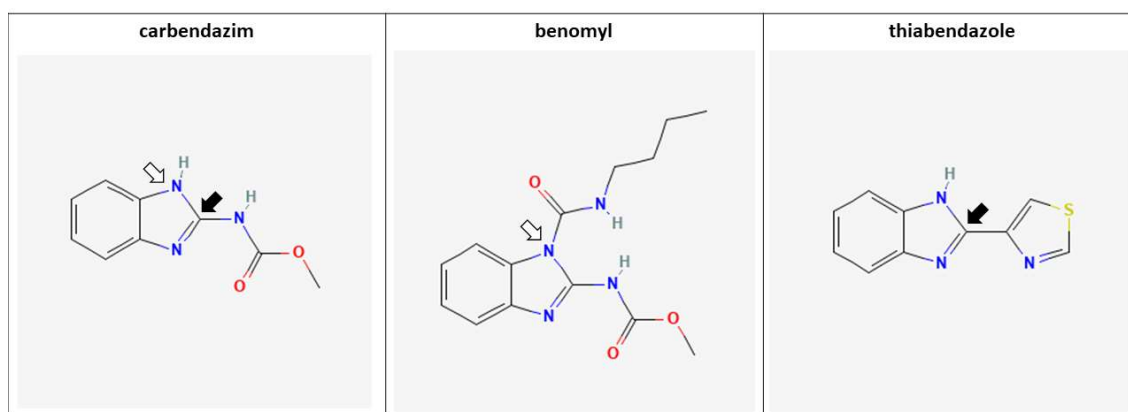


Figure 9: 2D structure of carbendazim, benomyl and thiabendazole

2D structure was downloaded from PubChem. The white arrow indicate position 1 and black arrow indicates position 2.

3.5.3 β -tubulins of *Homo sapiens*

There are 9 different β -tubulins encoded in human genome. 8 out of 9 isotypes have Tyr200 or Ala198, which are correlated with resistance against BZs. Only HsTubB8, does not have any residues associated with resistance. In fact, in the experiment by Garge et al, HsTubB8 is proved to be more susceptible to thiabendazole than the control HsTubB4. (Garge et al., 2021)

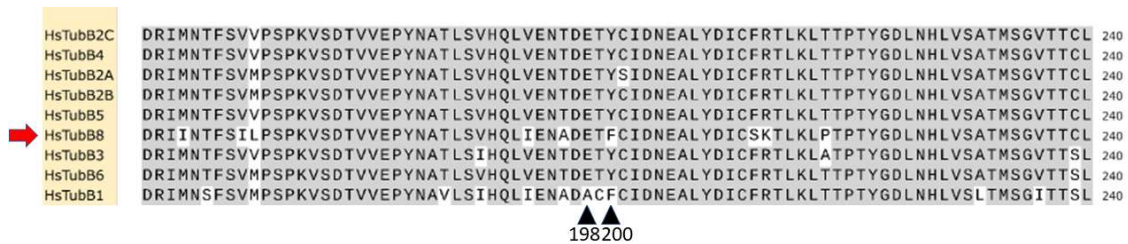


Figure 10: Alignment of human β -tubulin and amino acid of human β -tubulins
 All β -tubulins encoded in human genome were aligned with ClustalW . Grey highlights indicate consensus . Black arrowheads indicate positions correlated to BZ resistance . Red arrow indicates HsTubB8, which is susceptible to thiabendazole.

3.5.4 β -tubulins of *E. multilocularis*

In the genome of *Echinococcus multilocularis*, there are ten β -tubulins encoding genes (Tsai et al., 2013). Three out of ten are identified and named as tub-1, tub-2 and tub-3 (Brehm et al., 2000), but in this dissertation, we call them EmTubB1, EmTubB2 and EmTubB3, to distinguish them from tubulins of other organisms. Results of several experiments and analyses below strongly suggest that EmTubB2 is expressed specifically in stem cells.

Introduction

1. EmTubB2 shows the strongest expression throughout the life cycle (Koziol and Brehm, 2015; Tsai *et al.*, 2013).
2. EmTubB2 transcripts peak in primary cell culture day 2 of cultivation, when the percentage of stem cells is especially high (Koziol and Brehm, 2015; Tsai *et al.*, 2013).
3. When metacestode vesicles treated with HU or Bi2536 to eliminate stem cell compartment specifically, the expression level of EmTubB2 dropped. Such patterns were not observed with EmTubB1 or EmTubB3 (Brehm, personal communication).
4. When metacestode vesicles were stained with EmTubB2-specific antibody and *in situ* hybridization probe of EmTRIM, almost 100% signals from EmTubB2 and EmTRIM were co-localized (Brehm, personal communication). EmTRIM is a cell-cycle independent marker of stem cells (Koziol et al., 2015).

EmTubB2 has Tyr200 but EmTubB1/EmTubB3 have Phe200. (Koziol and Brehm, 2015). Later the importance of Tyr167 of EmTubB2 were also discussed. From the sequence, we can expect that EmTubB2 is likely to be more resistant against ABZ than EmTubB1/EmTubB3.

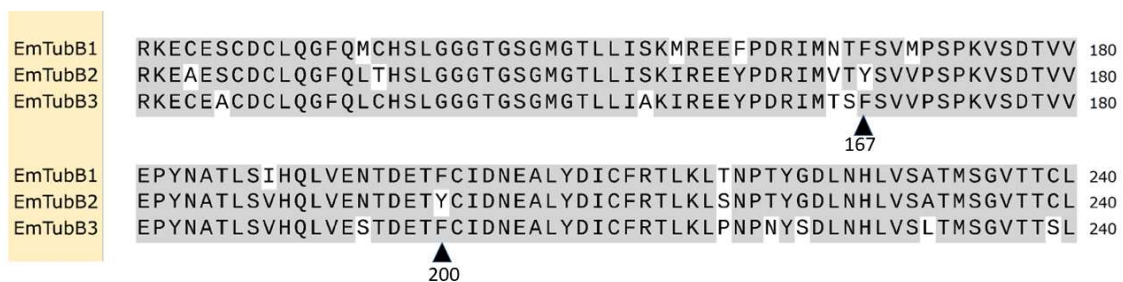


Figure 11: Alignment of β -tubulins of *E. multilocularis* and amino acid residues correlated with resistance

3 β -tubulins strongly expressed in metacestode vesicles of *E. multilocularis* were aligned with ClustalW. Grey highlights indicate consensus. Black arrowheads indicate positions correlated to BZ resistance.

3.5.5 β -tubulins of *Fasciola hepatica*

The common liver fluke *Fasciola hepatica* expresses 6 β -tubulins in the adult stage.

FhTubB1-3 have Tyr200, FhTubB5 has Leu200 and FhTubB4/6 have Phe200.

The expression level of FhTubB1 is the strongest among 6 β -tubulins in adult worms, and its expression is also specific to the adult. Therefore, Fuchs et al. discussed that FhTubB1 is likely to be expressed in reproductive organs (Fuchs et al., 2013). In fact, single cell RNA seq data indicate specific expression of FhTubB1 in the testes (Häberlein, personal communication).

Especially in 4 weeks old migrating juveniles in definitive hosts, only 3 β -tubulins, FhTubB2, FhTubB3 and FhTubB4 are expressed (Fuchs *et al.*, 2013). Because ABZ does not work on juveniles (Alvarez *et al.*, 2009; Fairweather and Boray, 1999; Kouadio *et al.*, 2021), these three isotypes are expected to have lower affinities with ABZ. However, in the experiment of affinity purification, ABZ has affinity with FhTubB2 and this isotype is likely to be the target of ABZ (Chambers et al., 2010). FhTubB2 has Tyr200, which is correlated with ABZ-resistance (Jung *et al.*, 1992; Prichard, 2001). This result of the affinity purification looks contradicting from the sequence information and ABZ resistance.



Figure 12: Alignment of β -tubulin of *F. hepatica* and amino acid residue correlated with resistance 6 β -tubulins expressed in adult stage of *F. hepatica* were aligned with ClustalW. Grey highlights indicate consensus. Black arrowheads indicate positions correlated to BZ resistance.

TCBZ-resistance *Fasciola hepatica* was found in Australia in 1995 (Overend and Bowen, 1995). Since then, a lot of worms with resistance have been found in cattle, sheep and human in Europe, South America and Australia (Fairweather et al., 2020). There are many hypotheses how they acquire drug resistance. Some people suspected that mutations of β -tubulin weakened the interaction between the drug and the target tubulins. However, no difference in the amino acid sequence or expression level of β -tubulins between resistant strains and susceptible strains has been found (Fuchs *et al.*, 2013; Robinson et al., 2002).

3.5.6 Colchicine binding site

Colchicine binds to non-polymerized tubulin subunits. Different from BZs, its binding site spans both α -tubulin and β -tubulin and generally called colchicine binding site. Massarotti et al. identified three zones of colchicine binding site on α/β -tubulins. Zone 1 is located at the α/β subunit interface. Zone 2 and zone 3 are located at the β -subunit but zone 3 is buried deeper in the subunit (Massarotti *et al.*, 2012).

Massarotti et al. used crystal structures of mammalian tubulin for his models, but Ranjan et al. applied these zones to *Haemonchus contortus*'s β -tubulin. According to his analysis, ABZ and ABZSX interact with zone 3, but TCBZ interact with zone 2 (Ranjan et al., 2017). In Fig.13, green arrowheads (zone 3 in Ranjan's model) overlap black arrowheads (ABZSX binding site in Robinson's model).

Introduction

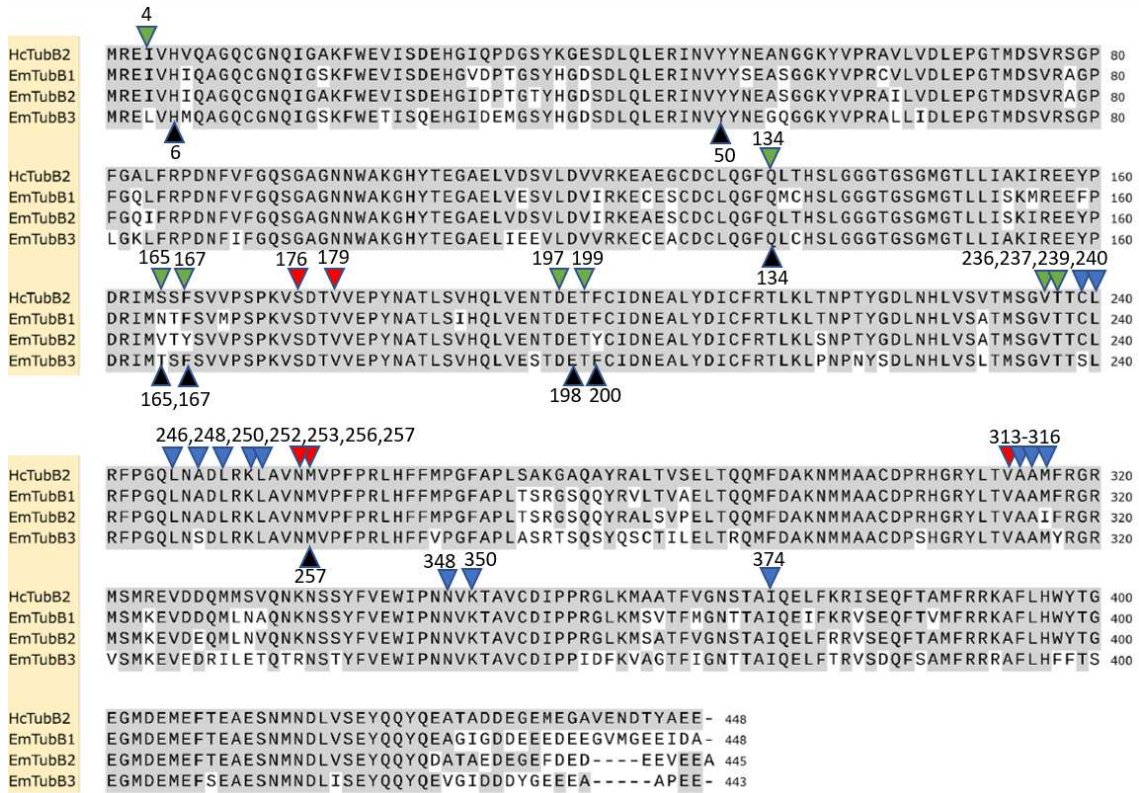


Figure 13: Comparison of Robinson's model and Ranjan's model

3 β -tubulins from *E. multilocularis* and 1 β -tubulin from *H. contortus* were aligned with ClustalW. Grey highlights indicate residues identical to HcTubB2. Black arrowheads indicate residues which from ABXSX binding site in the model of Robinson et al (2004). Red, blue and green arrowheads indicate residues which form zone 1, zone 2 and zone 3 respectively in the model of Ranjan et al. (2017).

In fact, colchicine and several BZs are known to be competitive each other. When tubulin homogenates from *Fasciola hepatica* are treated *in vitro* with ABZ first, the binding efficiency of colchicine was lowered. On the other hand, the binding efficiency of colchicine was not lowered by TCBZ (Fetterer, 1986; Robinson et al., 2001). This does not contradict to the analysis with Ranjan's model.

3.6 Purpose of this research

Current chemotherapy against AE depends on ABZ, but ABZ has two problems. It works only parasitostatically and it accompanies adverse side effects. The fundamental purpose of this research is, finding new compounds which can overcome these problems. More specific questions are,

- How can we perform screening of compounds more efficiently?
- How can we identify and evaluate compounds with selective toxicity?
- How can we identify and evaluate compounds with parasitocidal effect?

4 Materials and methods

4.1 Ethical statement

In vivo propagation of parasite material was performed in Mongolian jirds (*Meriones unguiculatus*), which were raised and housed at the local animal facility of the Institute of Hygiene and Microbiology, University of Würzburg. This study was performed in strict accordance with German (*Deutsches Tierschutzgesetz, TierSchG*, version from Dec-9-2010) and European (European directive 2010/63/EU) regulations on the protection of animals. The protocol was approved by the Ethics Committee of the Government of Lower Franconia (Regierung von Unterfranken) under permit numbers 55.2–2531.01-61/13 and 55.2.2-2532-2-1479-8.

4.2 Equipment and devices

| Usage | Product name | Manufacturer |
|---|------------------------|----------------|
| Transilluminator | TFX 35M | VILBER LOURMAT |
| Analytical balance | ABT 120-50M | KERN |
| Benchtop centrifuge | Mikro 200 | Hettich |
| Benchtop centrifuge (angle) | ROTINA 380R | Hettich |
| Benchtop centrifuge (plates) | Megafuge 1.0R | Heraus |
| Benchtop centrifuge (swing) | Bactifuge | Heraeus CHRIST |
| Biological Safety Cabinet for <i>Echinococcus</i> | Nu-437-400E | NUARE |
| Biological Safety Cabinet for yeast | MSC-ADVANTAGE | Thermo |
| Cell density meter | CO8000 | WPA |
| Colony Counter | ProtoCOLSR | SYMBIOSYS |
| Confocal microscope | Eclipse Ti2E | Nikon |
| Confocal Scanner Unit | CSU-W1 | Yokogawa |
| constant temperature dryer | FD240 | Binder |
| DC power supply | Power Pack P25 T | Biometra |
| DC power supply | El. Phor Powerpack P24 | Biometra |
| Deep freezer | minus 86 ULT Freezer | Thermo Forma |
| Electrophoresis chamber | Agagel Standard | Biometra |

Materials and methods

| Usage | Product name | Manufacturer |
|---|---|-----------------------------|
| Freezer | GS5216 | LIEBHERR |
| Heat Block | 50126101 | Liebisch |
| Heat Block | DB-3 | Techne |
| Haemocytometer | Neubauer precicolor depth 0.1mm, 0.0025mm ² | Neubauer Hemocytometry |
| Imaging System | ChemiDoc™ MP | Bio-Rad |
| Incubator for <i>E. coli</i> | kelvitron@t | Heraeus instruments |
| Incubator for Echinococcus/mammalian | Cell240 | HERA |
| Incubator for Echinococcus/mammalian | INC0246med | Memmert |
| Incubator for Echinococcus/mammalian | DHD AUTOFLOW | NUARE |
| Incubator for yeast | kelvitron@t | Heraeus |
| Laser Unit | LightHub+ | Omicron |
| Lateral shaker at cold room | DE24 | DESAGA |
| Lateral shaker at room temperature | KL2 | Edmund Buehler GmbH |
| Light microscope | Eclipse Ts2 | Nikon |
| Microcentrifuge | C1301B-230V | Labnet international |
| Microwave | MWS 1820 Duo | Bauknecht |
| pH meter | Lab850 | SCHOTT Instrument |
| Pipetman 0.5-10µl | Pipette 0.5-10µl | Eppendorf |
| Pipetman 100-1000µl | Pipette 100-1000µl | Eppendorf |
| Pipetman 10-100µl | Pipette 10-100µl | Eppendorf |
| Refrigerator | profil line | LIEBHERR |
| Shaking incubator for <i>E. coli</i> | TH30(shaker)+SH30(Heater) | Edmund Buehler GmbH |
| Shaking incubator for yeast | G24 | New Brunswick Scientific |
| Thermal Cycler | T1 Thermocycler | Biometra |
| Thermal Cycler | T Gradient | Biometra |
| Thermomixer | 5436 | Eppendorf |
| Vacuum pump | | ILMVAC |
| Voltex | HY-210/1 | Heidolph |
| Water bath | WB7 | Memmert |

Table 1

4.3 Chemicals and reagents

4.3.1 Commercially available kinase inhibitors

List 1

| Kinase inhibitor | Provider |
|------------------|-------------|
| GENE-0877 | Selleckchem |
| FRAX597 | Tocris |
| AZ-191 | Selleckchem |
| CHIR-99021 | Tocris |
| Dasatinib | Selleckchem |
| Tanzisertib | Selleckchem |
| Advosertib | Selleckchem |
| KN-62 | Selleckchem |
| SGL-1776 | Selleckchem |
| Tozasertib | Selleckchem |
| BX-912 | Selleckchem |
| Sotrastaurin | Selleckchem |
| Y-27632 | Selleckchem |
| Cabozantinib | Selleckchem |

Table 2

List2

| Kinase inhibitor | Provider |
|------------------|---------------|
| CHIR-99021 | Selleckchem |
| Dacomitinib | abcr GmbH |
| Danuserib | abcr GmbH |
| GSK690693 | Tocris |
| Imatinib | Sigma-aldrich |
| Palbociclib | Selleckchem |
| Ponatinib | abcr GmbH |
| SGL-1776 | Selleckchem |
| Sorafenib | abcr GmbH |
| SP600125 | Selleckchem |
| Bi2536 | Axon Medchem |
| Tozasertib | Selleckchem |

Table 3

List3

| Kinase inhibitor | Provider |
|------------------|----------------------------|
| A-92 | Axon Medchem |
| AZD1208 | Selleckchem |
| Afatinib | Cayman chemical |
| CX-6258 | Cayman chemical |
| Hesperadin | Cayman chemical |
| Lapatinib | Cayman chemical |
| Nilotinib | Selleckchem |
| PIM447 | Selleckchem |
| Sunitinib | Hölzel Diagnostika Handels |
| Volasertib | Cayman chemical |
| YKL-05-099 | Hölzel Diagnostika Handels |

Table 4

4.3.2 Commercially available inhibitors of tubulin polymerization

| inhibitor of tubulin polymerization | Provider |
|-------------------------------------|----------|
| Triclabendazole | Vetrenal |
| Triclabendazole-sulfoxide | Vetrenal |
| Albendazole | Fluka |
| Albendazole-sulfoxide | Vetrenal |

Table 5

4.3.3 Kits

| Kit | Manufacturer |
|--|-----------------------|
| Nucleospin® Gel and PCR clean-up | Macherey-Nagel |
| Nucleospin® Plasmid | Macherey-Nagel |
| PureLink™ RNA Mini kit | Invitrogen |
| Superscript® IV Reverse transcriptase | Invitrogen, Darmstadt |
| CloneJet™ PCR Cloning KIT | Fermentas |
| KOD Hot Start DNA Polymerase | Toyobo |
| Click-iT® EdU Alexa Fluor® 555 Imaging Kit | Life technologies |

Table 6

4.3.4 Reagent/media for *Echinococcus*/mammalian

| Product | Manufacturer |
|--|-------------------|
| Dulbecco's Modified Eagle Medium, high glucose(4.5g/l) GlutaMAX | Life Technologies |
| Fetal Calf Serum | Invitrogen |
| L-Cystein | Sigma-Aldrich |
| Bathocuproine disulfonic acid | Sigma-Aldrich |
| β -Mercaptoethanol | Sigma-Aldrich |
| Penicillin/Streptomycin | Invitrogen |
| Trypsin/EDTA solution | Biochrom |
| Dimethyl sulfoxide | Sigma-Aldrich |

Table 7

4.3.5 Reagent/media for yeast

| Product | Manufacturer |
|--|------------------------------|
| DO supplement -Ade/-His/-Leu/-Trp | Clontech |
| DO supplement -Leu/-Trp | Clontech |
| Adenine hemisulfate | Sigma-Aldrich |
| Difco™ Yeast Nitrogen Base w/o Amino Acids | Becton Dickinson and Company |
| Yeast extract | Thermo fishers |
| Pepton | Merck |
| Glucose monohydrate | Merck |
| Ecotainer® Sterile water for irrigation | B. Braun |

Table 8

4.3.6 Reagent/media for *E. coli* and plasmid construction

| Product | Manufacturer |
|---|-------------------------------|
| CutSmart Buffer | New England Biolabs |
| XhoI | New England Biolabs |
| PspOMI | New England Biolabs |
| BamHI-HF | New England Biolabs |
| Carbencilin | Invitrogen |
| Kanamycin sulfate | Sigma-Aldrich |
| Taq polymerase | New England Biolabs |
| LB Broth mix | Beckton Dickinson and Company |
| Difco Agar | Beckton Dickinson and Company |
| Agarose, biological grade | Roth |
| Midori Green Advance | Nippon Genetics Europe |
| Gel Loading Purple | New England Biolab |
| Smart Ladder | Eurogentec |
| Ecotainer® Sterile water for irrigation | B. Braun |

Table 9

4.3.7 Reagents /antibodies for imaging analysis

| Product | Manufacturer |
|--|------------------------|
| Fluoprep | Biomerieux Nutringen |
| Formamid | Sigma-Aldrich |
| Heparin | Sigma-Aldrich |
| NHS-Fluorescein | Sigma-Aldrich |
| nuclease-free water | Qiagen |
| Paraformaldehyde | Sigma-Aldrich |
| Sheep serum | Sigma-Aldrich |
| DIG RNA labeling mix 10× | Roche |
| Protease K | Fermentus |
| RQ1 Rnase-Free Dnase | Promega |
| SP6 polymerase | New England Biolabs |
| T7 polymerase | New England Biolabs |
| Denhardt solution | Sigma-Aldrich |
| Diethyl procarbonate | Applichem |
| Anti-digoxigenin, AP conjugated | Roche |
| Anti-Digoxigenin, POD conjugated | Roche |
| Anti-Acetylated α - Tubulin, mouse antibody | Santa Cruz |
| FITC-conjugated anti mouse goat antibody | Jackson Immunoresearch |
| TRITC-conjugated phalloidin | Sigma-Aldrich |
| Torula RNA | Sigma-Aldrich |
| Triton® X-100 | Sigma-Aldrich |
| Trizol® Reagent | Invitrogen |
| Tween® 20 | Sigma-Aldrich |
| β -Mercaptoethanol | Sigma-Aldrich |
| Albumin fraction V Blotting grade | Applichem |

Table 10

4.4 Oligonucleotides

All oligonucleotides below were purchased from Merck.

4.4.1 Primers for both projects

| name of plasmid | name of primer | 5'-sequence-3' |
|-----------------|---------------------|--|
| pJet1.2 | pJet1.2-Fw | CGA CTC ACT ATA GGG AGA GCG GC |
| pJet1.2 | pJet1.2-Rev | AAG AAC ATC GAT TTT CCA TGG CAG |
| pJet1.2 | T7 Plus2 | AGA AGA GTA ATA CGA CTC ACT ATA GG |
| pJet1.2 | 5-Sp6+pJet1.2 Rev-3 | ATA ATT TAG GTG ACA CTA TAG AAC ATC GAT TTT CCA TGG CAG |

Table 11

4.4.2 Primers for kinase projects

| name of plasmid | name of primer | 5'-sequence-3' |
|--------------------|--------------------------------|--|
| pGBKT7-EmPim | pGBKT7cloning_rev | caggtcctcctcgagatcagc |
| pGBKT7-EmPim | pGBKT7cloning_fwd | ataactagcataacccttggggc |
| pGBKT7-EmPim | pGBKT7-EmPimF | ctcagaggaggacctgGCAGTCGACCATTCAAGAGAC |
| pGBKT7-EmPim | pGBKT7-EmPimR | caaggggttatgctagttatcTAAAATTTACGCGGTTTAGA GCTAC |
| pGADT7- EmCdc25 | pGADT7-EmCdc25F | ccgggtgggcatcgatacggGGAAAGGGAAATGACTATG |
| pGADT7- EmCdc25 | pGADT7-EmCdc25R | atctacgattcatctgcagcTCACGATTTACACGAAGG |
| pJet-EmPim | pJet-EmPimF | CGACCATTCAAGAGACGTGA |
| pJet-EmPim | pJet-EmPimR | CCCGAACGAACAGTAATGGA |
| pGBKT7/pGADT7 | T7 sequencing primer | TAATACGACTCACTATAGGGC |
| pGBKT7 | 3' DNA BD sequencing primer | TAAGAGTCACTTTAAAATTTGTAT |
| pGADT7 | 3' AD sequencing primer | AGATGGTGCACGATGCACAG |

Table 12

4.4.3 Primers for tubulin project

| name of plasmid | name of primer | 5'-sequence-3' |
|----------------------------|---------------------|--|
| pCMV-chimericEmTubB1 | pCMVTubB1IGVPsXhF | gctgcggaattgtaccgcgATGCGTGAAATT GTGCAC |
| pCMV-chimericEmTubB1 | EmTubB1-QQYQ_rev | ccgtggcgtcCTGGTACTGTTGGTACTC |
| pCMV-chimericEmTubB1 | SyncHsTubB2BF1 | acagtaccaggacgccacggccgacgaacaaggggagt tcgaggaggaggagggcgaggacgaggcgtaggtacc gcgcccgcggggatc |
| pCMV-chimericEmTubB2 | pCMVTubB2PsXhF | gctgcggaattgtaccgcgATGCGTGAGAT TGTCATATTC |
| pCMV-chimericEmTubB2 | EmTubB2-QQYQ_rev | ccgtggcgtcCTGATACTGCTGATACTC |
| pCMV-chimericEmTubB2 | SyncHsTubB2BF2 | gcagtatcaggacgccacggccgacgaacaagggga gttcgaggaggaggagggcgaggacgaggcgtaggg taccgcccgcgggggatc |
| pCMV- chimericEmTubB1/2 | SyncHsTubB2BR | gatccccgcccgcggtaccctacgctcgtcctcgcc ctcctcctcgaactcccctgttcgctggccgtggcgtc |
| pCMV-chimericEmTubB3 | pCMVTubB3PsXhF | gctgcggaattgtaccgcgATGCGTGAGCTT GTTTCATATG |
| pCMV-chimericEmTubB3 | EmTubB3-QQYQ_rev | ccgtggcgtcTTGATACTGCTGATATTCA CTAATC |
| pCMV-chimericEmTubB3 | HsTubB2BforEmTubB3F | gcagtatcaagacgccacggccgacgaacaagggga gttcgaggaggaggag |
| pCMV-chimericEmTubB3 | HsTubB2BDATA-rev | gatccccgcccgcggtaccctacgctcgtcctcgccc tcctcctcctgaac |
| pCMV | pCMV-Fwforseq | TGTCTTTTATTTTCAGGTCCCGGA |
| pCMV | pCMV-Fwforseq | AAAACCTCCCACACCTCCCC |

Table 13

167th or 200th amino acids are far from the beginning and the end of tubulin. Therefore, the same primer can be used both for pCMV-chimericEmTubB2wt and pCMV-chimeric EmTubB2mut.

4.5 Other consumables

| Product | Manufacturer |
|--|-------------------------------|
| TC-Plate 6well, Standard, F | SARSTADT AG & Co. KG |
| TC-Plate, 12well, Standard, F | SARSTADT AG & Co. KG |
| TC-Plate, 96 well, Standard, F | SARSTADT AG & Co. KG |
| Microplate 384 well PS F-Bottom, μ CLEAR® Black, High binding, sterile | Greiner bio one |
| Lid, PS, High Profile(9MM) clear, sterile, single packed | Greiner bio one |
| Microplate 96 well, PS, F-bottom (Chimney well), μ Clear®, Black, Med. Binding | Greiner bio one |
| EASYSTRAINER 40 μ l, for 50ml tubes | Greiner bio one |
| 0.2ml 8-Strip PCR Tube, Individually Attached Flat Caps | STARLAB international GmbH |
| Nylon membrane, positively charged | Roche |
| Safe-lock tubes 0.5ml | Epperndorf |
| Safe-lock tubes 1.0ml | Epperndorf |
| Safe-lock tubes 2.0ml | Epperndorf |
| Semi-micro cuvettes | SARSTADT AG & Co. KG |
| Sterile tubes 15ml | Greiner bio one |
| Sterile tubes 50ml | Greiner bio one |
| Disposable Syringes and canula | Braun Melsungen AG |
| Pipette tip 20 μ l | SARSTADT AG & Co. KG |
| Pipette tip 200 μ l | SARSTADT AG & Co. KG |
| Pipette tip 1000 μ l | SARSTADT AG & Co. KG |
| gel nail colour 01 glass N' ROLL | Essence |
| Microscope Cover Glasses | Deckglaeser |
| Microscope Slides | Paul Marienfeld GmbH & Co. KG |

Table 14

4.6 *In vitro* cultivation

4.6.1 *In vitro* cultivation of *E. multilocularis*

In this doctoral dissertation, parts done by someone else are shown in bold letters. In our laboratory, Dirk Radloff, a technician is doing weekly maintenance and production of metacystode vesicles.

In vitro cultivated *Echinococcus multilocularis* isolate H95 was used for the experiments of *in situ* hybridization and drug treatment on matured vesicles. In the experiments of drug treatment on primary cells, another isolate GH09 was also used. H95 was originally isolated from a naturally infected fox found in Germany (Jura et al., 1996) and GH09 was originally isolated from a captive bred crab-eating macaque (*Macaca fascicularis*) in German primate center (Göttingen, Germany) (Tappe et al., 2007). **Mongolian gerbils (*Meriones unguiculatus*) were sacrificed for *in vivo* propagation of the parasite through intraperitoneal passages as described in previous papers (Spiliotis and Brehm, 2009; Spiliotis et al., 2004). Briefly, echinococcal tissues isolated from laboratory rodents are cut into small pieces and strained with tea strainer. These tissues are washed and treated with antibiotics. After antibiotics treatment, the tissues are washed again and transferred into DMEM culture together with Reuber hepatoma. Approximately after 5 weeks continuous maintenance including exchange of medium and feeder cells, new vesicles around 3mm in diameter will be found. The same tissues after antibiotics treatment can be intraperitoneally inoculated into another laboratory rodents**

***In vitro* cultures of metacystode vesicles were maintained in aerobic condition at 37°C with 25-175cm² culture bottles. Feeder cells and medium were rat cell line Reuber-hepatoma and DMEM (Dulbecco's Modified Eagle Medium) + GlutaMAX-I (life technologies) including 10% Fetal Bovine Serum Superior (life technologies). The medium and Reuber hepatoma are exchanged weekly.**

4.6.2 *In vitro* cultivation of mammalian cells

Cryostock tubes of HEK293T (DuBridge et al., 1987) cells and HepG2 (Aden et al., 1979) cells are stored in -80°C. Several weeks before the experiments, cryostock tubes are thawed as rapidly as possible with 37°C water bath, and centrifuged shortly. The supernatant including DMSO is removed, and cell pellets are resuspended with DMEM+GlutaMAX-I+FBS. The resuspension is moved to 25cm² bottle with 10ml DMEM and incubated at 37°C until they grow semiconfluent. After they grew semiconfluent, they are subcultured and maintained with the methods of ATCC until the use of experiments.

4.6.3 *In vitro* cultivation of *Saccharomyces cerevisiae*

Saccharomyces cerevisiae Gold strain (Clontech) was kindly provided by AG Grevelding in Justus-Liebig university in Gießen. They are stored as colonies of stationary phase on YPD plates at 4°C for maximal one month. After one month, one colony is picked up and inoculated in 6ml of liquid YPD. The tube is incubated at 30°C, 200rpm for 16hours. After 16 dhours, 10 µl is diluted by 100 times with fresh YPD. 100ul of diluted culture is inoculated on a new YPD plate and the plate is incubated at 30°C for two or more days, until the diameter of colony exceeds 2mm. After the diameter exceeds 2 mm, the plate will be stored up to one month.

4.7 *In vitro* screening

4.7.1 Matured vesicle assay

In matured vesicle assay, 10 matured metacystode vesicles were treated with inhibitors in 2mL of conditioned medium (100% A6 medium, 12 well plates) under axenic condition for 21 or 28 days as described in (Gelmedin *et al.*, 2008; Hemer and Brehm, 2012; Spiliotis *et al.*, 2008). The number of structurally intact vesicles were counted under an optical microscope (Nikon eclipse Ts2-FL) with 2×Objective lens. Most of the experiments were performed with 3 biological replicates, except for the initial screening of newly synthesized compounds against EmPIM and Colchicine binding site inhibitors, because there were too many candidates and it was impossible to prepare enough vesicles for replicates. The medium and inhibitors were exchanged every 3 or 4 days. For the experiment with biological replicates, the percentages of structurally intact vesicles were statistically analyzed with one-way ANOVA with Dunnet's multiple comparison tests in Graphpad prism 9.3.1 (Graphpad software). In this analysis, all concentrations were compared with the negative control DMSO.

A6 medium was prepared by seeding 1.0×10^6 rat Reuber hepatoma cells (Spiliotis and Brehm, 2009) in 175cm² culture flask with 50mL DMEM+GlutaMAX-I including 10% FBS and incubated for 6 days under aerobic condition. The supernatant was filtrated to remove hepatocytes and used as A6 medium.

4.7.2 Vesicle formation assay

Primary cells were isolated from matured metacystode vesicles with the protocol described in (Spiliotis et al., 2010) and the density of primary cells in the resuspension in Phosphate Buffered Saline (PBS) were measured indirectly by densitometry. The definition of 1 Unit primary cells is the amount which increases the value of OD600 by 0.01. 100 Units of isolated primary cells ($\sim 1.5 \times 10^4$ cells) /well were seeded into 96 well plates with 200 μ L of conditioned medium (50% A6 medium + 50% B4 medium) for 21 days under axenic condition with nitrogen atmosphere. Three biological replicates with each three technical replicates were performed for the experiment of commercially available inhibitors. For newly synthesized compounds, three technical replicates were prepared.

The number of newly formed vesicles were counted under an optical microscope (Nikon eclipse Ts2-FL) with 2 \times Objective lens. Kruskal-Wallis test followed by Dunn's multiple comparisons test was used for statistical analysis with GraphPad Prism version 9.3.1 (Graphpad software). In this analysis, all concentrations were compared with the negative control DMSO. Half of the medium (100 μ L/well) and inhibitors were exchanged every 3 or 4 days.

B4 medium was prepared similarly as A6. The difference is, the number of Reuber hepatoma (1.0×10^7) and incubation period (4 days)

4.7.3 Cell viability assay of *E.multilocularis*

15 Units of isolated primary cells ($\sim 2.25 \times 10^3$ cells)/well were seeded into 384 well plates with 100 μ L of conditioned medium (50% A6 medium + 50% B4 medium) including each concentration of inhibitors. The plates were incubated at 37°C under axenic condition. After 3 days, cell viability was measured with cell titer glo (Promega), basically with the protocol of the manufacture, but 1% TritonX was added to the mixture of the CellTiter-Glo reagent before it is added to samples. The luminescence was measured by Spectramax iD3 Multi-mode Microplate reader (Molecular Devices). Three technical replicates are prepared for each concentration/inhibitor combination. The measured luminescence unit was normalized to that of the control (DMSO treated) of each test, and visualized as heatmaps with GraphPad Prism version 9.3.1 (Graphpad software).

4.7.4 Screening with mammalian cell lines

The toxicity of inhibitors against mammals was evaluated through the treatment on commonly used mammalian cell lines, HEK293T (DuBridge *et al.*, 1987) and HepG2 (Aden *et al.*, 1979). Semi-confluent cultured cells up to ten passages after thawing the cryostock were trypsinized and 1.0×10^3 cells were seeded into 384 well opaque-wall plates with 50 μ L of DMEM+GlutaMAX-I including 10% FBS. After 24 hours, 50 μ L of DMEM+GlutaMAX-I+FBS including 0-60 μ M inhibitors, so that final concentrations are 0-30 μ M. These plates were incubated for 3 days aerobically, and cell viability was measured with cell titer glo (Promega), with the protocol of the manufacture. The luminescence was measured by Spectramax iD3 Multi-mode Microplate reader (Molecular Devices). Three independent experiment were prepared in triplicates for both of two cell lines. The value of luminescence unit was normalized with the control DMSO of each independent experiment, as percentage

Materials and methods

of luminescence unit. One-Way-ANOVA test followed by Turkey's multiple comparison test was applied with GraphPad Prism version 9.3.1 (Graphpad software) for statistical analysis, but only comparisons between the same concentration are shown on the graph.

4.7.5 Transfection of mammalian cell line and following cell viability assay

Dr. Spiliotis, a former member of our working group, made plasmids of wildtype and mutated (Y167F+Y200F) EmTubB2. The position and sequence of mutation is shown below (Fig.14). I constructed pCMV-myc based plasmids for transient expression in mammalian cells, by using his plasmids as templates.



Figure 14: Sequence of EmTubB2wt and EmTubB2mut

DNA and amino acid sequence around 167th and 200th AA positions are shown. Sequences and the feature were visualized with SnapGene viewer. EmTubB2wt stands for wildtype EmTubB2 and EmTubB2mut stands for mutated EmTubB2. The position of 167th and the 200th residues are shown in red and blue features, respectively.

Materials and methods

EmTubB2 has high similarity with human tubulins until 430th position (QQYQDATA), but its similarity is lowered at C-terminus. C-terminus of EmTubB1 and EmTubB3 are even more different from human tubulins like the alignment below. In Fig.15, HsTubB2B is aligned with tubulins of *E. multilocularis*, because it is most abundantly expressed in HEK293T cells. Because C terminus is important for the interaction with α -tubulins, full-length tubulins from *E. multilocularis* might not be able to form dimer with human α -tubulins in HEK cells and might not be successfully integrated into microtubule (Fig.15).

| | | | |
|----------|------------------|--|-----|
| HsTubB2B | DRIMNTFSVMPSPKVS | SDTVVEPYNATLSVHQLVENTDETYCIDNEALYDICFRTLKLTTPYGDNLHLVSATMSGVTTCL | 240 |
| EmTubB1 | DRIMNTFSVMPSPKVS | SDTVVEPYNATLSIHQLVENTDETFCIDNEALYDICFRTLKLTNPYGDNLHLVSATMSGVTTCL | 240 |
| EmTubB2 | DRIMVTYSVVPSPKVS | SDTVVEPYNATLSVHQLVENTDETYCIDNEALYDICFRTLKLSNPYGDNLHLVSATMSGVTTCL | 240 |
| EmTubB3 | DRIMTSFSVVPSPKVS | SDTVVEPYNATLSVHQLVESTDETFCIDNEALYDICFRTLKLPNPYSDLNHLVSLTMSGVTTSL | 240 |
| | | | |
| HsTubB2B | RFPGQLNADLRKLA | VNMVFPFRLHFFMPGFAPLTSRGSQQYRALTVPELTQQMFDSKNMMAACDPRHGRYLTVAEIFRGR | 320 |
| EmTubB1 | RFPGQLNADLRKLA | VNMVFPFRLHFFMPGFAPLTSRGSQQYRVLTVAELTQQMFDAKNMMAACDPRHGRYLTVAAMFRGR | 320 |
| EmTubB2 | RFPGQLNADLRKLA | VNMVFPFRLHFFMPGFAPLTSRGSQQYRALSVPELTQQMFDAKNMMAACDPRHGRYLTVAEIFRGR | 320 |
| EmTubB3 | RFPGQLNSDLRKL | AVNMVFPFRLHFFVPGFAPLASRTSQSYQSCITILELTRQMFDAKNMMAACDPSHGRYLTVAAMYRGR | 320 |
| | | | |
| HsTubB2B | MSMKEVDEQMLNVQ | NKSSYFVEWIPNNVKTAVCDIPPRGLKMSATFIGNSTAIQELFKRISEQFTAMFRRKAFLHWYTG | 400 |
| EmTubB1 | MSMKEVDDQMLNA | QNKSSYFVEWIPNNVKTAVCDIPPRGLKMSVTFMGNTTAIQEIFKRVSEQFTVMFRRKAFLHWYTG | 400 |
| EmTubB2 | MSMKEVDEQMLNV | QNKSSYFVEWIPNNVKTAVCDIPPRGLKMSATFVGNSTAIQELFRRVSEQFTAMFRRKAFLHWYTG | 400 |
| EmTubB3 | VSMKEVEDRILETQ | TRNSTYFVEWIPNNVKTAVCDIPPIDFVAGTFIGNTTAIQELFTRVSDQFSAMFRRRAFLHFFTS | 400 |
| | | | |
| HsTubB2B | EGMDEMEFTEAESNM | DLVSEYQQYQDATADEQGEFEFEFEDEEA --- | 445 |
| EmTubB1 | EGMDEMEFTEAESNM | DLVSEYQQYQEAAGIGDDEEEDDEEGVMGEEIDA | 448 |
| EmTubB2 | EGMDEMEFTEAESNM | DLVSEYQQYQDATADEGEFEDEEVEEA --- | 445 |
| EmTubB3 | EGMDEMEFSEAESNM | DLISEYQQYQEVGIDDD--YGEEEAAPEE --- | 443 |

Figure 15: Comparison of HsTubB2B and 3 tubulins of *E. multilocularis*

3 β -tubulins from *E. multilocularis* and 1 human β -tubulin were aligned with ClustalW. Grey highlights indicate residues identical to that of HsTubB2B. Red rectangle indicates C terminal region which is important for the interaction with α -tubulins.

Therefore, C terminal regions of these *Echinococcus* tubulins were exchanged by that of human tubulin isotype HsTubB2B. The plasmid map of constructs and exchanged part of tubulin is shown in Fig.16. The junction and structure of plasmid is largely the same also in other constructs. QQYQ of *Echinococcus* tubulins were fused to DATA of HsTubB2B. The primer sequence and detailed method of plasmid construction is described in 4.4.3 and 4.9.

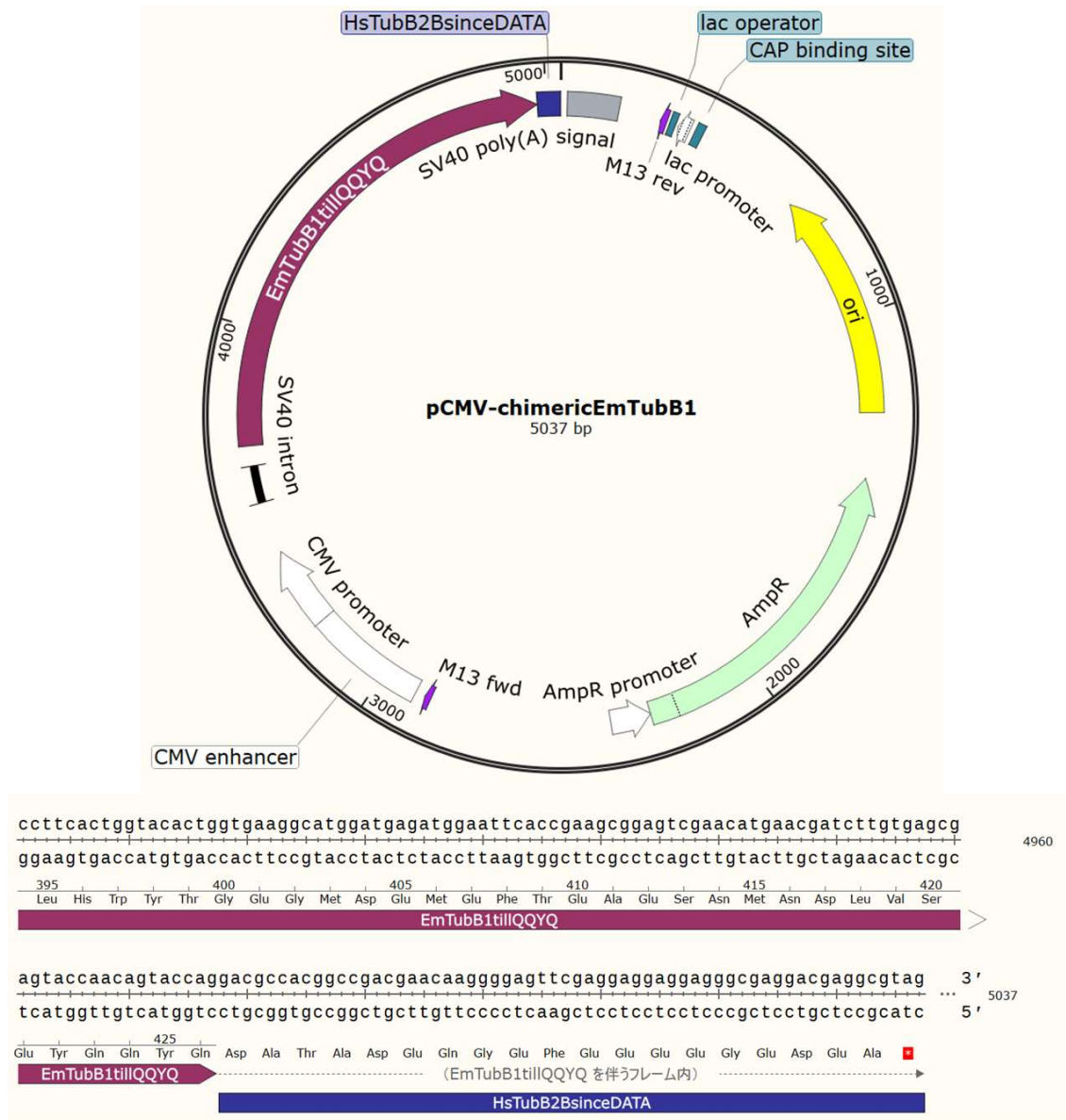


Figure 16: plasmid map and sequence of exchanged part
 Upper: plasmid map of pCMV-chimericEmTubB1
 Lower: plasmid sequence of pCMV-chimericEmTubB1
 The sequence and features were visualized with SnapGene Viewer. The indigo feature indicates C terminal part after DATA from HsTubB2B and the red-purple feature indicates EmTubB1 until QQYQ connected to the fragment of HsTubB2B. The junctions between HsTubB2B are the same also in other 3 constructs.

Materials and methods

The protocol for the transfection is basically the same as the instruction of the manufacture. Semi-confluent HEK293T cells were trypsinized and inoculated in 96 well plate with opaque wall (2×10^4 cells in 200ul of DMEM+GlutaMAX-I with 10% FBS) one day before the transfection. Next day, lipofectamine 3000 ($0.15 \mu\text{l} \times$ total well number) was diluted by DMEM + GlutaMAX-I WITHOUT FBS ($5 \mu\text{l} \times$ total well number). In different eppendorf tube, plasmid ($0.2 \mu\text{g} \times$ well number of each plasmid) and P3000 reagent ($0.4 \mu\text{l} \times$ well number of each plasmid) are diluted by DMEM+GlutaMAX-I WITHOUT FBS ($5 \mu\text{l} \times$ well number of each plasmid). The diluted lipofectamine were dispensed into each tube of plasmid (50%:50%) and the mixtures were incubated at room temperature for 5 minutes. After the incubation, the mixture were added to 96 well plate of HEK293T cells ($10 \mu\text{l}/\text{well}$).

2 days after transfection, 100ul of the medium was removed from each well and inhibitors in fresh $100 \mu\text{l}$ DMEM with 10% FBS ($2 \times$ final concentration) were added. 4 days after the transfection, $150 \mu\text{l}$ of the medium was removed from each well and $50 \mu\text{l}$ of Cell titer glo mixture was added. After this, the plates were incubated and chemiluminescence was measured, with the condition of user's guide from the manufacture. The value of chemiluminescence unit was normalized with that of DMSO-treated transfectants of the same plasmid as percentage. Non-linear regression curves were drawn with Graphpad Prism 9.3.1 (Graphpad software) and IC_{50} of 12 combinations of inhibitors and transfectants were calculated.

4.8 Bioinformatic analysis and handling of nucleic acids

4.8.1 Bioinformatic analysis

For kinase project, amino acid sequence of various human kinases, histon H3, CDK1/2 and HsCDC25A-C were acquired from UniProt (Bateman et al., 2021) through KEGG database Genomenet (Kanehisa et al., 2002). Amino acid sequences of PIM kinases and CDC25 phosphatases from other model organisms were also acquired from UniProt. If multiple transcript variants are deposited, isoform 1 was picked up for that protein. Kinase domain of each proteins were detected by SMART8.0 (Letunic and Bork, 2018; Letunic et al., 2015; Letunic et al., 2021). Amino acids sequences of various human kinases were aligned with CLUSTALW2.1 (Thompson et al., 1994) in MEGA11 (Tamura et al., 2021). The setting was, Gap Opening Penalty=10.00, Gap Extension Penalty=0.20, Delay Divergent Cutoff=30%. Based on these alignments, phylogenic tree was generated by MEGA11. The statistical method for this tree was maximum likelihood, substitution model was Jones-Taylor-Thompson model, ML Heuristic method was Nearest-Neighbor Interchange.

Amino acid sequences of human PIM kinases , CDC25 phosphatases, HASPIN, FLT3, histon H3 were used as queries for BLASTP (Altschul et al., 1997) analysis against protein database of *E. multilocularis* and *S. mansoni* through WormBase ParaSite (Howe et al., 2016; Howe et al., 2017). After identifying EmPIM, EmCDC25, SmPIM, SmCDC25A/B and EmHASPIN1/2 they were used as queries for BLASTP analysis against human genome through genomenet. The setting for both BLASTP analysis were default. The domains of proteins were detected by SMART8.0, aligned by MEGA11, with the same setting described above. The alignment was visualized with SnapGene Viewer (SnapGene software). Based on the alignments, phylogenetic trees were generated by MEGA with the same setting above and percent identity / similarity were culculated through Sequence manipulation suite (Stothard, 2000). The transcripts of empim kinase and emcdc25 phosphatase from the data

Materials and methods

of Tsai et al (Tsai *et al.*, 2013) were browsed with Integrative Genomics Viewer (Robinson et al., 2011; Thorvaldsdóttir et al., 2013) to see whether amino acid sequences available in UniProt are correctly predicted. The actual sequences cloned for yeast-two-hybrid were also compared with the prediction of EmPIM and EmCdc25.

For tubulin project, 10 β -tubulins encoded in the genome of *E. multilocularis* were already identified in the preceding research (Koziol and Brehm, 2015). Also β -tubulins in *Fasciola/*Caenorhabditis genomes were identified and named in the preceding researches. Therefore, I simply could acquire their amino acid sequences from UniProt, together with that human β -tubulins. HcTubB2 was identified by blastp analysis. The sequence on the figure 3 of Robinson et al. Was used as query (Robinson *et al.*, 2004). Multiple sequence alignment were performed with CLUSTALW 2.1 in Mega11 with the same setting above. The alignments were visualized with SnapGene Viewer. Based on these alignments, percent identity/similarity was calculated though Sequence manipulation suite and phylogenetic trees were generated with MEGA11, with the same setting described above.

4.8.2 *In silico* screening of compounds

In this doctoral dissertation, experiment/analysis by collaborators are described in bold letters. The analysis in this paragraph is done by Dr. Kim, Dr. Zhang, Dr. Becker, Dr. Hannus, and Dr. Sennhenn.

To identify compounds which potentially bind to EmPIM, Dr. Kim and Dr. Zhang of Immunerring corporation (MA/CA/NY) employed a proprietary deep learning -based platform named Fluency (Kim et al., 2020) which can predict binding strength between small compounds and proteins as predicted dissociation constant (nM). The query was kinase domain of EmPim, which was predicted by Pfam. The libraries were the Enamine Hinge Binders library (Enamine) (n=24,000) and Enamine Diverse REAL drug-like library version 2021q1-2 (Enamine), further filtered for drug-like properties based on Lipinski's rule of 5 (Lipinski et al., 2001) (n=21.4M). Two versions fluency models trained with various data sets and settings, v2c24 and v2c27 were applied for the predictions. In total 4 sets of predictions (2 libraries × 2 models) were performed and affinity of all molecules were ranked from strongest to weakest. From those predictions, the first list of 400 compounds was made, by combining the top ranked 200 compounds from each library (Appendix 8.1). Based on this list, 20 compounds of final lists (Appendix 8.2) were chosen with four criteria below, by Dr. Sennhenn, Dr. Hannus and Dr. Becker.

1. Fluency screening score
2. Diversity of structure
3. SeeSAR analysis of the ATP pocket binding mode, intermolecular clashes and torsion quality with BioSolveIT (version 11.2) (BioSolveIT GmbH)
4. Actural availability and budget

SIA Enamine (Riga, Latvijas) synthesized compounds of the final list in small scale and these compounds were used for in vitro screening of *E. multilocularis* and human cell lines.

4.8.3 *In silico* analysis of affinity between HsPim1 and inhibitors

In this dissertation, description with bold letters are results analyzed by someone else. The analysis in this paragraph was done by Dr. Sennhenn.

The binding strength between HsPIM1 and two inhibitors were analyzed with modeling software SeeSAR Version 12.0.1 (BioSolvelt GmbH), based on 3D structure of HsPIM1 available online. The integrated analyzer mode in the software identified poses which were clash-free and accompany statistically typical torsions (Schärfer et al., 2013).

4.9 Handling of nucleic acids

4.9.1 PCR with KOD DNA polymerase

When we are cloning DNA sequencing into plasmids, we use proofreading DNA polymerase. In our laboratory AG Brehm, KOD DNA polymerase (Toyobo, Kyoto, Japan) is used. In general, the pJG4-5 based library made by Hubert et al (Hubert et al., 2004) has been used as template. The mixture and program in the thermal cycler with KOD DNA polymerase are like below.

PCR mix with KOD DNA polymerase (1sample)

| | Concentration | Volume |
|------------------------|---------------|---------------------|
| 10×KOD reaction buffer | | 5µl |
| Forward primer | 10µM | 1.5µl |
| Reverse primer | 10µM | 1.5µl |
| dNTP mix | 2mM each | 5µl |
| MgSO ₄ | 25mM | 3µl |
| KOD DNA polymerase | | 1µl |
| template DNA | | depends on template |
| Distilled water | | up to 50µl |

Table 15

Thermal cycler program for KOD DNA polymerase

| Procedure | Temperature | Time | Cycle |
|------------------|-----------------------|---------------------------|-------|
| Initial denature | 95°C | 3min | ×1 |
| Denature | 95°C | 20sec | ×40 |
| Annealing | depend on primer pair | 20sec | |
| Extension | 70°C | 20sec/kbp | |
| final extension | 50°C | 20% longer than extension | ×1 |
| Hold | 4°C | ∞ | ×1 |

Table 16

Materials and methods

Plasmids provided from Dr. Spiliotis or AG Brehm was used as templates for EmTubB constructs. Because C terminus fragment of HsTubB2B was too short, no templates were necessary and double strand DNA fragments were synthesized just by annealing of forward and reverse primers. The combinations of templates and primers are below.

| Plasmid | Template |
|-------------------------|---------------------------------------|
| pCMV-chimericEmTubB1 | pCFJ601-TubB1-23 K1 (gelb1) |
| pCMV-chimericEmTubB2wt | pCFJ601-TubB2-31K4 (gelb4) |
| pCMV-chimericEmTubB2mut | pCFJ601-TubB2 2x Y-F mutiert (gelb42) |
| pCMV-chimericEmTubB3 | pCFJ601-TubB30-1K4 (gelb5) |

Table 17

| Plasmid | Forward | Reverse |
|------------------------|---------------------|------------------|
| pCMV-chimericEmTubB1/2 | SyncHsTubB2BF2 | SyncHsTubB2BR |
| pCMV-chimericEmTubB3 | HsTubB2BforEmTubB3F | HsTubB2BDATA-rev |

Table 18

4.9.2 Gel electrophoresis

1% agarose gels of Tris-acetate-EDTA (TAE) are prepared before the end of the PCR. To visualize the band, Midori Green Advance (Nippon Genetics Europe) is mixed before the gels are solidified (1:25000). The PCR products are mixed with loading dye (2µl of dye +5µl of PCR product) and loaded into the gel. Smart ladder (Eurogentec) is also loaded into the gel to estimate the size of PCR products. After 20 min or longer (depends on the size of the PCR product and gel) electrophoresis in TAE buffer at 125V, the bands of PCR products were visualized under ChemiDoc MP System (Bio-Rad). If there is a single band of desired size, the leftover of the PCR products will be purified. In case there are extra bands other than the band of desired size, all leftover of PCR products is loaded new Agarose gel. After electrophoresis again, only the band of desired size is excised from the gel and this part of gel will be used for the purification.

4.9.3 Purification and cloning of PCR products

The leftover of PCR products or gel including the band of desired size are purified with NucleoSpin® Gel and PCR clean-up (Macherey Nagel GmbH) with the procedure of its user's manual. After purification, the PCR products are quantified with nanodrop.

In the case of pJet1.2 based plasmids, the PCR fragments are cloned into pJet1.2 with CloneJET™ PCR Cloning kit with the procedure of its user's manual. In the case of other backbones, PCR fragments were integrated into linearized vectors with the method of aqua cloning described in (Beyer et al., 2015)

4.9.4 Transformation of chemically competent *E. coli*

In our laboratory AG Brehm, chemically competent *E. coli* strain TOP10 is regularly used.

Aliquots of competent cells are thawed on crashed ice, and 2.5µl (CloneJET™ PCR Cloning kit or 10µl (aqua cloning) of the reaction mixtures are added to the tubes. After 30 minutes of incubation on the crashed ice, the tubes are moved to heat block and heat-shocked at 42°C for 45 seconds. After the heat shock, the tubes are moved into the crashed ice and incubated for 5 minutes. After 5 minutes, the tubes are centrifuged at room temperature, 6000 × g for 1 minutes and the supernatants are removed. The *E. coli* pellets are resuspended with 100µl of SOC medium and incubated on thermomixer at 37°C, 200rpm for up to 1 hour. After 1 hour, all 100µl are inoculated on LB plates with selection marker (Kanamycin: 50mg/ml, Carbenicillin: 100mg/ml) and incubated at 37°C overnight.

4.9.5 Colony PCR

After overnight incubation at 37°C, colonies on selection plates come out. These colonies are picked up with sterile tips and resuspended into 30µl of ultrapure water independently. 9µl of PCR mix below are added to 1 µl of the resuspension in 8 strips.

PCR mix for Taq DNA polymerase (10 samples)

| | Concentration | Volume |
|---------------------|---------------|--------|
| 5×Midori PCR buffer | | 20µl |
| Forward primer | 50µM | 1µl |
| Reverse primer | 50µM | 1µl |
| Taq DNA polymerase | | 1µl |
| Distilled water | | 65µl |

Table 19

Primer pair

| Backborn plasmid | Forward | Reverse |
|------------------|---------------|----------------|
| pJet1.2 | pJet1.2 Fw | pJet1.2 Rev |
| pGBKT7 | T7 | pGBKT7-Rev |
| pGADT7 | T7 | pGADT7-Rev |
| pCMV-myc | pCMV_Fwforseq | pCMV_Revforseq |

Table 20

The sequences of each primer are written in 4.4. tables.

The 8 strips are moved into the thermal cycler and moved with the program below.

Thermal cycler Program for Taq polymerase

| Procedure | Temperature | Time | Cycle |
|------------------|-----------------------|---------------------------|-------|
| Initial denature | 94°C | 3min | ×1 |
| Denature | 94°C | 20sec | ×25 |
| Annealing | depend on primer pair | 20sec | |
| Extension | 72°C | 1min/kbp | |
| final extension | 72°C | 20% longer than extension | ×1 |
| Hold | 4°C | ∞ | ×1 |

Table 21

The size of PCR products is evaluated through electrophoresis.

4.9.6 Amplification of plasmid

If there is colony with PCR products of appropriate size, 10µl of colony resuspension is inoculated into a sterile tube with 5ml of LB media including antibiotics (Kanamycin 50mg/ml or Carbenicillin 100mg/ml). The tubes are incubated at 37°C 200rpm for 16hours. After 16hours, the plasmids are purified with Nucleospin ® plasmid (Macherey Nagel GmbH) and quantified with nanodrop.

4.9.7 Sequencing of plasmid

The plasmid was mixed with primer like below and sent to the sequencing service of Mycosynth SeqLab (Göttingen, Germany). The primers for sequencing are basically the same as those for colony PCR, but when inserts are too long to be covered by a pair of primers (approximately over 2000bp), additional primers need to be designed and ordered.

| sequencing sample | Concentration | Amount |
|-------------------|---------------|-------------|
| Plasmid | | up to 500ng |
| Primer | 5µM | 5µl |
| ultrapure water | | up to 10µl |

Table 22

4.9.8 Synthesis of probes for in situ hybridization

For the synthesis of DIG-labelled riboprobe for in situ hybridization, pJet1.2-based plasmids including maximum 1000kbp cDNA sequences from the gene of interest were constructed with the procedure above. After clarifying that desired sequences are included through sequencing, use the plasmid for the next PCR as template. The same as 4.7.2.1, PCR with KOD polymerase is necessary.

| | Concentration | Volume |
|--------------------------------|---------------|--------|
| 10×KOD reaction buffer | | 5µl |
| Forward primer | 10µM | 1.5µl |
| Reverse primer | 10µM | 1.5µl |
| dNTP mix | 2mM each | 5µl |
| MgSO ₄ | 25mM | 3µl |
| KOD DNA polymerase | | 1µl |
| Template pJet1.2 based plasmid | | 5µl |
| Distilled water | | 28µl |

Table 23

| Backborn plasmid | Forward | Reverse |
|------------------|----------|---------------------|
| pJet1.2 | T7 plus2 | 5-Sp6+pJet1.2 Rev-3 |

Table 24

Materials and methods

The sequence of each primer is written in 4.4 tables.

The thermal cycler program is completely the same as KOD PCR described above.

The PCR fragments should include both T7 and Sp6 sites. The size of PCR products should be checked by electrophoresis. The leftover of PCR products is purified as 4.7.2.3.

The purified PCR products are used as template for the synthesis of riboprobes with T7 and SP6 RNA polymerases. Depending on the direction of insertion, one will be the riboprobe (antisense) the other will be the control probe (sense)

The mixture for in vitro RNA transcription is like below. The polymerase should be added the last.

In vitro transcription mix (1 probe, 20 μ l)

| | Volume |
|---|------------------|
| 10 \times NEB in vitro transcription buffer | 2 μ l |
| 10 \times DIG Mix | 2 μ l |
| RNA polymerase | 2 μ l |
| RNAse inhibitor | 0.5 μ l |
| 10 \times BSA | 2 μ l |
| Template DNA | 1 μ g |
| RNAse free water | up to 20 μ l |

Table 25

These mixes are incubated at 37°C for 2 hours. After 2 hours, add 1ul of RQ1 DNase to each tube and incubate 15 more minutes at 37°C.

2 μ l of the transcribed RNA is mixed with 6 \times 2 μ l of loading dye (New England Biolabs) and loaded into 1% agarose gel. The same as 4.9.2.2., the size of products need to be evaluated. If the product size is appropriate, the leftover of transcribed RNA will be purified with the kit and its quality was evaluated through dot blot, as described in Koziol et al. (Koziol *et al.*, 2014) by comparing signal from control DIG-labelled RNA (Roche).

4.10 Yeast-two-hybrid

In AG Brehm, Matchmaker Gold Yeast Two Hybrid System (Takara) has been used for decades. The primer pairs were designed based on the sequence information from WormBase ParaSite (Howe *et al.*, 2016; Howe *et al.*, 2017; Tsai *et al.*, 2013), so that full-length cDNA of EmPIM and EmCDC25 are amplified. Their sequences of primers are shown in the table of 4.5.2. and vector construction process is described in 4.9.

Saccharomyces cerevisiae Gold strain (Takara) are transformed with plasmids by one step protocol described by Tripp et al in (Tripp et al., 2013) and were inoculated on the -Leu/-Trp double dropout agarose plates. After the incubation at 30°C for 2 days, three colonies were picked up from each transformants and inoculated independently into 2ml of liquid -Leu /-Trp medium and incubated at 30°C, 200rpm until they grew above OD₆₆₀=1.0. These yeasts are diluted so that the density is approximately equivalent to the level of OD₆₆₀=1.0, 0.1 and 0.01. The diluted yeast was inoculated on -Leu, -Trp, -Ade triple dropout plates and -Leu/ -Trp/ -Ade /-His quadruple dropout plates as 5µl droplet. After 48 to 72 hours of incubation at 30°C, the pictures of plates were taken with ProtoCOL SR colony counter (Synbiosis) and the growth was compared with the transformants of positive control (pGADT7-AntigenT+pGBKT7-p53) and negative control (pGADT7-AntigenT+pGBKT7-LamC)

The pictures were converted into gray scale, and processed with Fiji/imageJ (Schindelin et al., 2012), with the protocol described in (Petrovavlovskiy et al., 2020). The level of growth on quadruple dropout plates with the inoculation density OD₆₆₀=1.0 was quantified as gray value. The quantified level of growth was statistically analyzed with one-way ANOVA followed by Tukey's multiple comparison tests in Graphpad prism 9.3.1(Graphpad software). In this analysis, all plasmid combinations were compared one another but only the comparisons with corresponding controls are shown on the graph.

4.11 Imaging analysis

4.11.1 Whole-mount in situ hybridization

For kinase project, the construction process of pJet1.2-based plasmid for probe synthesis is described in 4.9.1-4.9.7. Following process of synthesizing in situ hybridization probes is described in 4.9.8.

In vitro cultivated untreated metacestodes vesicles (H95) were incubated in DMEM+GlutaMAX-I including 50 μ M 5-ethynyl-2'-deoxyuridine (EdU, included in invitrogen's Click-iT cell proliferation assay kit) and 10% Fetal Bovine Serum Superior (Life Technologies) at 37°C for 5 or 8 hours. The plates were gently tapped every 1 hour. After labeling, the vesicles were moved into DEPC-PBS and were torn with forceps to wash out hydatid fluid. After washing, the vesicles were fixed in 4% PFA in DEPC-treated PBS at 4°C overnight.

The next day, fixed vesicles were washed three times with DEPC-treated PBS and dehydrated gradually with 25%, 50% and 100% methanol. After dehydration, the samples were stored at -20°C.

The procedure of WISH was performed in the protocol described in (Koziol *et al.*, 2014). After the procedure of *in situ* hybridization, EdU developing procedures and 4', 6-diamidino-2-phenylindole (DAPI, Thermo Fisher) staining were carried out with the protocol of Koziol *et al.* (Koziol *et al.*, 2014). After DAPI staining, vesicles were washed 5 times with PBS and mounted on slide glasses together with histology mounting medium Fluoroshield (Sigma-aldrich).

Nikon eclipse Ti2E conjugated to the Laser Unit LightHub+ (Omicron) and Confocal Scanner Unit CSU-W1 (Yokogawa) was used to observe these slides. Series of pictures were taken at randomly chosen sections of the germinal layer of 5 metacestode vesicles with 40 \times objective lens as Z-stack. Among the picture of each Z-stack, the layer of strongest

Materials and methods

signal was selected by the function of Z project in Fiji/ImageJ and processed (Schindelin *et al.*, 2012).

EdU positive cells, WISH positive cells and double positive cells were counted manually and independently. The number of cells with each signal were calculated to cell number per mm² on the germinal layer.

For tubulin project, vesicles were treated with 30µM TCBZS or DMSO for 10 days before fixation. The pJet1.2-based plasmid including EmTRIM sequences was constructed by Dr. Koziol (Koziol *et al.*, 2015) and was still stored in -20°C. The process of probe syntehsis is described in 4.9.8. The process between fixation and acquisition of Z-Stack images is totally the same as kinase project.

After the layer of strongest signal was extracted with Fiji, the image was splitted into 3 channel. Thresholds are set for both green and blue channel independently, and area (mm²) with green (WISH) signal and area with blue (DAPI) signal are independently measured. By normalizing green area (WISH signal which reflects EmTRIM positive cell number) with Blue area (DAPI signal which reflects total cell number), the ratio of EmTRIM positive cells was quantified. The normalized values from each Z stack were statically analyzed with Mann Whitney test in GraphPad Prism 9.3.1 (GraphPad software).

4.11.2 Whole-mount immunofluorescence assay

Vesicles treated with inhibitors for 10 days were torn in PBS and washed to remove hydatid fluid. After washing, they were fixed with PBS including 4% PFA at 4 °C overnight. The next day, the vesicles were washed three times with PBS, and dehydrated with 50%, 75% and 100% methanol gradually. The vesicles were stored at -20°C until use.

On the 1st day of experiment, the vesicles were rehydrated with 100%, 75% and 50% ethanol gradually. After washing 3 times with PBSTx (including 0.3% TritonX-100), the vesicles were permeabilized with PBS including 1% SDS at room temperature for 20 min. After permeabilization, the vesicles were washed 3 times again with PBSTx, and blocked with PBSTx including 3% BSA and 5% sheep serum for 2 hours. After blocking, the vesicles were incubated in PBSTx including 3% BSA and the primary antibody (100 times diluted anti Acetylated α -tubulin mouse antibody) at 4°C overnight.

On the 2nd day of the experiment, the primary antibody was washed with PBSTx 5 times and incubated in PBSTx including 3% BSA and the secondary antibody (100 times diluted FITC-conjugated anti mouse goat antibody) at 4°C overnight.

On the 3rd day of the experiment, the vesicles were washed with PBSTx once, and stained in PBS including 1% BSA, 1 μ g/ml DAPI and 40 times diluted TRIC-conjugated Phalloidin at room temperature for 30 minutes. After staining with DAPI and phalloidin, washed with PBSTx 4 times and mounted on the slide glasses, the same as samples of WISH. The slides were observed under a confocal microscope and series of pictures were acquired as Z stack, the same as the sample of WISH. The number of cells with AcTub signal were calculated to cell number per mm² on the germinal layer, similarly as WISH against PIM.

4.11.3 EdU labeling and analysis of EdU positive cells

For the evaluation of BZs' effect on EdU cells, metacystode vesicles were treated with BZs for 10 days, and fixed with 4% PFA overnight after labeling with 50 μ M EdU for 5 hours, the same as 4.11.1. Next day, the vesicles were washed and dehydrated. On the day of development, the EdU was developed with the protocol of Koziol et al. (Koziol *et al.*, 2014). The process from DAPI staining to images acquisition was almost the same as 4.11.1., but images from 10 metacystode vesicles were acquired. The layers of the strongest signals were extracted with Z project of Fiji/imageJ (Schindelin *et al.*, 2012) and saved through a macro customized by myself. The threshold was set with NIS-element AR (Nikon, Tokyo, Japan) and EdU positive cells were counted with object count function in the software. The ratio of EdU positive cells (cell number /mm²) were statistically analyzed with Kruskal-Wallis test followed by Dunn's multiple comparison test in Graphpad Prism in 9.3.1 (Graphpad Software) and all combinations of BZs-treatment were compared with DMSO.

5. Results

5.1 *In vitro* screening with kinases inhibitors

Protein kinases are considered to be good targets for chemotherapy because of several characteristics (3.2.1). Therefore, AG Brehm, TransMedChem and Intana Bioscience acquired budget for the research of Echinococcus kinase, Kinase Inhibitoren als Therapeutika gegen Echinokokkose (KITE). The first experiment of the project was screening with commercially available inhibitors. Through the research of transcriptmics, it was already known that *E. multilocularis* has kinases in all 7 groups of human kinome (Tsai *et al.*, 2013). The first list of kinase inhibitors (Table 2) was made so that it covers all 7 major groups.

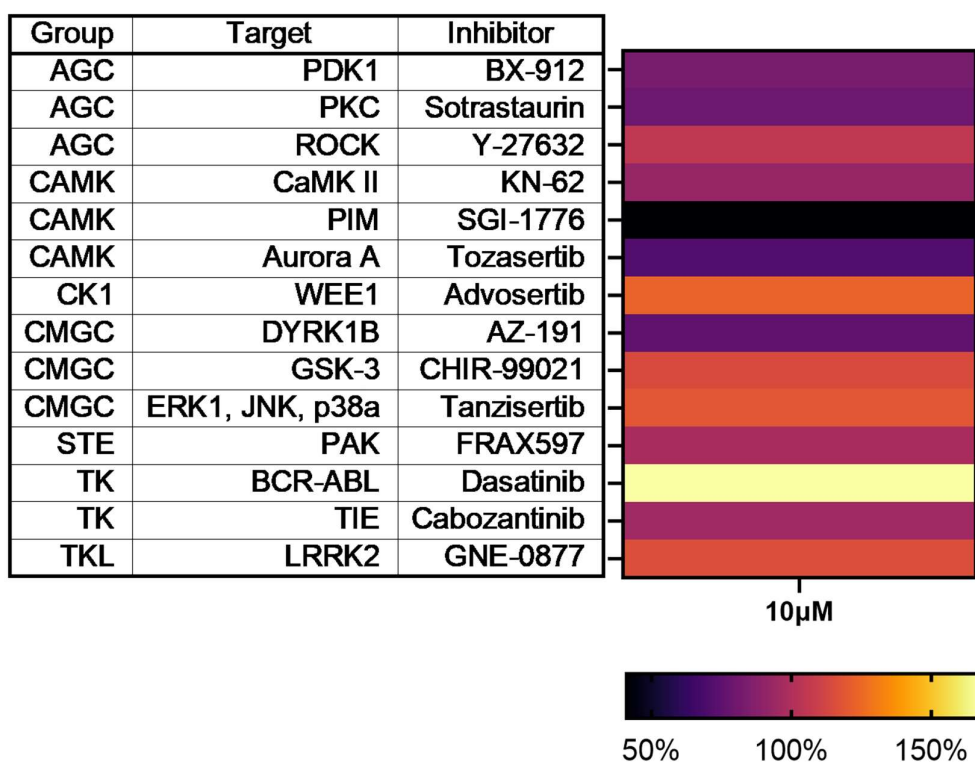


Figure 17: Screening result of kinase List1

The right heatmap shows luminescence units of primary cells treated with kinase inhibitors for 3 days. They are shown as percentage after normalized with that control, DMSO. The left table shows names of inhibitors in the list1, which target kinases in 7 major groups.

5. Results

I measured the effect of inhibitors as cell viability of primary cells, which include high percentage of geminative stem cells (Koziol *et al.*, 2014). The primary cells were incubated for 3 days with 10 μ M of each inhibitors before the measurement of cell viability. There were 14 inhibitors in the first list. SGI-1776, a commercially available pan-PIM inhibitor showed outstanding detrimental effect among these 14 inhibitors (Fig.17).

The second list for screening (Table 3) includes inhibitors against kinases which have been studied in previous research in AG Brehm (Gelmedin *et al.*, 2008; Gelmedin *et al.*, 2010; Hemer and Brehm, 2012; Montagne *et al.*, 2019; Schubert *et al.*, 2014). These inhibitors already have tried in various methods by each researcher and proved to have some detrimental effect against *E. multilocularis in vitro*, or at least their target kinases are important for *E. multilocularis*. The advantage of cell viability assay is that many inhibitors can be tried in shorter time with smaller consumption of parasitic material, but none of the previous researchers have tried this method and its validity was questionable. Resazurin assay has already been tried (Herz and Brehm, 2021) and it is also categorized into cell viability assay, but it is different from our assay. Our assay measures ATP concentration and resazurin measures oxidation-reduction reaction. Therefore, I tried SGI-1776, which showed the strongest toxicity in the 1st list, together with the inhibitors already tried by other researchers. However, GSK690693 and Palbociclib were exception. Previous researchers in AG Brehm have never published about AKT, CDK4 or CDK6. They were planned to be included in the first list, but simply they were delivered months later than the initial schedule and could not be used together with kinase inhibitors in the first list.

5. Results

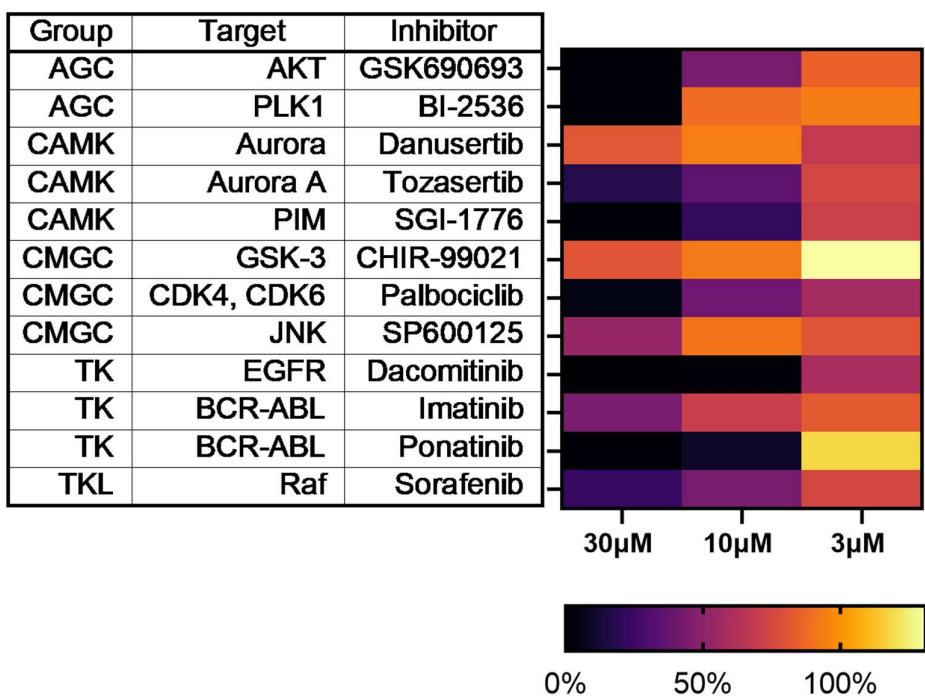


Figure 18: Screening result of List2

The right heatmap shows luminescence units of primary cells treated with kinase inhibitors for 3 days. They are shown as percentage after normalized with that control, DMSO. The concentration of inhibitors are shown under the heatmap. The left table shows names of inhibitors in the list 2, which target kinases studied by previous researchers in AG Brehm.

As I expected, PLK inhibitor or EGFR inhibitor showed stronger toxicity, the same as SGI-1776 and the result of cell viability assay with the first list was validated (Fig.18). Through the screening with two lists, we therefore decided to focus on PIM kinase and EGFR.

Because we decided to focus on PIM kinase and EGFR, the 3rd list (Table 4) includes multiple inhibitors against PIM kinase and EGFR, and against kinases closer to them. Because the toxicities of BCR-ABL inhibitors and Aurora kinase inhibitors in the 1st and 2nd list were different, additional inhibitor against them were also included into the 3rd list.

5. Results

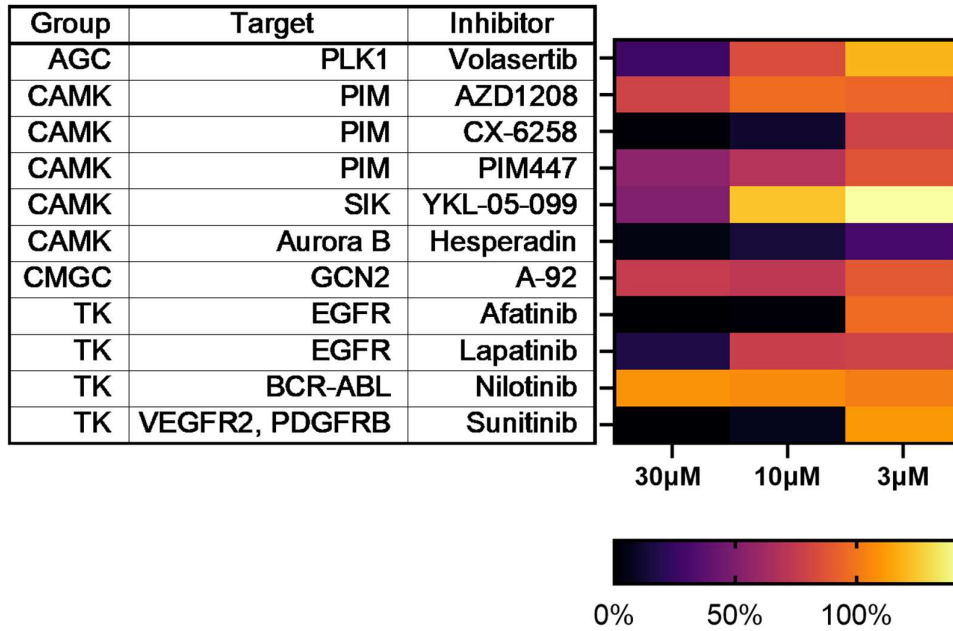


Figure 19: Screening result of List3

The right heatmap shows luminescence units of primary cells treated with kinase inhibitors for 3 days. They are shown as percentage after normalized with that control, DMSO. The concentration of inhibitors are shown under the heatmap. The left table shows names of inhibitors in the list 3.

There were several exceptions, but multiple inhibitors both against EGFR and PIM kinases showed stronger detrimental effect (Fig.19). Therefore, we decided to focus on these kinases, especially PIM kinase.

5. Results

5.2 PIM kinases

5.2.1 Characterization of EmPIM

During *in vitro* screening with kinase inhibitors in 7 major groups (5.1), at least two pan-Pim kinase inhibitor, SGI-1776 and CX-6258, showed outstanding detrimental effect on the cell viability of the primary cells. The original targets for these inhibitors are three isoforms in human genome, PIM1, PIM2, PIM3 (Cuypers et al., 1984; Konietzko et al., 1999). When I performed BLASTP analysis against protein database of *E. multilocularis* (Tsai et al., 2013), only one protein, EmuJ_000197100, had homology with the three queries, HsPim1, HsPim2 and HsPim3. Especially the similarity in the kinase domain of this protein and human PIM kinases were high. This protein also has homology with PIM kinases of other model organisms, PSK2 of *Caenorhabditis* and PRK2 of *Saccharomyces*. When I performed BLASTP analysis against genome of *Schistosoma mansoni* with the three queries, HsPIM1, HsPIM2 and HsPIM3, again only one protein, Smp_090890 was identified. We named them EmPIM and SmPIM, respectively.

Immediately after I identified EmPIM and SmPIM, I analyzed domains of full length of EmPIM, SmPIM and HsPIM1-3 through SMART (Letunic and Bork, 2018; Letunic et al., 2015; Letunic et al., 2021). All three human Pim kinases have only shorter sequences outside of kinase domain, both at N terminus and C terminus. On the other hand, EmPIM has long sequences at C terminus, after its kinase domain. SmPIM also has long sequences after kinase domain (Fig.20). No domain or motifs was detected in the lengthy C terminus tail of EmPIM and SmPIM, therefore the function of these longer C terminal tail is unknown.

5. Results

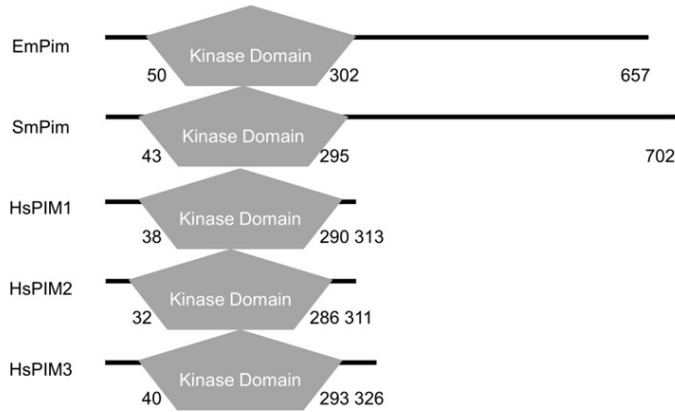


Figure 20: Schematic image of domains in PIM kinases

Domains detected by SMART and length of EmPIM, SmPIM, and human PIM kinases (HsPIM1-3). The total length of the proteins is shown to the right. The positions of the kinase domain are indicated.

Next, I aligned amino acid sequence of kinase domains (Fig.21).

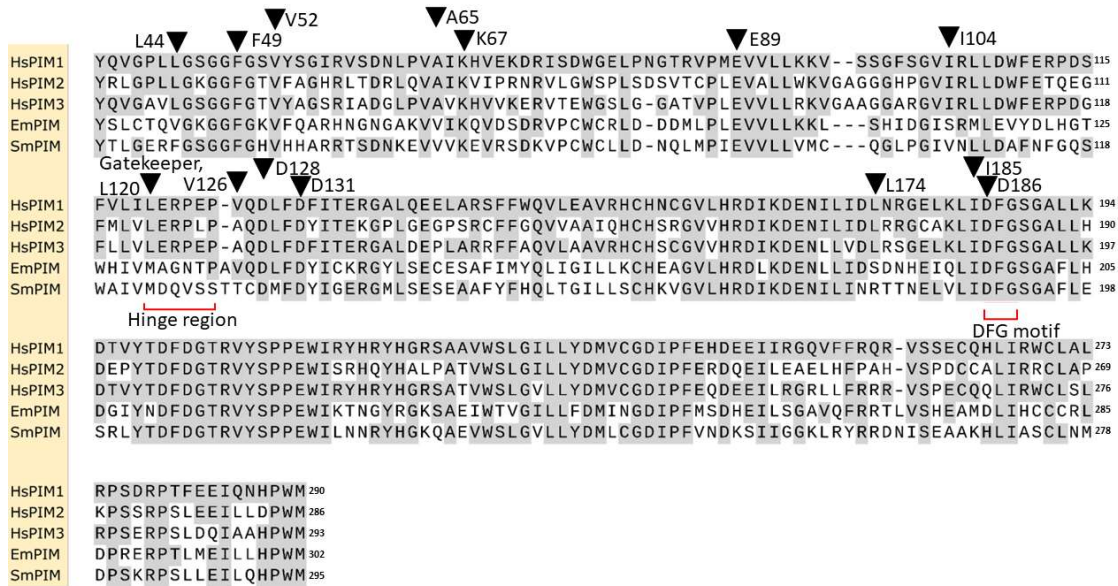


Figure 21: Alignment of kinase domain of PIM kinases

Amino acid sequence of the kinase domains of EmPIM, SmPIM, HsPIM1-3 were aligned with ClustalW. Grey highlights indicate residues identical to HsPIM1. DFG motifs and the hinge regions are shown under the alignment. 14 residues important for the interaction with CX-6258 (Bogus et al.) are shown with black arrowheads. The alphabet and number next to the arrowheads indicate the residue and position in HsPIM1.

5. Results

Based on the alignment (Fig.21), a phylogenetic tree of kinase domains was generated (Fig.22). According to the phylogenetic tree, EmPIM is not especially closer to any of three human kinases.

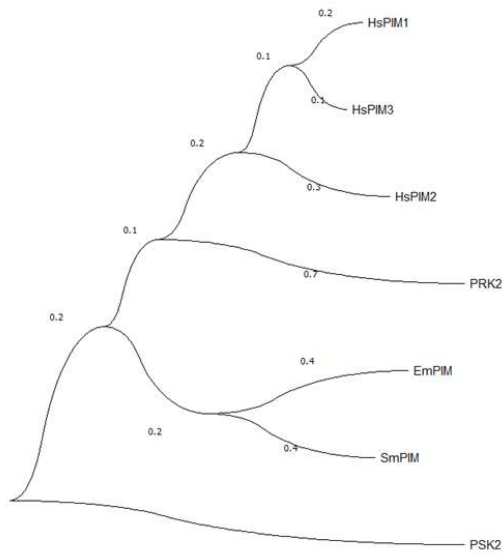


Figure 22: Phylogenetic tree of PIM kinases

Phylogenetic tree was generated based on the alignment of kinase domains of EmPIM, SmPIM, all three human PIM kinases (HsPIM1-3), PRK2 from *Caenorhabditis*, and PSK2 from *Saccharomyces*. The statistical method for the tree was maximum likelihood, substitution model was Jones-Taylor-Thompson model, ML Heuristic method was Nearest-Neighbor Interchange. The tree was visualized with MEGA11.

5. Results

5.2.2 Expression of *empim* in stem cells

HsPIM1 is a positive regulator of cell cycle progression (Morishita et al., 2008). In *E. multilocularis*, stem cells (germinative cells) are only mitotically active (Koziol et al., 2014). Therefore, I expected that *empim* are expressed in stem cells and play a similar role as HsPIM1. To estimate the expression level of *empim* in stem cells, I analyzed the expression data of Tsai et. al. (Tsai et al., 2013). The expression level of *empim* is lower in metacestode vesicle without brood capsules than in primary cells 2 days after isolation (Fig.23). Because the most of primary cells remain undifferentiated in 2 days after isolation (Koziol et al., 2014), the expression profile of primary cells day2, is considered to reflect that of stem cells. This indicates that *empim* expressed more in stem cells than differentiated cells. However, the difference in the expression level of *empim* between metacestode vesicles and primary cells is less clear than that of *emplk1*, which is known to be expressed specifically in primary cells (Schubert et al., 2014).

From the expression profile, the expression of *empim* in stem cells was indicated. Therefore, to see co-localization of *empim* mRNA and actively proliferating stem cell marker (EdU), I tried in situ hybridization. In AG Brehm, metacestode vesicles for in situ hybridization are labelled with EdU for 5 hours, according to the standard protocol of the laboratory (Koziol et al., 2014).

5. Results

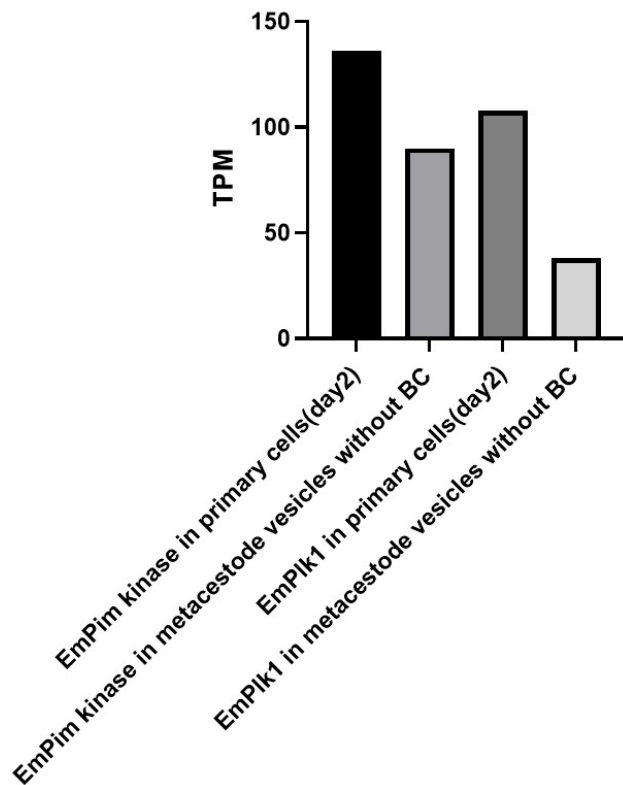


Figure 23: Expression level of EmPim

Expression data here were extracted from Tsai et al. Gene expression level (Transcripts Per kilobase of exon per Million transcripts mapped, TPM) of EmPim kinase and EmPlk1, in primary cell isolated after 2days and in metacystode vesicles without brood capsules (bc). Plk1 is specifically expressed in stem cells and its expression level is shown to compare with that of EmPim.

However, very limited number of cells show co-localization of EdU and WISH signal.

Therefore, I prolonged the incubation to 8 hours and 16 hours. The vesicles incubated for 16 hours were too fragile to keep their structure during the *in situ* hybridization process, which include repetitive wash and boiling at 57-60°C over 24 hours. Approximately 25% of WISH positive signals co-localized with EdU signals in the samples of 8 hours incubation (Fig.24).

5. Results

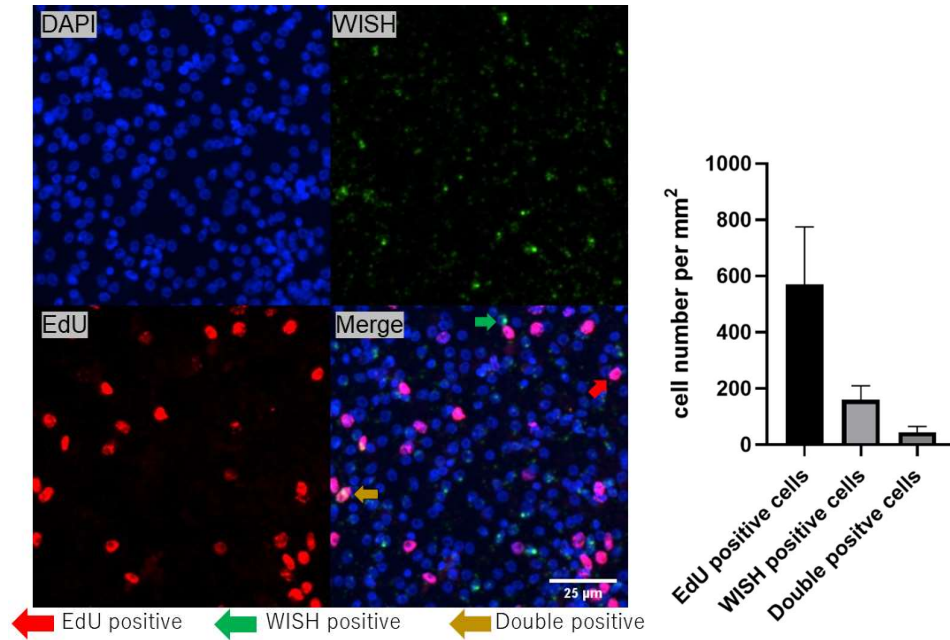


Figure 24 Co-localization of empim and stem cell marker

(Left) WISH sample observed under a confocal microscope. Green signal is from antisense probe against empim, red signal is from EdU (actively proliferating stem cells in S phase) and blue signal is from DAPI (nucleus). Red arrow indicates EdU positive cells, green arrow indicates WISH positive cells, and brown arrow indicates cells with both signals. The length of scale bar is 25 μm.

(Right) Mean number of cells with each signals per mm² observed in WISH samples under confocal microscope. The error bars represent standard deviation.

5. Results

5.2.3 Interaction between EmPIM and EmCDC25C

Human PIM1 positively regulate cell cycle progression through activation of CDC25 phosphatases (Bachmann *et al.*, 2006; Mochizuki *et al.*, 1999). CDC25 phosphatases are well-conserved among members of opisthokonta (metazoa and fungi), although the number of gene varies from species to species. After being activated by HsPIM1, CDC25A/C removes inhibitory phosphates from cyclin-CDK complexes and the signals for cell-cycle progression are transmitted (Bachmann *et al.*, 2006; Chow *et al.*, 2011; Donzelli and Draetta, 2003; Mochizuki *et al.*, 1999). If EmPIM is a positive regulator of cell cycle progression similarly as HsPIM1, CDC25 phosphatase should be encoded in the genome of *E. multilocularis*. Blastp analysis against protein database of *E. multilocularis* identified only one protein EmuJ_001174300, which had high similarity with the queries, human CDC25A, CDC25B and CDC25C. Similar blastp analysis against protein database of *S. mansoni* identified two proteins with homologies with human CDC25s. We named them EmCDC25, SmCDC25A and SmCDC25B respectively. When we analyzed amino acid sequences of these proteins with SMART (Letunic and Bork, 2018; Letunic *et al.*, 2015; Letunic *et al.*, 2021), rhodase homology domain (RHOD) were detected. RHOD domain is a hallmark of CDC25 family (Bordo and Bork, 2002). However, different from human CDC25s, M phase phosph domain was not detected in EmCDC25 and SmCDC25s (Fig.25)

5. Results

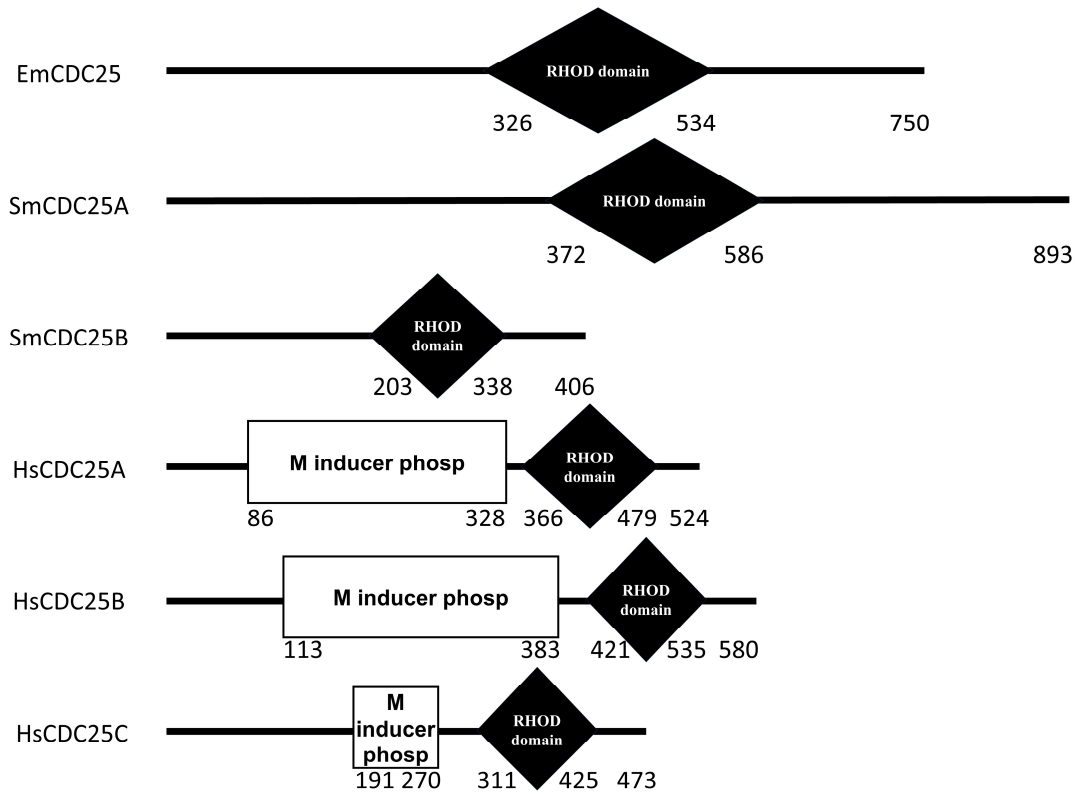


Figure 25: Schematic image of domains in CDC25 phosphatases from three species

Pfam domains detected through SMART are shown in this schematic image. The position of each domain and total length of the protein are shown.

5. Results

When I made an alignment of RHOD domain, one characteristic of EmCDC25 was found.

EmCDC25 has insert between DCR motif and Active site in its RHOD domain, and such inserts do not exist in huan CDC25s. SmCDC25A shares this characteristic, but SmCDC25B does not have the last and longer insert (Fig.26).

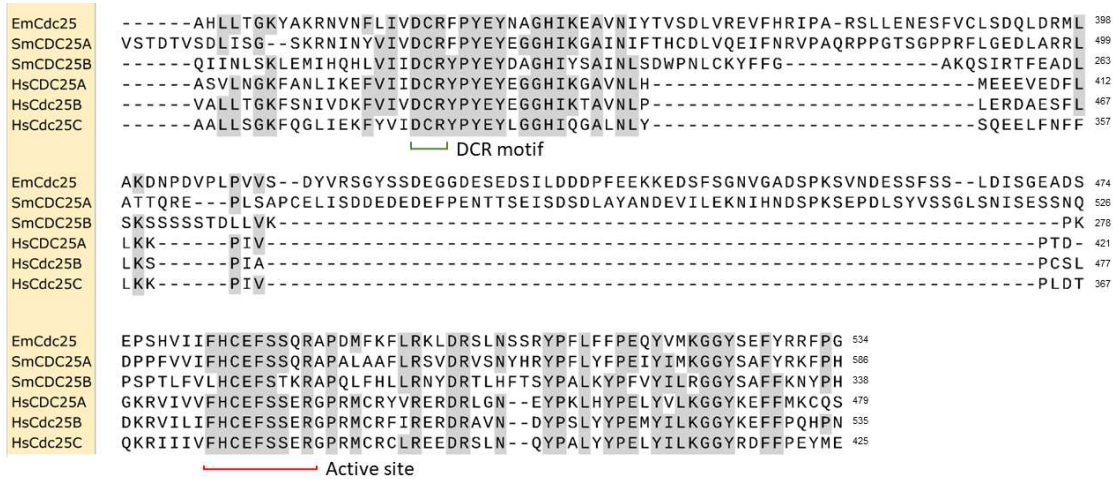


Figure 26: Alignment of rhodanese homology domain

The RHOD domains of each phosphatase were detected through the analysis with SMART and aligned with ClustalW. Gray highlights indicate consensus of residues on four or more phosphatases.

5. Results

Based on the alignment, a phylogenetic tree of CDC25 was generated. EmCDC25 and SmCDC25A are adjacent to each other in the phylogenetic tree, but SmCDC25B are far from EmCDC25 and SmCDC25A (Fig.27) , probably because of different pattern of inserts.

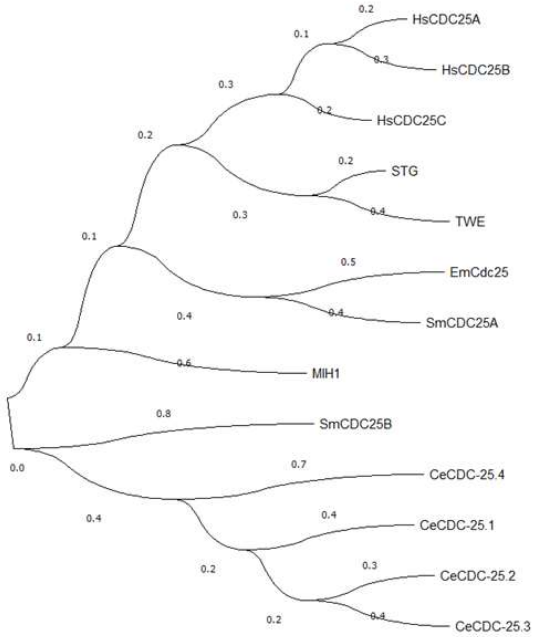


Figure 27: Phylogenetic tree of rhodase homology domains

The phylogenetic tree was generated based on the alignment of RHOD domains of CDC25 phosphatases. TWE and STG are CDC25s of *Drosophila*, MIH1 is CDC25 of *Saccharomyces*, and CeCDC25s are 4 CDC25s from *Caenorhabditis*. The statistical method for the tree was maximum likelihood, substitution model was Jones-Taylor-Thompson model, ML Heuristic method was Nearest-Neighbor Interchange. The tree was visualized with MEGA11

5. Results

To verify whether EmPIM and EmCDC25 have interactions like human PIM1-CDC25A, I tried yeast-two-hybrid assay. The transformant with pGBKT7-empim and pGADT7-emcdc25 clearly grew better on both triple dropout plate (moderate stringency) and quadruple dropout (high stringency) plate than the control transformants with empty vectors (Fig.28). This indicates that there is a specific interaction between these two proteins.

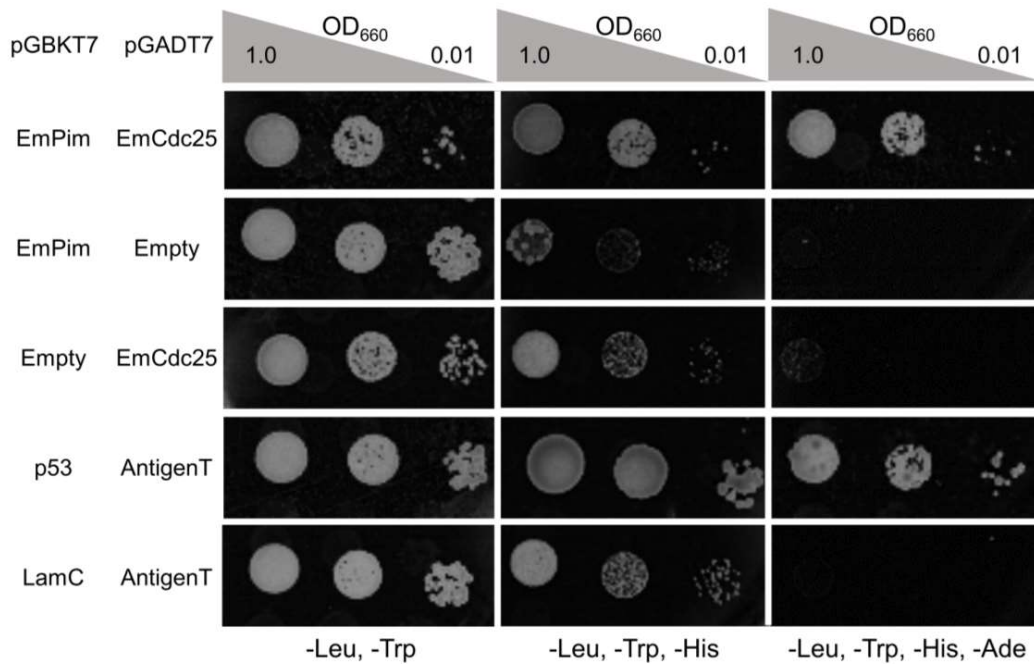


Figure 28: Yeast growth on selection plates

Pictures of yeast transformants grown on double dropout (-Leu/-Trp), triple dropout (-Leu/-Trp/-His), quadruple dropout (-Leu/-Trp/-His/-Ade) after being inoculated with three densities above and plasmid combination of each transformants are shown at the left. The pictures were converted into grayscale and the background was subtracted with the algorithm of sliding paraboloid.

When I quantify the growth of each transformants on quadruple dropout (inoculation density OD₆₆₀=1.0), the differences between pGBKT7-empim x pGADT7-emcdc25 and controls with empty vectors were also significant (Fig.29).

5. Results

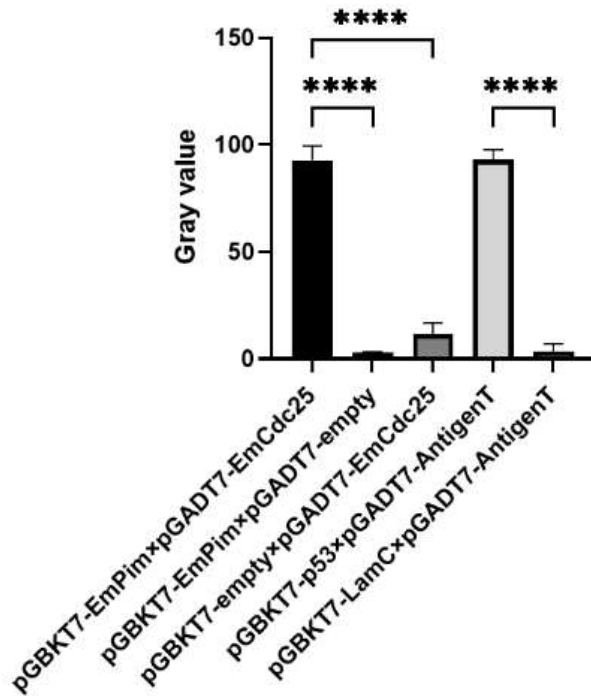


Figure 29: Quantified growth level of yeast

Mean level of growth was quantified as gray value. The error bars represent standard deviation. One way ANOVA followed by Tukey's multiple comparison test was used to compare all plasmid combinations, but only the comparisons of corresponding control are shown. P values less than 0.0001 are summarized with ****.

The target of human CDC25A/CDC25C are HsCDK2/HsCDK1 (Bachmann *et al.*, 2006; Donzelli and Draetta, 2003). EmCDK1 has already been identified in the expression data of Tsai et al (Tsai *et al.*, 2013). When I aligned EmCDK1 with human CDC25A and CDC25C, the amino acid sequence around Thr14/Tyr15, the target residues of human CDC25s, are relatively well conserved (Fig.30).

5. Results

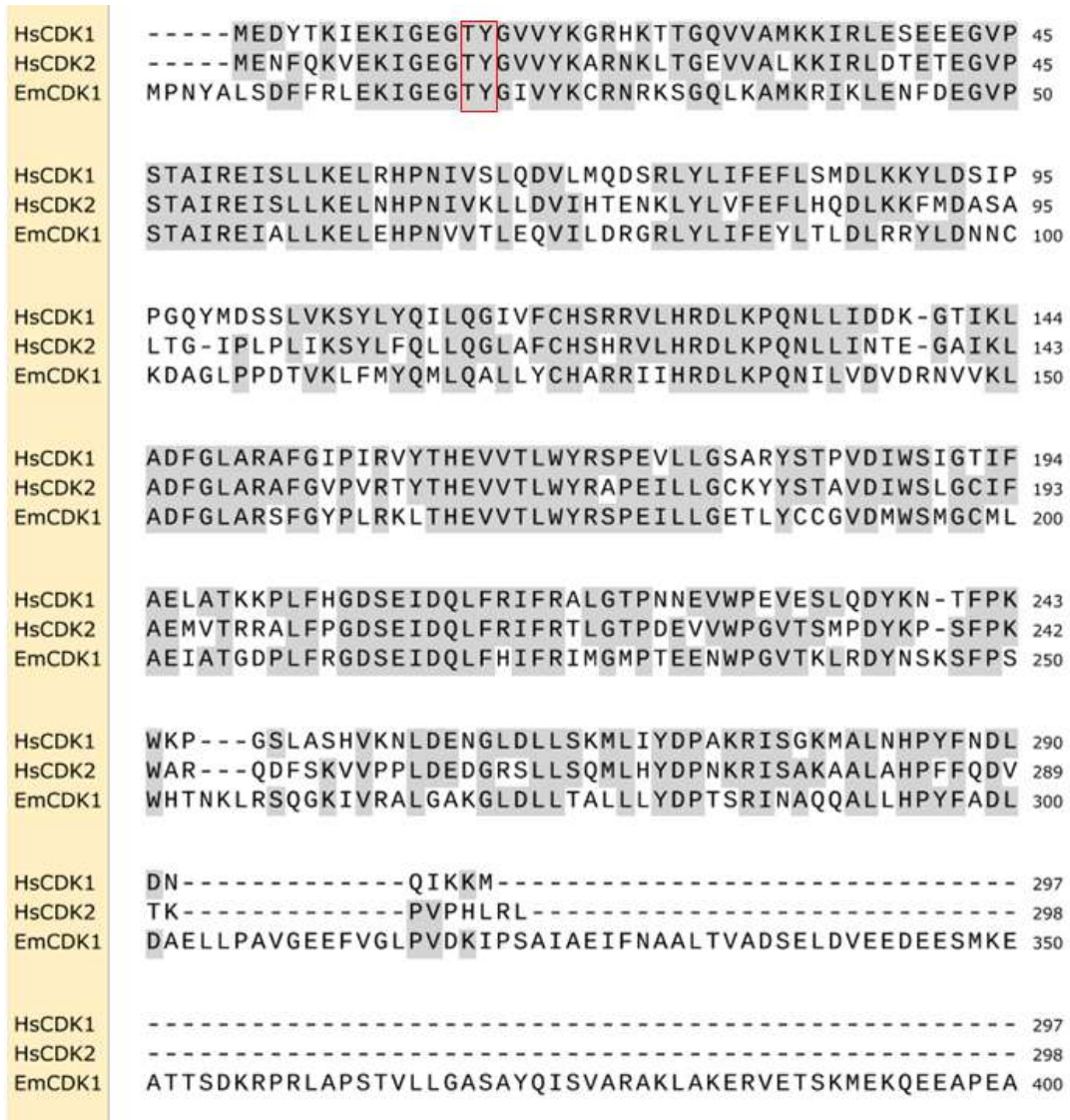


Figure 30: Alignment of human CDK1/2 and EmCDK1

Full-length human CDK1/2 and EmCDK1 are aligned with ClustalW. Gray highlights indicate consensus of residues. The red rectangular indicates target residues of HsPKMYT1, HsWEE1 and HsCDC25A/C.

5. Results

5.2.4 Effects of SGI-1776 and CX6258 on *E. multilocularis*

In the cell viability assay with primary cells (5.1), two pan-PIM inhibitor, SGI-1776 and CX-6258 showed clear detrimental effect. The advantage of cell viability assay is, that we can perform screening of many inhibitors at once with smaller amount of parasite samples. On the other hand, it has the disadvantage of being far away from the state of natural infection. Therefore, I tried these inhibitors on metacestode vesicles *in vitro*, a state closer to the natural infection. Both inhibitors had toxicity against matured metacestode vesicles and altered their structural integrity in dose dependent manner. Especially after 28 days incubation with 10 μ M inhibitors, the laminated layers and germinative layers were completely detached (Fig.31).

Stem cells (germinative cells) of *E. multilocularis* have totipotency and they can regenerate metacestode vesicles. This ability is likely to be correlated with the relapses of AE and impeding vesicle regeneration is important (Brehm and Koziol, 2014). Therefore, I tried vesicle formation assay and evaluated the ability of these two inhibitors to stop vesicle regeneration from primary cells, which include high percentage of stem cells. Without any inhibitor, stem cells in primary cells can differentiate and regenerate new metacestode vesicles even *in vitro*. However, the number of new vesicles were significantly smaller after 21 days incubation with 10 μ M and 30 μ M of CX-6258. In the case of SGI-1776, the difference was not statistically significant with 10 μ M but no vesicles were regenerated with 30 μ M (Fig.32).

5. Results

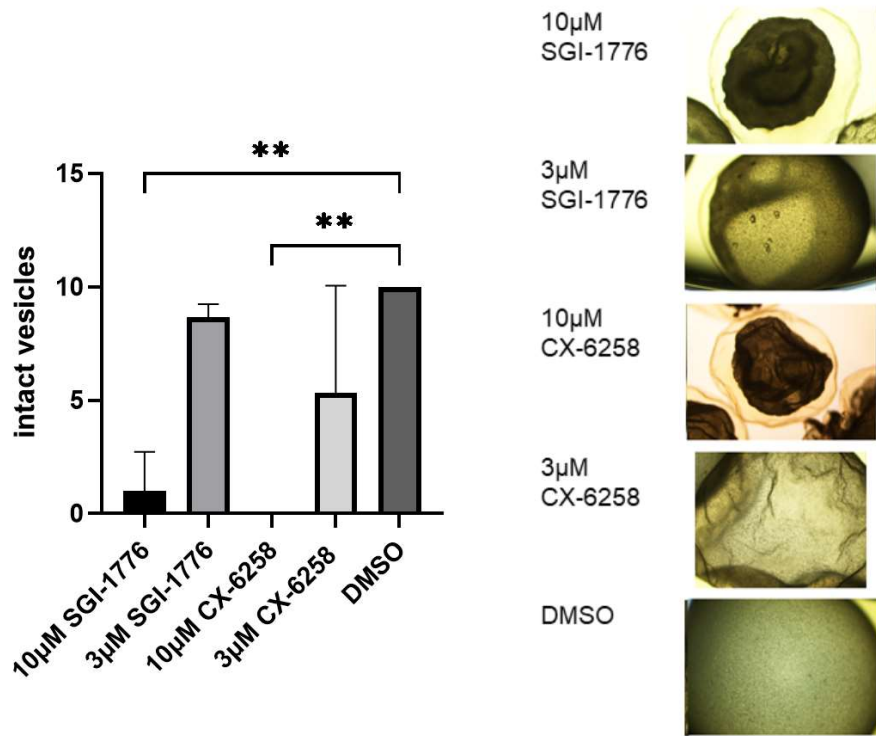


Figure 31: Damage on matured metacystode vesicles by commercially available inhibitors
Matured vesicles were treated with commercially available inhibitors for 28 days.
Left; The bar graph shows mean number of structurally intact vesicles. The error bars represent standard deviation. One way ANOVA followed by Dunnet's multiple comparison test was used to compare with the control group, DMSO. P values less than 0.0021 are summarized with **.
Right; The picture of structurally altered metacystode vesicles observed under an optical microscope.

5. Results

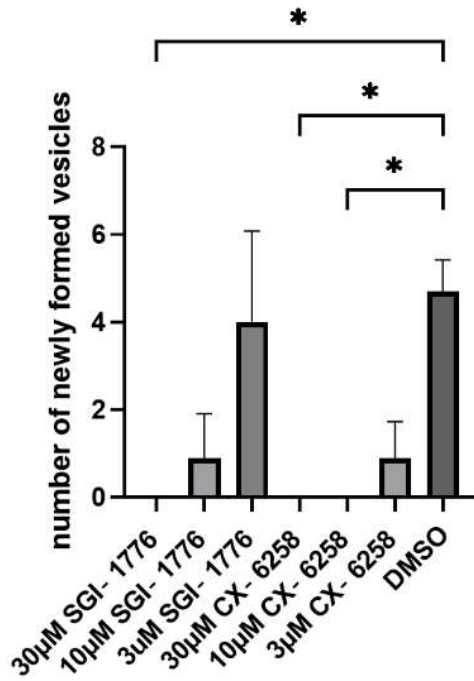


Figure 32: Inhibition of the vesicle regeneration by commercially available inhibitors

Primary cells were incubated with commercially available inhibitors for 21 days. The bar graph shows the number of newly formed vesicles. The error bars represent standard deviation. Kruskal-Wallis test followed by Dunn's multiple comparison test is used to compare with the control group, DMSO. P values less than 0.0332 are summarized with *.

In 5.2.1 and the experiments above (Fig.31-32), SGI-1776 and CX-6258 showed clear detrimental effect on matured vesicle and primary cells of *E. multilocularis*. However, both inhibitors are known to inhibit two kinases far away from CAMK group, receptor tyrosine kinase FLT3 and HASPIN (Chen *et al.*, 2009; Haddach *et al.*, 2012; Melms *et al.*, 2020). When I used HsFLT3 for the query of blastp analysis, no protein was identified in the protein database of *E. multilocularis*. In contrast, two proteins (EmuJ_000667600.1, EmuJ_001165000.1) were identified when I used HsHASPIN as the query. I named them HASPIN1 and HASPIN2, respectively. According to the expression data from Tsai *et al.*, the

5. Results

expression level of HASPIN1 was relatively stronger, but that of HASPIN2 was negligible (Tsai *et al.*, 2013).

There is no previous research about the interaction between SGI-1776 and HsPIM1, but the interaction between CX-6258 and HsPIM1 already has been studied (Bogusz *et al.*, 2017). They identified that 14 residues are especially important for the interaction. To consider whether CX-6258 inhibits EmpPIM, I detected kinase domain of HsFLT3 by SMART analysis (Letunic and Bork, 2018; Letunic *et al.*, 2015; Letunic *et al.*, 2021) When I aligned it with kinase domain of PIM kinases, at least gatekeepers and DFG motifs of PIM kinases and HsFLT3 were aligned like below (Fig.33).



Figure 33: Alignment of kinase domain of HsFLT3 and PIM kinases

Kinase domains of HsPIM1, EmPIM, and HsFLT3 were aligned with ClustalW. Grey highlights indicate residues identical to HsPIM1. DFG motifs is shown under the alignment. 14 residues important for the interaction with CX-6258 (Bogusz *et al.*) are shown with black arrowheads. The alphabet and number next to the arrowheads indicates the residue and position in HsPIM1.

5. Results

The same as alignment with HsFLT3, I detected HASPIN kinase domain of HASPINs by SMART analysis and aligned them with kinase domain of PIM kinases (Fig.34).

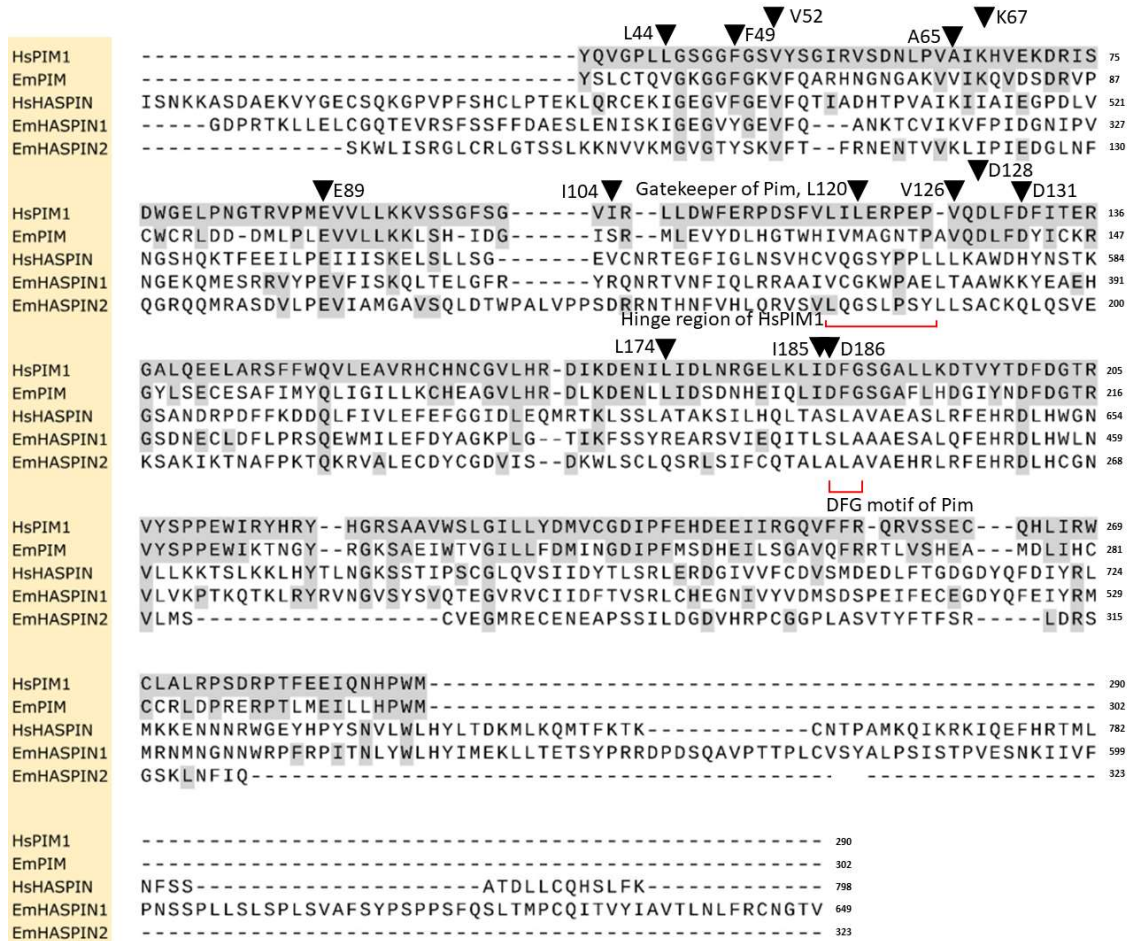


Figure 34: Alignment of kinase domain in PIM kinases and haspin kinase domain in HASPINs

Amino acid sequence of the kinase domains and haspin kinase domains were aligned with ClustalW. Grey highlights indicate residues identical to HsPim1. DFG motifs and the hinge region of HsPIM1 are shown under the alignment. 14 residues important for the interaction with CX-6258 (Bogus et al.) are shown with black arrowheads. The alphabet and number next to the arrowhead indicates the residue and position in HsPIM1.

As indicated in 3.2.2 (Fig.4), the structure of HsHASPIN is quite different from other kinases. Most of kinses have DFG motifs, but HASPINs are exception.

5. Results

Among 14 residues important for HsPIM1-CX-6258 interaction, 9 residues are identical in EmPIM (Fig.21). However, only 7 residues were identical in HsFLT3 (Fig.33). Therefore, we can expect that EmPIM has stronger affinity to CX-6258 than HsFLT3, which is known to interact weakly with CX-6258. On the other hand, 2 or 3 out of 14 residues were identical, when I compare HsPIM1 and HASPINs. As for the similar residues, 11 out of 14 residues in EmPIM are similar or identical to HsPIM1, but 4-6 residues in HASPINs are similar or identical (Fig.21, Fig.34). The similarities/identities of 14 important positions of each protein shown in three alignments (Fig.21, Fig.33, Fig.34) are summarized in Table 26 below.

| | HsPIM1 | HsPIM2 | HsPIM3 | EmPIM | SmPIM | HsFLT3 | HsHASPIN | EmHASPIN 1 | EmHASPIN 2 |
|-----------------------------------|-------------|--------|--------|-------|-------|--------|----------|------------|------------|
| | <u>L44</u> | L38 | L44 | V54 | F47 | L616 | I490 | I299 | M101 |
| | <u>F49</u> | F43 | F49 | F59 | F52 | F621 | F495 | Y304 | Y106 |
| | <u>V52</u> | V46 | V52 | V62 | V55 | V624 | V498 | V307 | V109 |
| | <u>A65</u> | A59 | A65 | V75 | V68 | V637 | K511 | K317 | K120 |
| | <u>K67</u> | K61 | K67 | K77 | K70 | I639 | I513 | F319 | I122 |
| | <u>E89</u> | E83 | E90 | E100 | E93 | E661 | E527 | E333 | E136 |
| | <u>I104</u> | I100 | I107 | S114 | V107 | V675 | V549 | R356 | D165 |
| | <u>L120</u> | L116 | L123 | M130 | M123 | F691 | G567 | G379 | G183 |
| | <u>V126</u> | A122 | A129 | V137 | T130 | S762 | L574 | T381 | L190 |
| | <u>D128</u> | D124 | D131 | D139 | D132 | D764 | A576 | A383 | A192 |
| | <u>D131</u> | D127 | D134 | D142 | D135 | E767 | H579 | K386 | Q195 |
| | <u>L174</u> | L170 | L177 | S185 | R178 | L175 | A623 | R428 | Q237 |
| | <u>I185</u> | I181 | I188 | I196 | I189 | C828 | A634 | L439 | L248 |
| | <u>D186</u> | D182 | D189 | D197 | D190 | D829 | S635 | S440 | A249 |
| identical residues | 14 | 13 | 13 | 9 | 8 | 7 | 3 | 2 | 2 |
| similar residues | 0 | 1 | 1 | 2 | 2 | 2 | 6 | 4 | 4 |
| IC ₅₀ of CX-6258 (nM) | 5 | 25 | 16 | | | 134 | | | |
| IC ₅₀ of SGI-1776 (nM) | 7 | 363 | 69 | | | 44 | 34 | | |

Table 26: 14 residues important for HsPIM-CX-6258 interaction in different kinases.

The number of identical or similar residues in PIM kinases, HASPINs and FLT3 are shown. Identical residues are indicated in yellow highlights and similar residues are indicated in green highlights. The total numbers of identical/similar residues in each protein are shown in the middle of the table. IC₅₀ of two inhibitors against each protein is shown in the below of the table.

5. Results

The target of HsHASPIN is Thr3 of HsHiston3. When I used human Histon H3.1-3.3 as queries of blastp analysis, only one protein was identified in the protein database of *E. multilocularis*. I named it EmHiston H3. These proteins were highly conserved and percent identity was over 96% regardless of the combination. Especially, percent identity and percent similarity between HsHiston H3.3 and EmHiston H3 were 99.26% and 100% respectively. Overall sequences, including those around the target residue Thr3 were very well-conserved (Fig.35). When human histon3 is translated, Thr3 and Ser10 are 4th and 11th residues, but the initiation methionine is removed later (Chen et al., 2021). Therefore, they are generally called Thr3 and Ser10.

| | ▼Thr3 | ▼Ser10 | |
|---------------|---|--------|-----|
| EmHiston H3 | MARTKQTARKSTGGKAPRKQLATKAARKSAPSTGGVKKPH | | 40 |
| HsHiston H3.1 | MARTKQTARKSTGGKAPRKQLATKAARKSAPATGGVKKPH | | 40 |
| HsHiston H3.2 | MARTKQTARKSTGGKAPRKQLATKAARKSAPATGGVKKPH | | 40 |
| HsHiston H3.3 | MARTKQTARKSTGGKAPRKQLATKAARKSAPSTGGVKKPH | | 40 |
| EmHiston H3 | RYRPGTVALREIRRYQKSTELLIRKLPFQRLVREIAQDFK | | 80 |
| HsHiston H3.1 | RYRPGTVALREIRRYQKSTELLIRKLPFQRLVREIAQDFK | | 80 |
| HsHiston H3.2 | RYRPGTVALREIRRYQKSTELLIRKLPFQRLVREIAQDFK | | 80 |
| HsHiston H3.3 | RYRPGTVALREIRRYQKSTELLIRKLPFQRLVREIAQDFK | | 80 |
| EmHiston H3 | TDLRFQSAAVGALQEASEAYLVGLFEDTNLCAIHAKRVTI | | 120 |
| HsHiston H3.1 | TDLRFQSSAVMALQEACEAYLVGLFEDTNLCAIHAKRVTI | | 120 |
| HsHiston H3.2 | TDLRFQSSAVMALQEASEAYLVGLFEDTNLCAIHAKRVTI | | 120 |
| HsHiston H3.3 | TDLRFQSAAIIGALQEASEAYLVGLFEDTNLCAIHAKRVTI | | 120 |
| EmHiston H3 | MPKDIQLARRIRGERA | | 136 |
| HsHiston H3.1 | MPKDIQLARRIRGERA | | 136 |
| HsHiston H3.2 | MPKDIQLARRIRGERA | | 136 |
| HsHiston H3.3 | MPKDIQLARRIRGERA | | 136 |

Figure 35: Alignment of human and *Echinococcus* Histon H3

Full-length Histon H3 from *E. multilocularis* and human are aligned with ClustalW. The black arrowheads indicate positions of Thr3 and Ser10.

5. Results

5.2.5 *In silico* screening of EmPIM inhibitors

In this doctoral dissertation, analysis described in bold letters is done by our collaborators.

SGI-1776 and CX-6258 showed toxicity strong enough to damage metacystode vesicles to stop regeneration from primary cells. However, their toxicities are also high to human and chemotherapeutic approach with pan-PIM kinase inhibitors accompanies adverse side effect (Chen et al., 2011; Cortes et al., 2018; Raab et al., 2019). SGI-1776 once proceeded to clinical trial of leukemia and non-hodgkin's lymphoma, but because of the adverse side effect such as QT-elongation, both clinical trials have been aborted (NCT00848601, NCT01239108). CX-6258 even has not proceeded to clinical trial. Therefore, clinical use of these inhibitors for the treatment of AE is clearly impractical. To target EmPIM as a parasiticide, it is necessary to develop compounds with selective toxicities. **As described in 4.8.2, Dr. Kim and Dr. Zhang in the United States analyzed EmPIM *in silico* and made the first list of compounds (Appendix 8.1) which potentially have affinities to EmPIM. Based on the first list, Dr. Becker, Dr. Sennhenn and Dr. Hannus made the final list of 20 compounds and ordered SIA Enamine to synthesize them in small scale.** The structure and detailed information of these 20 compounds are included in Appendix 8.2. In the first screening, 20 compounds are tested on matured vesicles in small scale without replicates. 4 out of 20 compounds (Z30898879, Z196138710, Z65225039, Z354576500) which showed some toxicities on the matured vesicles (Fig.36 left). They are also tested on primary cells and only Z196138170 among the 4 compounds inhibited vesicle regeneration with the concentration of 10 μ M (Fig.36 right).

5. Results

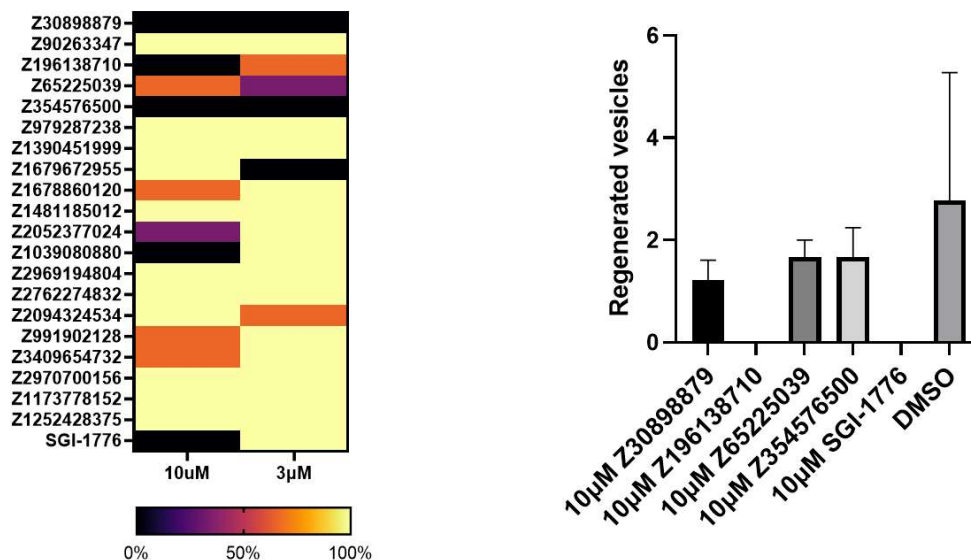


Figure 36: Screening of newly synthesized compounds with *E. multilocularis* in vitro

(Left) Newly synthesized 20 compounds are tested on matured vesicles with small scale. The percentage of structurally intact vesicles after 28 days of incubation are shown in the heatmap.

(Right) 4 compounds which showed relatively stronger toxicity on metacestode vesicels were tested on primary cells, together with DMSO and 10µM SGI-1776 to evaluate the effect on vesicle regeneration. Mean number of regenerated vesicles after 21 days of incubation is shown. The error bar represents standard deviation.

Because of the inhibition of vesicle regeneration, we focused on Z196138170 (*N*-(4-(difluoromethoxy)-3-methoxybenzyl)-thieno-[3,2-*d*]-pyrimidin-4-amine) and tried it on matured vesicles (Fig.37 left) and primary cells with 3 biological replicates (Fig.37 right). This compounds showed toxicity against matured vesicles and primary cells comparable to commercially available inhibitor SGI-1776.

5. Results

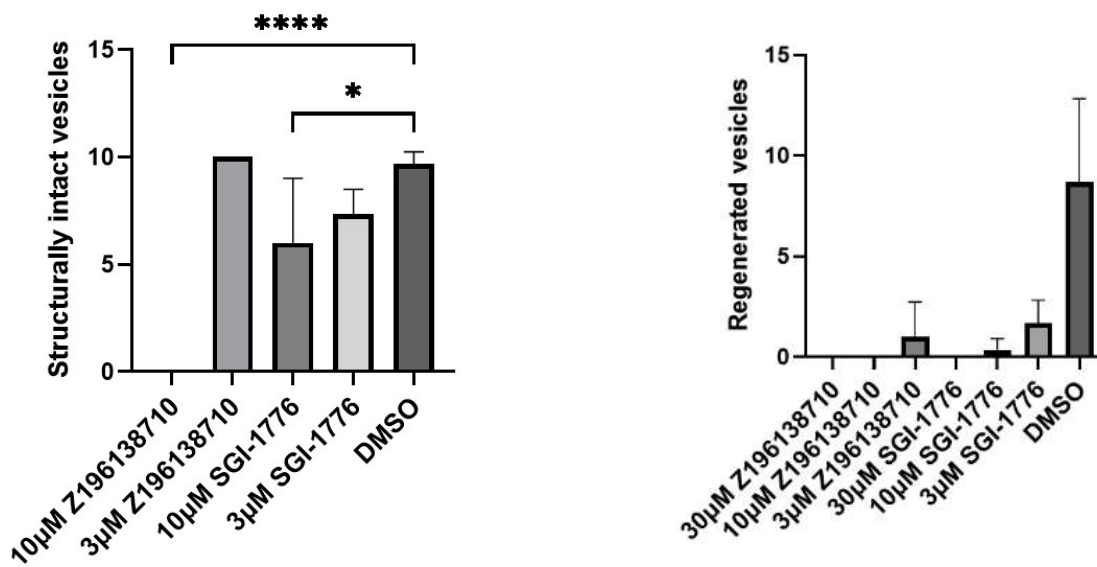


Figure 37: The effect of newly synthesized compound Z196138710 and commercially available inhibitor SGI-1776 against *E. multilocularis*

(left) The effect of Z196138710 on the matured metacestode vesicles was evaluated after 28 days of incubation. Mean number of structurally intact vesicles are shown. The error bar represents standard deviation. One way ANOVA followed by Dunnet's multiple comparison test was used to compare with the control group, DMSO. P values less than 0.0001 are summarized with **** and p values less than 0.0332 are summarized with *.

(right) The effect of Z196138710 on the regeneration of vesicles from primary cells was evaluated after 21 days of incubation. Mean numbers of regenerated vesicles are shown. The error bar represents standard deviation.

Because Z196138710 showed satisfactory toxicity against both matured vesicles and primary cells, I decided to evaluate its toxicity against human cell lines, HEK293T and HepG2. Several studies have shown that cell viability of these cell lines is likely to be correlated with functional PIM kinases (Herzog et al., 2015; Kronschnabl et al., 2020; Yu et al., 2014). The toxicity was evaluated with cell viability assay after 3 days of incubation with inhibitors. The toxicity against human cell lines HEK293T (Fig.38 left) and HepG2 (Fig.38 right) of the Z196138170 was relatively limited, compared with the severe toxicities of SGI-1776 and CX-6258. In fact, with all concentration from 3µM to 30µM, Z196138160 showed

5. Results

significantly weaker toxicity than both commercially available inhibitors. From the experiments of Fig.36-38, we can conclude that Z196138170 has selective toxicity.

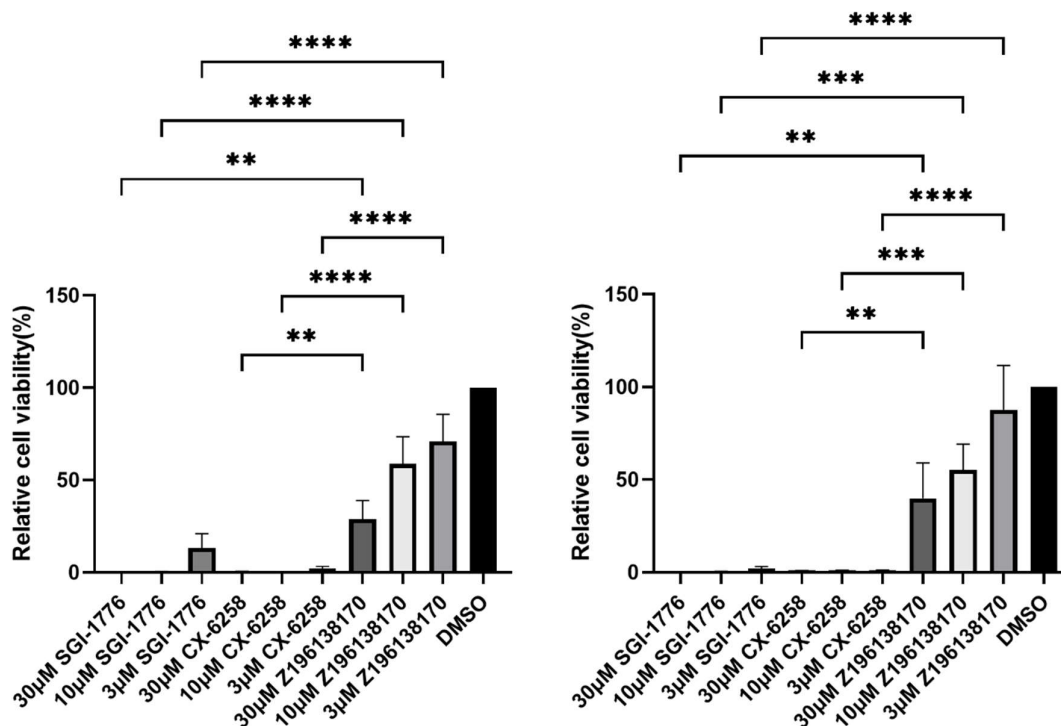


Figure 38: Effect of newly synthesized compound Z196138170 and commercially available inhibitor SGI-1776 against mammalian cell lines

After three days of incubation with SGI-1776, CX-6258 and Z196138170, the cell viability of mammalian cell lines HEK293T (left) and HepG2 (right) was measured. The relative cell viability normalized with DMSO is shown as percentage. The error bar represents standard deviation. P values less than 0.0021, 0.0002, and 0.00001 are summarized with **, *** and **** respectively.

The effect of Z196138170 on cell viability of human cell lines was relatively limited. However, cell viability just reflects number of alive cells, and it is difficult to conclude from this data that the affinity of Z196138170 against human PIM kinases is weaker than that of commercially available inhibitors. Therefore, I asked our collaborator to analyze affinities between HsPIM1 and Z196138170 *in silico*. For *in silico* analysis, 3D data of the protein was necessary. 3D data of EmPIM1 are not available, but the data of HsPIM1 are deposited in the databases. Therefore, only the affinity against HsPIM1 was predicted.

5. Results

Dr. Sennhenn used SeeSAR modelling analysis with the deposited 3D data of HsPIM1. The affinity of SGI-1776 against ATP binding pocket of PIM1 was nM level. This does not contradict to the previous research (Chen *et al.*, 2009). In contrast, the affinity of Z196138710 was μM level and it was weaker than that of SGI-1776 (Fig.36-38). Therefore, we can conclude that Z196138710 has lower toxicity to HsPIM1 than SGI-1776.

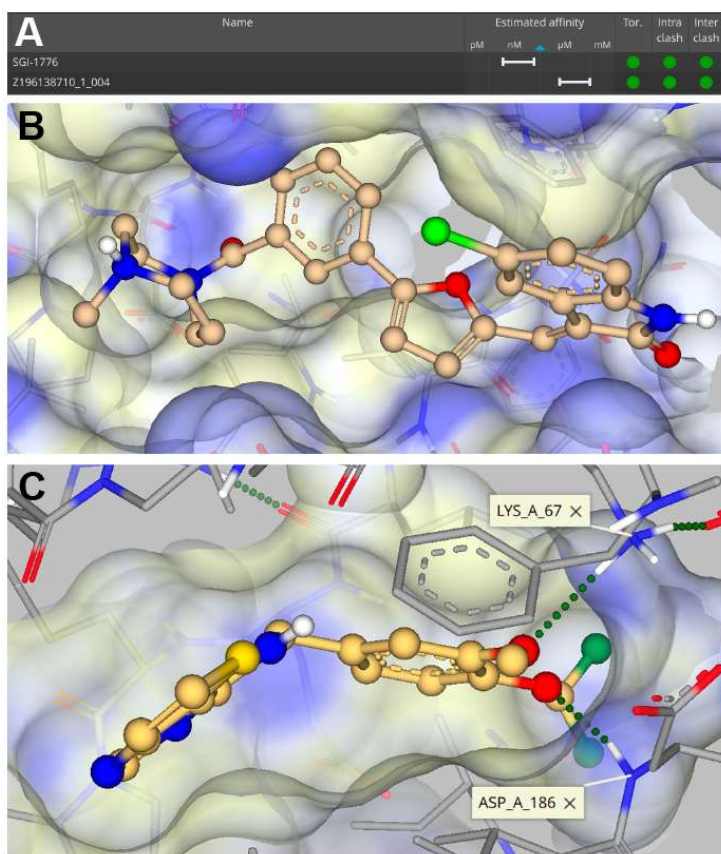


Figure 39: SeeSAR modeling analysis of binding to HsPIM1.

(A) Estimated binding affinity of SGI-1776 and Z196138710 to the ATP-binding pocket of HsPIM1.

(B) Model of SGI-1776 binding to the ATP-binding pocket of HsPIM1.

(C) Model of Z196138710 binding to the ATP-binding pocket of HsPIM1.

5. Results

5.3 Tubulins

5.3.1 Comparison of Echinococcus tubulins and Robinson's model of *H. contortus*

To consider which residues are important for the interaction of benzimidazoles and β -tubulins of *E. multilocularis*, I analyzed amino acid sequences of β -tubulins once more. The comparison of 200th position has been shown previously (Koziol and Brehm, 2015) and they focused on also to 167th position later, but not only 167th and 200th position is correlated with BZ resistance.

Robinson et. al. made a model of interaction between albendazole-sulfoxide (ABZSX) and *Haemonchus contortus*'s β -tubulin (deposited in theoretical models section of the RCSB Protein Data Bank, PDB entry: 1OJ0). In this model, residues which form the putative binding site are shown. Most of them are also residues correlated to BZ resistance. These residues are also They described that tubulin as isotype 12-16 (Robinson *et al.*, 2004). However, no protein data was deposited in WormBase ParaSite under that name. I analyzed the sequence on his paper with blastp and that tubulin proved to be identical to *Haemonchus contortus* β -tubulin isotype2 (tbb-isotype-2 HCON_00043670). Therefore, the sequence is used for the alignment here as HcTubB2.

5. Results

Based on the alignment (Fig.40), I summarized residues at important positions for the interaction between ABZSX and HcTubB2.

| Position | 6 | 50 | 134 | 165 | 167 | 198 | 200 | 257 |
|----------|---|----|-----|-----|-----|-----|-----|-----|
| HcTubB2 | H | Y | Q | S | F | E | F | M |
| EmTubB1 | H | Y | Q | N | F | E | F | M |
| EmTubB2 | H | Y | Q | V | Y | E | Y | M |
| EmTubB3 | H | Y | Q | T | F | E | F | M |

Table 27: Comparison of important residues in tubulins of *E. multilocularis* with Robinson's model of HcTubB2

Residues of HcTubB2 which form ABZSX binding site and residues in Echinococcus tubulins of those positions are shown. Yellow highlights indicate residues identical to those of HcTubB2, and green highlights indicate residues similar to those of HcTubB2. This table is based on the alignment of Fig.40

Other than 167th and 200th position, the difference in 165th might be important. Asn and Thr at 165th position of EmTubB1/EmTubB3 belong to the same group as Ser on HcTubB2, but Val at 165th position belongs to different group.

5. Results

5.3.2 Effect of TCBZ on metacestode vesicles

5.3.2.1 EdU positive cells and structural alternation detectable under an optical microscope

From the experiments of former members in AG Brehm, expression of EmTubB2 in stem cells and resistance of stem cells against ABZ have already been indicated (Brehm, personal communication). Therefore, AG Brehm members have looked for compounds which damage stem cells.

As we see in 5.3.1, the position around 165th - 200th in β -tubulins are generally important for the interaction with ABZSX and most of other benzimidazoles (BZs), and EmTubB2 has several residues important for BZ resistance (3.5).

Triclabendazole (TCBZ) and ABZ seems to interact with different regions in β -tubulin (Fetterer, 1986; Ranjan *et al.*, 2017; Robinson *et al.*, 2001). One β -tubulin isotype of *Fasciola hepatica* FhTubB1 has Tyr200, and this residue is correlated with BZ-resistance. In the experiment by Stitt and Fairweather, TCBZSX inhibited mitosis of spermatogenic cells in the testes of adult *Fasciola hepatica* (Stitt and Fairweather, 1992). According to the recent data from single cell RNA seq analysis of adult *F. hepatica*, FhTubB1 is expressed specifically and strongly in testes (Häberlein, personal communication). These results and analysis indicate that TCBZ works on FhTubB1 with Tyr200 in spermatogenic cells of *F. hepatica*. Therefore, we expected that TCBZ might have effect on EmTubB2 in stem cells, regardless of the sequences around 165th-200th.

As the first experiment of this project, triclabendazole-sulfoxide (TCBZSX, TCBZ is metabolized into TCBZSX in mammalian hosts) and combination of ABZ/TCBZSX on metacestode vesicles were tried, since we already had the idea of combining ABZ and TCBZ for AE treatment.

5. Results

Matured metacystode vesicles were treated with 0-30 μ M TCBZSX for 10 days, with or without 0-10 μ M ABZ. 30 μ M TCBZSX treatment without ABZ did not result in structural disintegration, even though this concentration is lethal for *Fasciola hepatica in vitro*. At least under an optical microscope, no detectable phenotypes were observed. In contrast, regardless of the concentration of TCBZSX, the structure of metacystode vesicles were severely altered by 10 μ M ABZ. Especially germinal layer and tegument of the vesicles were completely disintegrated after the treatment with 10 μ M ABZ + 30 μ M TCBZ (Fig.41).

5. Results

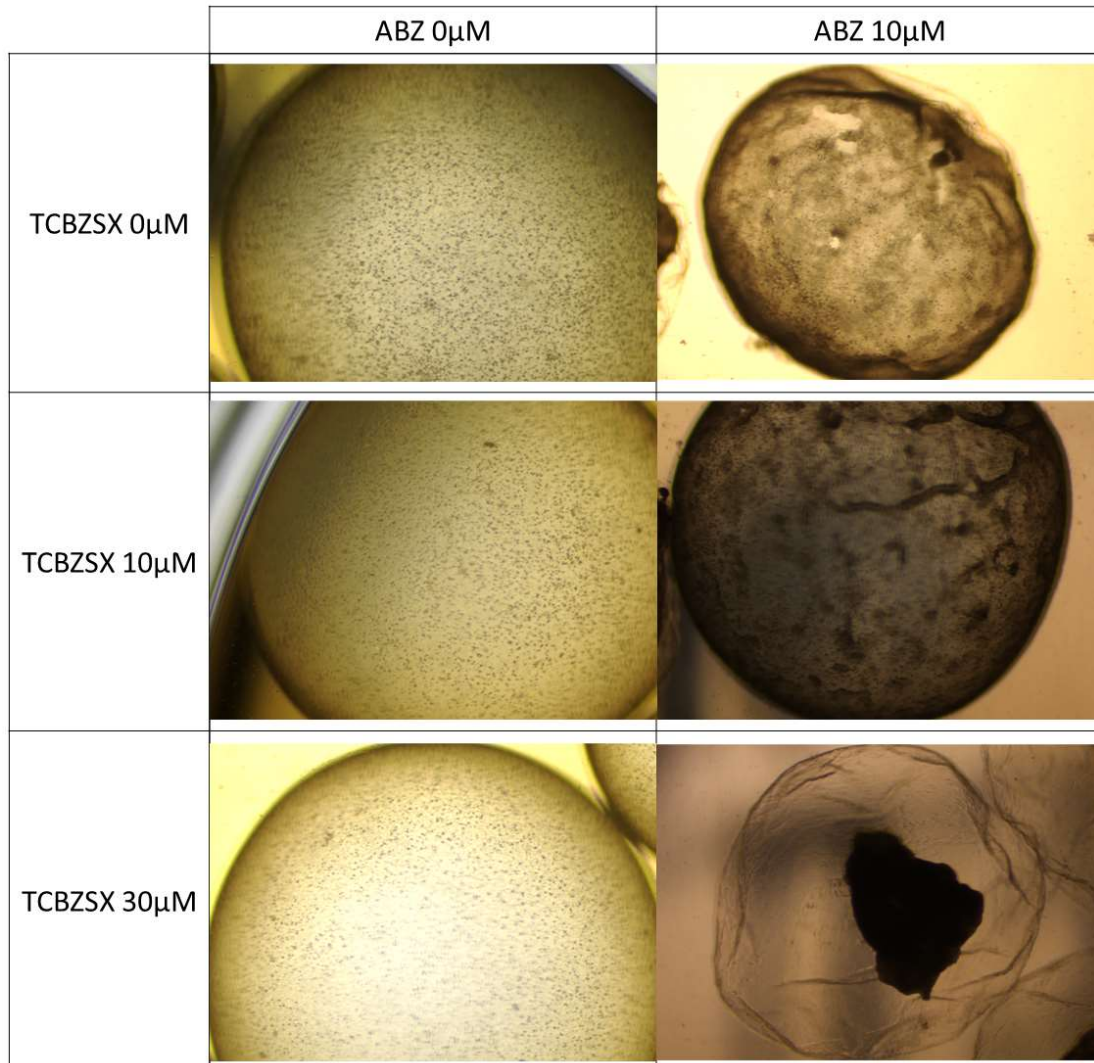


Figure 41: Matured vesicles treated with TCBZSX and ABZ

The vesicles were treated with 0-30 μ M TCBZSX and 0-10 μ M ABZ for 10 days. ABZ 0 μ M + TCBZSX 0 μ M means treatment with DMSO.

It is impossible to estimate the damage to stem cells just by observing vesicles through an optical microscope. To evaluate the damage to actively proliferating stem cells, I labelled these vesicles with 5-Ethynyldeoxy-2'-uridine (EdU), the marker of proliferating cells in S phase. After the development of EdU, clear phenotype was visualized through a confocal microscope (Fig.42).

5. Results

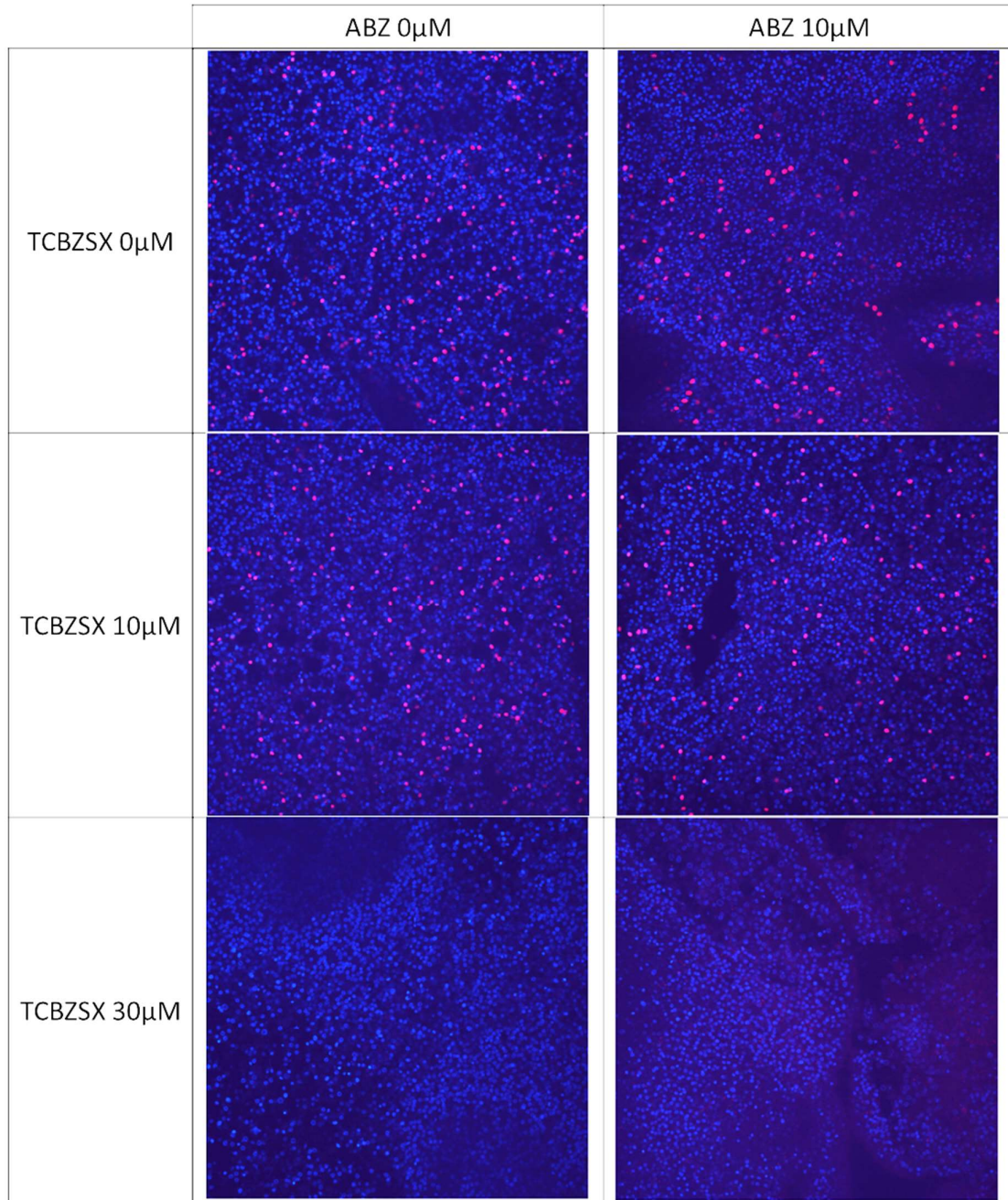


Figure 42: Matured vesicles labelled with EdU after BZ treatment

Red signals are from EdU (marker of actively proliferating cells in S phase) and blue signals are from DAPI (marker of nuclear DNA). 0 μ M ABZ + 0 μ M TCBZSX means DMSO treatment.

5. Results

The number of EdU positive cells in the germinal layer of each vesicles were counted independently and the density of EdU positive cells in germinal layer was calculated (Fig.43).

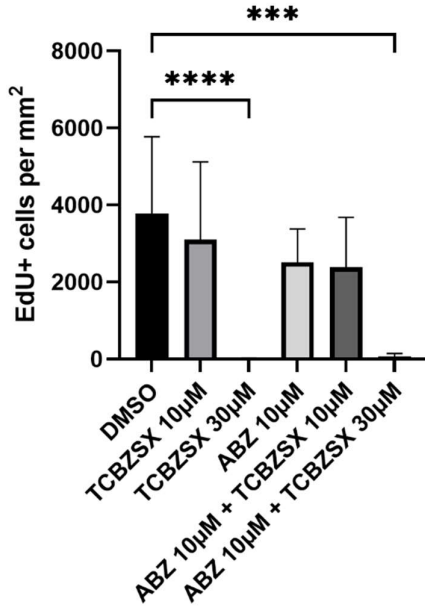


Figure 43: EdU positive cells after treatments with BZs

Metacostode vesicles were treated with TCBZSX 0-30µM, ABZ 0-10µM and combinations of them for 10 days. The number of EdU+ cells were counted and calculated as cell number per mm². The error bars represent standard deviation. Kruskal-Wallis test followed by Dunn's multiple comparison test was used to compare with the control group, DMSO. P values less than 0.0002 are summarized with *** and p values less than 0.0001 are summarized with ****.

From this experiments, treatment with 30µM TCBZSX for 10 days can eliminate most of EdU positive cells but it did not alter the structure. In contrast, 10µM ABZ treatment for 10 days was enough to destroy the structure of vesicles, but the damage against actively proliferating stem cells seems to be limited.

Next, I simply incubated the vesicles with TCBZ and TCBZSX, to try severer conditions. 10days was not enough to change the structure but the structures of the vesicles were damaged after 14 days and 28 days. The number of intact vesicles are shown in the figures below (Fig.44).

5. Results

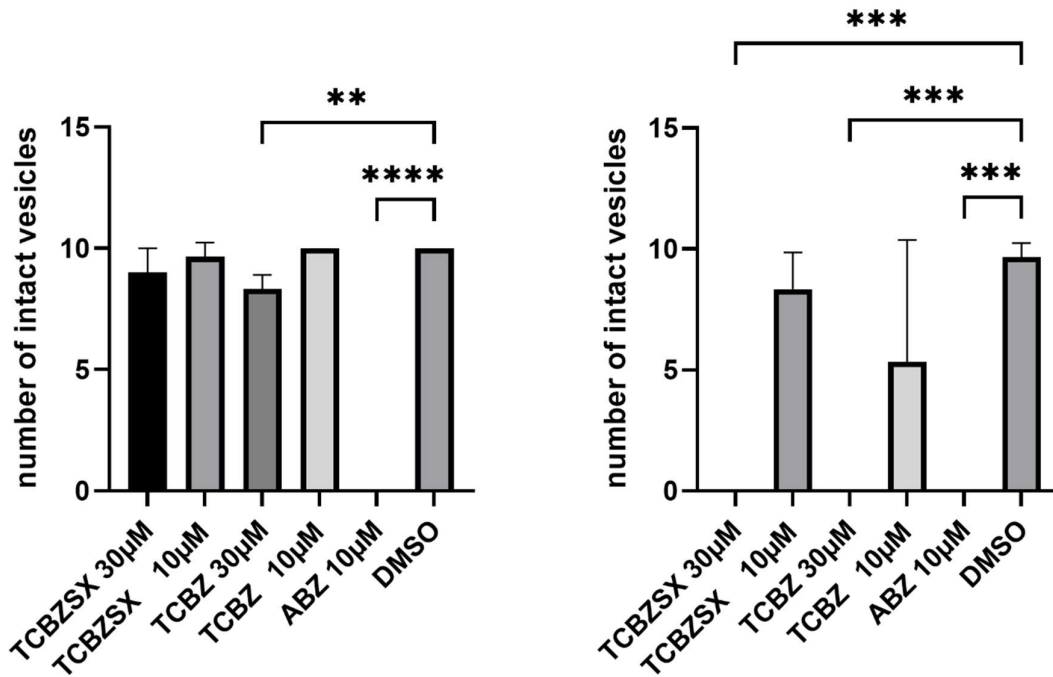


Figure 44: Damages of matured vesicles treated with 3 benzimidazoles
 Left: 14th day of treatment Right: 28th day of treatment
 The number of structurally intact vesicles are shown in the bar graph. The error bars represent standard deviation. One-way ANOVA followed by Dunnet's multiple comparison test is used to compare with the control group, DMSO. P values less than 0.0021, 0.002 and 0.0001 are summarized with **, *** and **** .

These results indicate that 30µM TCBZSX can cause structural damage with longer incubation, although ABZ can damage the structure with lower concentration and shorter time.

5. Results

5.3.2.2 TRIM positive cells

EdU only can label stem cells in S phase. In the experiment of 5.3.2.1, there were almost no EdU positive cells after 10 days of 30 μ M TCBZSX incubation. This result just means that there are no actively dividing cells and does not necessarily mean that all stem cells were depleted. To clarify whether there are still inactive stem cells, I tried *in situ* hybridization with EmTRIM. EmTRIM is another marker of stem cells, and different from EdU, it can visualize stem cells regardless of the cell cycle (Koziol *et al.*, 2015). Fortunately, the same plasmid used in the TRIM paper was still left in the freezer and I could synthesize probes from it.

I incubated 20 vesicles for 10 days with 30 μ M TCBZSX or control DMSO and used them for *in situ* hybridization. There were almost no signal with the sample of control probe (sense probe) but with antisense probe, there were very strong signals both with TCBZSX and DMSO samples (Fig.45). The series of images were acquired as Z stack, and layers of the strongest signal are extracted and analyzed.

5. Results

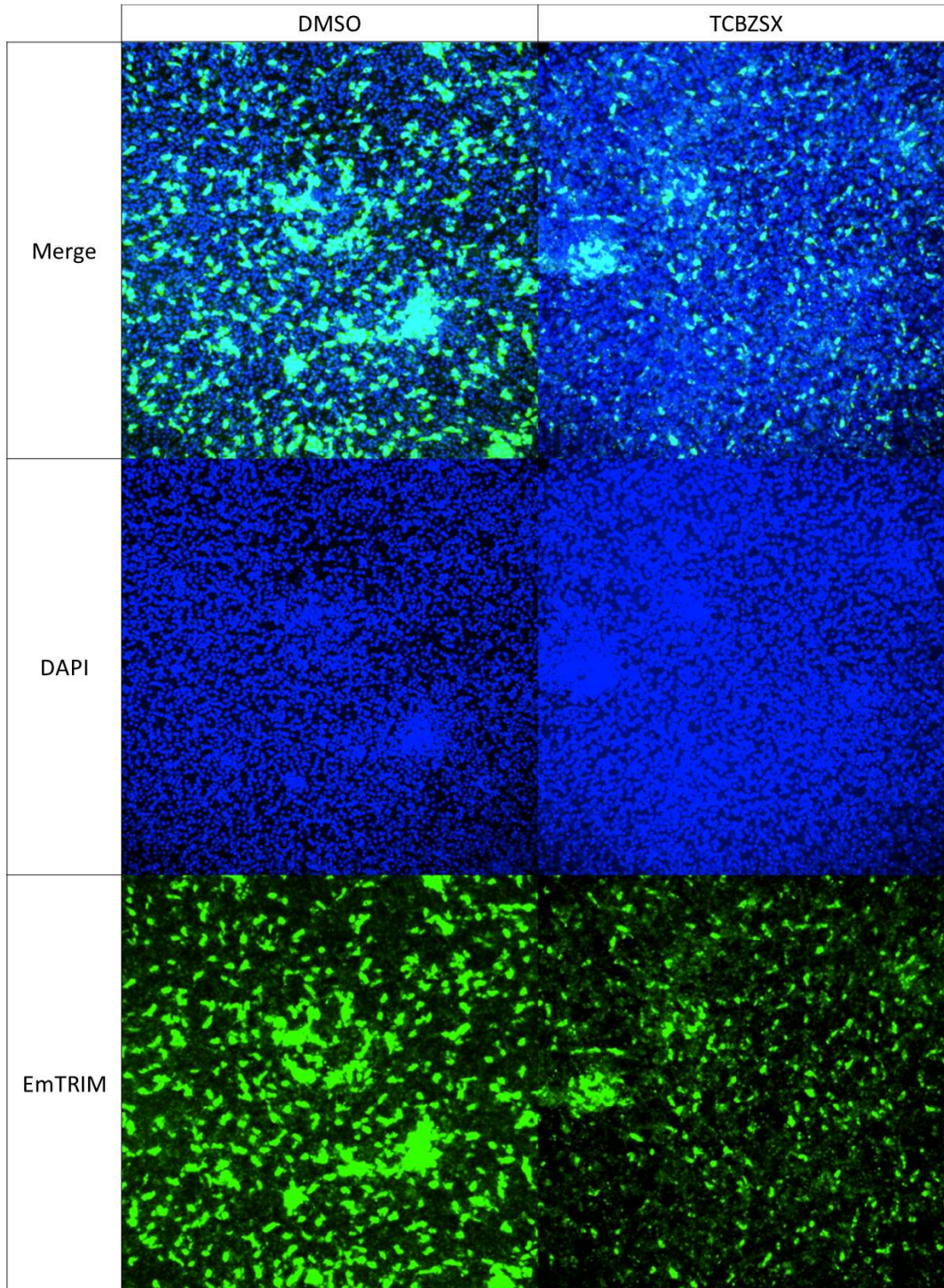


Figure 45: *In situ* hybridization with EmTRIM probe on vesicles treated with TCBZSX

EmTRIM is a marker of stem cells. Different from EdU, EmTRIM is expressed regardless of the cell cycles.

5. Results

Because the signal was too strong, it was impractical to count cells with green signal. Therefore, I divided the images into RGB and measured green and blue area independently. The green area (correlated with the number of EmTRIM positive cells) was normalized with blue area (DAPI signal, correlated with the total cell number). The difference between DMSO and TCBZSX treated samples were statistically significant (Fig.46).

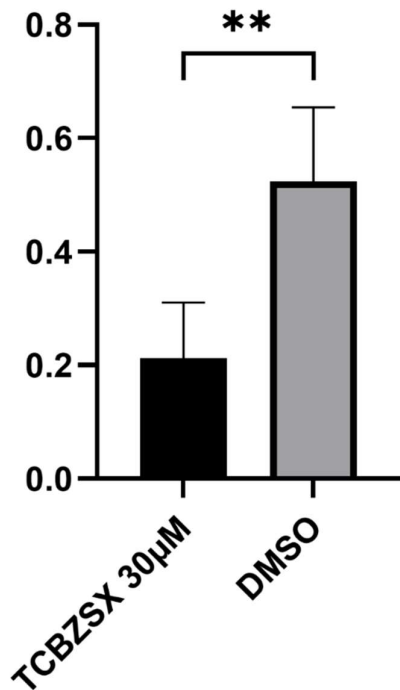


Figure 46: Comparison of EmTRIM signal from treated and untreated vesicles

The area with EmTRIM signal (correlated with stem cell number) was normalized with the area of DAPI signal (correlated with total cells number) and shown in the bar graph.

The error bars represent standard deviation. Mann Whitney test is used to compare with the control group, DMSO. P values less than 0.0021 is summarized with **.

Combined with the result of 5.3.2.1, 30µM TCBZSX can stop cell cycles in 10 days, but stem cells had not been completely depleted in 10 days. Although their number was decreased, some stem cells were alive and were continuously expressing EmTRIM.

5. Results

5.3.2.3 Nerve cells

As far as I observed under an optical microscope, the effect of TCBZSX against differentiated cells in the metacystode vesicles looked limited. Therefore, we tried a marker of nerve cells, as an example of differentiated cells. Acetylated α -tubulin (AcTub) is a marker of stable microtubule. In the stage of metacystode vesicles, only nerve cells include stable microtubule. Koziol et al showed that commercially available AcTub antibody also can recognize nerve cells of *E. multilocularis* and *Mesocystoides corti* (Koziol et al., 2010; Koziol et al., 2013). I treated vesicles with 30 μ M TCBZ, 30 μ M TCBZSX or control DMSO for 10 days and stained them with DAPI and anti AcTub antibody. The images were acquired as a series of layers as Z stack and layers with the strongest signal were extracted and analyzed. The images of each condition were like below (Fig.47). Cell bodies of nerve cell were manually counted and calculated as cells per mm² (Fig.48).

5. Results

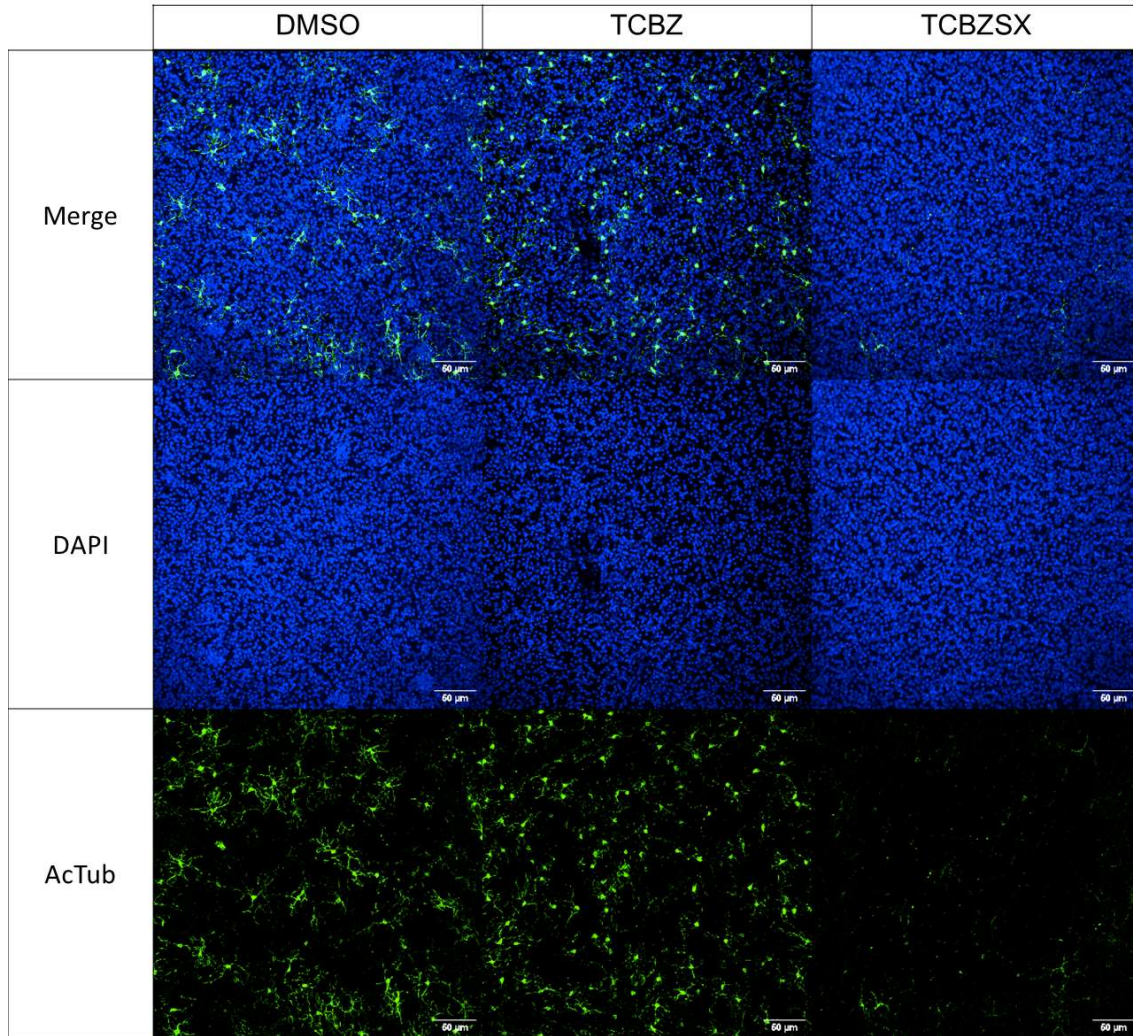


Figure 47: Whole-mount immunofluorescence assay with acetylated α -tubulin on metacestode vesicles treated with TCBZSX and TCBZ

Acetylated α -tubulin (green) is a marker for nerve cells and DAPI (blue) is a marker of nuclear DNA

5. Results

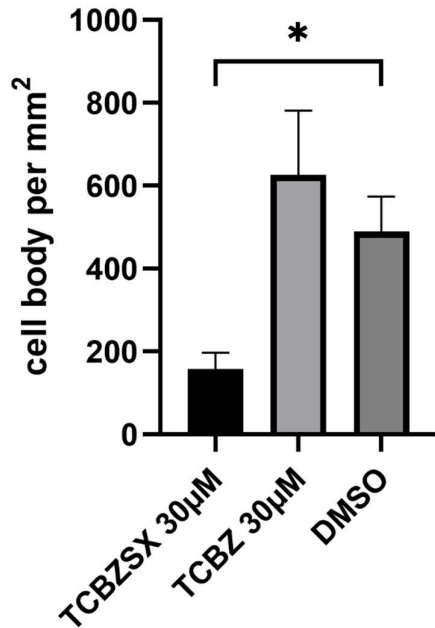


Figure 48: Comparison of the signal from nerve cells between treated and untreated vesicles

The density of cell bodies of nerve cells is shown in the bar graph. The error bars represent standard deviation. Kruskal-Wallis test followed by Dunn's multiple comparison test is used to compare treated groups with the control group, DMSO. P values less than 0.0332 is summarized with *.

There were differences in the number of AcTub positive cells between DMSO and TCBZSX treated vesicles. On the contrary to my expectation, TCBZSX seems to have some detrimental effect on nerve cells. I also tried to stain metacestode vesicles with phalloidin to evaluate the effect on muscle cells, but even the control vesicles, which were treated with DMSO, were not stained appropriately.

5. Results

5.3.3 Effect of TCBZ on the ability of regeneration

From the EdU labelling experiment in 5.4.2.1, we concluded that TCBZSX eliminated actively dividing cells. However, we could not know whether stem cells were irreversibly inactivated, or the cell cycle was transiently blocked. Therefore, I treated metacystode vesicles with 30 μ M TCBZSX for 10 days and isolated primary cells from these vesicles. After isolation of primary cells, no inhibitor was added. If stem cells were not irreversibly inactivated, they should aggregate and regenerate new vesicles. However, even after 28 days, no aggregation nor regeneration was observed in the well of primary cells from treated vesicles. On the other hand, vesicles were newly regenerated in the control well (Fig.49).

5. Results

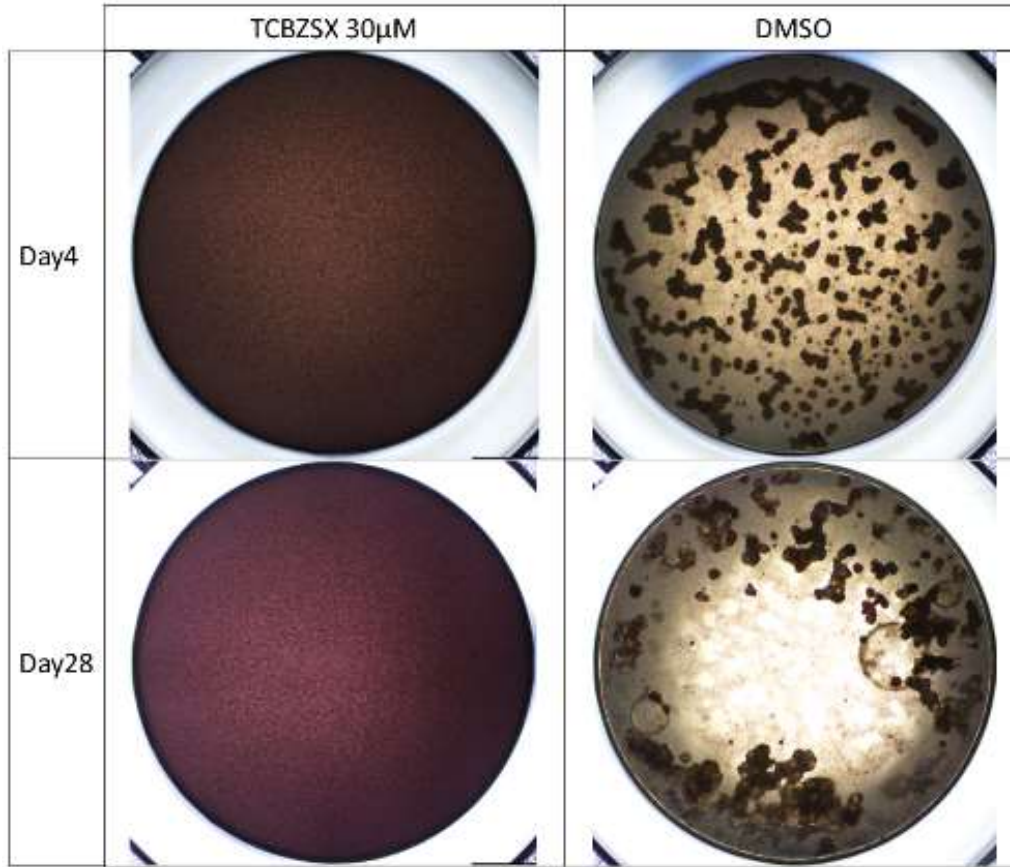


Figure 49: Vesicle regeneration out of primary cells from treated and untreated vesicles

Metacestode vesicles were treated with 30 μ M TCBZSX or DMSO for 10 days. The primary cells isolated from these vesicles were incubated for 28 days without any inhibitors. The pictures were taken on 4 the days to evaluate aggregation, and on 28 days to evaluate regeneration.

It was obvious even without calculation, but there was significant difference between treated and control groups (Fig.50).

5. Results

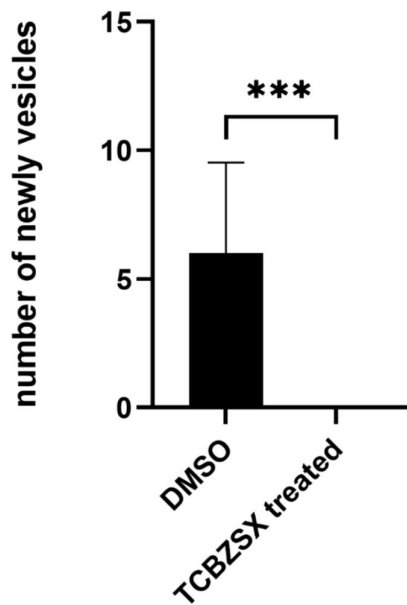


Figure 50: Number of newly formed vesicles from treated and untreated vesicles

Number of newly formed vesicles per well were counted and average number of vesicles are shown. The error bars represent standard deviation. Mann-Whitney test is used for the comparison.

P values less than 0.0002 is summarized with ***.

5. Results

5.3.4 Effect of TCBZ on isolated primary cells

Next, I tried TCBZSX on isolated primary cells. Opposite to the experiment in 5.4.3, the vesicle had never been treated with any inhibitors. Instead, primary cells after isolation were treated with TCBZSX for 21 days. The number of regenerated vesicles is shown in the figure below (Fig.51). The same as the experiment on vesicles with TCBZSX (5.3.2), 10 μ M seems to be not enough for both TCBZ and TCBZSX to completely inactivate stem cells.

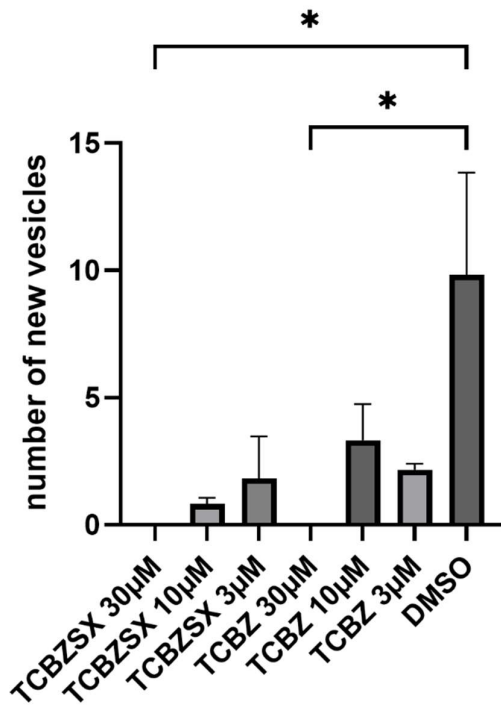


Figure 51: Number of newly formed vesicles from treated and untreated primary cells The bar graph shows the number of regenerated vesicles per well. The error bars represent standard deviation. Kruskal-Wallis test followed by Dunn's multiple comparison test is used to compare with the control group, DMSO. P values less than 0.0332 is summarized with *.

5. Results

5.3.5 Interaction between BZs and each β -tubulin of *E. multilocularis*

To analyze the effect of ABZSX and TCBZSX on each tubulin independently, we transfected HEK293T cells with expression vectors of 3 wildtype tubulins (EmTubB1, wild type EmTubB2=EmTubB2wt, EmTubB3) and 1 mutated tubulin (mutated EmTubB2=EmTubB2mut, Tyr167Phe+Tyr200Phe). The procedure of plasmid construction was described in 4.9 and the primer sequences for the plasmid construction were described in 4.4. The design of these vectors and the detailed procedure of transfection / inhibitor treatment are described in 4.7.5.

2 days after the transfection of expression vectors, 30, 10, 3 μ M of benzimidazoles were added to the wells of transfectants. 4 days after transfection, the growth level (cell viability) was quantified as ATP concentration with Promega Cell titer glo. Chemiluminescence unit was normalized with that of DMSO treated wells of the transfectants with the same plasmids. I took the logarithm of these normalized value and draw nonlinear regression curves. IC_{50} was calculated with these regression curves.

The result with TCBZSX was unclear, because the toxicity against HEK293T cells without plasmid was unexpectedly high (Fig.53). However, IC_{50} of ABZSX on EmTubB1 and EmTubB2 transformants were clearly smaller than that of others (Fig.52).

5. Results

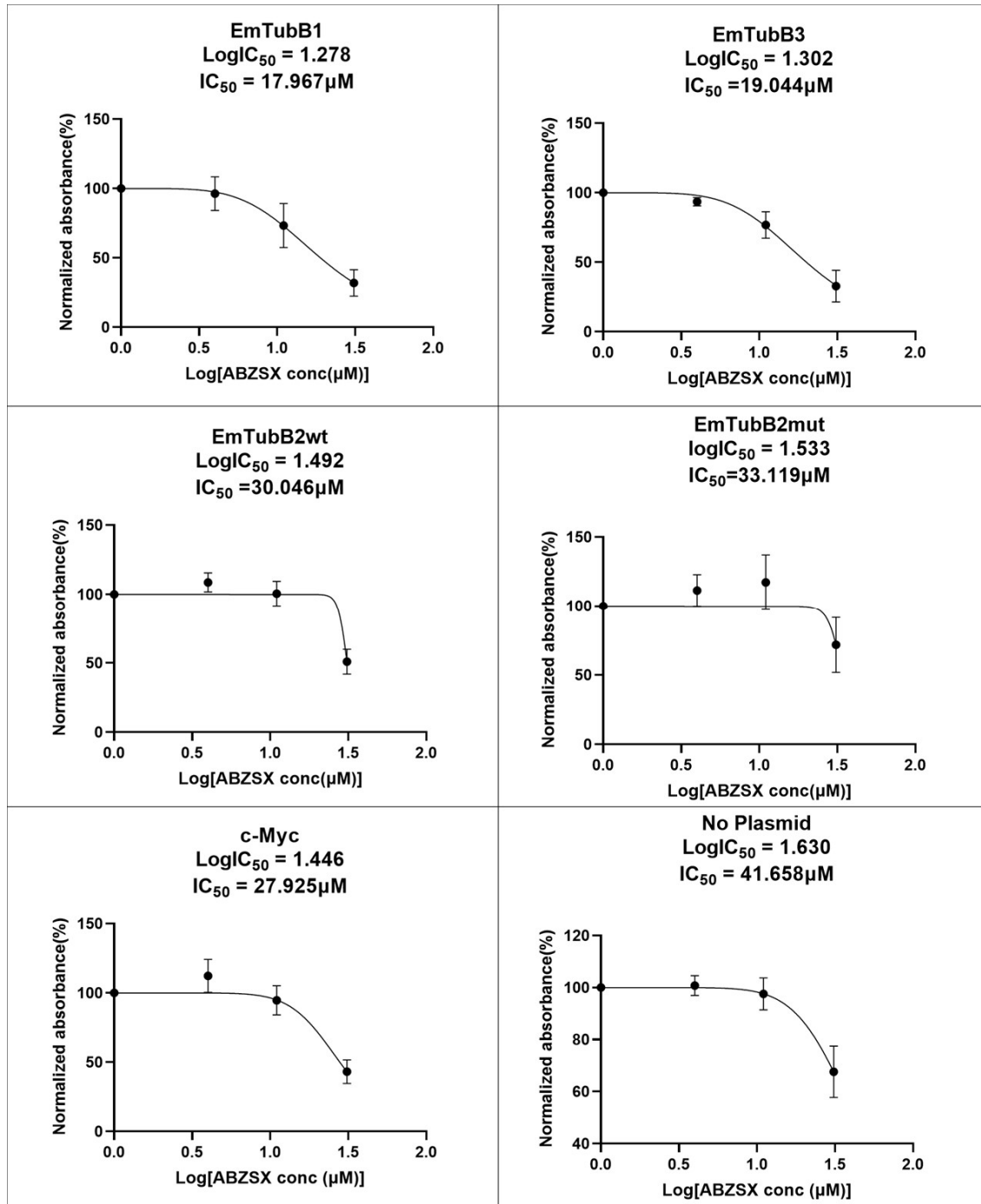


Figure 52: IC₅₀ of ABZSX for each transfectants and control
 2 days after transfection, 3 concentrations of ABZSX were added and transfectants were treated with ABZSX for 2 days. The cell viability was normalized with chemiluminescence of DMSO treated cells as percentage. The error bar represents standard deviation.

5. Results

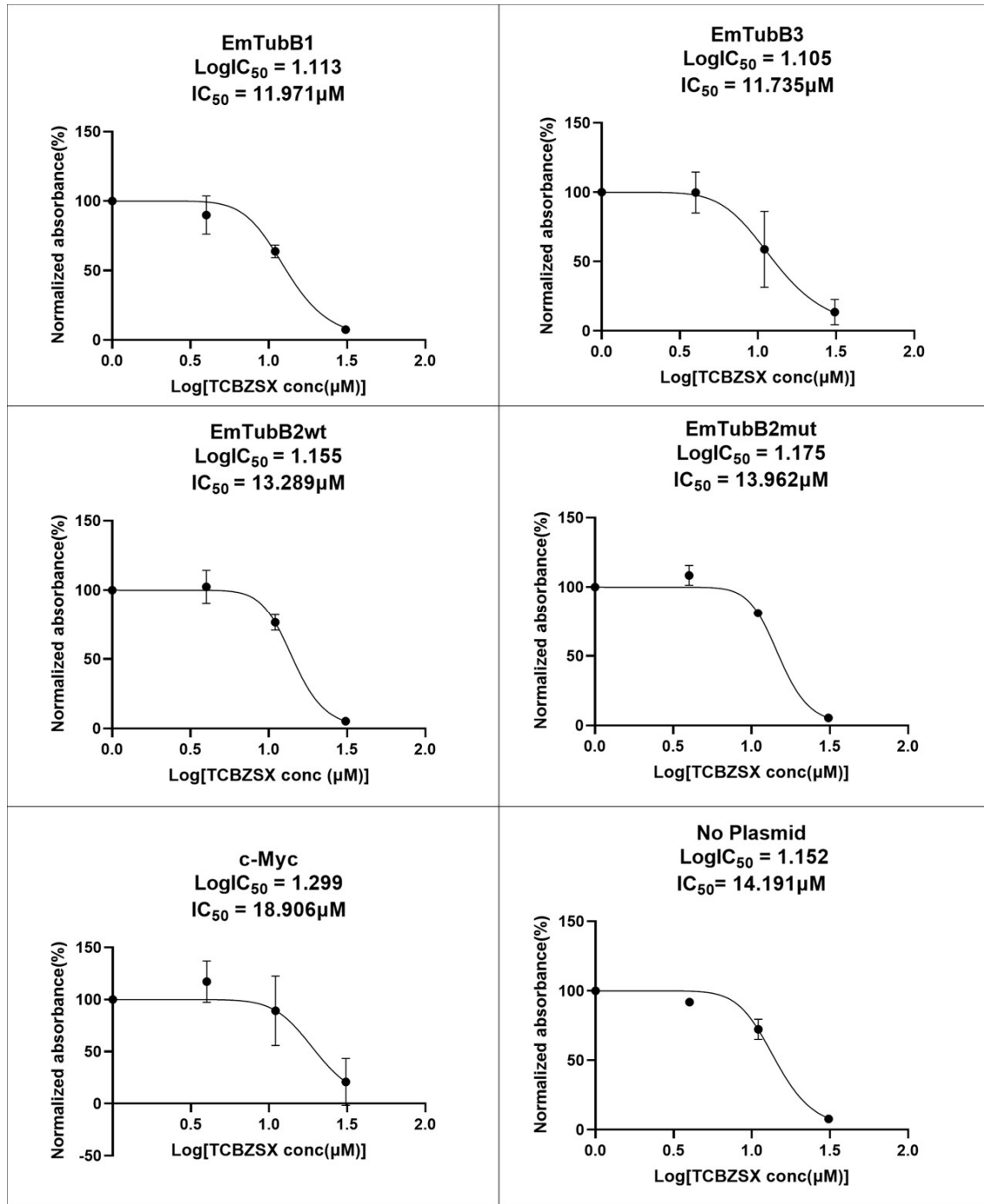


Figure 53: IC₅₀ of TCBZSX for each transfected cells and control

2 days after transfection, 3 concentrations of TCBZSX were added and transfected cells were treated with TCBZSX for 2 days. The cell viability was normalized with chemiluminescence of DMSO treated transfected cells as percentage. The error bar represents standard deviation.

5. Results

5.3.6 Trial of colchicine binding site inhibitors on *E. multilocularis* in vitro

Viruses in family Flaviviridae including Zika virus, West Nile virus and Dengue virus preferably target cells with high carboxylesterase (hCE1) expression. Klein laboratory in Heidelberg university synthesized 31 colchicine-binding site inhibitors with additional moieties, which weakens the toxicity of parental compound. When they reached cells with high hCE1 expression level, they are hydrolyzed by hCE1 and additional moieties are removed. After the hydrolysis, these compounds show selective toxicity against targets of the viruses. Hepatocytes also express hCE1 abundantly and are preferable target of such viruses (Richter *et al.*, 2019).

Initially, I tried all 31 compounds at 10 μ M on matured metacystode vesicles for 28 days without any replicate (Fig.54).

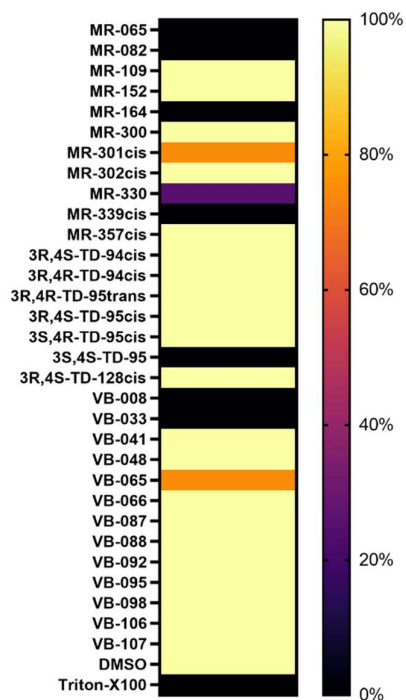


Figure 54: Initial screening of colchicine/combretastatin derivatives with matured vesicles
The vesicles were incubated with 10 μ M compounds for 28 days. The ratios of structurally intact vesicles (%) are shown in the heatmap.

5. Results

Based on the result of the 1st screening, I picked up 14 compounds and tried again on matured vesicles with three technical replicates. The period was one week shorter, 21 days.

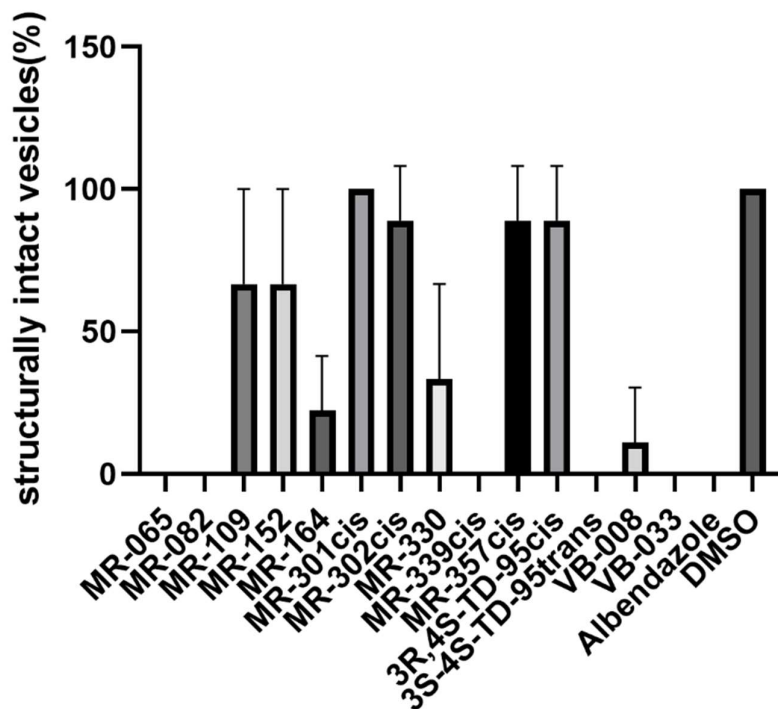


Figure 55: Secondary screening of colchicine/combretastatin derivatives with matured vesicles

The vesicles were treated with 10 μ M compounds for 21 days. Structurally intact vesicles (%) after 21 days treatment is shown in the bar graph. The error bar represents standard deviation.

All vesicles treated with MR-065, MR-082, MR-339cis 3S, 4S-TD-95 (trans), VB-033, were structurally altered. Most of vesicles treated with MR-164 and VB-008 were also severely damaged (Fig.55).

6 Discussion

6.1 In vitro screening with kinase inhibitors

Current chemotherapy against Alveolar Echinococcosis (AE) works only parasitostatically, and the development of parasitocidal drug is necessary. Kinases can be attractive targets for drugs against AE for three reasons. First, through the biological research of free-living or parasitic invertebrate species, it has been proven that the functions of kinases are relatively well-conserved (Canduri *et al.*, 2007). Second, a lot of human kinase inhibitors have been developed and even clinical data of such inhibitors and 3D structure of human kinases are available (Brooijmans *et al.*, 2010), because a lot of scientific resources have been invested for the research of human kinases, as main targets of anticancer reagents. Third, every kinases has an ATP binding pocket, which is especially suitable as target of small molecule inhibitors (Bode and Dong, 2009).

Therefore, I tried screening of human kinase inhibitors against *E. multilocularis* *in vitro*. Through screening, pan-PIM inhibitors and EGFR inhibitors showed relatively good toxicity. I tried 4 inhibitors against PIM kinase and EGFR. 2 out of 4 PIM kinase inhibitors showed stronger effect and 3 out of 4 EGFR inhibitors showed stronger effect. These two pan-PIM kinase inhibitors, SGI-1776 and CX-6258, will be discussed in 6.2.1. The kinase inhibitors which target multiple kinases such as Ponatinib or Sunitinib damaged *E. multilocularis* severely, but we did not work on them at this moment, simply because it is difficult to identify the targets in parasites. In addition, CDK4/CDK6 inhibitor Palbociclib also showed stronger effect, but we could not pursue the possibility, because its toxicity is too high also for humans. As for EGFR inhibitors, I will publish an independent paper (Fig.17-19).

6.2 PIM kinases

6.2.1 Characterization of EmPIM

The characteristic of EmPIM is, the length of C-terminal tail. As for the full length comparison, EmPIM is more than twice longer than any of three human PIM kinases (Fig.20). Initially we suspected that the sequence available in UniProt is wrongly predicted. However, when we browsed the transcript data from Tsai et al (Tsai *et al.*, 2013) through Integrated Genomics Viewer (Robinson *et al.*, 2011; Thorvaldsdóttir *et al.*, 2013), it proved to be correctly predicted. In addition, the sequence cloned into pGBKT7 for yeast two hybrid was identical to the prediction. Therefore, I concluded that EmPIM actually has the long C-terminal tail. I also analyzed the domain of EmPim with SMART to predict the function of the long C-terminal tail, but any domain was not detected. Therefore, the function of its C-terminal tail is unknown. Interestingly, SmPIM, PIM kinase of *Schistosoma mansoni* also seems to have the long C-terminal tail but no domain was detected there.

In contrast to EmPIM or SmPIM, human PIM kinases have very short sequences outside of the kinase domains. Human PIM kinases do not have regulatory domains and are considered to be constitutively active. Their activity is regulated by transcription, translation and proteosomal degradation (Amaravadi and Thompson, 2005; Qian *et al.*, 2005). The long C terminal tails of EmPIM or SmPIM might include phosphorylation sites for more sophisticated regulation. There is limitation on prediction tools such as SMART, because these programs are based largely on the data of mammalian or limited number of model organisms. Therefore, the accuracy of prediction tends to be lower when we analyzed proteins from non-model organisms.

If there are any reliable genome editing protocol or methods of overexpression for *E. multilocularis*, we might be able to make strains expressing EmPIM with shortened C-terminal tail and observe phenotype, but such method has not been established.

10 years has passed since the potential of CRISPR-Cas9 system for genome-editing has been shown (Jinek et al., 2012). During these 10 years, genome-editing protocols of protozoan and nematodes have been greatly developed (Adams et al., 2019; Sidik et al., 2014). In contrast, there are still limited number of successful experiments of genome editing with platyhelminthes (Ittiprasert et al., 2019). In the case of *E. multilocularis*, there are some examples of genetic manipulations (Spiliotis et al., 2008), but these protocols are still not as practical as those for protozoans or nematodes. The development of protocols for reverse genetics in platyhelminthes, especially protocols for genome-editing, will broaden the range of possible experiments.

6.2.2 Expression of empim in stem cells

Because HsPIM1 plays a key role in cell cycle regulation, I expected expression of EmPIM in stem cells, which is only mitotically active in *E. multilocularis*. When I tried whole mount *in situ* hybridization (WISH), approximately 25% of WISH positive cells were also positive with EdU (Fig.24).

The majority of WISH positive cells were negative for EdU signal. The reason might be cell-cycle dependent expression of EmPIM. HsPIM kinases are constitutively active and cannot be inactivated when they are not necessary. They need to be regulated by transcription, translation or proteosomal degradation (Amaravadi and Thompson, 2005; Qian et al., 2005). HsPIM1 is positive regulator of cell cycle progression from G1-S and G2-M. Therefore, HsPIM1 is likely to be transcribed/translated more in these two phase transitions. In human chronic myelogenous leukemia, the expression level of HsPIM1 is elevated exactly around G1-S and G2-M, but it is dropped in S phase (Liang et al., 1996).

Discussion

EdU is an analog of thymidine that labels only cells in S-phase but it remains in the nucleus for some time after S phase ends. If the expression level of EmPIM is elevated only at the G2-M or G1-S transition, similarly as that of HsPIM1, co-localization of both signal can be seen in only smaller fraction of stem cells. This is because such cells should have completed S phase during incubation with EdU and should have reached G2-M transition when vesicles were fixed with paraformaldehyde. On the other hand, if cells are in G1-S phase transition when the vesicles were fixed, only signal of WISH is likely to be observed in such cells. No one have tried to measure how long it takes for stem cells to complete cell cycle, but incubation time with EdU should have been much shorter than the duration of complete cell cycle of *E. multilocularis*, as far as I guess from the increase of stem cell number during clonal expansion (Kozioł *et al.*, 2014). This also can explain why the number of double positive cells were even smaller when the incubation time was 5 hours. In 5 hours, majority of the cells with EdU signal must be still in S phase or G2 phase, and had not reached to G2-M transition. However, as I discussed in 6.2.1, if the long C terminus tail includes regulation domains and EmPIM can be inactivated through phosphorylation, this explanation will be less convincing.

In addition, there were plenty of WISH positive cells without signal of EdU. Some part of such cells can be stem cells in G1-S transition, but differentiated cells might be included. In fact, HsPIM kinases have functions other than cell cycle regulation, such as negative regulation of apoptosis (Gu *et al.*, 2009). Furthermore, the difference in expression level of EmPIM between primary cells (enriched in stem cells) and metacestode vesicles is clearly smaller than that of EmPLK1, which is known to specifically expressed in stem cells (Fig.23) (Schubert *et al.*, 2014; Tsai *et al.*, 2013). It would not be too surprising even if EmPIM is expressed also in differentiated cells and has functions other than cell cycle regulation. To show the expression of EmPIM in differentiated cells, double-in situ hybridization of EmPIM and EmTRIM, which is a cell-cycle-independent marker of stem cells, would be necessary.

6.2.3 Interaction between EmPIM and EmCDC25

Because HsPIM1 regulates cell cycles through interaction with CDC25A/C, I expected that CDC25 like phosphatases should be encoded in the genome of *E. multilocularis*. Through blastp analysis, only one CDC25-like protein was identified.

When I suppose that EmCDC25 remove inhibitory phosphorylation from CDKs in *E. multilocularis*, one question comes out. Can just one CDC25 phosphatase control both G1-S and G2-M transition? As far as I searched through BLASTP analysis, most of model organisms and *Schistosoma mansoni* have multiple CDC25-like protein (Fig.27). As for this question, it seems to be not impossible at least for mammals. Knockout mice of *cdc25a* is lethal but the knockout mice of *cdc25b* and *cdc25c* survived (Ferguson et al., 2005). The result of this research indicates that CDC25C and CDC25B are dispensable and can be substituted by CDC25A or other phosphatase. Another study showed that CDC25C usually work on CDK1 during G2-M transition but CDC25A also can interact with CDK1 (Donzelli and Draetta, 2003). Therefore, it is not that strange to suppose that two phase-transitions are regulated by one CDC25 phosphatase.

RHOD domain of EmCDC25 and SmCDC25A includes large insertions (Fig.26). Similarly as C terminal tail of EmPim, we suspected that EmCdc25 phosphatase is wrongly predicted, but it proved to be correct. These inserts also included in the cloned sequence in pGADT7 and in the transcript data from Tsai et al. (Tsai et al., 2013) browsed through Integrated Genomics Viewer (Robinson et al., 2011; Thorvaldsdóttir et al., 2013). Different from long C terminal tail of EmPIM, these insertions are located in the middle of functional domain. In addition, M phase inducer phospho domain was not detected in the sequence of EmCDC25 and SmCDC25s during SMART analysis (Fig.20). Therefore, I am not sure whether EmCDC25 might have the same function as HsCDC25s. It might be interesting if I could remove these insertions and observe phenotype, but it is currently impossible, as I

Discussion

discussed in 6.2.1. I also would like to try CDC25 inhibitor to see phenotype, but there were not any commercially available CDC25 specific inhibitor.

Anyhow, this strange insertions in RHOD domain might be important if we try to develop selective inhibitor against EmCDC25 phosphatase, but we did not pursue such a possibility, because we are working on the budget from Kinase Inhibitoren als Therapeutika gegen Echinokokkose (KITE), not from Phosphatase Inhibitoren als Therapeutika gegen Echinokokkose.

If EmCDC25 plays a similar role as human CDC25s in cell cycle regulation, its substrate is most likely to be EmCDK1 and amino acid sequences of substates also should be similar. HsCDC25C removes inhibitory phosphorylations at T14 and Y15 on HsCDK1 (Bachmann *et al.*, 2006) and HsCDC25A removes them on HsCDK2 (Mochizuki *et al.*, 1999). EmCDK1 has T19/Y20 and amino acid sequences around there were well-aligned with those of T14/Y15 of HsCDK1/HsCDK2 (Fig.30).

In yeast-two-hybrid assay, interaction between EmPIM and EmCDC25 was indicated (Fig.28, Fig.29). Together with the localization of EmPim kinase in stem cells and amino acid sequence of EmCDK1, these data can indicate that EmPIM and EmCDC25 regulate G1-S or G2-M cell cycle transision, similarly as HsPIM1 and HsCDC25A/C. If I plan additional experiment to support this possibility, validating interaction between EmCDC25 and EmCDK1 through yeast-two-hybrid might be interesting.

Planarians are free-living platyhelminthes and famous for the ability to regenerate. Their adult stem cells named neoblasts play key roles for the regeneration capacity (Newmark and Sanchez Alvarado, 2002). In one study of gene expression pattern of planarians during the process of regeneration, three pim kinases are categorized into “immediate early genes” whose expression levels are elevated soon after amputation (Wenemoser *et al.*,

2012). This indicates that these planarian pim kinases can be important for the regeneration. Of course regeneration process accompanies rapid cell divisions. If planarian pim kinases control cell-cycle transition during the regeneration process, EmPIM also might control cell-cycle transition, because stem cells of *E. multilocularis* have a lot in common with planarian neoblasts. On the other hand, different from PIM kinases, HsCDC25-like-phosphatases were not included in the list. This difference might be attributed to the difference in the regulation of PIM kinases and CDC25 phosphatases. At least in mammals, CDC25 phosphatases can be inactivated thorough phosphorylation (Bachmann *et al.*, 2006; Mochizuki *et al.*, 1999) but PIM kinases only can be regulated through transcription, transcription, and proteosomal degradation (Amaravadi and Thompson, 2005; Qian *et al.*, 2005).

6.2.4 Effects of SGI-1776 and CX6258 on *E. multilocularis*

In addition to the initial screening of 5.1., I tried two commercially available pan-PIM inhibitors on *E. multilocularis* with replicate. Both inhibitors showed detrimental effect to matured vesicle and vesicle formation from stem cells (Fig.31-32).

Both CX-6258 and SGI-1776 have affinities also to HsHASPIN and HsFLT3 (Chen *et al.*, 2009; Haddach *et al.*, 2012; Melms *et al.*, 2020). However, HsFLT3-like protein was not identified in the protein database of *E. multilocularis* by blastp analysis. This does not contradict to the fact that FLT3 kinases have evolved after the lineage of protostomes (including platyhelminthes) and deuterostomes (including vertebrates) was separated (Grassot *et al.*, 2006). On the other hand, two HsHASPIN-like protein, EmHASPIN1 and EmHASPIN2 were identified from the protein database of *E. multilocularis*.

EmPIM1 has more residues identical or similar to the 14 residues important for the interaction between HsPIM1 and CX-6258, than EmHASPIN1/2, other potential CX-6258

Discussion

targets. Therefore, we can expect that the toxicity of CX-6258 on *E. multilocularis* comes, at least partially from the affinity between CX-6258 and EmPIM (Fig.21, Fig.33-34, Table26).

Melms et. al. showed that CX-6258 and SGI-1776 have off-traget effect against HsHASPIN. On the other hand, other pan-PIM kinase inhibitors, AZ1206 and PIM447 were also tried in their paper and did not show such off-target effects (Melms *et al.*, 2020). When I see the screening data of list 3 kinase inhibitors (Fig.19) again, AZ1206 and PIM447 showed lower toxicity against primary cells of *E. multilocularis* than CX-6258. Therefore, it is still possible that CX-6258 showed detrimental effect not only from the affinity against EmPIM1 but also from that against EmHASPIN1/2.

To show actual interaction between CX-6258/SGI-1776 and EmPIM, I considered to try a kinase activity assay, the same as Melms et al. did in their paper (Melms *et al.*, 2020). However, there are no available combination of substrates for EmPIM and commercially available antibodies which can recognize phosphrylation of the target residue on that substrate. To try a kinase assay without such antibodies, [$\gamma^{32}\text{P}$]ATP and an appropriate facilities to handle radioisotopes are required. Therefore, it is difficult to demonstrate wether SGI-1776 and CX-6258 actually inhibit EmPIM. In contrast, Histon H3, the substrate of HASPIN, is extremely well conserved among metazoa (Fig.35) and commercially available Histon H3 is likely to be phosphorylated also by EmHASPIN. In fact, previous work in our laboraotry showed that phosphorylation of Ser10 on H3 could be recognized by a commercially available antibody for mammals/fruit flies (Koziol *et al.*, 2014). In addition, antibodies which recognize phosphorylation of Thr3 of HsHASPIN is commercially available. It might be interesting to try kinase activity assay with recombinant EmHASPIN. If such an experiment deny inhibition of EmHASPIN by SGI-1776 and CX-6258, inhibition of EmPIM by these inhibitors might be shown indirectly. However, this experiment is too time consuming to be included in our PIM paper and it should be tried for another independent paper.

6.2.5 *In silico* screening of EmPim inhibitors

Because of the lack of parasitocidal effect in current chemotherapy with albendazole (ABZ), the development of new drug against alveolar echinococcosis (AE) is necessary. To find lead compounds for new drug effectively, several methods of medium-throughput *in vitro* screening have been developed. One of them is PGI assay of Hemphil laboratory in Bern. It actually could handle hundreds of compounds (Stadelmann *et al.*, 2014), but it can be time-consuming to prepare metacestode vesicles of appropriate age and size for this assay and it is difficult to identify slow-acting drugs like ABZ. To deal with such problems, narrowing down candidates compounds before proceeding to *in vitro* experiments is necessary. Fortunately, the publicly available transcriptome (Tsai *et al.*, 2013) and development of computational platforms such as Fluency (Kim *et al.*, 2020) allowed us to try high-throughput *in silico* screening.

Through the experiment until 5.2.4, I concluded that EmPIM can be a good target. However, it is impractical to apply commercially available PIM inhibitors for the patients of AE. In fact, some of PIM kinase inhibitors proceeded to clinical trial, but none of them has reached to the practical use for the patients. I would like to try high throughput screening to identify compounds with selective toxicity against EmPIM, but at the same time, I would like to downsize the list of candidate compounds because of the limitation of available resources. By *in silico* analysis with Fluency model and SeeSAR analysis of our collaborators, we successfully downsized the list from 21.4 million to 20. The 20 compounds are actually synthesized and tried on *E. multilocularis in vitro*. One out of 20, Z196138710, showed comparable toxicity against matured vesicle and primary cells as that of commercially available inhibitors (Fig.37). In addition, the toxicity against mammalian cell lines were clearly different (Fig.38). Furthermore, *in silico* analysis with SeeSAR predicted that SGI-1776 has stronger affinity against HsPIM1 than Z196138710 (Fig.39). I believe that this *in*

silico high throughput screening method showed enough potential for the development of compounds with selective toxicities.

6.2.6 Summary of kinase project and how this research advance the field

Currently ABZ is used for chemotherapy against Echinococcosis. It prolonged life expectancy of patients, but it also compromises the quality of life, because of its side effects. To identify compounds with less side effect, several methods for screening had been tried on *in vitro* cultivated *E. multilocularis*, but all of them were relatively time-consuming.

In this study, through *in vitro* trial, pan-PIM kinase inhibitors proved to have strong toxicities against *E. multilocularis*. EmPIM, a PIM kinase of *E. multilocularis* was identified and it had relatively high percent similarity to human PIM kinases. However, commercially available pan-PIM kinase inhibitors are also highly toxic to the host. Therefore, high-throughput *in silico* screening was employed to identify compounds with selective toxicity against *E. multilocularis* and one compound, Z196138710 actually showed selective toxicity.

The discovery of Z196138710, can be a good example that it is not impossible to identify promising compounds with selective toxicity against well-conserved targets. This research paved a way to more efficient screening method, and I hope this method will be developed further. It might be interesting to try this *in silico* approach to other kinases, which showed relatively good toxicity during the initial screening of 5.1 in the near future.

6.3 Tubulins

6.3.1 Comparison of Echinococcus tubulin and Robinson's model of *H. contortus*

Since 1980s, ABZ prolonged life expectancy of AE patients, but there is demand for new drugs, because ABZ only works parasitostatically. Because stem cells are responsible for the regenerative capacity and longevity of *E. multilocularis*, toxicity to stem cells is of particular importance in the development of new anthelmintics (Koziol *et al.*, 2014).

Expression data indicates that EmTubB2 is expressed in stem cells (Koziol and Brehm, 2015; Tsai *et al.*, 2013). In addition, the combination of immunofluorescence and in situ hybridization showed co-localization of EmTubB2 and EmTRIM, a cell cycle-independent marker of stem cells (Brehm, personal communication; Koziol *et al.*, 2015). When we try compounds against tubulins on *E. multilocularis*, the analysis of their sequence is especially important.

The importance of 200th residue of β -tubulins, has already been discussed in former publication of AG Brehm (Koziol and Brehm, 2015) and that of 167th residue was also discussed later. As for another important position in the model of *H. contortus* by Robinson *et al.* (Robinson *et al.*, 2004), 165th residue might be worth noting. EmTubB1, EmTubB3, HcTubB2 have Asn165, Thr165, Ser165 respectively. These Ser, Asn and Thr belong to the same group of polar, uncharged amino acids. However, EmTubB2 has Val165, and Val belongs to another group of aliphatic amino acids (Fig.40, Table 27). Val165 in EmTubB2 also can be important for the resistance, because it is impossible for ABZSX to form hydrogen bond at 165th position with hydrophobic residue like Val. In addition, A165V mutation of benA make *Aspergillus nidulans* supersensitive to carbendazim, nocodazole and benomyl, but resistant to thiabendazole (Jung and Oakley, 1990). It might be interesting to try carbendazim on *E. multilocularis in vitro*. However, carbendazim is not approved for medical or veterinary use

but for various crops as fungicide. Even if *E. multilocularis* is supersensitive to carbendazim, it must be difficult to use carbendazim for clinical purpose.

6.3.2 Effect of TCBZ on metacestode vesicles

Because several experimental data indicates that triclabendazole (TCBZ) works on FhTubB1, which has similar residues correlated with benzimidazole (BZ) resistance as EmTubB2 in stem cells, we tried TCBZ on *E. multilocularis*.

6.3.2.1 EdU incorporation and structural alternation under optical microscope

Because EmTubB2 is expressed in stem cells, and we expected that TCBZSX affect EmTubB2, I labelled metacestode vesicles with stem cell marker EdU, after drug treatment. Structural disintegration of matured vesicles was not found after 10 days treatment with 30 μ M TCBZSX as far as I observed them under the optical microscope (Fig.41). However, almost no EdU positive cells were found under the confocal microscope. On the other hand, there was not statistically significant difference between the control and vesicles treated with 10 μ M TCBZS. 30 μ M sounds high, but this is almost the same concentrations lethal to *Fasciola in vitro* (Fairweather et al., 1984; Robinson *et al.*, 2002). This result indicates that 30 μ M TCBZSX can make stem cells mitotically inactive, at least temporary. In the experiment of combined treatment with ABZ and TCBZSX, clear disintegration in the vesicle structure was detected. However, 30 μ M TCBZSX was still required to reduce the number of EdU-positive cells with or without ABZ (Fig.42-43). This result also indicates that ABZ affects differentiated cells but does not affect stem cells.

I would like to try various treatment periods to determine the minimum duration of treatment to remove EdU positive cells. This information is important to consider the conditions for *in*

vivo experiments, especially because TCBZ treatment for Fascioliasis is relatively shorter and information on side effect after longer period of TCBZ treatment is limited.

When we incubate vesicles with TCBZ or TCBZSX for longer period, structural disintegration was observed (Fig.44). People in Ulm university hospital already have tried TCBZ *in vitro*, and the necessary concentration to cause structural disintegration in their experiment was largely similar (Richter et al., 2013). Even if TCBZ or TCBZSX do not affect differentiated cells directly, the vesicles cannot sustain its structure without normal mitotic activity of stem cells, presumably because the maintenance and renewal of differentiated cells are impossible without stem cells.

6.3.2.2 TRIM positive cells

To evaluate the effect of TCBZ/TCBZSX against stem cells not in S phase, I tried cell-cycle independent stem cell marker, EmTRIM (Kozioł *et al.*, 2015). The difference between control vesicles and TCBZS treated vesicles were statistically significant, but there were still clear signals from EmTRIM on the treated vesicles (Fig.45-46). On the other hand, in the previous experiment, EdU positive cells had been mostly disappeared in 10 days (Fig.42-43). This indicates that TCBZSX stops stem cell proliferation faster than it stops EmTRIM expression.

6.3.2.3 Nerve cells

In the experiments of 5.3.2.1, the effect of TCBZSX on differentiated cells looked limited. To evaluate actual effect of TCBZ/TCBZSX on differentiated cells, I stained nerve cells with anti-acetylated α -tubulin antibody, as an example of differentiated cells. At least TCBZSX had detrimental effect on nerve cells. It was unknown whether TCBZSX affected directly or indirectly. In contrast, there were no statistically significant difference between DMSO and

TCBZ (Fig.47-48). TCBZSX is a metabolite of TCBZ, but the effect of TCBZ and TCBZSX against helminths might be slightly different at least *in vitro*. In fact, as for the comparison of TCBZ and TCBZSX, there is interesting description in the paper of Fairweather et al. TCBZ caused an overall inhibition of Fasciola's movement *in vitro*. In contrast, TCBZ-SX stimulated activity initially but caused long-term decline in physical activity (Fairweather *et al.*, 1984). This difference in the motility of flukes might come from the difference in damages of nerve cells. However, before concluding like that, reproducibility is necessary to be confirmed.

6.3.3 Effect of TCBZ on the ability of regeneration

Through the experiment of 5.3.2, TCBZSX proved to eliminate mitotically active stem cells (Fig.42). To clarify whether TCBZSX stops cell cycles just temporary or irreversibly, I tried vesicle formation assay with primary cells isolated from TCBZSX-treated vesicles. Because stem cells are only mitotically active, and vesicle regeneration accompanies cell division, regeneration of vesicles should be impossible if the stem cells were damaged irreversibly. In fact, no aggregation or regeneration of vesicles had been observed in the primary cells from treated vesicles, even after 28 days incubation (Fig.49-50). Therefore, even though stem cells still could express EmTRIM after 10-day treatment (Fig.45-46), TCBZS had already inactivated mitotic activity of stem cells irreversibly.

6.3.4 Effect of TCBZ on isolated primary cells

To evaluate the effect on the ability of vesicle regeneration, I treated primary cells from non-treated metacestode vesicles, with TCBZ/TCBZSX. In the wells of 30 μ M TCBZ or TCBZSX treatment, no regenerated vesicles were observed. However, in the samples with 3-10 μ M TCBZ/TCBZSX, small number of regenerated vesicles were observed. The same as the

experiment with matured vesicles (Fig.42-43), higher concentration seems to be necessary to inactivate mitotic activity of stem cells (Fig.51). As for the number of regenerated vesicles, the difference between control DMSO and 3 μ M samples were insignificant, but the vesicles in control DMSO looked bigger in diameter. It might be interesting to measure and compare the diameter and calculate the growth speed as another criterion of toxicity.

The expression pattern of β -tubulins can be different from stage to stage. In metacystode vesicles without brood capsules, only EmTubB1, EmTubB2, EmTubB3 shows stronger expression. However, in primary cells 11 days after isolation, the expression level of another β -tubulin, EmuJ_000955100, is higher than EmTubB1 (Koziol and Brehm, 2015). Because visible vesicles appear from approximately 10 days after isolation, it is possible that these newly regenerated vesicles express this tubulin. This tubulin has Asn165, Phe167, Glu198 and Tyr200, but further experiments are necessary to see localization of this tubulin and to estimate the affinity of TCBZ/TCBZSX and this tubulin.

6.3.5 Interaction between BZs and each β -tubulin of *E. multilocularis*

To evaluate the effect of benzimidazoles on three EmTubBs independently, human cell line HEK293T were transfected with expression vector encoding these tubulins. The effect of TCBZSX was unclear, because HEK293T cells were more susceptible to it than I expected (Fig.53).

In contrast, there were clear difference in IC_{50} between cells with with pCMV-c-Myc (control) and those with pCMV-chimericEmTubB1/EmTubB3. This indicates that these chimeric tubulins were successfully integrated, and they are likely to be more susceptible to ABZ than human β -tubulins. In contrast, there were no clear differences in IC_{50} among pCMV- c-Myc and pCMV-chimericEmTubB2wt/EmTubB2mut (Fig.52). Possible explanations for the insignificant difference between wildtype and mutant constructs are,

Discussion

1. In addition to Tyr167 and Tyr200 there are other important residues for the resistance against ABZSX
2. The partner α -tubulin from human cells affect the resistance against ABZSX
3. The chimeric tubulins of EmTubB2 were not integrated.

Both for 1st and 2nd explanations, there is example of FhTubB2. FhTubB2 has Tyr200, but it is most probable target of ABZ (Chambers *et al.*, 2010). In addition, there are countless reports on resistant strains of *Fasciola hepatica*, but no clear difference in amino acid sequences of tubulins between resistant and susceptible strains have been found (Fuchs *et al.*, 2013; Robinson *et al.*, 2002). Tyr200 and Tyr167 are correlated with the resistance, but they might not be the only important factor for the resistance.

As for the 1st explanation, Val165 in EmTubB2 might be important, the same as I discussed in 6.3.1. Asn165 in *Haemonchus contortus*'s β -tubulin is known to form hydrogen bond with ABZSX (Robinson *et al.*, 2004). When asparagine, a polar residue is exchanged with a hydrophobic residue like valine, the affinity between tubulins and ABZSX can be weakened.

As for the 2nd explanation, there is example. In the genome of baker's yeast (*Saccharomyces cerevisiae*) there are only two α -tubulins. By knocking out one of them, ScTub3, the yeast became susceptible to thiabendazole (Garge *et al.*, 2020). This means that not ScTub2(β -tubulin) but ScTub3 is responsible for the resistance, at least in the case of wildtype yeast.

As for the 3rd explanation, it is impossible to verify it through IFA with our EmTubB2 specific antibody. This antibody has affinities to C-terminus of EmTubB2. However, in this experiment, C-terminus of EmTubB2 is exchanged with that of HsTubB2B to encourage integration with the partner α -tubulin from human cells. However, EmTubB2 is more likely to be integrated to human microtubule than EmTubB1 and EmTubB3, because EmTubB2 has

Discussion

higher percent identity / similarity with HsTubB2A-C, HsTubB4 and HsTubB5. The percent identity and similarity of EmTubB2 and these 5 human tubulins are, 93.9-95.5% and 97.3-98.7% respectively. In the case of EmTubB1, percent identity and similarity are 88.2-90.6% and 93.1-94.4%. EmTubB3's percent identity and similarity are 76.5-79.7% and 84.7-88.1%.

There is another experiment with *Caenorhabditis elegans* about susceptibility of mutated EmTubB2 against ABZ. **In this doctoral dissertation, experiments done by collaborators are written in bold letters. This experiment was done by people in Stigloher laboratory of Würzburg university.** *Caenorhabditis's* β -tub4 (CeTubB4) has high percent similarity with EmTubB2. CeTubB4 is expressed in the cilia of sensory neurons and together with CeTubA6 and CeTubA9, it is required for the optimal response behavior (Hurd et al., 2010; Nishida et al., 2021). **When EmTubB2wt and EmTubB2mut were introduced into nematodes instead of CeTubB4, regardless of the 167th/200th residues, these nematodes could gather to the source of smell (optimal response behavior). However, when ABZ was added, nematodes with EmTubB2wt could gather to the source of smell but nematodes with EmTubB2mut could not (Stigloher and Brehm, personal communication)**

This result clearly contradicts to the result of my experiment. However, if we think about the effect of α -tubulin like the 2nd explanation, we can solve this contradiction. In the experiment with nematode, the partner of EmTubB2 to form heterodimer should be an α -tubulin from nematodes. In the experiment with HEK293T cells, the partner is an α -tubulin from human. Because the partner is different, the susceptibility could be different.

Other than these explanations, there is one difference between the nematode experiment and HEK293T experiment. As far as I heard, nematodes were treated with ABZ but HEK293T cells were treated with ABZSX. I am not sure whether this difference affected to the results. As for this point, I had to adjust the condition when I planned my experiment.

Discussion

I believe that the 2nd explanation sounds the most plausible. However, to prove it, further experiment is necessary. In fact, my experiment with HEK293T had several important problems below.

1. It was difficult to exclude the effect of tubulins originally expressed in human cells. Human genome includes 8 β -tubulins and 9 α -tubulins. It was impractical to knock out or knock down all 8 β -tubulins, and it is difficult to consider the effect of 9 α -tubulins on the resistance.
2. Even though HEK 293T cells can be transfected with high efficiency, there should be plenty of cells without plasmids. It was impossible to remove them because there was no selection marker.
3. HEK293T is an adherent cell line, and it was impossible to quantify its growth noninvasively. In our experiment, I used cell viability assay (measurement of ATP concentration), but it includes invasive procedure (lysis of the cells). Therefore, repetitive measurement of growth level was impossible. With mammalian floating cell lines, the growth level can be quantified easily, noninvasively, and repeatedly by measuring optical density, but there are no floating mammalian cell lines with higher transfection efficiency.

All three problems can be solved by using genome editing with *Saccharomyces cerevisiae*. As for the 1st problem, *Saccharomyces* have only one β -tubulin (Garge *et al.*, 2020) and if it is replaced with tubulins from *E. multilocularis* by genome editing, there is no other β -tubulins. In addition, as I discussed above, only two α -tubulins are encoded in the genome of *S. cerevisiae* and ScTub3, the one which affect drug resistance, is not essential. Also through genome-editing, ScTub3 can be knocked out. As for the 3rd problem, yeasts can be cultured in a shaking incubator, and growth level can be quantified easily, noninvasively, and repeatedly. I am planning this yeast experiment after I submit my doctoral dissertation.

If we would like to predict the interaction between each tubulin and BZs, generating homology models of EmTubBs might be interesting. If we try to acquire real 3D data of protein binding, X-ray crystallography will be required, and it costs a lot. However, Robinson et al. did not have 3D data of *Haemonchus*'s β -tubulin (HcTubB2). They generated the model structure by combining bovine $\alpha\beta$ -tubulin dimer atomic structure (PDB entry 1JFF) and the amino acid sequence of HcTubB2 (Robinson *et al.*, 2004). Once the homology models of Echinococcus tubulins are constructed, we might be able to calculate interaction score. In fact, Ranjan et al. calculated interaction scores between HcTubB2 and various BZs through FlexX docking algorithm in LeadIT (Ranjan *et al.*, 2017). LeadIT is not supported anymore, but FlexX is still available as one component of SeeSAR (BioSolveIT GmbH). According to their calculation, the interaction scores with ABZ, ABZSX and TCBZ are -18.16, -17.96 and -5.13kJ/mol respectively (Ranjan *et al.*, 2017). Even though the model was not based on real X-ray crystallography, this computation does not look contradicting to the fact that TCBZ generally does not show strong effect against nematodes (Coles, 1986; Guralp and Tinar, 1984; Wolff et al., 1983).

6.3.6 Trial of colchicine binding site inhibitors on *E. multilocularis in vitro*

To evaluate toxicities of colchicine binding site inhibitors from Klein laboratory, I tried them on *E. multilocularis in vitro*. MR-065, MR-082, MR-339cis, 3S, 4S-TD-95 (trans), and VB-033 showed stronger toxicity against matured metacystode vesicles. The toxicity of MR-164 and VB-008 was slightly weaker (Fig.54-55).

In their paper, Richter et al. picked up VB-033 and VB-087. Both of them are derivatives of colchicine and showed good activity in viral replication assays, while its cytotoxicity is much lower than parental compound colchicine. Especially VB-033 showed considerable antiviral activity. On the other hand, its effect on tubulin polymerization itself was marginal. They

Discussion

discussed that antiviral activity might come from other kind of microtubule dynamics or interactions with other host cellular mechanisms (Richter et al, 2019). I do not know how they worked on *E. multilocularis*, but in the case of *E. multilocularis*, VB-033 had strong effect and VB-087 showed weaker activity.

When I tried these compounds, I just arrived at Germany, and I did not have the mental capacity to design an experiment based on the background. Therefore, I did not ask anything about the background then to people in Klein laboratory. The postdoctoral fellow who synthesized them already have left Klein laboratory, and no one knows his intention now. However, I can guess from the design of compounds now. These compounds are designed to have weakened toxicity until they are hydrolyzed by human carboxylesterase 1 (hCE1). These compounds were sent to our laboratory presumably because both flaviviruses and *E. multilocularis* have organ tropism toward the liver (Förster *et al.*, 2018), where hCE1 is strongly expressed. I tried them under axenic condition without feeder cells. However, I should have tried them with Reuber hepatoma to evaluate toxicity after hydrolysis if I could have considered the background of this experiment.

6.3.7 Summary of tubulin project and how this research advance the field

Although ABZ has been used for chemotherapy against Echinococcosis since the 1980s, it has a problem that it does not have parasitocidal effect.

In this study, TCBZ, which is approved for the treatment of Fascioliasis, proved to damage stem cells of *E. multilocularis* irreversibly. After 10 days of treatment, stem cells lost their ability to proliferate and could not regenerate the vesicles anymore.

Since ABZ damages differentiated cells and TCBZ damages stem cells, these two BZs can complement each other. This study may lead to the development of practical and parasitocidal chemotherapy for echinococcosis.

7 Bibliography and approval of secondary publication

7.1 Bibliography

Adams, S., Pathak, P., Shao, H., Lok, J.B., and Pires-daSilva, A. (2019). Liposome-based transfection enhances RNAi and CRISPR-mediated mutagenesis in non-model nematode systems. *Sci Rep* 9, 483. 10.1038/s41598-018-37036-1.

Aden, D.P., Fogel, A., Plotkin, S., Damjanov, I., and Knowles, B.B. (1979). Controlled synthesis of HBsAg in a differentiated human liver carcinoma-derived cell line. *Nature* 282, 615-616. 10.1038/282615a0.

Altschul, S.F., Madden, T.L., Schäffer, A.A., Zhang, J., Zhang, Z., Miller, W., and Lipman, D.J. (1997). Gapped BLAST and PSI-BLAST: a new generation of protein database search programs. Oxford University Press.

Alvarez, L., Moreno, G., Moreno, L., Ceballos, L., Shaw, L., Fairweather, I., and Lanusse, C. (2009). Comparative assessment of albendazole and triclabendazole ovicidal activity on *Fasciola hepatica* eggs. *Vet Parasitol* 164, 211-216. 10.1016/j.vetpar.2009.05.014.

Amaravadi, R., and Thompson, C.B. (2005). The survival kinases Akt and Pim as potential pharmacological targets. *The Journal of clinical investigation* 115, 2618-2624. 10.1172/JCI26273.

Bachmann, M., Kosan, C., Xing, P.X., Montenarh, M., Hoffmann, I., and Möröy, T. (2006). The oncogenic serine/threonine kinase Pim-1 directly phosphorylates and activates the G2/M specific phosphatase Cdc25C. *International Journal of Biochemistry and Cell Biology* 38, 430-443. 10.1016/j.biocel.2005.10.010.

Bateman, A., Martin, M.J., Orchard, S., Magrane, M., Agivetova, R., Ahmad, S., Alpi, E., Bowler-Barnett, E.H., Britto, R., Bursteinas, B., et al. (2021). UniProt: The universal protein knowledgebase in 2021. *Nucleic Acids Research* 49, D480-D489. 10.1093/nar/gkaa1100.

- Beyer, H.M., Gonschorek, P., Samodelov, S.L., Meier, M., Weber, W., and Zurbriggen, M.D. (2015). AQUA cloning: A versatile and simple enzyme-free cloning approach. *PLoS ONE* 10. 10.1371/journal.pone.0137652.
- BioSolveIt GmbH, S.A.G. . SeeSAR version 12.1. www.biosolveit.de/SeeSAR.
- Bischoff, R., and Holtzer, H. (1968). The effect of mitotic inhibitors in myogenesis in vitro. *J Cell Biol* 36, 111-127.
- Blackley, S., Kou, Z., Chen, H., Quinn, M., Rose, R.C., Schlesinger, J.J., Coppage, M., and Jin, X. (2007). Primary human splenic macrophages, but not T or B cells, are the principal target cells for dengue virus infection in vitro. *J Virol* 81, 13325-13334. 10.1128/JVI.01568-07.
- Bode, A.M., and Dong, Z. (2009). Signal transduction molecules as targets for cancer prevention. *Sci Signal* 2, mr2. 10.1126/scisignal.259mr2.
- Bogusz, J., Zrubek, K., Rembacz, K.P., Grudnik, P., Golik, P., Romanowska, M., Wladyka, B., and Dubin, G. (2017). Structural analysis of PIM1 kinase complexes with ATP-competitive inhibitors. *Scientific Reports* 7. 10.1038/s41598-017-13557-z.
- Boray, J.C., Crowfoot, P.D., Strong, M.B., Allison, J.R., Schellenbaum, M., Von Orelli, M., and Sarasin, G. (1983). Treatment of immature and mature *Fasciola hepatica* infections in sheep with triclabendazole. *Vet Rec* 113, 315-317. 10.1136/vr.113.14.315.
- Bordo, D., and Bork, P. (2002). The rhodanese/Cdc25 phosphatase superfamily. Sequence-structure-function relations. *EMBO reports* 3, 741-746. 10.1093/embo-reports/kvf150.
- Brasó-Maristany, F., Filosto, S., Catchpole, S., Marlow, R., Quist, J., Francesch-Domenech, E., Plumb, D.A., Zakka, L., Gazinska, P., Liccardi, G., et al. (2016). PIM1 kinase regulates cell death, tumor growth and chemotherapy response in triple-negative breast cancer. *Nature Medicine* 22, 1303-1313. 10.1038/nm.4198.

- Brehm, K. (2010a). Echinococcus multilocularis as an experimental model in stem cell research and molecular host-parasite interaction. *Parasitology*.
- Brehm, K. (2010b). The role of evolutionarily conserved signalling systems in Echinococcus multilocularis development and host-parasite interaction. *Med Microbiol Immunol* 199, 247-259. 10.1007/s00430-010-0154-1.
- Brehm, K., and Koziol, U. (2014). On the importance of targeting parasite stem cells in anti-echinococcosis drug development. *Parasite* 21. 10.1051/parasite/2014070.
- Brehm, K., Kronthaler, K., Jura, H., and Frosch, M. (2000). Cloning and characterization of beta-tubulin genes from Echinococcus multilocularis. 01666851/00. www.elsevier.com/locate/parasitology.
- Brehm, K., Spiliotis, M., Zavala-Gongora, R., Konrad, C., and Frosch, M. (2006). The molecular mechanisms of larval cestode development: first steps into an unknown world. *Parasitol Int* 55 Suppl, S15-21. 10.1016/j.parint.2005.11.003.
- Brooijmans, N., Chang, Y.W., Mobilio, D., Denny, R.A., and Humblet, C. (2010). An enriched structural kinase database to enable kinome-wide structure-based analyses and drug discovery. *Protein Sci* 19, 763-774. 10.1002/pro.355.
- Brunetti, E., Kern, P., Vuitton, D.A., and Writing Panel for the, W.-I. (2010). Expert consensus for the diagnosis and treatment of cystic and alveolar echinococcosis in humans. *Acta tropica*, 1-16. 10.1016/j.actatropica.2009.11.001.
- Canduri, F., Perez, P.C., Caceres, R.A., and de Azevedo, W.F., Jr. (2007). Protein kinases as targets for antiparasitic chemotherapy drugs. *Curr Drug Targets* 8, 389-398. 10.2174/138945007780058979.
- Chambers, E., Ryan, L.A., Hoey, E.M., Trudgett, A., McFerran, N.V., Fairweather, I., and Timson, D.J. (2010). Liver fluke beta-tubulin isotype 2 binds albendazole and is thus a probable target of this drug. *Parasitol Res* 107, 1257-1264. 10.1007/s00436-010-1997-5.

Chaudhuri, A.R., Seetharamalu, P., Schwarz, P.M., Hausheer, F.H., and Luduena, R.F. (2000). The interaction of the B-ring of colchicine with alpha-tubulin: a novel footprinting approach. *J Mol Biol* 303, 679-692. 10.1006/jmbi.2000.4156.

Chen, J., Horton, J., Sagum, C., Zhou, J., Cheng, X., and Bedford, M.T. (2021). Histone H3 N-terminal mimicry drives a novel network of methyl-effector interactions. *Biochem J* 478, 1943-1958. 10.1042/BCJ20210203.

Chen, L.S., Redkar, S., Bearss, D., Wierda, W.G., and Gandhi, V. (2009). Pim kinase inhibitor, SGI-1776, induces apoptosis in chronic lymphocytic leukemia cells. *Blood* 114, 4150-4157. 10.1182/blood.

Chen, L.S., Redkar, S., Taverna, P., Cortes, J.E., and Gandhi, V. (2011). Mechanisms of cytotoxicity to Pim kinase inhibitor, SGI-1776, in acute myeloid leukemia. *Blood* 118, 693-702. 10.1182/blood-2010-12-323022.

Chen, W.W., Chan, D.C., Donald, C., Lilly, M.B., and Kraft, A.S. (2005). Pim family kinases enhance tumor growth of prostate cancer cells. *Molecular Cancer Research* 3, 443-451. 10.1158/1541-7786.MCR-05-0007.

Cheng, Z., Liu, F., Li, X., Dai, M., Wu, J., Guo, X., Tian, H., Heng, Z., Lu, Y., Chai, X., and Wang, Y. (2017). EGF-mediated EGFR/ERK signaling pathway promotes germinative cell proliferation in *Echinococcus multilocularis* that contributes to larval growth and development. *PLoS Neglected Tropical Diseases* 11. 10.1371/journal.pntd.0005418.

Cheng, Z., Xu, Z., Tian, H., Liu, F., Li, X., and Luo, D. Running Title: Effects of EGFR/ERK inhibitors on *E. multilocularis* 4 5 Authors.

Cheng, Z., Xu, Z., Tian, H., Liu, F., Li, X., Luo, D., and Wang, Y. (2020). In vitro and in vivo efficacies of the EGFR/MEK/ERK signaling inhibitors in the treatment of alveolar echinococcosis. *Antimicrobial Agents and Chemotherapy* 64. 10.1128/AAC.00341-20.

- Chow, J.P.H., Poon, R.Y.C., and Ma, H.T. (2011). Inhibitory Phosphorylation of Cyclin-Dependent Kinase 1 as a Compensatory Mechanism for Mitosis Exit. *Molecular and Cellular Biology* 31, 1478-1491. 10.1128/mcb.00891-10.
- Cohen, A.M., Grinblat, B., Bessler, H., Kristt, D.A., Kremer, A., Shalom, S., Schwartz, A., Halperin, M., Merkel, D., and Don, J. (2004). Increased expression of the hPim-2 gene in human chronic lymphocytic leukemia and non-Hodgkin lymphoma. *Leukemia and Lymphoma* 45, 951-955. 10.1080/10428190310001641251.
- Coles, G.C. (1986). Anthelmintic activity of triclabendazole. *J Helminthol* 60, 210-212. 10.1017/s0022149x00026110.
- Collins, J.J., 3rd, and Newmark, P.A. (2013). It's no fluke: the planarian as a model for understanding schistosomes. *PLoS Pathog* 9, e1003396. 10.1371/journal.ppat.1003396.
- Cortes, J., Tamura, K., Deangelo, D.J., De Bono, J., Lorente, D., Minden, M., Uy, G.L., Kantarjian, H., Chen, L.S., Gandhi, V., et al. (2018). Phase i studies of AZD1208, a proviral integration Moloney virus kinase inhibitor in solid and haematological cancers. *British Journal of Cancer* 118, 1425-1433. 10.1038/s41416-018-0082-1.
- Cuyper, H.T., Selten, G., Quint, W., Zijlstra, M., Maandag, E.R., Boelens, W., van Wezenbeek, P., Melief, C., and Berns, A. (1984). Murine leukemia virus-induced T-cell lymphomagenesis: integration of proviruses in a distinct chromosomal region. *Cell* 37, 141-150. 10.1016/0092-8674(84)90309-x.
- Dalbeth, N., Lauterio, T.J., and Wolfe, H.R. (2014). Mechanism of action of colchicine in the treatment of gout. *Clin Ther* 36, 1465-1479. 10.1016/j.clinthera.2014.07.017.
- Dhanasekaran, N., and Premkumar Reddy, E. (1998). Signaling by dual specificity kinases. *Oncogene* 17, 1447-1455. 10.1038/sj.onc.1202251.
- Dixon, J.B. (1997). Echinococcosis. *Comp Immunol Microbiol Infect Dis* 20, 87-94. 10.1016/s0147-9571(96)00019-7.

- Donzelli, M., and Draetta, G.F. (2003). Regulating mammalian checkpoints through Cdc25 inactivation. *EMBO reports* 4, 671-677. 10.1038/sj.embor.embor887.
- DuBridge, R.B., Tang, P., Hsia, H.C., Leong, P.M., Miller, J.H., and Calos, M.P. (1987). Analysis of mutation in human cells by using an Epstein-Barr virus shuttle system. *Molecular and cellular biology* 7, 379-387. 10.1128/mcb.7.1.379-387.1987.
- Dyachenko, V., Pantchev, N., Gawlowska, S., Vrhovec, M.G., and Bauer, C. (2008). Echinococcus multilocularis infections in domestic dogs and cats from Germany and other European countries. *Vet Parasitol* 157, 244-253. 10.1016/j.vetpar.2008.07.030.
- Eckert, J., and Deplazes, P. (2004). Biological, Epidemiological, and Clinical Aspects of Echinococcosis, a Zoonosis of Increasing Concern. *Clinical Microbiology Reviews*.
- Enamine. Real Compound Libraries. <https://enamine.net/compound-collections/real-compounds/real-compound-libraries>.
- Enamine. Hinge Binders Library. <https://enamine.net/compound-libraries/targeted-libraries/kinase-library/hinge-binders-library>.
- Engelhardt, J., Scheer, O., Stadler, P.F., and Prohaska, S.J. (2022). Evolution of DNA Methylation Across Ecdysozoa. *J Mol Evol* 90, 56-72. 10.1007/s00239-021-10042-0.
- Fabbro, D., Cowan-Jacob, S.W., and Moebitz, H. (2015). Ten things you should know about protein kinases: IUPHAR Review 14. *Br J Pharmacol* 172, 2675-2700. 10.1111/bph.13096.
- Fairweather, I., and Boray, J.C. (1999). Fasciolicides: efficacy, actions, resistance and its management. *Vet J* 158, 81-112. 10.1053/tvjl.1999.0377.
- Fairweather, I., Brennan, G.P., Hanna, R.E.B., Robinson, M.W., and Skuce, P.J. (2020). Drug resistance in liver flukes. *International Journal for Parasitology: Drugs and Drug Resistance*. Elsevier Ltd.
- Fairweather, I., Holmes, S.D., and Threadgold, L.T. (1984). Fasciola hepatica: motility response to fasciolicides in vitro. *Exp Parasitol* 57, 209-224. 10.1016/0014-4894(84)90094-8.

- Ferguson, A.M., White, L.S., Donovan, P.J., and Piwnica-Worms, H. (2005). Normal Cell Cycle and Checkpoint Responses in Mice and Cells Lacking Cdc25B and Cdc25C Protein Phosphatases. *Molecular and Cellular Biology* 25, 2853-2860. 10.1128/mcb.25.7.2853-2860.2005.
- Fetterer, R.H. (1986). The effect of albendazole and triclabendazole on colchicine binding in the liver fluke *Fasciola hepatica*. *J Vet Pharmacol Ther* 9, 49-54. 10.1111/j.1365-2885.1986.tb00011.x.
- Findeisen, P., Muhlhausen, S., Dempewolf, S., Hertzog, J., Zietlow, A., Carlomagno, T., and Kollmar, M. (2014). Six subgroups and extensive recent duplications characterize the evolution of the eukaryotic tubulin protein family. *Genome Biol Evol* 6, 2274-2288. 10.1093/gbe/evu187.
- Foo, K.Y., and Chee, H.Y. (2015). Interaction between Flavivirus and Cytoskeleton during Virus Replication. *Biomed Res Int* 2015, 427814. 10.1155/2015/427814.
- Förster, S., Koziol, U., Schäfer, T., Duvoisin, R., Cailliau, K., Vanderstraete, M., Dissous, C., and Brehm, K. (2018). The role of fibroblast growth factor signalling in *Echinococcus multilocularis* development and host-parasite interaction. *PLoS Neglected Tropical Diseases* 13. 10.1371/journal.pntd.0006959.
- Fuchs, M.A., Ryan, L.A., Chambers, E.L., Moore, C.M., Fairweather, I., Trudgett, A., Timson, D.J., Brennan, G.P., and Hoey, E.M. (2013). Differential expression of liver fluke β -tubulin isotypes at selected life cycle stages. *International Journal for Parasitology* 43, 1133-1139. 10.1016/j.ijpara.2013.08.007.
- Garge, R.K., Cha, H.J., Lee, C., Gollihar, J.D., Kachroo, A.H., Wallingford, J.B., and Marcotte, E.M. (2021). Discovery of new vascular disrupting agents based on evolutionarily conserved drug action, pesticide resistance mutations, and humanized yeast. *Genetics* 219. 10.1093/genetics/iyab101.

- Garge, R.K., Laurent, J.M., Kachroo, A.H., and Marcotte, E.M. (2020). Systematic humanization of the yeast cytoskeleton discerns functionally replaceable from divergent human genes. *Genetics* 215, 1153-1169. 10.1534/genetics.120.303378.
- Gelmedin, V., Caballero-Gamiz, R., and Brehm, K. (2008). Characterization and inhibition of a p38-like mitogen-activated protein kinase (MAPK) from *Echinococcus multilocularis*: Antiparasitic activities of p38 MAPK inhibitors. *Biochemical Pharmacology* 76, 1068-1081. 10.1016/j.bcp.2008.08.020.
- Gelmedin, V., Spiliotis, M., and Brehm, K. (2010). Molecular characterisation of MEK1/2- and MKK3/6-like mitogen-activated protein kinase kinases (MAPKK) from the fox tapeworm *Echinococcus multilocularis*. *International Journal for Parasitology* 40, 555-567. 10.1016/j.ijpara.2009.10.009.
- Grassot, J., Gouy, M., Perrière, G., and Mouchiroud, G. (2006). Origin and molecular evolution of receptor tyrosine kinases with immunoglobulin-like domains. *Molecular biology and evolution* 23, 1232-1241. 10.1093/molbev/msk007.
- Greber, U.F. (2002). Signalling in viral entry. *Cell Mol Life Sci* 59, 608-626. 10.1007/s00018-002-8453-3.
- Gu, J.J., Wang, Z., Reeves, R., and Magnuson, N.S. (2009). PIM1 phosphorylates and negatively regulates ASK1-mediated apoptosis. *Oncogene* 28, 4261-4271. 10.1038/onc.2009.276.
- Gull, K., Dawson, P.J., Davis, C., and Byard, E.H. (1987). Microtubules as target organelles for benzimidazole anthelmintic chemotherapy. *Biochemical Society transactions* 15, 59-60. 10.1042/bst0150059.
- Guralp, N., and Tinar, R. (1984). Trematodiasis in Turkey: comparative efficacy of triclabendazole and niclofolan against natural infections of *Fasciola hepatica* and *F. gigantica* in sheep. *J Helminthol* 58, 113-116. 10.1017/s0022149x00028595.

- Haddach, M., Michaux, J., Schwaebe, M.K., Pierre, F., O'Brien, S.E., Borsan, C., Tran, J., Raffaele, N., Ravula, S., Drygin, D., et al. (2012). Discovery of CX-6258. A potent, selective, and orally efficacious pan-pim kinases inhibitor. *ACS Medicinal Chemistry Letters* 3, 135-139. 10.1021/ml200259q.
- Haller, M., Deplazes, P., Guscelli, F., Sardinas, J.C., Reichler, I., and Eckert, J. (1998). Surgical and chemotherapeutic treatment of alveolar echinococcosis in a dog. *J Am Anim Hosp Assoc* 34, 309-314. 10.5326/15473317-34-4-309.
- Hemer, S., and Brehm, K. (2012). In vitro efficacy of the anticancer drug imatinib on *Echinococcus multilocularis* larvae. *International Journal of Antimicrobial Agents* 40, 458-462. 10.1016/j.ijantimicag.2012.07.007.
- Hemer, S., Konrad, C., Spiliotis, M., Koziol, U., Schaack, D., Förster, S., Gelmedin, V., Stadelmann, B., Dandekar, T., Hemphill, A., and Brehm, K. (2014). Host insulin stimulates *Echinococcus multilocularis* insulin signalling pathways and larval development. *BMC Biology* 12. 10.1186/1741-7007-12-5.
- Herz, M., and Brehm, K. (2021). Serotonin stimulates *Echinococcus multilocularis* larval development. *Parasites and Vectors* 14. 10.1186/s13071-020-04533-0.
- Herzog, S., Fink, M.A., Weitmann, K., Friedel, C., Hadlich, S., Langner, S., Kindermann, K., Holm, T., Bohm, A., Eskilsson, E., et al. (2015). Pim1 kinase is upregulated in glioblastoma multiforme and mediates tumor cell survival. *Neuro Oncol* 17, 223-242. 10.1093/neuonc/nou216.
- Horiuchi, D., Camarda, R., Zhou, A.Y., Yau, C., Momcilovic, O., Balakrishnan, S., Corella, A.N., Eyob, H., Kessenbrock, K., Lawson, D.A., et al. (2016). PIM1 kinase inhibition as a targeted therapy against triple-negative breast tumors with elevated MYC expression. *Nature Medicine* 22, 1321-1329. 10.1038/nm.4213.

- Hosokawa, M. (2008). Structure and catalytic properties of carboxylesterase isozymes involved in metabolic activation of prodrugs. *Molecules* *13*, 412-431. 10.3390/molecules13020412.
- Howe, K.L., Bolt, B.J., Cain, S., Chan, J., Chen, W.J., Davis, P., Done, J., Down, T., Gao, S., Grove, C., et al. (2016). WormBase 2016: Expanding to enable helminth genomic research. *Nucleic Acids Research* *44*, D774-D780. 10.1093/nar/gkv1217.
- Howe, K.L., Bolt, B.J., Shafie, M., Kersey, P., and Berriman, M. (2017). WormBase ParaSite – a comprehensive resource for helminth genomics. *Molecular and Biochemical Parasitology* *215*, 2-10. 10.1016/j.molbiopara.2016.11.005.
- Hubert, K., Zavala-Góngora, R., Frosch, M., and Brehm, K. (2004). Identification and characterization of PDZ-1, a N-ERMAD specific interaction partner of the *Echinococcus multilocularis* ERM protein Elp. *Molecular and Biochemical Parasitology* *134*, 149-154. 10.1016/j.molbiopara.2003.10.018.
- Hurd, D.D., Miller, R.M., Nunez, L., and Portman, D.S. (2010). Specific alpha- and beta-tubulin isoforms optimize the functions of sensory Cilia in *Caenorhabditis elegans*. *Genetics* *185*, 883-896. 10.1534/genetics.110.116996.
- Ingold, K., Bigler, P., Thormann, W., Cavaliero, T., Gottstein, B., and Hemphill, A. (1999). Efficacies of albendazole sulfoxide and albendazole sulfone against *In vitro*-cultivated *Echinococcus multilocularis* metacestodes. *Antimicrob Agents Chemother* *43*, 1052-1061. 10.1128/AAC.43.5.1052.
- Ittiprasert, W., Mann, V.H., Karinshak, S.E., Coghlan, A., Rinaldi, G., Sankaranarayanan, G., Chaidee, A., Tanno, T., Kumkhaek, C., Prangtaworn, P., et al. (2019). Programmed genome editing of the omega-1 ribonuclease of the blood fluke, *Schistosoma mansoni*. *Elife* *8*. 10.7554/eLife.41337.

- Jaroch, K., Karolak, M., Gorski, P., Jaroch, A., Krajewski, A., Ilnicka, A., Sloderbach, A., Stefanski, T., and Sobiak, S. (2016). Combretastatins: In vitro structure-activity relationship, mode of action and current clinical status. *Pharmacol Rep* 68, 1266-1275. 10.1016/j.pharep.2016.08.007.
- Jinek, M., Chylinski, K., Fonfara, I., Hauer, M., Doudna, J.A., and Charpentier, E. (2012). A programmable dual-RNA-guided DNA endonuclease in adaptive bacterial immunity. *Science* 337, 816-821. 10.1126/science.1225829.
- Johnson, L.N., and Noble, M.E.M. (1996). Active and Inactive Protein Kinases: Review Structural Basis for Regulation.
- Jung, M.K., and Oakley, B.R. (1990). Identification of an amino acid substitution in the benA, beta-tubulin gene of *Aspergillus nidulans* that confers thiabendazole resistance and benomyl supersensitivity. *Cell Motil Cytoskeleton* 17, 87-94. 10.1002/cm.970170204.
- Jung, M.K., Wilder, I.B., and Oakley, B.R. (1992). Amino acid alterations in the benA (beta-tubulin) gene of *Aspergillus nidulans* that confer benomyl resistance. *Cell Motil Cytoskeleton* 22, 170-174. 10.1002/cm.970220304.
- Jura, H., Bader, A., Hartmann, M., Maschek, H., and Frosch, M. (1996). Hepatic tissue culture model for study of host-parasite interactions in alveolar echinococcosis. *Infection and immunity* 64, 3484-3490. 10.1128/iai.64.9.3484-3490.1996.
- Kanehisa, M., Goto, S., Kawashima, S., and Nakaya, A. (2002). The KEGG databases at GenomeNet. *Nucleic acids research* 30, 42-46. 10.1093/nar/30.1.42.
- Kanev, G.K., de Graaf, C., de Esch, I.J.P., Leurs, R., Würdinger, T., Westerman, B.A., and Kooistra, A.J. (2019). The Landscape of Atypical and Eukaryotic Protein Kinases. *Trends in pharmacological sciences* 40, 818-832. 10.1016/j.tips.2019.09.002.

- Keiser, J., Engels, D., Buscher, G., and Utzinger, J. (2005). Triclabendazole for the treatment of fascioliasis and paragonimiasis. *Expert Opin Investig Drugs* *14*, 1513-1526. 10.1517/13543784.14.12.1513.
- Kern, P. (2010). Clinical features and treatment of alveolar echinococcosis. *Current opinion in infectious diseases* *23*, 505-512. 10.1097/QCO.0b013e32833d7516.
- Kim, J., Zhang, J., Cha, Y., Kolitz, S., Funt, J., Chong, R.E., Barrett, S., Kusko, R., Zeskind, B., and Kaufman, H. (2020). Advanced bioinformatics rapidly identifies existing therapeutics for patients with coronavirus disease-2019 (COVID-19). *Journal of Translational Medicine* *18*. 10.1186/s12967-020-02430-9.
- Konietzko, U., Kauselmann, G., Scafidi, J., Staubli, U., Mikkers, H., Berns, A., Schweizer, M., Waltereit, R., and Kuhl, D. (1999). Pim kinase expression is induced by LTP stimulation and required for the consolidation of enduring LTP. *The EMBO journal* *18*, 3359-3369. 10.1093/emboj/18.12.3359.
- Kouadio, J.N., Giovanoli Evack, J., Achi, L.Y., Balmer, O., Utzinger, J., N'Goran, E.K., Bonfoh, B., Hattendorf, J., and Zinsstag, J. (2021). Efficacy of triclabendazole and albendazole against *Fasciola* spp. infection in cattle in Côte d'Ivoire: a randomised blinded trial. *Acta tropica* *222*, 106039-106039. 10.1016/j.actatropica.2021.106039.
- Koziol, U., and Brehm, K. (2015). Recent advances in *Echinococcus* genomics and stem cell research. *Veterinary Parasitology*. Elsevier.
- Koziol, U., Domínguez, M.F., Marín, M., Kun, A., and Castillo, E. (2010). Stem cell proliferation during in vitro development of the model cestode *Mesocestoides corti* from larva to adult worm. *Frontiers in Zoology* *7*. 10.1186/1742-9994-7-22.
- Koziol, U., Jarero, F., Olson, P.D., and Brehm, K. (2016). Comparative analysis of Wnt expression identifies a highly conserved developmental transition in flatworms. *BMC Biology* *14*. 10.1186/s12915-016-0233-x.

- Koziol, U., Krohne, G., and Brehm, K. (2013). Anatomy and development of the larval nervous system in *Echinococcus multilocularis*. *Frontiers in zoology* 10, 24-24. 10.1186/1742-9994-10-24.
- Koziol, U., Radio, S., Smircich, P., Zarowiecki, M., Fernández, C., and Brehm, K. (2015). A novel terminal-repeat retrotransposon in miniature (TRIM) is massively expressed in *Echinococcus multilocularis* stem cells. *Genome Biology and Evolution* 7, 2136-2153. 10.1093/gbe/evv126.
- Koziol, U., Rauschendorfer, T., Zanon Rodríguez, L., Krohne, G., and Brehm, K. (2014). The unique stem cell system of the immortal larva of the human parasite *Echinococcus multilocularis*. *EvoDevo* 5. 10.1186/2041-9139-5-10.
- Kronschnabl, P., Grunweller, A., Hartmann, R.K., Aigner, A., and Weirauch, U. (2020). Inhibition of PIM2 in liver cancer decreases tumor cell proliferation in vitro and in vivo primarily through the modulation of cell cycle progression. *Int J Oncol* 56, 448-459. 10.3892/ijo.2019.4936.
- Kwa, M.S., Veenstra, J.G., and Roos, M.H. (1994). Benzimidazole resistance in *Haemonchus contortus* is correlated with a conserved mutation at amino acid 200 in beta-tubulin isotype 1. *Mol Biochem Parasitol* 63, 299-303. 10.1016/0166-6851(94)90066-3.
- Lartillot, N., and Philippe, H. (2008). Improvement of molecular phylogenetic inference and the phylogeny of Bilateria. *Philos Trans R Soc Lond B Biol Sci* 363, 1463-1472. 10.1098/rstb.2007.2236.
- Letunic, I., and Bork, P. (2018). 20 years of the SMART protein domain annotation resource. *Nucleic Acids Research* 46, D493-D496. 10.1093/nar/gkx922.
- Letunic, I., Doerks, T., and Bork, P. (2015). SMART: Recent updates, new developments and status in 2015. *Nucleic Acids Research* 43, D257-D260. 10.1093/nar/gku949.

Letunic, I., Khedkar, S., and Bork, P. (2021). SMART: Recent updates, new developments and status in 2020. *Nucleic Acids Research* 49, D458-D460. 10.1093/nar/gkaa937.

Li, J., Katiyar, S.K., and Edlind, T.D. (1996). Site-directed mutagenesis of *Saccharomyces cerevisiae* beta-tubulin: interaction between residue 167 and benzimidazole compounds. *FEBS Lett* 385, 7-10. 10.1016/0014-5793(96)00334-1.

Liang, H., Hittelman, W., and Nagarajan, L. (1996). Ubiquitous expression and cell cycle regulation of the protein kinase PIM-1. *Archives of biochemistry and biophysics* 330, 259-265. 10.1006/abbi.1996.0251.

Lin, Y.W., Beharry, Z.M., Hill, E.G., Song, J.H., Wang, W., Xia, Z., Zhang, Z., Aplan, P.D., Aster, J.C., Smith, C.D., and Kraft, A.S. (2010). A small molecule inhibitor of Pim protein kinases blocks the growth of precursor T-cell lymphoblastic leukemia/lymphoma. *Blood* 115, 824-833. 10.1182/blood-2009-07-233445.

Lipinski, C.A., Lombardo, F., Dominy, B.W., and Feeney, P.J. (2001). Experimental and computational approaches to estimate solubility and permeability in drug discovery and development settings. *Advanced drug delivery reviews* 46, 3-26. 10.1016/s0169-409x(00)00129-0.

Macaev, F., Boldescu, V., Geronikaki, A., and Sucman, N. (2013). Recent advances in the use of cyclodextrins in antifungal formulations. *Curr Top Med Chem* 13, 2677-2683. 10.2174/15680266113136660194.

Manning, G., Whyte, D.B., Martinez, R., Hunter, T., and Sudarsanam, S. (2002). The protein kinase complement of the human genome. *Science* 298, 1912-1934. 10.1126/science.1075762.

Martina, B.E., Koraka, P., and Osterhaus, A.D. (2009). Dengue virus pathogenesis: an integrated view. *Clin Microbiol Rev* 22, 564-581. 10.1128/CMR.00035-09.

- Massarotti, A., Coluccia, A., Silvestri, R., Sorba, G., and Brancale, A. (2012). The tubulin colchicine domain: a molecular modeling perspective. *ChemMedChem* 7, 33-42. 10.1002/cmdc.201100361.
- Maurer, G., Tarkowski, B., and Baccarini, M. (2011). Raf kinases in cancer-roles and therapeutic opportunities. *Oncogene* 30, 3477-3488. 10.1038/onc.2011.160.
- Melms, J.C., Vallabhaneni, S., Mills, C.E., Yapp, C., Chen, J.Y., Morelli, E., Waszyk, P., Kumar, S., Deming, D., Moret, N., et al. (2020). Inhibition of haspin kinase promotes cell-intrinsic and extrinsic antitumor activity. *Cancer Research* 80, 798-810. 10.1158/0008-5472.CAN-19-2330.
- Mochizuki, T., Kitanaka, C., Noguchi, K., Muramatsu, T., Asai, A., and Kuchino, Y. (1999). Physical and functional interactions between Pim-1 kinase and Cdc25A phosphatase. Implications for the Pim-1-mediated activation of the c-Myc signaling pathway. *The Journal of biological chemistry* 274, 18659-18666. 10.1074/jbc.274.26.18659.
- Montagne, J., Preza, M., Castillo, E., Brehm, K., and Koziol, U. (2019). Divergent Axin and GSK-3 paralogs in the beta-catenin destruction complexes of tapeworms. *Dev Genes Evol* 229, 89-102. 10.1007/s00427-019-00632-w.
- Morishita, D., Katayama, R., Sekimizu, K., Tsuruo, T., and Fujita, N. (2008). Pim kinases promote cell cycle progression by phosphorylating and down-regulating p27kip1 at the transcriptional and posttranscriptional levels. *Cancer Research* 68, 5076-5085. 10.1158/0008-5472.CAN-08-0634.
- Morris, D.L., Dykes, P.W., Dickson, B., Marriner, S.E., Bogan, J.A., and Burrows, F.G. (1983). Albendazole in hydatid disease. *British medical journal (Clinical research ed.)* 286, 103-104. 10.1136/bmj.286.6359.103-a.
- Nair, J.R., Caserta, J., Belko, K., Howell, T., Fetterly, G., Baldino, C., and Lee, K.P. (2017). Novel inhibition of PIM2 kinase has significant anti-tumor efficacy in multiple myeloma. *Leukemia* 31, 1715-1726. 10.1038/leu.2016.379.

Needham, L.A., Davidson, A.H., Bawden, L.J., Belfield, A., Bone, E.A., Brotherton, D.H., Bryant, S., Charlton, M.H., Clark, V.L., Davies, S.J., et al. (2011). Drug targeting to monocytes and macrophages using esterase-sensitive chemical motifs. *J Pharmacol Exp Ther* 339, 132-142. 10.1124/jpet.111.183640.

Newmark, P.A., and Sanchez Alvarado, A. (2002). Not your father's planarian: a classic model enters the era of functional genomics. *Nat Rev Genet* 3, 210-219. 10.1038/nrg759.

Nishida, K., Tsuchiya, K., Obinata, H., Onodera, S., Honda, Y., Lai, Y.C., Haruta, N., and Sugimoto, A. (2021). Expression Patterns and Levels of All Tubulin Isoforms Analyzed in GFP Knock-In *C. elegans* Strains. *Cell Struct Funct* 46, 51-64. 10.1247/csf.21022.

Olson, P.D., Zarowiecki, M., Kiss, F., and Brehm, K. (2012). Cestode genomics - progress and prospects for advancing basic and applied aspects of flatworm biology. *Parasite Immunology*.

Orbach, M.J., Porro, E.B., and Yanofsky, C. (1986). Cloning and characterization of the gene for beta-tubulin from a benomyl-resistant mutant of *Neurospora crassa* and its use as a dominant selectable marker. *Mol Cell Biol* 6, 2452-2461. 10.1128/mcb.6.7.2452-2461.1986.

Overend, D.J., and Bowen, F.L. (1995). Resistance of *Fasciola hepatica* to triclabendazole. *Aust Vet J* 72, 275-276. 10.1111/j.1751-0813.1995.tb03546.x.

Petropavlovskiy, A.A., Tauro, M.G., Lajoie, P., and Duennwald, M.L. (2020). A Quantitative Imaging-Based Protocol for Yeast Growth and Survival on Agar Plates. *STAR Protocols* 1. 10.1016/j.xpro.2020.100182.

Prichard, R. (2001). Genetic variability following selection of *Haemonchus contortus* with anthelmintics. *Trends Parasitol* 17, 445-453. 10.1016/s1471-4922(01)01983-3.

- Qian, K.C., Wang, L., Hickey, E.R., Studts, J., Barringer, K., Peng, C., Kronkaitis, A., Li, J., White, A., Mische, S., and Farmer, B. (2005). Structural basis of constitutive activity and a unique nucleotide binding mode of human Pim-1 kinase. *Journal of Biological Chemistry* 280, 6130-6137. 10.1074/jbc.M409123200.
- Raab, M.S., Thomas, S.K., Ocio, E.M., Guenther, A., Goh, Y.T., Talpaz, M., Hohmann, N., Zhao, S., Xiang, F., Simon, C., et al. (2019). The first-in-human study of the pan-PIM kinase inhibitor PIM447 in patients with relapsed and/or refractory multiple myeloma. *Leukemia* 33, 2924-2933. 10.1038/s41375-019-0482-0.
- Ranjan, P., Kumar, S.P., Kari, V., and Jha, P.C. (2017). Exploration of interaction zones of beta-tubulin colchicine binding domain of helminths and binding mechanism of anthelmintics. *Comput Biol Chem* 68, 78-91. 10.1016/j.compbiolchem.2017.02.008.
- Reuter, S., Beisler, T., and Kern, P. (2010). Combined albendazole and amphotericin B against *Echinococcus multilocularis* in vitro. *Acta Trop* 115, 270-274. 10.1016/j.actatropica.2010.04.009.
- Richter, D., Richter, J., Gruner, B., Kranz, K., Franz, J., and Kern, P. (2013). In vitro efficacy of triclabendazole and clorsulon against the larval stage of *Echinococcus multilocularis*. *Parasitol Res* 112, 1655-1660. 10.1007/s00436-013-3321-7.
- Richter, M., Boldescu, V., Graf, D., Streicher, F., Dimoglo, A., Bartenschlager, R., and Klein, C.D. (2019). Synthesis, Biological Evaluation, and Molecular Docking of Combretastatin and Colchicine Derivatives and their hCE1-Activated Prodrugs as Antiviral Agents. *ChemMedChem* 14, 469-483. 10.1002/cmdc.201800641.
- Rishi, S., and Rishi, K.K. (1979). Chromosomal analysis of *Trabala vishnu* Lef. (Lasiocampidae, Lepidoptera) with clear indications of localized centromeres. *Cytobios* 24, 33-42.
- Robinson, J.T., Thorvaldsdóttir, H., Winckler, W., Guttman, M., Lander, E.S., Getz, G., and Mesirov, J.P. (2011). Integrative genomics viewer. *Nature biotechnology* 29, 24-26. 10.1038/nbt.1754.

- Robinson, M.W., Hoey, E.M., Fairweather, I., Dalton, J.P., McGonigle, S., and Trudgett, A. (2001). Characterisation of a beta-tubulin gene from the liver fluke, *Fasciola hepatica*. *Int J Parasitol* 31, 1264-1268. 10.1016/s0020-7519(01)00240-5.
- Robinson, M.W., McFerran, N., Trudgett, A., Hoey, L., and Fairweather, I. (2004). A possible model of benzimidazole binding to beta-tubulin disclosed by invoking an inter-domain movement. *J Mol Graph Model* 23, 275-284. 10.1016/j.jmglm.2004.08.001.
- Robinson, M.W., Trudgett, A., Hoey, E.M., and Fairweather, I. (2002). Triclabendazole-resistant *Fasciola hepatica*: beta-tubulin and response to in vitro treatment with triclabendazole. *Parasitology* 124, 325-338. 10.1017/s003118200100124x.
- Ross, A.G., Bartley, P.B., Sleight, A.C., Olds, G.R., Li, Y., Williams, G.M., and McManus, D.P. (2002). Schistosomiasis. *N Engl J Med* 346, 1212-1220. 10.1056/NEJMra012396.
- Santio, N.M., K-J Landor, S., Vahtera, L., Ylä-Pelto, J., Paloniemi, E., Imanishi, S.Y., Corthals, G., Varjosalo, M., Babu Manoharan, G., Uri, A., et al. Phosphorylation of Notch1 by Pim kinases promotes oncogenic signaling in breast and prostate cancer cells. www.impactjournals.com/oncotarget.
- Schärfer, C., Schulz-Gasch, T., Hert, J., Heinzerling, L., Schulz, B., Inhester, T., Stahl, M., and Rarey, M. (2013). CONFECT: conformations from an expert collection of torsion patterns. *ChemMedChem* 8, 1690-1700. 10.1002/cmdc.201300242.
- Schindelin, J., Arganda-Carreras, I., Frise, E., Kaynig, V., Longair, M., Pietzsch, T., Preibisch, S., Rueden, C., Saalfeld, S., Schmid, B., et al. (2012). Fiji: an open-source platform for biological-image analysis. *Nature methods* 9, 676-682. 10.1038/nmeth.2019.
- Schubert, A., Koziol, U., Cailliau, K., Vanderstraete, M., Dissous, C., and Brehm, K. (2014). Targeting *Echinococcus multilocularis* Stem Cells by Inhibition of the Polo-Like Kinase EmPlk1. *PLoS Neglected Tropical Diseases* 8. 10.1371/journal.pntd.0002870.

- Sekar, P., Ravitchandirane, R., Khanam, S., Muniraj, N., and Cassinadane, A.V. (2022). Novel molecules as the emerging trends in cancer treatment: an update. *Med Oncol* 39, 20. 10.1007/s12032-021-01615-6.
- Shen, T., and Huang, S. (2012). The role of Cdc25A in the regulation of cell proliferation and apoptosis. *Anticancer Agents Med Chem* 12, 631-639. 10.2174/187152012800617678.
- Sidik, S.M., Hackett, C.G., Tran, F., Westwood, N.J., and Lourido, S. (2014). Efficient genome engineering of *Toxoplasma gondii* using CRISPR/Cas9. *PLoS One* 9, e100450. 10.1371/journal.pone.0100450.
- Siemann, D.W., Chaplin, D.J., and Walicke, P.A. (2009). A review and update of the current status of the vasculature-disabling agent combretastatin-A4 phosphate (CA4P). *Expert Opin Investig Drugs* 18, 189-197. 10.1517/13543780802691068.
- Smyth, J.D. (1968). In vitro studies and host-specificity in *Echinococcus*. *Bull World Health Organ* 39, 5-12.
- Spickler, A.R. (2020). *Echinococcosis*.
- Spiliotis, M., and Brehm, K. (2009). Axenic in vitro cultivation of *Echinococcus multilocularis* metacystode vesicles and the generation of primary cell cultures. *Methods in molecular biology* (Clifton, N.J.) 470, 245-262. 10.1007/978-1-59745-204-5_17.
- Spiliotis, M., Konrad, C., Gelmedin, V., Tappe, D., Brückner, S., Mösch, H.U., and Brehm, K. (2006). Characterisation of EmMPK1, an ERK-like MAP kinase from *Echinococcus multilocularis* which is activated in response to human epidermal growth factor. *International Journal for Parasitology* 36, 1097-1112. 10.1016/j.ijpara.2006.05.008.
- Spiliotis, M., Lechner, S., Tappe, D., Scheller, C., Krohne, G., and Brehm, K. (2008). Transient transfection of *Echinococcus multilocularis* primary cells and complete in vitro regeneration of metacystode vesicles. *International Journal for Parasitology* 38, 1025-1039. 10.1016/j.ijpara.2007.11.002.

- Spiliotis, M., Mizukami, C., Oku, Y., Kiss, F., Brehm, K., and Gottstein, B. (2010). Echinococcus multilocularis primary cells: Improved isolation, small-scale cultivation and RNA interference. *Molecular and Biochemical Parasitology* 174, 83-87. 10.1016/j.molbiopara.2010.07.001.
- Spiliotis, M., Tappe, D., Sesterhenn, L., and Brehm, K. (2004). Long-term in vitro cultivation of Echinococcus multilocularis metacestodes under axenic conditions. *Parasitology Research* 92, 430-432. 10.1007/s00436-003-1046-8.
- Stadelmann, B., Aeschbacher, D., Huber, C., Spiliotis, M., Müller, J., and Hemphill, A. (2014). Profound activity of the anti-cancer drug bortezomib against Echinococcus multilocularis metacestodes identifies the proteasome as a novel drug target for cestodes. *PLoS Negl Trop Dis* 8, e3352. 10.1371/journal.pntd.0003352.
- Stadelmann, B., Scholl, S., Müller, J., and Hemphill, A. (2010). Application of an in vitro drug screening assay based on the release of phosphoglucose isomerase to determine the structure-activity relationship of thiazolides against Echinococcus multilocularis metacestodes. *The Journal of antimicrobial chemotherapy* 65, 512-519. 10.1093/jac/dkp490.
- Stitt, A.W., and Fairweather, I. (1992). Spermatogenesis in Fasciola hepatica: an ultrastructural comparison of the effects of the anthelmintic, triclabendazole ("Fasinex") and the microtubule inhibitor, tubulozole *Invertebrate Reproduction and Development* 22: 1-3, 139- 150. 10.1080/07924259.1992.9672266.
- Stoll, K., Bergmann, M., Spiliotis, M., and Brehm, K. (2021). A MEKK1 – JNK mitogen activated kinase (MAPK) cascade module is active in Echinococcus multilocularis stem cells. *PLoS Neglected Tropical Diseases* 15. 10.1371/journal.pntd.0010027.
- Stothard, P. (2000). The sequence manipulation suite: JavaScript programs for analyzing and formatting protein and DNA sequences. *BioTechniques* 28, 1102, 1104-1102, 1104. 10.2144/00286ir01.

- Talbott, J.H. (1978). Treating gout: successful methods of prevention and control. *Postgrad Med* 63, 175-180.
10.1080/00325481.1978.11714839.
- Tamura, K., Stecher, G., and Kumar, S. (2021). MEGA11: Molecular Evolutionary Genetics Analysis Version 11. *Molecular Biology and Evolution* 38, 3022-3027. 10.1093/molbev/msab120.
- Tappe, D., Brehm, K., Frosch, M., Blankenburg, A., Schrod, A., Kaup, F.-J., and Mätz-Rensing, K. (2007). Echinococcus multilocularis infection of several Old World monkey species in a breeding enclosure. *The American journal of tropical medicine and hygiene* 77, 504-506.
- Thayan, R., Huat, T.L., See, L.L., Khairullah, N.S., Yusof, R., and Devi, S. (2009). Differential expression of aldolase, alpha tubulin and thioredoxin peroxidase in peripheral blood mononuclear cells from dengue fever and dengue hemorrhagic fever patients. *Southeast Asian J Trop Med Public Health* 40, 56-65.
- Thompson, J.D., Higgins, D.G., and Gibson, T.J. (1994). CLUSTAL W: improving the sensitivity of progressive multiple sequence alignment through sequence weighting, position-specific gap penalties and weight matrix choice. *Nucleic acids research* 22, 4673-4680.
10.1093/nar/22.22.4673.
- Thompson, R.C., and Eckert, J. (1982). The production of eggs by Echinococcus multilocularis in the laboratory following in vivo and in vitro development. *Z Parasitenkd* 68, 227-234. 10.1007/BF00935064.
- Thompson, R.C., and Eckert, J. (1983). Observations on Echinococcus multilocularis in the definitive host. *Z Parasitenkd* 69, 335-345.
10.1007/BF00927875.
- Thorvaldsdóttir, H., Robinson, J.T., and Mesirov, J.P. (2013). Integrative Genomics Viewer (IGV): High-performance genomics data visualization and exploration. *Briefings in Bioinformatics* 14, 178-192.
10.1093/bib/bbs017.
- Torgerson, P.R., Keller, K., Magnotta, M., and Ragland, N. (2010). The global burden of alveolar echinococcosis. *PLoS Negl Trop Dis* 4, e722.
10.1371/journal.pntd.0000722.

- Tripp, J.D., Lilley, J.L., Wood, W.N., and Lewis, L.K. (2013). Enhancement of plasmid DNA transformation efficiencies in early stationary-phase yeast cell cultures. *Yeast* 30, 191-200. 10.1002/yea.2951.
- Tsai, I.J., Zarowiecki, M., Holroyd, N., Garcarrubio, A., Sanchez-Flores, A., Brooks, K.L., Tracey, A., Bobes, R.J., Fragoso, G., Sciotto, E., et al. (2013). The genomes of four tapeworm species reveal adaptations to parasitism. *Nature* 496, 57-63. 10.1038/nature12031.
- van Durme, C.M., Wechalekar, M.D., Landewe, R.B., Pardo Pardo, J., Cyril, S., van der Heijde, D., and Buchbinder, R. (2021). Non-steroidal anti-inflammatory drugs for acute gout. *Cochrane Database Syst Rev* 12, CD010120. 10.1002/14651858.CD010120.pub3.
- Vicogne, J., Cailliau, K., Tulasne, D., Browaeys, E., Yan, Y.T., Fafeur, V., Vilain, J.P., Legrand, D., Trolet, J., and Dissous, C. (2004). Conservation of epidermal growth factor receptor function in the human parasitic helminth *Schistosoma mansoni*. *J Biol Chem* 279, 37407-37414. 10.1074/jbc.M313738200.
- Wenemoser, D., Lapan, S.W., Wilkinson, A.W., Bell, G.W., and Reddien, P.W. (2012). A molecular wound response program associated with regeneration initiation in planarians. *Genes & Development* 26, 988-1002. 10.1101/gad.187377.112.
- World Health Organization. (2015). WHO estimates of the global burden of foodborne diseases: foodborne disease burden epidemiology reference group 2007-2015.
- Wolff, K., Eckert, J., Schneider, G., and Lutz, H. (1983). Efficacy of triclabendazole against *Fasciola hepatica* in sheep and goats. *Vet Parasitol* 13, 145-150. 10.1016/0304-4017(83)90074-2.
- Yu, Z., Zhao, X., Ge, Y., Zhang, T., Huang, L., Zhou, X., Xie, L., Liu, J., and Huang, G. (2014). A regulatory feedback loop between HIF-1alpha and PIM2 in HepG2 cells. *PLoS One* 9, e88301. 10.1371/journal.pone.0088301.

Zhang, N., Bao, Y., Xie, Z., Huang, X., Sun, Y., Feng, G., Zeng, H., Ren, J., Li, Y., Xiong, J., et al. (2019). Efficient Characterization of Tetraploid Watermelon. *Plants (Basel)* 8. [10.3390/plants8100419](https://doi.org/10.3390/plants8100419).

7.2 Approval of secondary publication

Kinase project part of this dissertation includes the same experimental data and materials from our manuscript below, submitted to PLOS Neglected diseases.

The title of that manuscript is,

Targeting *Echinococcus multilocularis* PIM kinase for improving anti-parasitic chemotherapy

The author list is,

Akito Koike, DVM Frank Becker, PhD Peter Sennhenn, PhD Jason Kim, PhD

Jenny Zhang, PhD Stefan Hannus, PhD Klaus Brehm, PhD

In addition, I contacted the officer of journal to know their policy on secondary publication.

Eoin O'connor, a journal assistant answered that

Thank you for your email. You are welcome to re-use the content from any PLOS articles.

All PLOS articles are published under a Creative Commons Attribution license (CC BY), further information about the terms of the license can be found at: <https://www.plos.org/license>.

All of our articles are available (through our websites) for anyone to download, re-use, reprint, modify, distribute, and/or copy so long as the original authors and source are cited.

8 Appendix and curriculum vitae

8.1 List of 400 compounds against EmPim

| Compound ID | Library | SMILES |
|-----------------|-----------------|--|
| Z991902128 | enamine_hinge | <chem>CC(C)c1nc(C)cc(N(CC2)CCN2c2ncnc3c2cc[nH]3)n1</chem> |
| Z4072835003 | enamine_diverse | <chem>CC1=C([C@@H]2C[C@H]2NC2=NC(C3CC3)=NC=C2C#N)C=NN1C</chem> |
| Z1678860120 | enamine_hinge | <chem>O=C(c1c(C2CCCC2)ncs1)Nc1cc(-c2ccncc2)n[nH]1</chem> |
| Z3888246969 | enamine_diverse | <chem>COCC1CCN(C2=CC=C(C(=O)NC3=CC(C4=CC=NC(C)=C4)=N[NH]3)C=C2)C1</chem> |
| Z1679672955 | enamine_hinge | <chem>CN(CCCc1n[nH]c(N)c1C#N)c1nnc(-c2ncccc2)s1</chem> |
| Z4229921168 | enamine_diverse | <chem>CN1C=C(CNC(C)(C)C2=N[NH]C(C3=CC=CS3)=N2)N2N=CC(C#N)=C12</chem> |
| Z979287238 | enamine_hinge | <chem>O=C(c1cn(-c(cc2)ccc2Cl)nc1)Nc1cc(-c2ccncc2)n[nH]1</chem> |
| PV-002785215900 | enamine_diverse | <chem>O=C(NCCC1(NC2=NN=CO2)CCC1)C1=C(C2=CC=CS2)[NH]N=C1</chem> |
| Z2053652475 | enamine_hinge | <chem>COC(CC1)(CCN1c1ncnc2c1cc[nH]2)c1nc(C2CCOCC2)no1</chem> |
| PV-002995981769 | enamine_diverse | <chem>CC1=CC=C(F)C2=C1C=C(C(=O)NC1=CN(C)N=C1C1=CC=NN1C)O2</chem> |
| Z1039064876 | enamine_hinge | <chem>FC(c(cc1)cn2c1nnc2C(CCC1)CN1c1ncnc2c1cc[nH]2)(F)F</chem> |
| Z3606267270 | enamine_diverse | <chem>CCN(C1=CC=C(C(=O)NC2=CN(C)N=C2C2=CC=NN2C)C=N1)C(C)C</chem> |
| Z2272316662 | enamine_hinge | <chem>O=C(NC1CC1)NC(CC1)CN1c1ncnc2c1c(cccc1)c1[nH]2</chem> |
| Z4341639935 | enamine_diverse | <chem>N#CC1=CC=C(NCC2=NC3=C(CCCC3)[NH]2)C=C1C1=CC=NC=C1</chem> |
| Z2997391675 | enamine_hinge | <chem>COCC1(CC1)c1noc(-c2c3nc(CC4CC4)[nH]c3ncc2)n1</chem> |
| PV-002877018476 | enamine_diverse | <chem>CC1=CC2=C(C=C1C#N)[NH]N=C2NC(=O)C1=CSC(C2=CN=C[NH]2)=N1</chem> |
| Z3686137214 | enamine_hinge | <chem>CN(C)c1nccc(N[C]C@H]2NC(NC3=O)=NC=C3Cl)C[C@@H]2OC)n1</chem> |
| Z3299201507 | enamine_diverse | <chem>CC(C)C1=NC(C(C)NC(=O)CC2=C[NH]C3=NC=CC(Cl)=C23)=N[NH]1</chem> |
| Z298641114 | enamine_hinge | <chem>CC(C)C(C(N(CC1)CC=C1c1c[nH]c2c1cccn2)=O)NC(c(F)ccc1)c1F)=O</chem> |
| Z4353162286 | enamine_diverse | <chem>O=C(NC1=CC=C(F)C(C2=CC=NC=C2)=C1)[C@H]1CC[C@H](C2=NC=N[NH]2)CC1</chem> |
| Z651752060 | enamine_hinge | <chem>O=C(c(cc1)cc(N2)c1OCC2=O)Nc(cc1)cc2c1[nH]c(-c(cc1)ccc1F)n2</chem> |
| Z4436022980 | enamine_diverse | <chem>CCN1C(=O)N(CC)C2=CC(NC3=NC(C4CC4)=NC=C3C#N)=CC=C21</chem> |
| Z3144202871 | enamine_diverse | <chem>CCCOC1=CC=C(C(=O)NC2=CN([C@@H]3COC[C@H]3N)N=C2)C=C1C(C)C</chem> |
| Z2951705193 | enamine_hinge | <chem>O=C1NC(CN(CCC2)CC2c2c[nH]c3c2cccn3)=Nc(cc2)c1cc2Cl</chem> |
| Z4145387080 | enamine_diverse | <chem>CN1N=CC(CN)=C1NC(=O)C1=CN(C(C)(C)C)N=C1C1=CC=C(F)C=C1F</chem> |
| Z2067253656 | enamine_hinge | <chem>Cc(ccc(NC(C1CC1)=O)c1)c1NC(c1cc(NC(C2CC2)=O)ncc1)=O</chem> |
| Z1671544587 | enamine_hinge | <chem>O=C(Nc1c[nH]nc1-c1ncccc1)N(CCCC1)C1c1c[nH]nc1</chem> |
| Z4272323057 | enamine_diverse | <chem>CCCN(CC1=CC=C(F)C=C1F)C(=O)NC1=CN(C)N=C1C1=CC=NN1C</chem> |
| Z1432828032 | enamine_hinge | <chem>CN(CCOC)c(cc1)cnc1NC(c(cc1)ccc1-c1nc(C2CC2)n[nH]1)=O</chem> |
| PV-002931613198 | enamine_diverse | <chem>N#CC1=CC=C(NC(=O)NC2=NN3CCCC3=C2)C=C1C1=CC=NC=C1</chem> |
| Z2365128081 | enamine_hinge | <chem>C[C@](C1)(C[C@@H]1Nc1nccc(-c(cc2)ccc2OC)n1)O</chem> |
| PV-002732961802 | enamine_diverse | <chem>CCC1=C[NH]C2=NC=C(C3=CC=C(C(=O)O)C(N4C=NN=N4)=C3)C=C12</chem> |
| Z4074472362 | enamine_diverse | <chem>CN1C=CN=C1C(NC1=NC(C2CC2)=NC=C1C#N)C1=CC=C(F)C=C1F</chem> |

8 Appendix and curriculum vitae

| | | |
|-----------------|-----------------|---|
| Z4081605925 | enamine_hinge | COc(ccc(-c1ccncc1)c1)c1-c1nc(N2CCNCC2)ncc1 |
| Z3094888956 | enamine_hinge | CC(C1)N(Cc2ccccc2)CCN1c1nnc(-c2cnc3[nH]ncc3c2)n1C |
| Z4239013469 | enamine_diverse | CN1C=C(CNC2=CC=C(CI)C(NC(=O)C3CC3)=C2)N2N=CC(C#N)=C12 |
| Z1280614515 | enamine_hinge | CNC(c1cccc(C(Nc2cc(-c3ccncc3)n[nH]2)=O)c1)=O |
| PV-002744692403 | enamine_diverse | N#CC1=CC=C(NC(=O)C2=C(O)N3N=CC=C3N=C2)C=C1C1=CC=NC=C1 |
| Z2365085666 | enamine_hinge | CN(C(CC1)C2)C1CC2Nc(nc1-c2csc2)ncc1F |
| PV-002834442825 | enamine_diverse | CCC1=C[NH]C2=NC=C(C3=CC(C4(C(=O)OC)CC4)=CC(F)=C3)C=C12 |
| Z4150465616 | enamine_diverse | CC(C)CC1=N[NH]C2=CC=C(C(=O)NC3=CN(C)N=C3C3=CC=NN3C)C=C12 |
| Z1147318407 | enamine_hinge | O=C(c1c[nH]nc1-c1cnccc1)Nc(cc1)ccc1-c1n[nH]cc1 |
| Z3144195577 | enamine_diverse | CN1CCN(C2=CC=C(C(=O)NC3=CN([C@@H]4COC[C@@H]4N)N=C3)C=C2F)C1 |
| Z3772051498 | enamine_hinge | Cc1nn(CC(F)(F)F)cc1Nc(nc1)nc(NCCNC(C2CCC2)=O)c1Br |
| Z3649641075 | enamine_diverse | CC1(O)CCN(C2=CC(NCC3=N[NH]C4=CC=C(CI)C=C34)=NC=N2)CC1 |
| Z1039080880 | enamine_hinge | C(CN(CC1)c2nnc3c2cc[nH]3)C1c1c[nH]c2c1ccn2 |
| Z1349148161 | enamine_hinge | COCCN(CCC1)CC1Nc(cc1)nn2c1nnc2C1CC1 |
| Z4343145856 | enamine_diverse | C[C@@H](NC1=NC=C2SC(N[C@H](C)C3=CC=NN3C)=CC2=N1)C1=CC=NN1C |
| Z2143800551 | enamine_hinge | FC(Oc1cc(C(C2)OCCN2c2nnc3c2cc[nH]3)ccc1)(F)F |
| PV-002814907453 | enamine_diverse | O=C(NCCC1(NC2=NN=CO2)CCC1)C1=CC=NC(C2=NC=C[NH]2)=C1 |
| Z1863838555 | enamine_hinge | OC[C@H](C1)C=C[C@H]1Nc(nc(N[C@@H]1C=C[C@H](CO)C1)nc1)c1Cl |
| Z3606265204 | enamine_diverse | CN1CCC(=O)NC2=CC(C(=O)NC3=CN(C)N=C3C3=CC=NN3C)=CC=C21 |
| Z4055346469 | enamine_diverse | CC1(C(=O)NC2=CN([C@@H]3COC[C@@H]3N)N=C2)CCN(C2=CC=NC=C2)CC1 |
| Z2770864932 | enamine_hinge | C(C(CC1)CCN1c1nnc2c1cc[nH]2)c1nc(cccc2)c2[nH]1 |
| Z1631504029 | enamine_hinge | O=C(c1cc(-c2nnc[nH]2)ccc1)Nc1nccc(C(F)(F)F)c1 |
| Z3888247203 | enamine_diverse | CC1=CC(C2=N[NH]C(NC(=O)C3=C(C)N(CC4CCOC4)C(C)=C3)=C2)=CC=N1 |
| Z1801657178 | enamine_hinge | CC(N(CC1)CCN1c1ccc(CNc2nn3c(-c(cccc4)c4F)nnc3cc2)cc1)=O |
| Z2190156351 | enamine_diverse | CN1C=C(NC(=O)NC2=NN(C3=CC=C(C#N)C=C3C)C=C2)C(C2CC2)=N1 |
| Z1139201870 | enamine_hinge | CC(CN(CC1)c2nnc3c2cc[nH]3)N1c(cc1)nn2c1nnc2 |
| Z3712341675 | enamine_diverse | CCN1CCN(C2=CC=C(C(=O)NC3=NN(C4=CN(C)N=C4)N=C3)C=C2F)CC1 |
| PV-002919752942 | enamine_diverse | CC1=C[NH]C2=NC=C(C(=O)NC3=CC(C4=CN(C)N=C4)=CC=N3)C=C12 |
| Z641415982 | enamine_hinge | Cn1c(-c2c(-c3ccccc3)nc(NC(c3n[nH]c4c3CCC4)=O)s2)ncc1 |
| Z1743912850 | enamine_hinge | O=C(c(c[nH]1)c1N1)N=C1N(CC1)CCN1c1cc(C2CC2)n[nH]1 |
| PV-002785833291 | enamine_diverse | CC1=CC=C2C(C(=O)NC3=CN(C)N=C3C3=CC=NN3C)=CC=NC2=C1 |
| Z1230400425 | enamine_hinge | O=C1NC(CN(CC2)CCC2c2c[nH]c3c2ccn3)=Nc(cc2)c1cc2Cl |
| PV-002917326625 | enamine_diverse | CCC1=C[NH]C2=NC=C(C3=C(F)C=C4NC(=O)C(C)(C)C4=C3)C=C12 |
| Z2630815440 | enamine_hinge | CCC(C=C1C(Nc2n[nH]c(C3CCCCC3)c2)=O)=CNC1=O |
| Z4008303813 | enamine_diverse | CC1=CC=C(NCC2=NC=C(C(=O)OC(C)(C)N2C)C2=C1C(C#N)=C[NH]2 |
| Z1979301510 | enamine_hinge | Cc1cc(C(Nc(cc(CCC(N2)=O)c2c2)c2F)=O)nc(NC)n1 |
| PV-002965683171 | enamine_diverse | N#CC1=CC=C(N2N=CN=C2NC(=O)C2=CC(C3CC3)=CC=C2F)C=C1 |
| Z1534432517 | enamine_hinge | C=CCNc1ncc(C(Nc2n[nH]c(cc3)c2cc3[N+]([O-])=O)=O)s1 |

8 Appendix and curriculum vitae

| | | |
|-----------------|-----------------|---|
| PV-003018051685 | enamine_diverse | N#CC1=CC=C(NC(=O)NC2=C3NCCCN3N=C2)C=C1C1=CC=NC=C1 |
| Z1715352094 | enamine_hinge | Cn1c(-c2n[nH]c3c2ccc(C(O)=O)c3)nc2c1cccc2OC |
| Z3175745907 | enamine_diverse | CC1=CC=C(NC(=O)NC2=CN(C)N=C2C2CC2)C2=C1C(C#N)=C[NH]2 |
| Z1423688478 | enamine_hinge | O=C(c1cnccc1)Nc1cc(-c2ccc(F)c2F)n[nH]1 |
| Z3833067008 | enamine_diverse | CC1=NC(NC2CCCN(C3=CC(=O)[NH]C=N3)C2)=CC(C2=CC=NC=C2)=N1 |
| Z2890437514 | enamine_hinge | O=C(C1=CC(COCC2)=C2NC1=O)N(CC1)CC=C1c1c[nH]c2c1cccn2 |
| PV-002982183422 | enamine_diverse | CC1=CC=C(CNC2=C(C(N)=O)C(C(C)C)=N[NH]2)C(C2=CN(C)N=C2)=C1 |
| Z1725346549 | enamine_hinge | O=C(c(c[nH]1)c1N1)N=C1N(CC1)CCC1c1c[nH]c2c1cccn2 |
| PV-002886983380 | enamine_diverse | CN1C=C(C2=CC=NC(NC(=O)C3=CC=C4[NH]C=C(C#N)C4=C3)=C2)C=N1 |
| PV-002866207541 | enamine_diverse | CC(C)C1=N[NH]C2=CN=CC(C3=CC(S(N)(=O)=O)=CC=C3C1)=C12 |
| Z1241143852 | enamine_hinge | O=C1NC(CN(CC2)CC=C2c2c[nH]c3c2cccn3)=Nc(cc2)c1cc2Cl |
| Z1242163269 | enamine_hinge | Cc1ccc(-c2n[nH]c(NC(C3=CC(CCCCC4)=C4NC3=O)=O)c2)s1 |
| PV-002814491924 | enamine_diverse | CC(C)(C)C1=C(C2=NC(C3=CC(C(N)=O)=C[NH]3)=NO2)N2CCCCC2)=N1 |
| Z2076067815 | enamine_hinge | O=C(C1CC1)Nc1nccc(C(Nc2c[nH]nc2-c(cccc2)c2F)=O)c1 |
| PV-002804071204 | enamine_diverse | CC1=NC2=C(C#N)C=NN2C(NC2=CC=C3CC(C)(C)CC3=C2)=C1 |
| Z3847603739 | enamine_hinge | C(CNc1c(C2CC2)cnc(Nc2cccc(CN3CCOCC3)c2)n1)c1c[nH]cn1 |
| Z4272309690 | enamine_diverse | COC1=CC=C(C(OC)C(C)NC(=O)NC2=CN(C)N=C2C2=CC=NN2C)C=C1 |
| Z3884859974 | enamine_hinge | CNc(nc(Nc(cc1)cc2c1OCCN2C)nc1)c1Cl |
| PV-002747354668 | enamine_diverse | N#CC1=CC(C2=CC=NC=C2)=CC(NC(=O)NC2=C3CCCCN3N=C2)=C1 |
| Z1671815711 | enamine_hinge | Cn1c(-c2nn(C)c(NC(NC(C3)Cc4c3[nH]nc4)=O)c2)nc1 |
| Z3506642551 | enamine_diverse | COC1=CC(C2=CC3=C(N4CCC4)N=C(C)N=C3S2)=CN=C1C#N |
| Z4521999237 | enamine_hinge | CC(C(N(C1)C[C@@H](C2)[C@H]1CN2c1ncnc2c1cc[nH]2)=O)n1cncc1 |
| PV-002920142336 | enamine_diverse | CC1=NC(C2=CC=NC(NC(=O)C3=CSC(C4=CN=C[NH]4)=N3)=C2)=N[NH]1 |
| Z4148638379 | enamine_diverse | CC(C)CC1=N[NH]C2=CC=C(C(=O)NC3=CC(C4CCCOC4)=NN3C)C=C12 |
| Z1897709996 | enamine_hinge | Cc1cc(F)c(CS(Nc2cc(-c3ccncc3)n[nH]2)(=O)=O)cc1 |
| Z224669120 | enamine_hinge | CCn(c1nc(-c2cccs2)c2)nc1c2C(Nc1nc(CCN(C)C2)c2s1)=O |
| PV-003025269455 | enamine_diverse | N#CC1=C2CCCC2=CN=C1NCC1=N[NH]C2=CC=C(CI)C=C12 |
| Z785206520 | enamine_hinge | O=S(CCC1)(N1c(cc1)cc(Nc2nc(C(F)(F)F)ccn2)c1F)=O |
| Z4429422034 | enamine_diverse | CN1C=C(NC(=O)C2=CC=C3CC(N)CCC3=C2)C(C2=CC=NC=C2)=N1 |
| Z1723428223 | enamine_hinge | CN(CCC1CNC(c2cc(C(C=C3N4C)=CNC3=NC4=O)ccc2)=O)C1c1cccs1 |
| Z3384716171 | enamine_diverse | CN1C=C(C2=CC=NC(NC(=O)C3=CSC(N4CCNCC4)=N3)=C2)C=N1 |
| Z2052377024 | enamine_hinge | Cn1nccc1[C@@H]1OCC[C@H]1CNc1c[nH]nc1-c1ncccc1 |
| Z4064028866 | enamine_diverse | CC1=NC(C2=CC(NC(=O)C3=C4CNCCN4C=C3)=CC(C(F)(F)F)=C2)=N[NH]1 |
| Z1872361171 | enamine_hinge | Cc1cnc(C(CC2)CCN2c2ncnc3c2cc[nH]3)s1 |
| PV-002944532109 | enamine_diverse | CC1=CC(C2=N[NH]C(NC(=O)NC3=NC=C(C#N)C=C3C)=C2)=CC=N1 |
| Z1527067014 | enamine_hinge | FC(Oc1cc(C(C2)OCCN2c2ncnc3c2cc[nH]3)ccc1)F |
| Z4185241582 | enamine_diverse | FC1=CN=CC=C1C1(CNC2=NC=C(F)C(C3=CSC=C3)=N2)CCNCC1 |
| Z1070433012 | enamine_hinge | Clc(ccc(C1)OCCN1c1ncnc2c1cc[nH]2)c1c1Cl |

8 Appendix and curriculum vitae

| | | |
|-----------------|-----------------|--|
| PV-002746815583 | enamine_diverse | CNC1=CC(NCC2=N[NH]C3=CC=C(C)C=C23)=NC(C2=COC=C2)=N1 |
| Z44542174 | enamine_hinge | O=C1NC(CNc2cc(CCC3)c3cc2)=Nc2c1c(-c(cccc1)c1Cl)cs2 |
| PV-002588600081 | enamine_diverse | CN1C=C(CNC2=C(C#N)C(C3CC3)=N[NH]2)C(C2=CC=NN2C)=N1 |
| Z1953282117 | enamine_hinge | O=C(C(COCC1)N1C1CCCC1)Nc1n[nH]c2c1ccc(F)c2 |
| PV-002738249423 | enamine_diverse | N#CC1=CC(C2=CC=NC=C2)=CC(NC(=O)[C@H]2C[C@H](N3C=CN=N3)C2)=C1 |
| Z1661110183 | enamine_hinge | NC(N(CCC1)CC1Nc1cc(C#N)c(cc(cc2)Cl)c2n1)=O |
| PV-002900331067 | enamine_diverse | COC(=O)C1=C2CN(C(=O)C3=CC=C4[NH]C=C(C#N)C4=C3)CCN2C=C1 |
| Z3606258171 | enamine_diverse | CC(C)C1=CC(C(=O)NC2=CN(C)N=C2C2=CC=NN2C)=C(C(C)C)[NH]1 |
| Z1874227393 | enamine_hinge | Cc1cc(C(CCC2)Nc3c(cc(cc4)S(C)(=O)=O)c4ncn3)c2cc1 |
| Z2198299248 | enamine_hinge | Cc1n[nH]c(-c2ccccc2)c1NC(c1cc(NC(C2CC2)=O)nc1)=O |
| Z4233590640 | enamine_diverse | CC1=CC(NCC2CCN(C3=NC=NC4=C3C=C[NH]4)CC2)=C(C#N)C=N1 |
| Z1533617251 | enamine_hinge | O=S(CCC1)(N1c(cc(cc1)NCc2nc[nH]2)c1F)=O |
| PV-002870224141 | enamine_diverse | COC1=CC(C#N)=CC=C1C(=O)NC1=CC(C2=CC=NC(C)=C2)=N[NH]1 |
| Z2722929943 | enamine_hinge | C[C@H]1NCCO[C@H]1c(cc1)ccc1-c1cnc2[nH]ccc2c1 |
| Z3562247574 | enamine_diverse | CC(C)C[C@H]1C[C@H](NC2=NC=C(C#N)C3=C2SC=C3)C(=O)N1 |
| Z2762045227 | enamine_hinge | Cc1c(C)[nH]c2c1c(N(C[C@H]1COCC3)C[C@]13C(NC)=O)ncn2 |
| PV-002907578606 | enamine_diverse | CC(C)C1=NC(C2=CC=C(C3=CN4N=CC(C#N)=C4N=C3)C=C2)=N[NH]1 |
| Z229742824 | enamine_hinge | CC(C)n1ncc(c(C(Nc2nc(CC(N)=O)cs2)=O)c2)c1nc2-c1c(C)sc(C)c1 |
| Z4025846504 | enamine_diverse | O=C(NC1=CN(C2=C(F)C=CC=C2F)N=C1)[C@H]1CCCO[C@H]1C1=NC=C[NH]1 |
| Z1357562157 | enamine_hinge | Cc(c1c2)n[nH]c1ncc2NC(C(CC1)C(c2cn(C)nc2)N(C)C1=O)=O |
| PV-002743070947 | enamine_diverse | N#CC1=CC=C(NC(=O)NC2=CN(CCF)N=C2)C=C1C1=CC=NC=C1 |
| Z1696310077 | enamine_hinge | CC(C)n1ncc2cc(CNc3nc(cc(cc4)F)c4n3C)cnc12 |
| Z4272307227 | enamine_diverse | CC(C1CC1)N1C=C(NC(=O)NC2=CN(C)N=C2C2=CC=NN2C)C=N1 |
| Z1958597427 | enamine_hinge | Cc1nc(cccc2)c2n1C(CC1)CCN1c1ncnc2c1cc[nH]2 |
| PV-002781563131 | enamine_diverse | CN1N=CC2=C1SC(C(=O)NC1=CC=C(C#N)C(C3=CC=NC=C3)=C1)=C2 |
| Z1642775153 | enamine_hinge | N#Cc1c(NC(CC2)CCN2c(cc2)nc2C#N)nc2n1cccc2 |
| Z4013386833 | enamine_diverse | CN1CCN(C(=O)NC2=CN(C3=C(F)C=CC=C3F)N=C2)CC1C1=NC=C[NH]1 |
| Z2274404638 | enamine_hinge | FC(c1cc(C(C2)CN2c2ncnc3c2cc[nH]3)ccc1)(F)F |
| PV-003024575700 | enamine_diverse | CN1C=C(CNC2=NC3=CC(C#N)=CC=C3N2C)C(C2=CC=NN2C)=N1 |
| Z2761199587 | enamine_hinge | Cc1c(C)[nH]c2c1c(N(C[C@H]1CCC3)C[C@]13c1nnc(C)O1)ncn2 |
| Z3888246704 | enamine_diverse | COC1(C2=CC=CC(C(=O)NC3=CC(C4=CC=NC(C)=C4)=N[NH]3)=C2)COC1 |
| Z3772051632 | enamine_hinge | Cc1nn(CC(F)(F)F)cc1Nc1nc(NCCc2cnc[nH]2)c(C2CC2)cn1 |
| PV-002796152175 | enamine_diverse | CC1(C)COC2=CC(NC3=NC(C4CC4)=NC=C3C#N)=CC=C21 |
| Z3950742997 | enamine_hinge | CNc(nc(Nc(cc1)cc2c1ncs2)nc1)c1Cl |
| PV-002763471892 | enamine_diverse | CCCC1=N[NH]C2=CC=C(C(=O)NC3=NN(CC)C(C4CC4)=C3)C=C12 |
| Z2272518272 | enamine_hinge | CS(C(CCCC1)CN1c1ncnc2c1c(cccc1)c1[nH]2)(=O)=O |
| PV-003009688818 | enamine_diverse | CC1=CC(N2C=CN=C2C)=CC=C1CNC1=C(C2=CC=NN2C)[NH]N=N1 |
| Z1623354286 | enamine_hinge | Cc1ccc(-c2n[nH]c(NC(c3cnc4n(C)nc4c3)=O)c2)s1 |

8 Appendix and curriculum vitae

| | | |
|-----------------|-----------------|--|
| Z4274715050 | enamine_diverse | CC1=C[NH]C(C2(NC(=O)NC3=CN(C4=C(F)C=CC=C4F)N=C3)CCC2)=N1 |
| Z4414586244 | enamine_diverse | CC1(C2=NOC(C3=NC=NC4=C3C(Br)=C[NH]4)=N2)CCNCC1 |
| Z26215952 | enamine_hinge | Cc(cccc1)c1Nc1nc(N)nc(COn2nnc(cc3)c2cc3S(C)(=O)=O)n1 |
| Z229257634 | enamine_hinge | FC(c1nnc(cc2)n1nc2Nc(cc1)cc2c1nc(N1CCCC1)s2)(F)F |
| PV-000578091755 | enamine_diverse | O=C(NC1CCCN(C(=O)C2=N[NH]C(C3CC3)=C2)CC1)C1=NC=C[NH]1 |
| Z3686278238 | enamine_hinge | CN(C=C(N1)N(CC2)C[C@@H]2Nc2hccc(-c(cccc3)c3F)n2)=O)C1=O |
| Z4449016638 | enamine_diverse | N#CC1=CC(C2=CC=NC=C2)=CC(NC(=O)C23COC(CN2)C3)=C1 |
| Z224443506 | enamine_hinge | O=C(c1c[nH]nc1-c(cc1)cc2c1OCCO2)Nc1nc(cccc2)c2[nH]1 |
| Z3832851705 | enamine_diverse | CCN1N=CC2=C1CCC(NC1=NC(C3=CC=NC=C3)=NC(C)=C1C)C2 |
| Z2205469925 | enamine_hinge | Cc(cc(c(C(NCC(F)(F)F)=O)c1)NC(c(cc2nn[nH]c2c2)c2OC)=O)c1F |
| Z3606252530 | enamine_diverse | COCCN1C=C(C(=O)NC2=CN(C)N=C2C2=CC=NN2C)C=CC1=O |
| Z52593003 | enamine_hinge | Cc1nc(Nc(cc2)ccc2C(N)=O)c(c(-c(cc2)cc(OC)c2OC)cs2)c2n1 |
| PV-002957303960 | enamine_diverse | CCC1=C(C(=O)NC2CCN(C3=C(C#N)C=NC(C)=C3)CC2)N=C(C)[NH]1 |
| Z1534432318 | enamine_hinge | CCNc1nccc(C(Nc2n[nH]c(cc3)c2cc3[N+](O)=O)=O)c1 |
| PV-002883150620 | enamine_diverse | CC(C)(C#N)C1=CC=CC(NC(=O)C2=CN=CC(C3=N[NH]C=C3)=C2)=C1 |
| Z1659270565 | enamine_hinge | CC[C@@H](C(Nc1cc(-c2ccncc2)n[nH]1)=O)NC(c1ccccc1)=O |
| Z4255631373 | enamine_diverse | CN1C(F)=NC(Cl)=C1C1=NOC(C2=NC(C3CC3)=NC=C2Br)=N1 |
| Z1600302705 | enamine_hinge | CCc(cncc1)c1C(Nc1n[nH]c(C2CCOCC2)c1)=O |
| Z2762269922 | enamine_diverse | CC1=CC=C(C2=CC=C(C(=O)NC3=C(C4CCNC4)[NH]N=C3)C(F)=C2)C=C1C |
| Z1462285873 | enamine_hinge | O=S(CCC1)(N1c1cc(NCc2c3[nH]ncc3ccc2)ccc1)=O |
| Z3809196940 | enamine_diverse | CC1=C(C2=NC(C3=C(N)N(CCC(C)C)N=C3)=NO2)C2=CC=NC=C2C=C1 |
| Z1723434154 | enamine_hinge | CN(c1c(N2)hcc(-c3cc(C(NC4CCOCC4)=O)ccc3)c1)C2=O |
| PV-002980361582 | enamine_diverse | O=C(NC1=CC(CC2=CC=CC=C2)=CC=N1)C1=CC=NC(C2=NC=C[NH]2)=C1 |
| Z3841381688 | enamine_diverse | COC1=CC([C@@H]2C[C@H]2NC(=O)NC2=CN(C)N=C2C2=CC=NC=C2)=CC=C1F |
| Z3077896328 | enamine_hinge | CCOc1c(N(CC2)CCN2c2nnc3c2cc[nH]3)nccc1 |
| Z2646616091 | enamine_hinge | CCn1nccc1[C@H]1OCC[C@@H]1NC(c1c2nc(C)[nH]c2ncc1)=O |
| Z3337830877 | enamine_diverse | CN1C=C(CNC2=CC=C(C(N)=O)C(N3CCCC3)=C2)C(C2=CC=NN2C)=N1 |
| Z2069984535 | enamine_hinge | Cc(ccnc1)c1NC(c1cc(NC(C2CC2)=O)ncc1)=O |
| Z3367330572 | enamine_diverse | CCC(C)OC1=CC(C2=NOC(C3=CN(C)N=C3C3=CC=NN3C)=N2)=CC=N1 |
| Z3356046392 | enamine_hinge | CNC(c1nccc(Oc2cccc(NC(c3cncc4c3[nH]c(C(F)(F)F)n4)=O)c2)c1)=O |
| Z4148599016 | enamine_diverse | CC(C)CC1=N[NH]C2=CC=C(C(=O)NC3=CC(C4=CN(C)N=C4)=NN3C)C=C12 |
| Z1614095645 | enamine_hinge | C(CC(C1)c2n[nH]c(-c3cccc3)n2)CN1c1ncnc2c1cc[nH]2 |
| PV-003000550853 | enamine_diverse | COC1=CC=C2[NH]C=CC2=C1C(=O)NC1=CN(C)N=C1C1=CC=NN1C |
| Z1576596711 | enamine_hinge | CC(N(C)Cc1cccc(Nc(cc2)nn3c2nnc3C(F)F)c1)=O |
| Z4211227894 | enamine_diverse | CN1C=C(CNCC2=CC=CC(N3CCOCC3)=N2)N2N=CC(C#N)=C12 |
| Z1546984393 | enamine_hinge | Cc(cc(C1)OCCN1c1ncnc2c1cc[nH]2)cc1c1F |
| Z4217513103 | enamine_diverse | CN1C=C(CNC2=CN=C3CCC(N)CC3=C2)C(C2=CC=NN2C)=N1 |
| Z2973449868 | enamine_hinge | CCc1c[nH]c2c1c(NC[C@@H]1[C@@H](c3ccnn3C)OCC1)ncc2 |

8 Appendix and curriculum vitae

| | | |
|-----------------|-----------------|---|
| Z2190136975 | enamine_diverse | CC1=CN(C2=CC=C(C(N)=O)C=C2NC(=O)NC2=CN(C)N=C2C2CC2)N=C1 |
| Z1268225168 | enamine_hinge | CNC(c(cc1)hcc1C(Nc1n[nH]c(C2C(CC3)CC3C2)c1)=O)=O |
| Z3832846113 | enamine_diverse | CCN1N=CC2=C1CCC(NC1=CC(C3=CC=CC=C3)=C(C)N=N1)C2 |
| Z3772051647 | enamine_hinge | Cc1nn(CC(F)(F)F)cc1Nc1ncc(C2CC2)c(NCc(cc2)ccc2S(N)(=O)=O)n1 |
| PV-002904720952 | enamine_diverse | CN1C=C(C2=CC=NC(NC(=O)C3=CC=CC(F)=C3C3CC3)=N2)C=N1 |
| Z573976144 | enamine_hinge | O=C(c1n[nH]c(C2CC2)c1)NCc(cc1)nn1-c(cccc1)c1F |
| Z4456494918 | enamine_diverse | CC1=CN=C2CC(NC3=CC(C4=CC=CC(CO)=C4)=CC=C3C#N)CCN12 |
| Z1272280382 | enamine_hinge | O=C1NC(NC2c(cccc3)c3OC2)=Nc2c1cnn2-c1cccc1 |
| Z4233590504 | enamine_diverse | CC1=NSC(NCC2CCN(C3=NC=NC4=C3C=C[NH]4)CC2)=C1C#N |
| Z339154168 | enamine_hinge | O=C(c1cc(CCC2)c2s1)N(CC1)CC=C1c1c[nH]c2c1cccc2 |
| PV-002734594439 | enamine_diverse | CC1=NC=C2C=CC(C(=O)NC3=CC=C(C4=N[NH]C(CN)=N4)C=C3)=CN12 |
| Z1465281292 | enamine_hinge | CCOc1cc(CCN(C2)c3ncnc4c3cc[nH]4)c2cc1 |
| PV-003010455145 | enamine_diverse | CC1=CC(C2=CN3N=CC(C#N)=C3N=C2)=CC2=C1NC(=O)C2(C)C |
| Z1823644534 | enamine_hinge | CN(C)C(CNc1c(cc(cc2)S(C)(=O)=O)c2ncn1)c(cc1)ccc1F |
| PV-002877163242 | enamine_diverse | CCC1=C[NH]C2=NC=C(C3=CC(C(C)C)=NN3C)C=C12 |
| Z2768571033 | enamine_hinge | Cc1c(C)[nH]c2c1c(N(C[C@H]1COC3)C[C@@]13c1nnc(C)o1)ncn2 |
| PV-002897667894 | enamine_diverse | O=C(NC1CC1)C1=CC=C(NC2=CN(C3=C(F)C=CC=C3F)N=C2)N=C1 |
| Z62737036 | enamine_hinge | Cc(c(-n1c(SCC(Nc2cc(C(N)=O)cc(C(N)=O)c2)=O)hcc1)ccc1)c1Cl |
| Z3293603813 | enamine_diverse | COC1=CC=C(C2=CC=NC=C2)C=C1CNC1=NC=C2COC(C)(C)C2=N1 |
| Z298640894 | enamine_hinge | CC(C)C(C(N(CC1)CC=C1c1c[nH]c2c1cccc2)=O)NC(c(cc1)ccc1Cl)=O |
| Z3794499819 | enamine_diverse | CC1=CC=C2C=NC=CC2=C1C(=O)NC1=CN([C@@H]2COC[C@@H]2N)N=C1 |
| Z1953282051 | enamine_hinge | Oc1cc(C(Nc2n[nH]c3c2ccc(F)c3)=O)c(C(F)(F)F)cc1 |
| PV-002999634520 | enamine_diverse | N#CC1=CC(C2=CC=NC=C2)=CC(NC(=O)NC2=NN(C3CCC3)C=C2)=C1 |
| Z991898772 | enamine_hinge | FC(c1cc(N(CC2)CCN2c2ncnc3c2cc[nH]3)ccc1)(F)F |
| PV-002949767030 | enamine_diverse | CN1N=CC2=CC(C3=CC=C4C(N)=C(C#N)C=NC4=C3)=CN=C21 |
| Z2967714693 | enamine_hinge | CCc1c[nH]c2c1c(N(CCC1)CC1c1nnc3n1cccc3)ncn2 |
| Z3606264919 | enamine_diverse | CC(C)C1=CN=C2C=C(C(=O)NC3=CN(C)N=C3C3=CC=NN3C)[NH]C2=C1 |
| Z1730062884 | enamine_hinge | CC(C)c1cnc(CNc(cc2)ccc2N(CCN2)C2=O)s1 |
| Z3337740546 | enamine_diverse | COC1=CC=C(NC2=NC(C3=CN([C@H]4CC[C@@H](N)CC4)N=N3)=CS2)C=C1F |
| Z1966281351 | enamine_hinge | O=C(c1c2)NC(c3c[nH]c4c3cccc4)=Nc1cc(Cl)c2Cl |
| PV-002923008066 | enamine_diverse | CN1N=CC(C2CC2)=C1C1=CC=C2C(N)=C(C#N)C=NC2=C1 |
| Z1725358463 | enamine_hinge | O=C(c(c[nH]1)c1N1)N=C1N1CC(CNc2ncccc2)CC1 |
| Z4101861755 | enamine_diverse | CC1=NN=CN1C1=CC=CC(NC(=O)C2=CC(NC3CC3)=NC=C2Cl)=C1 |
| Z785458586 | enamine_hinge | O=S(c1c[nH]c2c1cccc2)(N1CCN(Cc2nccn2C(F)F)CC1)=O |
| Z4216599240 | enamine_diverse | CC1=CC=C(NCC2=C(C)N=C(N(C)C)N2C)C2=C1C(C#N)=C[NH]2 |
| Z786281110 | enamine_hinge | O=C1NCCCC1Nc(cc1)nn2c1nnc2C(F)(F)F |
| Z4272303629 | enamine_diverse | CCOC1=CC=CC([C@@H]2C[C@H]2NC(=O)NC2=CN(C)N=C2C2=CC=NN2C)=C1 |
| Z1875036578 | enamine_hinge | CC(Nc(ccc(C(Nc1n[nH]c(C2CCOCC2)c1)=O)c1)c1F)=O |

8 Appendix and curriculum vitae

| | | |
|-----------------|-----------------|---|
| Z4028413203 | enamine_diverse | CC(C)(C#N)C1=CC(C(=O)NC2=C(C3CCNC3)[NH]N=C2)=CC(C(F)(F)F)=C1 |
| Z825782506 | enamine_hinge | CC(C)C(N(CCC1)C1C(Nc1cnc2[nH]nc(C)c2c1)=O)=O |
| Z4163994616 | enamine_diverse | CN(C)C1=CC(C(=O)NC2=C(C(F)F)N(C3=CC=NC=C3)N=C2)=NN=C1C1CC1 |
| Z4027450995 | enamine_hinge | C[C@H](C1)O[C@H](CO)CN1c1ncnc2c1c(cccc1)c1[nH]2 |
| Z3606268549 | enamine_diverse | COCCN(C)C1=CC=NC(C(=O)NC2=CN(C)N=C2C2=CC=NN2C)=C1 |
| Z340521968 | enamine_hinge | Cc(n(-c1cccc(Cl)c1)c1)nc1c1C(Nc(cc1)cc2c1[nH]nc2)=O |
| PV-003042472738 | enamine_diverse | CN1N=CC(CN)=C1NC(=O)C1=CC(C2=CN=C3[NH]C=CC3=C2)=CC=N1 |
| Z1663390302 | enamine_hinge | Cn1c(C2CCC2)nnc1CNC(Cc1c[nH]c2c1ccc2)=O |
| Z4310656126 | enamine_diverse | CN(C)C[C@@H]1CC[C@H](C(=O)NC2=CN(C)N=C2C2=CC=NC=C2)O1 |
| Z3547799409 | enamine_diverse | COC1=CC=CC(CN2C=CC=C(NCC3=C(Cl)[NH]N=C3C3CC3)C2=O)=N1 |
| Z2347721785 | enamine_hinge | C(CN(CC1)c2ncnc3c2cc[nH]3)C11OCCc2c1cccc2 |
| Z1757705914 | enamine_hinge | CC(NC1c1cccc(OC(CC2)CN2c2ncnc3c2cn[nH]3)c1)=O |
| PV-003006761255 | enamine_diverse | CN1N=CC2=CC(CNC3=C(C#N)N4C=CC(Cl)=CC4=N3)=CN=C21 |
| Z1317599619 | enamine_hinge | Cc1nc([nH]cc2)c2c(Nc(cc2)cc3c2[nH]nc3)n1 |
| Z4342827179 | enamine_diverse | C[C@H](NC1=CC(C(N)=O)=NC(C2CC2)=N1)C1=CC=NC=C1Br |
| Z1070432114 | enamine_hinge | Fc(ccc(C(C1)OCCN1c1ncnc2c1cc[nH]2)c1)c1F |
| Z3562247527 | enamine_diverse | CC(C)(C)[C@@H]1C[C@H](NC2=NN3C(C4=CC=NC=C4)=NN=C3C=C2)C(=O)N1 |
| Z106550938 | enamine_hinge | O=C1NC(CN(Cc(cc2)ccc2F)C2CC2)=Nc2c1c(-c1cccc1)cs2 |
| PV-002740943136 | enamine_diverse | CC1=CC2=C(C(C)=C1)C(NC1=NC(C3CC3)=NC=C1C#N)CC2 |
| Z196138710 | enamine_hinge | COc(cc(CNc1c2sccc2nnc1)cc1)c1OC(F)F |
| PV-002875435369 | enamine_diverse | N#CC1=CC=C(NC(=O)CC2=C3CCCCN3N=C2)C=C1C1=CC=NC=C1 |
| Z1622152395 | enamine_hinge | O=C(C1NCCC1)NCc1cn(-c2cccc2)nc1-c1ccncc1.Cl |
| Z4230030431 | enamine_diverse | CCC1=NN=C(C[C@@H]2CC[C@H](NC3=CC(C)=NC=C3C(=O)OC)C2)O1 |
| Z1834347005 | enamine_hinge | Cc(n(C1CCOCC1)nc1)c1C(Nc1n[nH]c2c1ccc(F)c2)=O |
| Z4144498914 | enamine_diverse | CNCC1=NC=C(C(=O)NC2=C(C)N(C3=CC(C)=CC=C3C)N=C2)C=N1 |
| Z2073045218 | enamine_hinge | Cc(ccc(CO)c1)c1NC(c1cc(NC(C2CC2)=O)ncc1)=O |
| PV-003039793887 | enamine_diverse | CC(N)(CNC1=C(C#N)C=NC2=C(F)C=CC(Cl)=C12)CN1C=CC=N1 |
| Z2762265035 | enamine_hinge | Cc(c(C)c1)cc2c1occ2CC(Nc1c(C2CNCC2)[nH]nc1)=O |
| PV-002719781073 | enamine_diverse | CC(NC(=O)NC1=CC2=C(C=N1)[NH]C=C2)C1=N[NH]C(C2=CC=CS2)=N1 |
| Z979286080 | enamine_hinge | CCOc(ccc(C(Nc1cc(-c2ccncc2)n[nH]1)=O)c1)c1OC |
| Z3653434344 | enamine_diverse | CN1N=CC(NC(=O)C2CCCC3=CC(C#N)=CC=C32)=C1C1=CN=CC=N1 |
| Z1758193983 | enamine_hinge | CC(C)(C)[C@H]1OCC[C@@H]1c1nnc(Cc2c[nH]c3c2ccc3)o1 |
| Z4449016569 | enamine_diverse | N#CC1=CC(C2=CC=NC=C2)=CC(NC(=O)[C@@H]2CCO[C@@H]2CC2CCNCC2)=C1 |
| Z1665944963 | enamine_hinge | Cc1ccnc(C(CC2)CCN2c2ncnc3c2cc[nH]3)n1 |
| Z4311251766 | enamine_diverse | CN(C)C[C@@H]1CC[C@H](C(=O)NC2=CC=C(Cl)C(N3CCNC3=O)=C2)O1 |
| Z1739540848 | enamine_hinge | Fc1cccc(F)c1C(CC1)CCN1c1ncnc2c1cc[nH]2 |
| PV-002729852227 | enamine_diverse | COC(=O)C1=CC2=C(C)C(C3=CN4N=CC(C#N)=C4N=C3)=CC=C2[NH]1 |
| Z52523797 | enamine_hinge | O=C(c1cccc(S(Nc(cc2)cc3c2[nH]nc3)(=O)=O)c1)Nc(cc1)cc2c1OCCCO2 |

8 Appendix and curriculum vitae

| | | |
|-----------------|-----------------|--|
| PV-002813282580 | enamine_diverse | N#CC1=CC(C2=CC=NC=C2)=CC(NC(=O)N2CCC[C@H]2C2=NOC=C2)=C1 |
| Z2093418700 | enamine_hinge | Cc1n[nH]cc1C(CC1)CCN1c1ncnc2c1cc[nH]2 |
| Z3842727524 | enamine_diverse | CC1=CC=C(NC(=O)N2CCC(CN(C)C)C2(C)C)C2=C1C(C#N)=C[NH]2 |
| Z1491594831 | enamine_hinge | CC(C)(C)n(c(C1CC1)c1)nc1C(Nc(ncc1c2)nc1ccc2C#N)=O |
| PV-002861941210 | enamine_diverse | CN1C=C(CNC2=NC3=C(C=C(CI)C(F)=C3)[NH]2)C(C2=CC=NN2C)=N1 |
| Z1587709311 | enamine_hinge | Fc(cc1)cnc1N(CC1)CCN1c1ncnc2c1cc[nH]2 |
| Z4232208022 | enamine_diverse | CC1=CC(N2CCC3=C(C2)C(CO)=N[NH]3)=NC=C1C#N |
| Z106498018 | enamine_hinge | CC(c(cc1)ccc1-n1ncnc1)N(C)CC(NC1=O)=Nc2c1oc1c2cccc1 |
| Z4421265565 | enamine_diverse | CN1C=C(C2=CC=NC(NC(=O)C3=CC4=C(CCNC4)N3C)=C2)C=N1 |
| Z1665646061 | enamine_hinge | COc1noc(C(Nc2cc(-c3cccc(F)c3F)n[nH]2)=O)c1 |
| Z3356558707 | enamine_diverse | CC(C)(C)C1=NC(CNC(=O)CC2=C[NH]C3=NC=CC(CI)=C23)=N[NH]1 |
| Z1039077300 | enamine_hinge | Clc1cc(CI)c(N(CC2)CCN2c2ncnc3c2cc[nH]3)nc1 |
| PV-002972008103 | enamine_diverse | O=C(NC1=CC(C2=NN=N[NH]2)=CC=C1F)C1=CN=C2NCCOC2=C1 |
| Z1537918417 | enamine_hinge | CCc1c(NC(c2cccc(OC)c2F)=O)[nH]nc1-c1ccncc1 |
| PV-002899034339 | enamine_diverse | CC1=CC(F)=CC(CO)=C1C1=CC2=C(C=C1C(F)(F)F)[NH]C=N2 |
| Z3383760531 | enamine_diverse | O=C(NC1=N[NH]C(C2=C(CI)C(CI)=CC=C2)=C1)C1CC2(CCOCC2)CN1 |
| Z2347732760 | enamine_hinge | COC(c1ccc(N(CC2)CCN2c2ncnc3c2cc[nH]3)s1)=O |
| Z1302789469 | enamine_hinge | Cc1nn(C)c2c1c(NC(c1cc(NC3CCCC3)nc1)=O)n[nH]2 |
| PV-002830448824 | enamine_diverse | CC1=CC(C(=O)NC2=CN(C)N=C2C2=CC=NN2C)=CC2=C1[NH]C=N2 |
| Z2972765817 | enamine_hinge | CCc1c[nH]c2c1c(Nc(cc1)cc(S(C)(=O)=O)c1OC)ncn2 |
| Z4063779764 | enamine_diverse | NCC1(C2=CC=C(C(=O)NC3=CC(C4=CC=CC(F)=C4F)=N[NH]3)C=N2)CCC1 |
| Z649765000 | enamine_hinge | O=C1NC(CN(CCC2)C2c2ccc[nH]2)=Nc2c1ccc(CI)c2 |
| Z3512028671 | enamine_diverse | CN1N=CC(C2CC2)=C1C1=CC=C2CC(N)(CO)CCC2=C1 |
| Z73488292 | enamine_hinge | O=C(C1)Nc(cc2)c1cc2-c1csc(Nc2cc(C(F)(F)F)ccc2)n1 |
| PV-002914165654 | enamine_diverse | CC1(C)CNC2=C1C=CC=C2C1=CN2N=CC(C#N)=C2N=C1 |
| Z1559985788 | enamine_hinge | O=C(c1n[nH]c2c1cccc2)Nc1c[nH]nc1-c1ncccc1 |
| PV-002729091047 | enamine_diverse | N#CC1=CC(C2=CC=NC=C2)=CC(NC(=O)C2CNC3=C(C=N[NH]3)C2)=C1 |
| Z3564291978 | enamine_hinge | Cc1cccc(CI)c1NC(c1nc(Nc2ncnc3c2CN(C)CC3)s1)=O.Oc(C(F)(F)F)=O |
| Z2092502849 | enamine_diverse | CC(NC1=CC(C2=CC=NC=C2)=NC(CI)=N1)C1=CC=C(N2CCCS2(=O)=O)C=C1 |
| Z1759675449 | enamine_hinge | CN(C)c1nccc(N(C2)[C@H](CNC(c3n[nH]c4c3CCC4)=O)C[C@@H]2F)n1 |
| PV-002814982933 | enamine_diverse | CCC1=C[NH]C2=NC=C(C3=CC(C4=NC(C)=NO4)=CN=C3)C=C12 |
| Z1225949377 | enamine_hinge | O=C(CC1c(cccc2)c2OCC1)Nc1cc(-c2ccncc2)n[nH]1 |
| PV-002964238309 | enamine_diverse | O=C(NCC1=CC2=CN=CC=C2[NH]1)C1=CC=NC(C2=NC=C[NH]2)=C1 |
| Z237522248 | enamine_hinge | CC(Nc(cc1)ccc1S(N(CC1)CC=C1c1c[nH]c2c1ccn2)(=O)=O)=O |
| PV-002794781466 | enamine_diverse | N#CC1=CC=C(NCC2=NC(C3CC3)=NC(O)=C2)C=C1C1=CC=NC=C1 |
| Z3137268093 | enamine_diverse | CC(C)C1=NC(C2=CC=CC=C2CI)=NC=C1C(=O)NC1=NN2CCNCC2=C1 |
| Z236016972 | enamine_hinge | Cn(cc1C(N(CCC2)CC2c2nc(cccc3)c3[nH]2)=O)nc1-c(cc1)cc2c1OCCCCO2 |
| Z1241145439 | enamine_hinge | C(c1nnc(-c2cccc2)o1)N(CC1)CC=C1c1c[nH]c2c1ccn2 |

8 Appendix and curriculum vitae

| | | |
|-----------------|-----------------|---|
| PV-002733662135 | enamine_diverse | O=C(NC1=CC(C2=C(F)C(F)=CC=C2)=N[NH]1)C1=NC=C(C2CC2)O1 |
| Z2163277696 | enamine_hinge | O=C([C@@H](CC1)O[C@@H]1c1cccc1)Nc1n[nH]c(cc2)c1cc2F |
| Z4254680099 | enamine_diverse | CCC1=NC=C(CI)C(C(=O)NCC2CCN(C3=NC=NC4=C3C=C[NH]4)CC2)=N1 |
| Z298640018 | enamine_hinge | O=C(Cc(cc1)ccc1F)N(CC1)CC=C1c1[nH]c2c1cccn2 |
| Z2189829175 | enamine_diverse | CN1C=C(NC(=O)NC2=CC=C(N3N=CC(C#N)=C3N)C=C2)C(C2CC2)=N1 |
| PV-002709802771 | enamine_diverse | NC1=NN2C=CC=CC2=C1C(=O)NC1=CC=C(F)C(C2=CC=NC=C2)=C1 |
| Z62878553 | enamine_hinge | O=C(c1n[nH]c2c1cccc2)Nc(cc1)cc2c1nc(N1CCOCC1)s2 |
| Z1612627107 | enamine_hinge | CC(c1cc(-c2ccncc2)ccc1)Nc1cc(C(NC2)=O)c2cc1 |
| Z3686134492 | enamine_diverse | CO[C@@H]1CN(C2=CC=NC(N(C)C)=N2)C[C@@H]1NC1=CC(=O)[NH]C2=CN=CC=C12 |
| Z1757781974 | enamine_hinge | Cn1nccc1[C@@H]1OCC[C@H]1CNc(ncc(C(N)=O)c1)c1Cl |
| Z4291364166 | enamine_diverse | CC(C)C(C1=CN=C(C(=O)NC2=CC=C(CI)C(N3CCNC3=O)=C2)O1 |
| Z2073189755 | enamine_hinge | Oc(ccc(NC(c1cc(NC(C2CC2)=O)ncc1)=O)c1)c1Cl |
| Z4233310566 | enamine_diverse | CCN1N=CC2=C1CCC(NC1=CC(C3CCCO3)=C(CI)N=N1)C2 |
| Z2378442098 | enamine_hinge | O=C(COC1CCNCC1)Nc(c1ccc2)n[nH]c1c2Cl |
| Z3606252965 | enamine_diverse | CC1=CC(C(=O)NC2=CN(C)N=C2C2=CC=NN2C)=CC=C1N1CCNC1=O |
| Z1544332989 | enamine_hinge | CCNc1ncc(C(Nc2cn(-c(nccc3)c3Cl)nc2)=O)s1 |
| Z1929584552 | enamine_diverse | CN1CCN(C2=NC=C(C(=O)NC3=C(C(F)F)N(C4=CC=NC=C4)N=C3)S2)CC1 |
| Z1039090602 | enamine_hinge | Cc1ccc(C(NC(CC2)CCN2c2ncnc3c2cc[nH]3)=O)s1 |
| PV-003005733604 | enamine_diverse | CNC1=CC=C(C(=O)NC2=CC3=C(C=C2C(=O)OC)[NH]C=C3)C(CI)=C1 |
| Z2218223010 | enamine_hinge | C(c1c(C2)n(-c3cccc3)nc1)N2c1nnc2c1cn[nH]2 |
| Z3151724655 | enamine_diverse | CC(C)CN1C(C2=N[NH]C3=CC=CC=C23)=NN=C1N1CCN(CCC#N)CC1 |
| Z354363402 | enamine_hinge | Cc1nc(NCc2cc(C(NC)=O)ccc2)c(c(-c2cccs2)cs2)c2n1 |
| Z3990037411 | enamine_diverse | CCC1=C[NH]C2=NC=C(C3=CC=NC4=C3CN(C(=O)OC)CC4)C=C12 |
| Z424981970 | enamine_hinge | CC1Oc(ccc(NC(c2c(C)n(C(C)(C)C)nc2)=O)c2)c2NC1=O |
| PV-002990544308 | enamine_diverse | CN1N=CC(NC(=O)C2CNC3=C(C=N[NH]3)C2)=C1C1=CC=CC=C1 |
| Z1559777197 | enamine_hinge | O=C(c1cc(F)cc2cccnc12)Nc1n[nH]c(C2CCOCC2)c1 |
| Z3834034884 | enamine_diverse | CN1CCC(N2CCC(NC3=C(C#N)C=NC4=C(F)C=CC(F)=C34)C2=O)CC1 |
| Z4561573892 | enamine_hinge | CCC(N(CC1)c2c1ccc(Nc1c(c(Br)c(C(OC)=O)[nH]3)c3nnc1)c2)=O |
| Z4353161447 | enamine_diverse | O=C(NC1=CC=C(F)C(C2=CC=NC=C2)=C1)[C@@H]1CCCO[C@H]1C1=NC=C[NH]1 |
| Z2969650561 | enamine_hinge | CCc1c[nH]c2c1c(NCCC(C(C)=NN1)C1=O)ncn2 |
| PV-002712264396 | enamine_diverse | CC1=CC2=C(C=C1NC(=O)C1=C[NH]N=C1C1=CC=C(C#N)C=C1)[NH]C=C2 |
| Z1658089838 | enamine_hinge | O=C(c1c2[nH]ncc2ccc1)Nc(cc1)nc1C(N1CCCC1)=O |
| PV-003033371733 | enamine_diverse | NC1=NC=C2CC(C(=O)NC3=C[NH]N=C3C(=O)NC3CC3)CCC2=N1 |
| Z2764131426 | enamine_hinge | CN(C[C@@H]1OCC[C@H]1c1nnc[nH]1)C(c(cc1)cc2c1[nH]nc2)=O |
| PV-000265026222 | enamine_diverse | O=C(NC1CCC(CNC(=O)C2=NC=C[NH]2)C1)C1=CC2=CN=CC=C2[NH]1 |
| Z51869695 | enamine_hinge | CC(C)n(c1nc(C2CC2)c2)nc1c2C(Nc(cc(cc1)Cl)c1-n1nnc1)=O |
| Z4385081296 | enamine_diverse | COC1=CC(NC(=O)C2=NC(C3CC3)=NC=C2Cl)=C(F)C=C1C#N |
| Z1607926386 | enamine_hinge | N#Cc(ccc(NC(c(cc(CCC(N1)=O)c1c1)c1F)=O)c1)c1C#N |

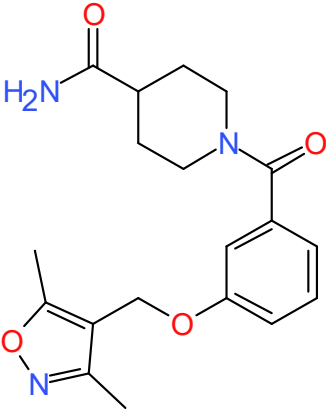
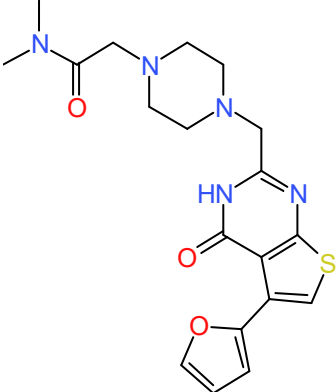
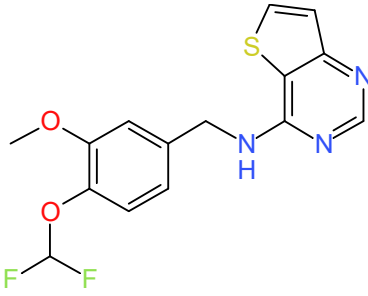
8 Appendix and curriculum vitae

| | | |
|-----------------|-----------------|--|
| Z3837563367 | enamine_diverse | CC1=C(C(=O)NC2=CN=CC=C2N2CCN(C)CC2)SC(C2=NC=C[NH]2)=N1 |
| Z3063592964 | enamine_hinge | O=C(c1n[nH]c(C2CC2)c1)Nc1n[nH]c2c1ccc(C(F)(F)F)n2 |
| Z4272282359 | enamine_diverse | CN(CC1=NC=C(CI)C=C1CI)C(=O)NC1=CN(C)N=C1C1=CC=NN1C |
| Z450065016 | enamine_hinge | O=C(c1c2CCCC1)nn2-c(cc1)cc(F)c1F)Nc1nc(cccc2)c2[nH]1 |
| PV-002709745589 | enamine_diverse | CC1=CC=C2N=CC(C#N)=C(N[C@@H](CO)CNC(=O)C3=NOC=C3)C2=C1 |
| Z3333528035 | enamine_hinge | O=C(N(CC1)CCN1c1ncnc2c1c(cccc1)c1[nH]2)OCc1cccc1 |
| Z4119176686 | enamine_diverse | COC(=O)C[C@H]1C[C@@H](NC2=NC(C3=CC=NC=C3Cl)=CS2)C1 |
| Z28536502 | enamine_hinge | CCn1nnc2c1ccc(C(Nc(cc(cc1)Cl)c1-n1ncnc1)=O)c2 |
| Z4409848142 | enamine_diverse | CC1(C)CN(C2=CC=NC(C3=CN4N=CC(C#N)=C4N=C3)=N2)CCN1 |
| Z1678860086 | enamine_hinge | Cc1nc(C(Nc2cc(-c3ccncc3)n[nH]2)=O)c(-c2cccc2)o1 |
| PV-002919206869 | enamine_diverse | CN1N=C(NCC2=CC(C3=CC=NC=C3)=N[NH]2)C=C1C#N |
| Z86317454 | enamine_hinge | Cc(cc1)ccc1-c1csc2ncnc(NCCc3n[nH]c(N)c3C#N)c12 |
| PV-002747489246 | enamine_diverse | CC1=CC=C2C=C[NH]C2=C1C1=CN2N=CC(C#N)=C2N=C1 |
| Z2700346964 | enamine_hinge | O=C(c(c[nH]1)c1N1)N=C1N(CC1)CCC1OCc(cc1)ccc1F |
| PV-002912080040 | enamine_diverse | N#CC1=CC(C2=CC=NC=C2)=CC(NC(=O)C2=CC3=C(CCCC3=O)[NH]2)=C1 |
| Z381645104 | enamine_hinge | Cc(cc1)ccc1-c1cnc(-c(ccc2)c2C(Nc2c[nH]nc2)=O)o1 |
| PV-002829057767 | enamine_diverse | O=C(NC1=CC=C(C2=N[NH]N=C2)C=C1)C1=CC=C(C2=CC=NC=C2)[NH]C1=O |
| Z1521955084 | enamine_hinge | O=C(c(cc1)ccc1C(Nc1n[nH]c(cc2)c1cc2F)=O)NC1CC1 |
| Z2869123619 | enamine_diverse | CN1C=C(NC(=O)NC2=C(C#N)C(C(C)C)=CS2)C(C2CC2)=N1 |
| Z2504758937 | enamine_hinge | CNC(c1nccc(Oc(ccc(NC2c3nccn3CCC2)c2)c2F)c1)=O |
| Z4264476336 | enamine_diverse | CN1N=CC(NC(=O)C2=CC=C(C3=NC=C[NH]3)N=C2)=C1CCC(F)(F)F |
| Z196131726 | enamine_hinge | Cc1nn2c(cccc3)c3c(Nc(cc3)cc(N4)c3OCC4=O)nc2c1Cl |
| Z3606260278 | enamine_diverse | CCN(CC)C1=CC=C(C(=O)NC2=CN(C)N=C2C2=CC=NN2C)C(O)=C1 |
| Z3048354414 | enamine_hinge | CC(C)(C)c1c(C(Nc2n[nH]c(cc3)c2cc3F)=O)scn1 |
| Z3833234996 | enamine_diverse | C[C@H](NC1=NC(N[C@@H](C)C2=CC=NN2C)=C(F)C(C2CC2)=N1)C1=CC=NN1C |
| Z1142722587 | enamine_hinge | CC(C)c1nc(CN(CC2)c3ncnc4c3cc[nH]4)c2n1C |
| PV-002775997025 | enamine_diverse | CN1N=CC(NC(=O)NCC2=CC3=CN=CC=C3[NH]2)=C1C1=CC=CC=C1 |
| Z2732441070 | enamine_hinge | C[C@@H](C[C@@H](C(Nc1cncc(-c2cnc3[nH]ccc3c2)c1)=O)N1)CC1=O |
| Z3081935015 | enamine_diverse | CC1=CC(C2CC2)=NC=C1C(=O)NC1=CN(C)N=C1C1=CC=NC=C1 |
| Z1613920204 | enamine_hinge | [O-][N+](c(cc(cc1)C(N(CC2)CC=C2c2c(cc[nH]3)c3ncc2)=O)c1NC1CC1)=O |
| PV-002738907074 | enamine_diverse | O=C(NC1=CC=C2C=NC=C(F)C2=C1)C1=CC=CC(C2=NC=N[NH]2)=C1 |
| Z2002922388 | enamine_hinge | O=C(C(CCC1)CC1(F)F)Nc1n[nH]c(cc2)c1cc2F |
| PV-002465580757 | enamine_diverse | CC1=N[NH]C2=C1N(C(=O)NC1=NN(C3=CC=CC=C3F)C(C)=C1)CCC2 |
| Z951386758 | enamine_hinge | N#Cc1c(NC2c2n(-c3cccc3)nc2-c2ccncc2)nc1 |
| PV-002931822629 | enamine_diverse | N#CCCN1C(C2=N[NH]C3=CC=CC=C23)=NN=C1N1CC[C@H](C(F)F)C1 |
| Z645644002 | enamine_hinge | FC(c1nnc(cc2)n1nc2NCCCNc1ncccc1)(F)F |
| PV-002962986688 | enamine_diverse | N#CC1=CC(N2CCCC2)=CC(C2=CN3N=CC(C#N)=C3N=C2)=C1 |
| Z1956680261 | enamine_hinge | O=C(c1c2)NC(c3ccc[nH]3)=Nc1cc(Br)c2F |

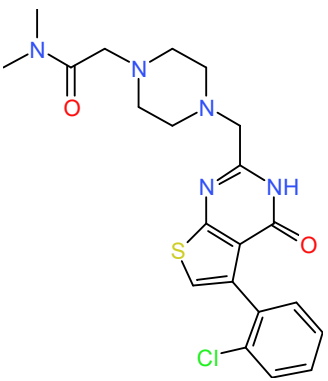
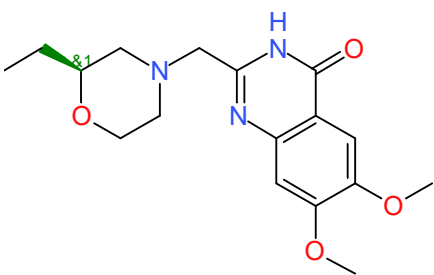
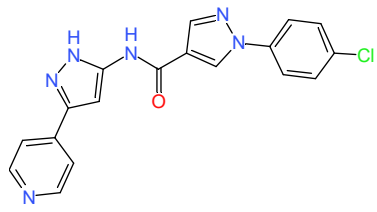
8 Appendix and curriculum vitae

| | | |
|-----------------|-----------------|---|
| PV-002919006773 | enamine_diverse | <chem>COC1=CC=C2C=NC(C3=CN4N=CC(C#N)=C4N=C3)=CC2=C1F</chem> |
| Z234513432 | enamine_hinge | <chem>O=C(c1cn(-c2cccc2)nc1)N(CC1)CC=C1c1c[nH]c2c1ccn2</chem> |
| Z4343432082 | enamine_diverse | <chem>CN1CCN(C2=CC(F)=CC(CNC3=NC(C4CC4)=NC=C3C#N)=C2)CC1</chem> |
| Z1737110153 | enamine_hinge | <chem>Cn1c(CC(Nc(cc2)cc3c2[nH]c(-c(cc2)F)c2F)n3)=O)cnc1</chem> |
| Z3774108580 | enamine_diverse | <chem>FC(F)(F)C1=CC(CNC2=NC=C3CCOCC3=N2)=C2C=C[NH]C2=C1</chem> |
| Z2834321565 | enamine_hinge | <chem>O=C1NC(CN(CC2)CC=C2c2c[nH]c3c2cccn3)=NC2=C1COCC2</chem> |
| PV-002816656911 | enamine_diverse | <chem>CCN1N=CC2=CC=C(NC(=O)C3=CC=C(C4=NN=N[NH]4)C=C3F)C=C21</chem> |
| Z2970701737 | enamine_hinge | <chem>O[C@H](CC1)CC[C@H]1Nc1ccnc(N[C@H](CC2)CC[C@H]2O)n1</chem> |
| Z3585590523 | enamine_diverse | <chem>CC1=C2N=CC(NC(=O)[C@H]3C[C@H]3C3=CC=NC=C3Cl)=CN2N=C1</chem> |
| Z1757858634 | enamine_hinge | <chem>C(c1cc([nH]nc2)c2cc1)N(CCC1)C1c1nc(CCCC2)c2[nH]1</chem> |
| PV-002877771020 | enamine_diverse | <chem>CC1CCN(C2=C(C#N)C=CC=C2C#N)CCN1C1=NC=NC2=C1C=C[NH]2</chem> |
| Z203982424 | enamine_hinge | <chem>Clc(cc1)cc(Cl)c1-c([nH]c1c2cccc1)c2-c1ncc[nH]1</chem> |
| Z4101799575 | enamine_diverse | <chem>CC1=C(NC(=O)C2=CC(NC3CC3)=NC=C2Cl)[NH]N=C1C1=CC=NC=C1</chem> |
| Z1768896238 | enamine_hinge | <chem>CC[C@H](CO)NC(C(CCC1)CN1C(c(cc1)cc2c1[nH]nc2)=O)=O</chem> |
| PV-002911432526 | enamine_diverse | <chem>CC1=CC(C2=N[NH]C(NC(=O)NC3=CC=C(C4=C[NH]N=C4)C=C3)=C2)=CC=N1</chem> |
| Z2378442101 | enamine_hinge | <chem>O=C(C1C(CC2)NCC2C1)Nc(c1ccc2)n[nH]c1c2Cl</chem> |
| PV-002856838327 | enamine_diverse | <chem>CN1C=C(CNC2=CC3=C(C=C2F)CCNC3=O)N2N=CC(C#N)=C12</chem> |
| Z3048354234 | enamine_hinge | <chem>O=C(C1N(CC(F)F)CCOC1)Nc1n[nH]c(cc2)c1cc2F</chem> |
| Z4211361205 | enamine_diverse | <chem>NC1=CC(C2=CC3=C(CCN3)S2)=C(C2CC2)S1</chem> |
| Z298642486 | enamine_hinge | <chem>CCN(c(ccc(C(N(CC1)CC=C1c1c[nH]c2c1ccn2)=O)c1)c1NC1=O)C1=O</chem> |
| Z3614131624 | enamine_diverse | <chem>N#CC1=CC=C(N2N=CN=C2NC(=O)C[C@H]2CCCC[C@H](C3CC3)O2)C=C1</chem> |
| PV-002973422314 | enamine_diverse | <chem>C[C@H](CNC(=O)CC1CC2(CC2)C1)NC1=NC=CC(C2=CN=CC=N2)=N1</chem> |
| Z1981589582 | enamine_hinge | <chem>O=C(c(cc1)cn2c1ncc2)Nc(cc(cc1)-c2n[nH]cn2)c1F</chem> |
| Z27652417 | enamine_hinge | <chem>CCc1c(C)sc(N=C(c(cc2)ccc2C(Nc(cc2)ccc2NC(C)=O)=O)N2)c1C2=O</chem> |
| Z4225430629 | enamine_diverse | <chem>O=C(NC1=NOC(C2=CC=CS2)=C1)[C@H]1CC[C@H](C2=NC=N[NH]2)CC1</chem> |

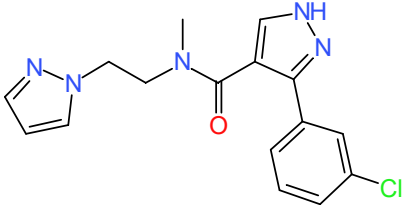
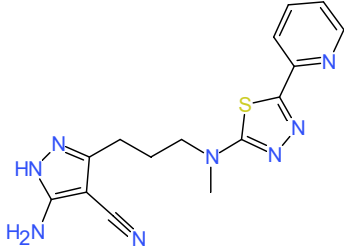
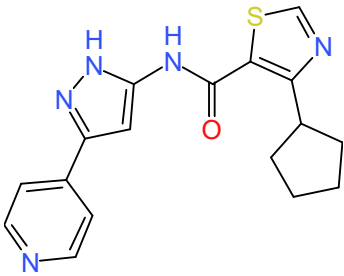
8.2 List of 20 compounds against EmPim

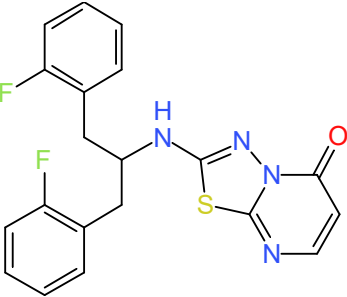
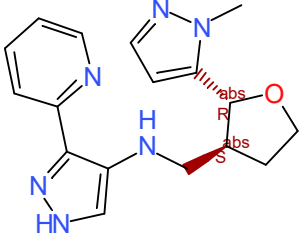
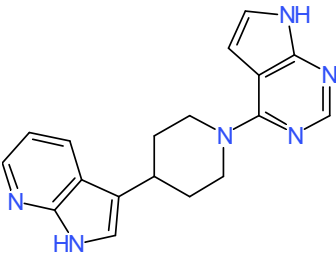
| Structure | Smile | Catalog-ID Enamine | Formula | MW |
|---|--|-----------------------|---|-----------|
|  | <chem>Cc1noc(C)c1 COc2cccc(c2)C(=O)N3CC C(CC3)C(=O)N</chem> | Z30898879 | C ₁₉ H ₂₃ N ₃ O ₄ | 357.40362 |
|  | <chem>CN(C)C(=O) CN1CCN(Cc 2nc3scc(c4cc co4)c3c(=O)[nH]2)CC1</chem> | Z90263347 | C ₁₉ H ₂₃ N ₅ O ₃ S | 401.48262 |
|  | <chem>COc1cc(CNc 2ncnc3ccsc2 3)ccc1OC(F) F</chem> | Z196138710 | C ₁₅ H ₁₃ F ₂ N ₃ O ₂ S | 337.34443 |

8 Appendix and curriculum vitae

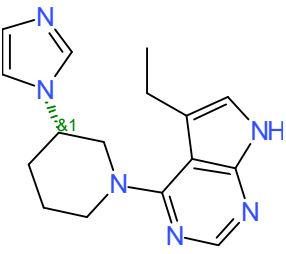
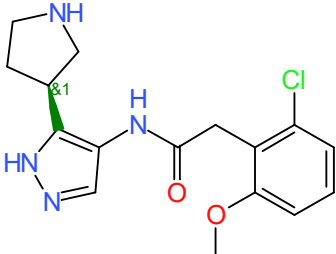
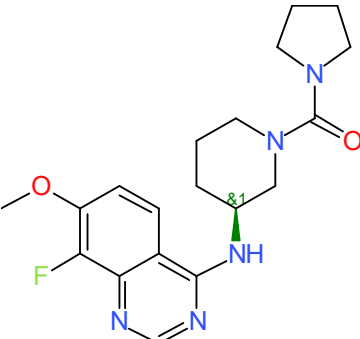
| | | | | |
|--|--|-------------------|---|-----------|
|  | <chem>CN(C)C(=O)CN1CCN(Cc2nc3sc(c4ccc(Cl)c3c(=O)[nH]2)CC1</chem> | Z65225039 | C ₂₁ H ₂₄ ClN ₅ O ₂ S | 445.96556 |
|  <p style="text-align: center;">racemate</p> | <chem>CCC1CN(Cc2nc3cc(OC)c(OC)cc3c(=O)[nH]2)CCO1</chem> | Z354576500 | C ₁₇ H ₂₃ N ₃ O ₄ | 333.38222 |
|  | <chem>Clc1ccc(cc1)n2cc(cn2)C(=O)Nc3cc(n[nH]3)c4ccncc4</chem> | Z979287238 | C ₁₈ H ₁₃ ClN ₆ O | 364.78842 |

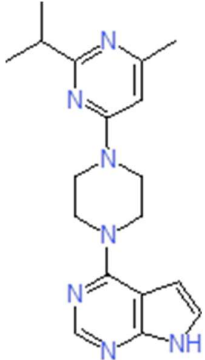
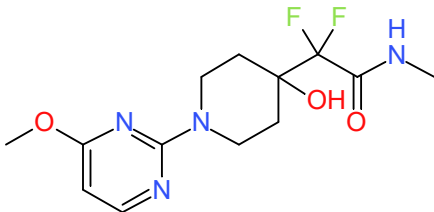
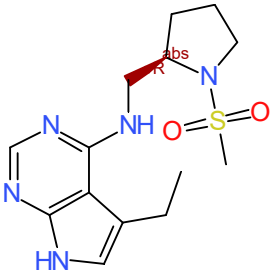
8 Appendix and curriculum vitae

| | | | | |
|---|--|-------------------------------|---|-----------|
|  | <chem>CN(CCn1ccc[n1])C(=O)c2c[nH]nc2c3ccc(Cl)c3</chem> | Z139045199 9 | C ₁₆ H ₁₆ ClN ₅ O | 329.78414 |
|  | <chem>CN(CCCc1[nH]c(N)c1C#N)c2nnc(s2)c3cccc3</chem> | Z167967295 5 | C ₁₅ H ₁₆ N ₈ S | 340.40614 |
|  | <chem>O=C(Nc1cc[nH]1)c2ccncc2)c3scnc3C4CCCC4</chem> | Z167886012 0 | C ₁₇ H ₁₇ N ₅ O ₂ S | 339.41478 |

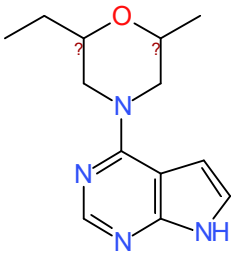
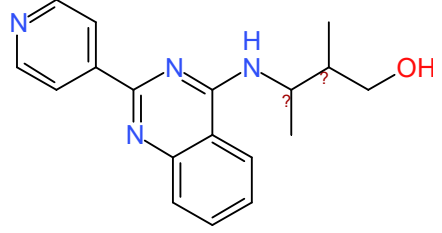
| | | | | |
|---|--|------------------------|---|-----------|
|  | <chem>Fc1ccccc1C(Cc2ccccc2F)Nc3nn4c(=O)ccnc4s3</chem> | Z148118501 2 | C ₂₀ H ₁₆ F ₂ N ₄ O OS | 398.42905 |
|  <p>this enantiomer</p> | <chem>Cn1ccc1[C@@H]2OCC[C@H]2CNc3c[nH]nc3c4cccn4</chem> | Z205237702 4 | C ₁₇ H ₂₀ N ₆ O | 324.3803 |
|  | <chem>C1CN(CCC1c2c[nH]c3ncc(=O)c23)c4ncnc5[nH]ccc45</chem> | Z103908088 0 | C ₁₈ H ₁₈ N ₆ | 318.37572 |

8 Appendix and curriculum vitae

| | | | | |
|---|---|------------------------|---|-----------|
|  <p style="text-align: center;">racemate</p> | <chem>CCc1c[nH]c2ncnc(N3CCCC(C3)n4ccnc4)c12</chem> | Z296919480 4 | C ₁₆ H ₂₀ N ₆ | 296.3702 |
|  <p style="text-align: center;">racemate</p> | <chem>COc1cccc(Cl)c1CC(=O)Nc2cn[nH]c2C3CCNC3</chem> | Z276227483 2 | C ₁₆ H ₁₉ ClN ₄ O ₂ | 334.80066 |
|  <p style="text-align: center;">racemate</p> | <chem>COc1ccc2c(NC3CCCN(C3)C(=O)N4CCCC4)ncnc2c1F</chem> | Z209432453 4 | C ₁₉ H ₂₄ FN ₅ O ₂ | 373.42456 |

| | | | | |
|--|---|---------------------|--------------|-----------|
|  | <chem>CC(C)c1nc(C)cc(n1)N2CCN(CC2)c3ncnc4[nH]ccc34</chem> | Z991902128 | C18H23N7 | 337.42212 |
|  | <chem>CNC(=O)C(F)(F)C1(O)CCN(CC1)c2ncnc(OC)n2</chem> | Z340965473 2 | C13H18F2N4O3 | 316.30383 |
|  <p style="color: red; text-align: center;">this enantiomer</p> | <chem>CCc1c[nH]c2ncnc(NC[C@H]3CCCN3S(=O)(=O)C)c12</chem> | Z297070015 6 | C14H21N5O2S | 323.41384 |


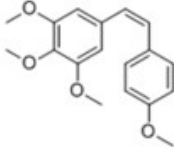
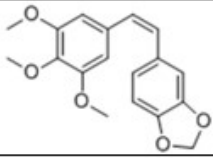
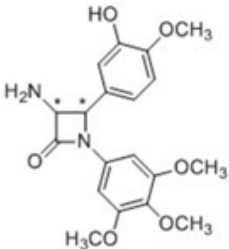
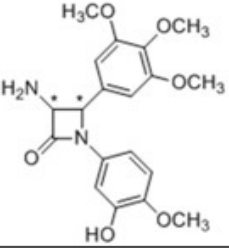
8 Appendix and curriculum vitae

| | | | | |
|---|---|------------------------|-----------|-----------|
|  <p>unknown chirality</p> | <chem>CCC1CN(CC(C)O1)c2ncnc3[nH]ccc23</chem> | Z117377815 2 | C13H18N4O | 246.30822 |
|  <p>unknown chirality</p> | <chem>CC(CO)C(C)Nc1nc(nc2ccc3ccccc23)c3ccnc1</chem> | Z125242837 5 | C18H20N4O | 308.3776 |

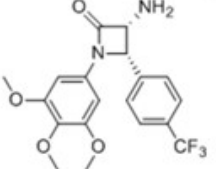
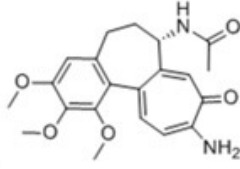
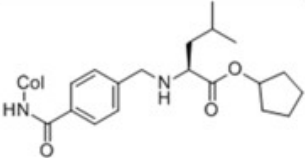
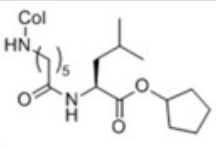
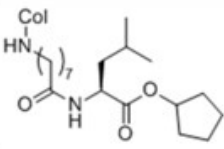
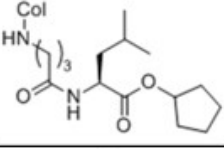
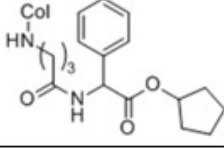
8.3 List of 31 combretastatin/colchicine-related compounds

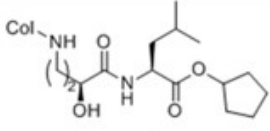
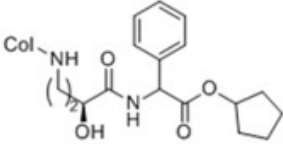
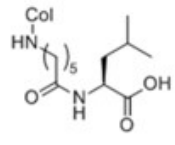
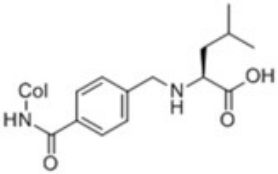
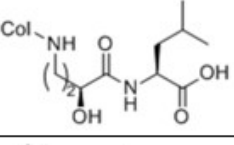
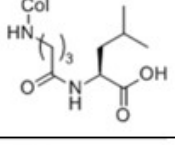
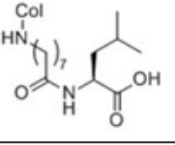
In the table below, Com stands for combretastatin residue and Col stands for colchicine residue.

| Name | Structure | Tubulin polymerization @ 10 μ M | CC ₅₀ (72 h) | |
|--------------------------------|-----------|-------------------------------------|-------------------------|----------|
| | | (DMSO = 100%) | HeLa | Huh-7 |
| MR-065 (Combretastatin A-4) | | 39.7% | 0.428 nM | 1.05 nM |
| MR-082 ("Combretamin") | | 66.9% | 1.47 nM | 1.65 nM |
| MR-109 | | 39.0% | 37.7 nM | 26.9 nM |
| MR-152 | | 105.7% | 78.2 nM | 172 nM |
| MR-164 | | 88.0% | 39700 nM | 26100 nM |
| MR-300 cis | | 71.7% | 726 nM | 1023 nM |
| MR-301 cis | | 53.0% | 33.8 nM | 143 nM |
| MR-302 cis | | 54.0% | 3070 nM | 3640 nM |

| Name | Structure | Tubulin Poly- merization @ 10 μ M | CC ₅₀ (72 h) | |
|---|--|---|-------------------------|----------|
| | | (DMSO = 100%) | HeLa | Huh-7 |
| MR-330 |  | 68.6% | 52.9 nM | 1490 nM |
| MR-339 cis |  | 49.0% | < 3.2 nM | < 3.2 nM |
| MR-357 cis |  | 45.9% | 1.28 nM | 1.06 nM |
| 3R,4S-TD-95 (cis) ("Combeta- lactam") |  | 32.0% | 29.9 nM | 17.6 nM |
| 3S,4R-TD-95 (cis) | | 83.0% | 9370 nM | 12700 nM |
| 3R,4R-TD-95 (trans) | | 48.1% | 5110 nM | 6870 nM |
| 3S,4S-TD-95 (trans) | | 43.4% | 27.2 nM | 20.8 nM |
| 3S,4R-TD-94 (cis) | |  | 102.0% | 46400 nM |
| 3R,4S-TD-94 (cis) | 57.0% | | 5900 nM | 3859 nM |

8 Appendix and curriculum vitae

| Name | Structure | Tubulin Poly- merization @ 10 μ M | CC ₅₀ (72 h) | |
|------------------|---|---|-------------------------|---------|
| | | (DMSO = 100%) | HeLa | Huh-7 |
| 3R,4S-TD-128 cis |  | 69.5% | 8145 nM | 5690 nM |
| VB-008 |  | 33% | 6,7 nM | 8,0 nM |
| VB-033 |  | 118% | 1480 nM | 4950 nM |
| VB-041 |  | 97% | 4620 nM | 6080 nM |
| VB-048 |  | 100% | 4930 nM | 4480 nM |
| VB-065 |  | 86% | 1190 nM | 2790 nM |
| VB-066 |  | 71% | 1240 nM | 5400 nM |

| Name | Structure | Tubulin Poly- merization @ 10 μ M | CC ₅₀ (72 h) | |
|--------|---|---|-------------------------|-------------|
| | | (DMSO = 100%) | HeLa | Huh-7 |
| VB-087 |  | 95% | 230 nM | 680 nM |
| VB-088 |  | 110% | 220 nM | 620 nM |
| VB-092 |  | 88% | 1070 nM | 1190 nM |
| VB-095 |  | 92% | 730 nM | 1170 nM |
| VB-098 |  | 120% | 960 nM | 3270 nM |
| VB-106 |  | 106% | > 50 000 nM | > 50 000 nM |
| VB-107 |  | 103% | > 50 000 nM | > 50 000 nM |

8.4 Accession numbers of proteins described in this doctoral dissertation

8.4.1 Kinase project

Human kinase

| Protein | UniProt ID |
|----------|------------|
| ABL1 | P00519 |
| AKT1 | Q96B36 |
| Aurora A | O14965 |
| Aurora B | Q96GD4 |
| CAMK2B | Q13554 |
| CDK1 | P06493 |
| CDK2 | P24941 |
| CDK4 | P11802 |
| CDK6 | Q00534 |
| DYRK1B | Q9Y463 |
| EGFR | P00533 |
| ERK1 | P27361 |
| FLT3 | P36888 |
| GCN2 | Q9P2K8 |
| GSK3B | P49841 |
| HASPIN | Q8TF76 |
| JNK1 | P45983 |
| LRRK2 | Q5S007 |
| MAPK14 | Q16539 |
| PAK1 | Q13153 |
| PDGFRB | P09619 |
| PDK1 | O15530 |
| PIM1 | P11309 |
| PIM2 | Q9P1W9 |
| PIM3 | Q86V86 |
| PKCA | P17252 |
| PLK1 | P53350 |
| ROCK1 | Q13464 |
| SIK1 | P57059 |
| TIE1 | P35590 |
| VEGFR2 | P35968 |
| WEE1 | P30291 |

Human phosphatase

| Protein | UniProt ID |
|---------|------------|
| CDC25A | P30304 |
| CDC25B | P30305 |
| CDC25C | P30307 |

Human histon

8 Appendix and curriculum vitae

| Protein | UniProt ID |
|-------------|------------|
| Histon H3.1 | P68431 |
| Histon H3.2 | Q71DI3 |
| Histon H3.3 | P84243 |

Fungi kinase

| Organism | Protein/gene | UniProt ID |
|----------------------|--------------|------------|
| <i>S. cerevisiae</i> | PSK2 | Q08217 |

Fungi phosphatase

| Organism | Protein/gene | Uniprot ID |
|----------------------|--------------|------------|
| <i>S. cerevisiae</i> | MIH | P23748 |

Insect phosphatase

| Organism | Protein/gene | Uniprot ID |
|------------------------|--------------|------------|
| <i>D. melanogaster</i> | STG | P20483 |
| <i>D. melanogaster</i> | TWE | Q03019 |

Nematode kinase

| Organism | Protein/gene | UniProt ID | WormBase ID |
|-------------------|--------------|------------|-------------|
| <i>C. elegans</i> | PRK2 | Q20443 | F45H7.4 |

Nematode phosphatase

| Organism | Protein/gene | Uniprot ID | WormBase ID |
|-------------------|--------------|------------|-------------|
| <i>C. elegans</i> | cdc-25.1 | O44552 | K06A5.7 |
| <i>C. elegans</i> | cdc-25.2 | O44628 | F16B4.8 |
| <i>C. elegans</i> | cdc-25.3 | P30634 | ZK637.11 |
| <i>C. elegans</i> | cdc-25.4 | Q21762 | R05H5.2 |

Platyhelminth kinase

| Organism | Protein/gene | UniProt ID | WormBase ParaSite | GenBANK ID |
|--------------------------|--------------|------------|-------------------|------------|
| <i>E. multilocularis</i> | EmPim | A0A087W0F2 | EmuJ_000197100.1 | ON005010 |
| <i>E. multilocularis</i> | EmHASPIN1 | A0A068YA64 | EmuJ_000667600.1 | |
| <i>E. multilocularis</i> | EmHASPIN2 | A0A068XTX4 | EmuJ_001165000.1 | |
| <i>E. multilocularis</i> | EmCDK1 | A0A087VXA1 | CDKD1.1 | |
| <i>S. mansoni</i> | SmPim | G4V8L0 | Smp_090890.1 | |

Platyhelminth phosphatase

| Organism | Protein/gene | Uniprot ID | WormBase ParaSite ID | GenBANK ID |
|--------------------------|--------------|------------|----------------------|------------|
| <i>E. multilocularis</i> | EmCdc25 | A0A068XY79 | EmuJ_001174300.1 | ON005011 |
| <i>S. mansoni</i> | SmCdc25a | A0A3Q0KFE7 | Smp_046810.1 | |
| <i>S. mansoni</i> | SmCdc25b | A0A3Q0KQ13 | Smp_152200.1 | |

Platyhelminth histon

| Organism | Protein/gene | Uniprot ID | WormBase ParaSite ID |
|--------------------------|--------------|------------|----------------------|
| <i>E. multilocularis</i> | EmHiston H3 | A0A068Y7V0 | EmuJ_000579800 |

8.4.2 Tubulin project

Platyhelminthes tubulin

| Organism | Protein/gene | UniProt ID | family |
|--------------------------|---------------------------|------------|---------|
| <i>E. multilocularis</i> | EmuJ_000041100 | A0A087VWR6 | β |
| <i>E. multilocularis</i> | EmuJ_000069900 | A0A087VXD6 | β |
| <i>E. multilocularis</i> | EmuJ_000202500 (EmuTubB3) | Q9NFZ5 | β |
| <i>E. multilocularis</i> | EmuJ_000202600 (EmuTubB1) | A0A087W137 | β |
| <i>E. multilocularis</i> | EmuJ_000569000 | A0A068Y7X2 | β |
| <i>E. multilocularis</i> | EmuJ_000617000 | A0A068Y8U8 | β |
| <i>E. multilocularis</i> | EmuJ_000672200 (EmuTubB2) | Q9NFZ6 | β |
| <i>E. multilocularis</i> | EmuJ_000955100 | A0A068YEW5 | β |
| <i>E. multilocularis</i> | EmuJ_001081200 | A0A068YEW6 | β |
| <i>E. multilocularis</i> | EmuJ_001126150 | A0A068YJS2 | β |
| <i>F. hepatica</i> | FhTubB1 | B0B5G8 | β |
| <i>F. hepatica</i> | FhTubB2 | B0RZ77 | β |
| <i>F. hepatica</i> | FhTubB3 | B0RZ78 | β |
| <i>F. hepatica</i> | FhTubB4 | A0A2H1CS84 | β |
| <i>F. hepatica</i> | FhTubB5 | B0B5H2 | β |
| <i>F. hepatica</i> | FhTubB6 | A0A6G5XRL6 | β |

Mammalian tubulin

| Organism | Protein | UniProt ID | Family |
|------------------|----------|------------|---------|
| <i>H.sapiens</i> | HsTubB2C | Q9BVA1 | β |
| <i>H.sapiens</i> | HsTubB4 | P04350 | β |
| <i>H.sapiens</i> | HsTubB2A | Q13885 | β |
| <i>H.sapiens</i> | HsTubB2B | Q9BVA1 | β |
| <i>H.sapiens</i> | HsTubB5 | P07437 | β |
| <i>H.sapiens</i> | HsTubB8 | Q3ZCM7 | β |
| <i>H.sapiens</i> | HsTubB3 | Q13509 | β |
| <i>H.sapiens</i> | HsTubB6 | Q9BUF5 | β |
| <i>H.sapiens</i> | HsTubB1 | Q9H4B7 | β |

Nematode tubulin

| Organism | Protein/gene | UniProt ID | Family |
|--------------------|--------------|------------|---------|
| <i>H.contortus</i> | HcTubB2 | C5J0J6 | β |
| <i>C.elegans</i> | CeTubB6 | G5EF01 | β |
| <i>C.elegans</i> | CeTubB1 | O17921 | β |
| <i>C.elegans</i> | CeTubB4 | P41937 | β |
| <i>C.elegans</i> | CeBen1 | Q18817 | β |
| <i>C.elegans</i> | CeMec7 | P12456 | β |

9. Acknowledgement and affidavit

9.1 Acknowledgement

First of all, I would like to thank Prof. Dr. Brehm, who accepted me into his research group, the best laboratory for the research of *Echinococcus multilocularis* and gave me the chance to work for my ph.D. In addition to let me work in his group, he also provided me financial support to stay continuously in Germany after the fellowship from Heiwa Nakajima foundation expired. Without him, I had to give up my research years ago. I was always astonished by his knowledge, accomplishment throughout his career, enthusiasm for the research, and networks with research groups all over the world. I learned a lot about his broad knowledge on cestodes and was stimulated by his attitude towards his profession as a researcher through discussion with him.

I also thank other members of my thesis committee, Prof. Dr. Stigloher and Prof Dr. Stich. As my second and third supervisors, they spared their time for my annual presentations.

Next, I would like to thank Heiwa Nakajima foundation. It provided me fellowship and chance to work for 2 years outside of Japan. Also, without this fellowship, I had to give up my research career years ago.

AG Brehm members also supported me in various ways. When Dr. Spiliotis was in AG Brehm, he taught me many experimental technique and knowledge with *E.multilocularis*. As the same doctoral candidates, I spend a lot of time with Philippa Brosch and Ruth Herrmann, both in the laboratory and in the office. They helped me when I cannot understand documents written in German or I had to communicate with people who only speak German. They also explained me German culture or system of German society. Other members also helped me directly and indirectly, through the daily tasks for the lab management. Especially Dirk Radloff has taken care of parasites in the laboratory almost alone. He must be one of

9. Acknowledgement and affidavit

the most essential persons to keep the special environment of our laboratory, where researcher can work on abundant materials of *E. multilocularis*.

The former members of AG Brehm, Dr. Herz and Dr. Koziol also helped me a lot. After Dr. Spiliotis left for Switzerland, there were no postdoctoral fellow in our laboratory. Therefore, I depended on Dr. Herz, because she is now working at another research group in the same building. She helped me a lot especially when I was writing our manuscript of PIM paper and this doctoral dissertation, because nobody in our laboratory, except for Prof. Dr. Brehm, had experience for writing manuscript or doctoral dissertation. I have never met Dr. Koziol in person, but I got a lot of advice on my experiment though Email and I am always using countless protocols he established. He also provided me a lot of his papers through Research Gate, because not all of them are available through the network of Würzburg university.

After the fellowship from Heiwa Nakajima foundation finished, I was employed through the budget from KITE and KITE members became co-author of the PIM paper later. Also without them, I could not have finished ph.D course.

Collins lab members also helped me indirectly even after I left Texas. Without a reference letter from Dr. Collins, probably Dr. Brehm did accept a total stranger from Far East to his laboratory. *In situ* hybridization protocol I learned through experiments with Dr. Wang, helped me in AG Brehm, because protocol for *S. mansoni* and *E. multilocularis* have a lot in common. I also learned Y2H from Dr. Paz. I and he expected to see again on Hydra Island, but it never happened. Unfortunately, all meetings there have been cancelled, because of the corona-pandemic.

9. Acknowledgement and affidavit

Lastly, I have to thank German system of higher education and laboratory environment. The system of higher education in Japan, is largely different from Japan. In Japan, most of ph.D candidates in universities had to work full time without salary. They are just students and not employees, and they had to pay expensive tuitions. The tuition per semester is, 15 times higher in Japanese public university than Würzburg university. It is difficult to be a ph.D candidate in Japan without supports from their families. I could not afford to pay the tuition without any income. That is why I decided to leave Japan, although I had never learned Germany, and I was not especially good at English. In addition, there are no employees to keep the laboratory environment for the research in most of Japanese universities. Students including ph.D candidates had to do all chores without salary, in parallel with their research. In Germany, at least in the institute of hygiene and microbiology, there are plenty of people like a janitor, people who take care of experimental animals, people who prepare basic media /plates and so on. Their support lets us ph.D candidates concentrate on the research. The most important reason why I came to Germany is, the fact that there is the best laboratory of *Echinococcus*, but the difference in the higher education system and environment of the laboratories were also very important. I am not a citizen of Germany or EU, but I could work in better environment with lower cost. I cannot thank enough for the system and people who supported me for these 3 years.

9. Acknowledgement and affidavit

9.2 Affidavit / Eidesstattliche Erklärung

Affidavit

I hereby confirm that my thesis entitled Molecular and cell biological approach towards novel drugs against *Echinococcus multilocularis* is the result of my own work. I did not receive any help or support from commercial consultants. All sources and / or materials applied are listed and specified in the thesis.

Furthermore, I confirm that this thesis has not yet been submitted as part of another examination process neither in identical nor in similar form.

Würzburg, 2022July18

Place, Date

Signature

Eidesstattliche Erklärung

Hiermit erkläre ich an Eides statt, die Dissertation Molekular und zellbiologischer Ansatz hin zu neuartigen Medikamenten gegen *Echinococcus multilocularis* eigenständig, d.h. insbesondere selbständig und ohne Hilfe eines kommerziellen Promotionsberaters, angefertigt und keine anderen als die von mir angegebenen Quellen und Hilfsmittel verwendet zu haben.

Ich erkläre außerdem, dass die Dissertation weder in gleicher noch in ähnlicher Form bereits in einem anderen Prüfungsverfahren vorgelegen hat.

Würzburg, 2022 July 18

Ort, Datum

Unterschrift